CHARLES UNIVERSITY IN PRAGUE

1st Faculty of Medicine
Institute of Inherited Metabolic Disorders

MOLECULAR BASIS OF FAMILIAL HYPERURICEMIC NEPHROPATHIES

Ph.D. Thesis

Prague 2010 **Martina ŽIVNÁ**

ACKNOWLEDGEMENT

My special thanks go to:

Stanislav Kmoch - my advisor, always encouraging, helping, criticizing and ready for discussion

Milan Elleder - head of the institute (during my Ph.D. study) where he cultivated scientific atmosphere and academic background full of discussions

Kateřina Hodaňová - workgroup colleague, always friendly and cheerful, ready to share her work experiences

Petr Vyleťal - workgroup colleague, always friendly, discussing and ready to help

Other colleagues:

Marie Kalbáčová, Jakub Sikora, Robert Ivánek, Helena Hůlková, Veronika Barešová, Hana Blažková - for discussions, their opinions and working experiences

Technicians:

Jana Sovová, Eva Richterová, Mirek Votruba, Eva Oliveriusová - for their excellent technical support, accuracy and reliability

Colleagues from other laboratories:

Zdislava Vaníčková, Květa Pelinková - from Institute of Clinical Biochemistry and Laboratory Diagnostics, helpful during development of ELISA method and analysis of urine samples

Family:

Jan Živný - my husband, always willing to listen to my troubles, ready for discussion and encouragement and patiently shared all my successes as well as failures

My parents Ivan a Blanka, my grandmother Blanka Mezteková and sister Lucie - for their interest in my Ph.D. and their support

...and my friends

FUNDING

This work was supported by the Grant Agency of Charles University of Prague, projects number – registration number 1/2005 (accounting number 203 200)

- registration number 81708 (accounting number 258 105)
- registration number 75007 (accounting number 257 750)
- registration number 67207 (registration number 257 672)
- registration number 44309 (accounting number 259 064).

Institutional support was provided by the Ministry of Education of the Czech Republic, projects MSM0021620806 and 1M6837805002.

Table of contents

Molecular basis of familial hyperuricemic nephropathies

1 Introduction and commented results

In 1960 Duncan and Dixon described family which suffered from chronic tubulointerstitial kidney disease associated with juvenile onset of hyperuricemia and gout. Based on combination of these clinical symptoms they named the disease familial juvenile hyperuricemic nephropathy (FJHN) [Duncan et al. 1960]. Disease with very similar clinical presentation but different age of onset and kidney histology was described as a medullary cystic kidney disease (MCKD) in 1977 [Chamberlin et al. 1977]. Since then, more than 250 families with more than 600 affected individuals fulfilling these basic clinical and biochemical criteria have been identified. Until recently the molecular basis and pathogenesis of this syndrome remained unknown.

The long term aim of our research group is to elucidate the genetic basis of the disease and to solve pathogenetic mechanisms leading to the individual clinical and biochemical symptoms (e.g. hyperuricemia) and kidney damage in general. In our research we mostly apply methods of linkage analysis, candidate gene prioritization and candidate gene sequencing. We systematically identify patients with this disease and healthy family members and collect relevant clinical information and samples for classification (urine, blood, tissue biopsies) and subsequent clinical, biochemical, molecular biology and cell pathology correlations.

In the last decade this approach greatly advanced our knowledge and understanding of FJHN phenotype. We [Stiburkova et al. 2000; Hodanova et al. 2003; Stiburkova et al. 2003; Hodanova et al. 2005] and others [Fuchshuber et al. 1998; Christodoulou et al. 1998; Cohn et al. 2000; Kamatani et al. 2000; Auranen et al. 2001; Fuchshuber et al. 2001; Stacey et al. 2003; Wolf et al. 2003] have proved genetic heterogeneity of FJHN and defined four

FJHN loci on chromosomes 1q21, 1q41, 16p11.2. and 17q21.3. Further research have defined disease causing mutations in three genes - uromodulin (*UMOD)* [Hart et al. 2002], hepatonuclear factor 1-beta (*HNF-1β)* [Bingham et al. 2003] and renin (*REN)* [Zivna et al. 2009], which however explain only about 40% of the FJHN cases. Interestingly, we also found that most of the FJHN cases have altered expression and urinary excretion of UMOD which suggest central role of UMOD protein in development of hyperuricemia and FJHN pathogenesis [Vylet'al et al. 2006]. Our surprising finding, has been corroborated recently by results of genome-wide association studies (GWAS) showing association of *UMOD* polymorphisms with development of chronic kidney disease [Kottgen et al. 2009; Kottgen et al. 2009]. This is a reason of revived and currently growing interest in still mysterious UMOD biology and function and positioning FJHN as a very hot topic in current nephrology research.

In this thesis I therefore decided to present results of my four published papers and one submitted manuscript in the context of actual knowledge in the field.

1. 1 Primary tubulointerstitial kidney diseases

Primary tubulointerstitial diseases of kidney are characterized by histologic and functional abnormalities that involve tubules and interstitium to a greater degree than glomeruli and renal vasculature. Based on the progression rate of the disease acute and chronic forms can be distinguished. Acute forms of the disease are caused by chemical intoxication, infection, and inflammatory or autoimmune mechanisms. Chronic forms of the disease are caused by exogenous or metabolic toxins, autoimmunity or neoplasia. Indispensable group of chronic tubulointerstitial nephropathies are genetically determined familial hyperuricemic nephropathies [Yu et al. 2004].

1. 2 Hyperuricemia and gout

Uric acid (or urate) is the end product of purine metabolism in humans and great apes. Hyperuricemia, accumulation of urate within the body, develops either from overproduction of uric acid (10 - 15% of cases) or defects in excretion of uric acid (85 - 90% of cases). The excretion of uric acid depends on glomerular filtration rate and net tubular reabsorption [Fig. 1]. Gout, clinical manifestation of the deposition of uric acid crystals in the joints, develops when the concentration of uric acid reaches the individual crystallization threshold [Gaffo et al. 2008]. Gout is the most common cause of inflammatory arthritis in men and its incidence is increasing [Wallace et al. 2004].

Hyperuricemia is strongly associated with kidney diseases, metabolic syndrome, cardiovascular diseases, and obesity, although the cause and relationship has not been established in most cases [Masuo et al. 2003; Riches et al. 2009].

The group of primary inherited hyperuricemias includes enzymatic defects in urate metabolism (e.g. hypoxanthine-guanine phosphoribosyl transferase defect, OMIM 300323 or phosphoribosylpyrophosphatase synthetase overactivity, OMIM 300661) and patients

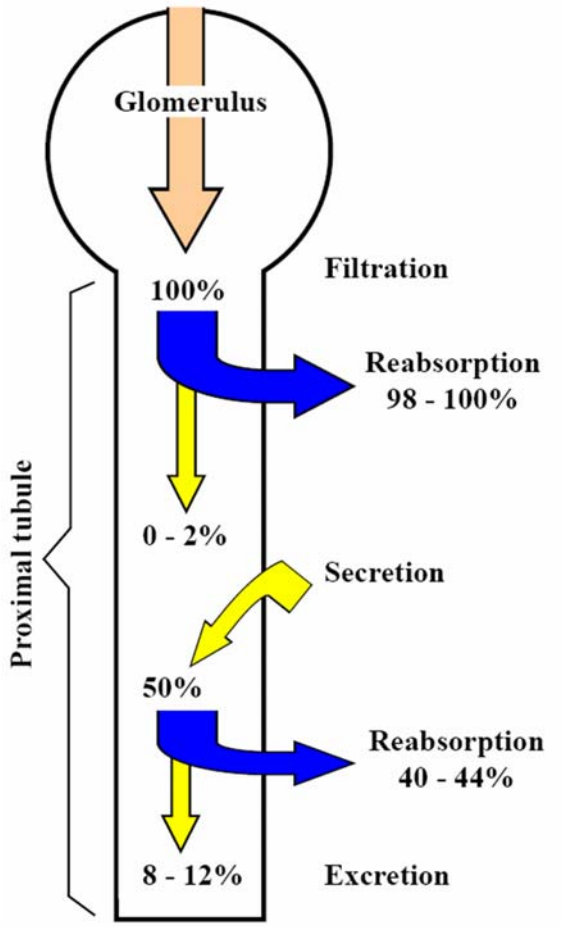

Figure 1: Model of the uric acid transport within the kidney nephron. Glomerularfiltration, tubular secretion and reabsorption are shown as percentage of filtered uric acid in individual nephron parts. (From the [McCarty et al. 1989]).

with glycogen storage diseases [Cameron et al. 2005]. Primary inherited hyperuricemias also include a group of familial autosomal dominant hyperuricemic nephropathies, including familial juvenile hyperuricemic nephropathy type 1 (OMIM 162000), familial juvenile hyperuricemic nephropathy type 2 (OMIM 613092), and medulary cystic kidney disease type 1 (OMIM 174000) and medullary cystic kidney disease type 2 (OMIM 603860) [Gaffo et al. 2008]. In these diseases the hyperuricemia develops at early stages, before clinical signs of kidney failure. The cause of hyperuricemia in cases of familial hyperuricemic nephropathies, however, has not been successfully explained yet.

Secondary hyperuricemias are caused by excessive purine turnover (diet, malignancies, medications, and toxins) or defects in uric acid excretion (kidney failure, tubulointrestitial defects).

Uric acid secretion and reabsorption is tuned in kidney tubules by several urate transporters. Known mutations in urate transporters, loss of function mutations in *SLC22A12* (UART-1) and *SLC2A9* are associated, however, with hypouricemia, hypouricuria and progressive kidney failure [Enomoto et al. 2002; Ichida et al. 2004]. The relation of urate transporters function and expression in patients with hyperuricemic nephropathies remains unclear [Gaffo et al. 2008; Riches et al. 2009].

1. 3 Familial hyperuricemic nephropathies (FHN)

Familial hyperuricemic nephropathies (FHN) are group of primary chronic forms of tubulointerstitial nephropathies with distinct clinical and histological features, various types of inheritance with either juvenile or adulthood onset. FHN with autosomal dominant inheritance, based on clinical and pathological finding, comprise following kidney diseases:

i) familial juvenile hyperuricemic nephropathy type 1 (FJHN1, OMIM 162000) also known as familial juvenile gouty nephropathy (FJGN)

ii) familial juvenile hyperuricemic nephropathy type 2 (FJHN2, OMIM 613092)

iii) medullary cystic kidney disease type 1 (MCKD1, OMIM 174000)

iv) medullary cystic kidney disease type 2 (MCKD2, OMIM 603860), [Fig. 2].

Clinical signs and symptoms of familial hyperuricemic nephropathies (FHN)

The typical clinical features for FHN are alteration of urinary concentration ability, hyperuricemia and tubulointerstitial fibrosis [Rampoldi et al. 2003]. Renal impairment

usually reaches clinical significance between 15 and 40 years of age and inevitably leads to end-stage renal failure (ESRF) within 10 to 20 years [Simmonds et al. 1980; Richmond et al. 1981; Cameron et al. 1993; Dahan et al. 2001].

Familial juvenile hyperuricemic nephropathy type 1 (FJHN1) as well as medullary cystic kidney disease type 2 (MCKD2) are autosomal dominant tubulointerstitial nephropathies characterized by juvenile onset of hyperuricemia, gouty arthritis, and progressive renal failure at an early age. Several investigators suggest FJHN1 and MCKD2 to be the same disease.

The familial juvenile hyperuricemic nephropathy type 2 (FJHN2) phenotype is characterized by early anemia, hypouricosuric hyperuricemia, small sized kidney with no evidence of cysts formation, progressive kidney failure resulting in end-stage renal failure between ages 43 - 68 [Hodanova et al. 2005; Zivna et al. 2009].

Medullary cystic kidney disease type 1 (MCKD1) is characterized by late onset of hyperuricemia, gouty arthritis, progressive renal failure and hypertension. Common biochemical hallmarks of FJHN1/MCKD2 and FJHN2 are hyperuricemia and reduced fractional excretion of uric acid. Imaging studies show decreased kidney size, parenchymal atrophy and abnormal echogenicity in a majority of patients. Medullary cysts, of a small size, are seen in approximately 30% of cases in later age [Prieto et al. 1994; Sebesta et al. 1994; Saeki et al. 1995; Stiburkova et al. 2000]. MCKD1 patients often develop cysts at the corticomedullary junction [Gardner 1971; Swenson et al. 1974; Hateboer et al. 2001]. Occasionally urate deposits are detected in tubulointerstitial region of the kidney in patients with familial hyperuricemic nephropathy [Cameron et al. 1993; Puig et al. 1993; Sebesta et al. 1994; Saeki et al. 1995; Pavelka et al. 1996; Lhotta et al. 1998; Stiburkova et al. 2000].

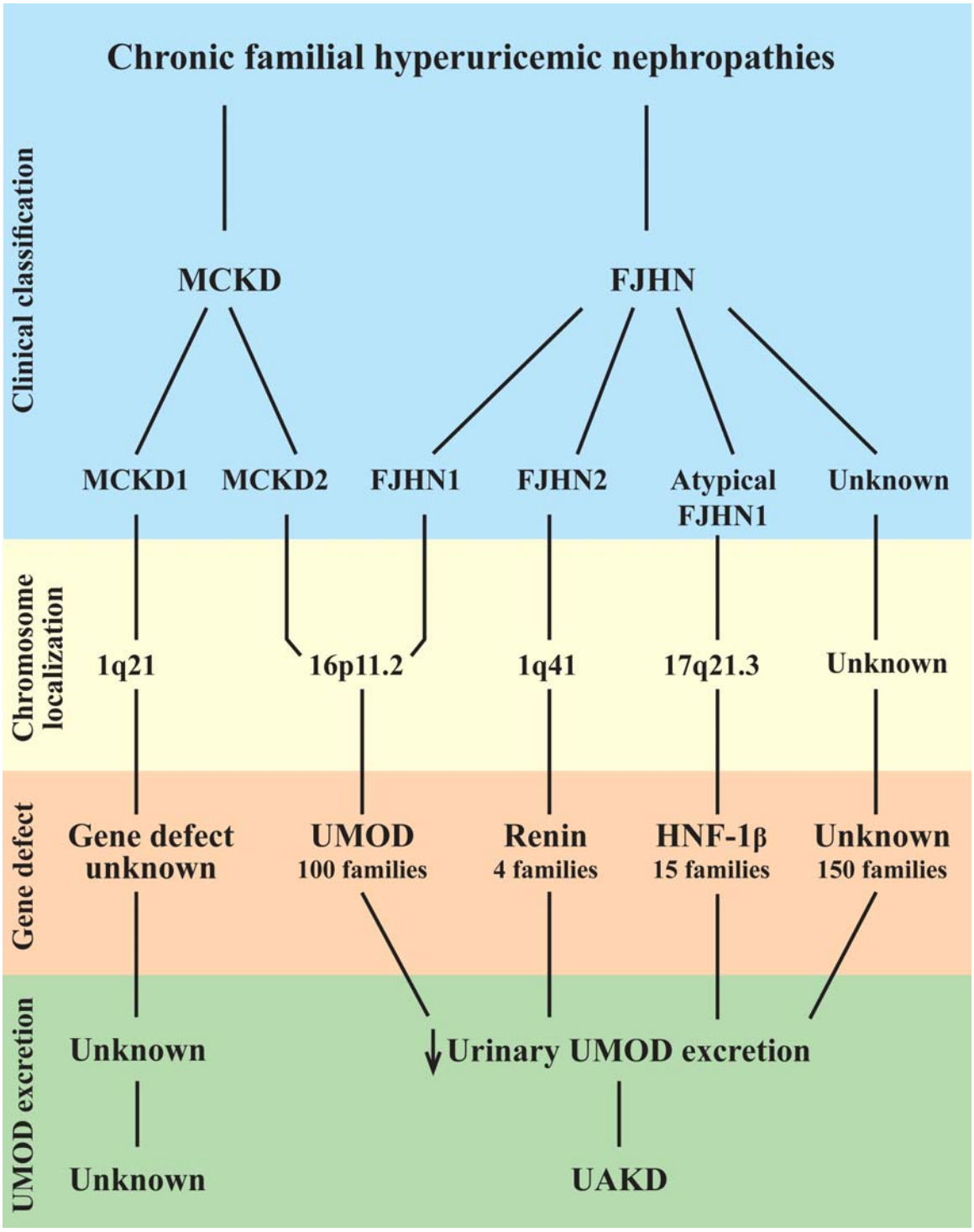

Figure 2: Chromosome localization of gene defect associated with chronic familial hyperuricemic nephropathies.
Abbreviations: MCKD - medullary cystic kidney disease; FJHN - familial juvenile hyperuricemic nephropathy; UMOD - uromodulin; HNF-1β - hepatocyte nuclear factor-1β; UAKD - uromodulin-associated kidney disease

Genetic heterogeneity of familial hyperuricemic nephropathies (FHN)

FHN are genetically heterogeneous diseases [Fuchshuber et al. 1998; Stiburkova et al. 2000]. FJHN1 and MCKD2 segregate with overlapping regions on 16p11.2 and 16p12 respectively [Scolari et al. 1999; Stiburkova et al. 2000; Dahan et al. 2001; Hateboer et al. 2001; Stiburkova et al. 2003]. FJHN2 is linked with chromosome 1q41 [Hodanova et al. 2005]. MCKD1 was further associated with region on chromosome 1q21 [Christodoulou et al. 1998; Wolf et al. 2006] [Fig. 2].

Locus 1q21 for MCKD1 was the first locus discovered to segregate with hyperuricemic nephropathy. However, the genetic defect from this region was not found yet [Christodoulou et al. 1998; Auranen et al. 2001; Fuchshuber et al. 2001; Wolf et al. 2006].

FJHN1 and MCKD2 were found to be associated with mutation in uromodulin *(UMOD)* which is localized in candidate region 16p11.2 [Hart et al. 2002; Rampoldi et al. 2003; Turner et al. 2003; Vylet'al et al. 2006; Wolf et al. 2007; Lhotta et al. 2009; Williams et al. 2009].

In families with features of FJHN1 complicated by early onset of diabetes was identified heterozygous mutation in *HNF-1β* gene [Bingham et al. 2003]. However, *HNF-1β* region on 17q21.3 suggests that *HNF-1β* mutations are a minor cause of FJHN1.

Within the other locus, linked with FJHN2, on chromosome 1q41 mutation in signal peptide of renin gene *(REN)* was found recently **[see results, paper 4. 1; Hodanova et al. 2005 and paper 4. 4; Zivna et al 2009]**. With regard to recent publication, the mutation in *REN* was found in approximately 2% of FHN cases to these days. However, the genetic testing of other families with tubulointerstitial nephropathies is underway, thus the real number of patients with mutation in *REN* could be higher [Fig. 2].

The common name uromodulin-associated kidney disease (UAKD) or uromodulin-related kidney disease was established for FJHN1 and MCKD2 [Bleyer et al. 2003; Bleyer et al. 2004; Bernascone et al. 2006; Vylet'al et al. 2006; Lhotta et al. 2009] as well as for FJHN2. Mutation in *UMOD* was identified only in approximately 30% of FJHN1/MCKD2 families.

1. 4 Uromodulin - Associated Kidney Disease (UAKD)

The term uromodulin-associated kidney disease (UAKD) or uromodulin-related kidney disease includes disease FJHN1, MCKD2 and FJHN2. Juvenile onset of hyperuricemia, gouty arthritis, reduced fractional excretion of uric acid, normal or small-sized kidney sometimes with cysts and progressive renal impairment leading to ESRD are typical presentations of UAKD [Hart et al. 2002; Turner et al. 2003; Bleyer et al. 2004; Vylet'al et al. 2006]. All UAKD patients have decreased urinary UMOD excretion independent on presence or absence of *UMOD* mutation **[see results, paper 4. 1; Hodanova et al. 2005 and paper 4. 2; Vyletal et al. 2006]**. Mutation in *UMOD* gene encoding uromodulin protein (UMOD) known as Tamm-Horsfall protein (THP) was identified in only 30% of UAKD cases. Kidney biopsies from UAKD patients revealed several different patterns of UMOD staining. Massive intracellular accumulation of UMOD in tubular cells is detected in all kidney sections of UAKD patients, which link on 16p11.2 and have mutation in *UMOD* [Dahan et al. 2003; Bleyer et al. 2004]. Kidney biopsy from UAKD patients associated with locus 16p11.2, i.e. without mutation in *UMOD*, shows different pattern of staining with uromodulin in hyaline casts and low intracellular positivity. Kidney section of patients from family FJHN2 mapped on 1q41 locus shows strongly reduced expression of UMOD without accumulation. In case of other UAKD family in which no linkage to known UAKD loci was found irregular pattern of UMOD

staining. While in patients UMOD in kidneys is found accumulated or decreased, the urinary UMOD excretion is invariably significantly decreased **[see results, paper 4. 1; Hodanova et al. 2005 and paper 4. 2; Vyletal et al. 2006]**.

1. 5 Uromodulin (UMOD), Tamm-Horsfall glycoprotein (THP)

Tamm-Horsfall protein (THP), also known as uromodulin (UMOD), was the first time isolated from human urine of healthy individuals by Igor Tamm and Frank Horsfall jr. in 1950 [Tamm et al. 1950]. Thirty five years later Muchmore and Decker identified 85kDa glycoprotein isolated from urine of pregnant women. Because of *in vitro* immunosuppressive activity of the protein was observed the name uromodulin was chosen [Muchmore et al. 1985; Muchmore et al. 1986]. Two years later, 1987, sequence analysis showed Tamm-Horsfall glycoprotein and uromodulin to be identical [Pennica et al. 1987].

Uromodulin (UMOD) expression

UMOD is exclusively expressed in the thick ascending limb (TAL) of the Henle´s loop and the early distal convoluted tubule (DCT) [Cavallone et al. 2001; Serafini-Cessi et al. 2003; Bleyer et al. 2004; Vylet'al et al. 2006; Williams et al. 2009]. The microscopic observations revealed that UMOD is targeted to the apical cell membrane of the TAL epithelial cells by glycosylphosphatydilinositol (GPI) anchor. From the apical pole of TAL epithelial cells is UMOD cleaved by unknown protease into the tubule lumen and excreted into the urine. UMOD is the most abundant protein in normal human urine [Thornley et al. 1985; Dahan et al. 2003; Serafini-Cessi et al. 2003; Devuyst et al. 2005; Vylet'al et al. 2006].

Uromodulin (UMOD) structure

UMOD is a synthesized as 640 amino acids precursor. Upon translocation into the endoplasmic reticulum, the 24 amino acid signal peptide and the hydrophobic portion of C-terminus are removed. After the glycosylphosphatidylinositol (GPI) anchor is attached to the C-terminus UMOD is transported to the cell surface. UMOD exposed on the tubular cell surface is cleaved again near the C-terminus, resulting in urinary UMOD [Kudo et al. 2004].

UMOD is 85kDa glycoprotein which contains up to 30% of its mass in carbohydrates. Eight potential sites of N-glycosylation are present, explaining high carbohydrate content of UMOD. The mature protein contains 48 cystein residues potentially involved in 24 disulfide bridges, which are important for its conformation. The correct formation of disulfide bonds seems to be limiting step for the subsequent export of UMOD from the endoplasmic reticulum of TAL cells [Malagolini et al. 1997; Serafini-Cessi et al. 2003; Devuyst et al. 2005; Choi et al. 2005; Williams et al. 2009]. Uromodulin consists of 3 epidermal growth factor-like (EGF) domains, a cystein-rich region, and a *zona pellucida* (ZP) domain. Second and third EGF-like domain contain calcium binding motif (cbEGF II and cbEGF III). Cystein-rich region includes a domain of 8 cysteines (D8C) [Fig. 3]. In general, EGF-like domains represent one of the most frequent parts of protein involved in protein-protein interactions. CbEGF-like domains are important to orient neighboring modules relative to each other in a manner that is required for biological activity and are predicted to form a rod like structure [Stenflo et al. 2000; Yuan et al. 2002]. Cystein residues form disulphide bridges to yield a stable tertiary structure [Yuan et al. 2002]. ZP domain is responsible for polymerization of UMOD [Jovine et al. 2005; Monne et al. 2008; Schaeffer et al. 2009].

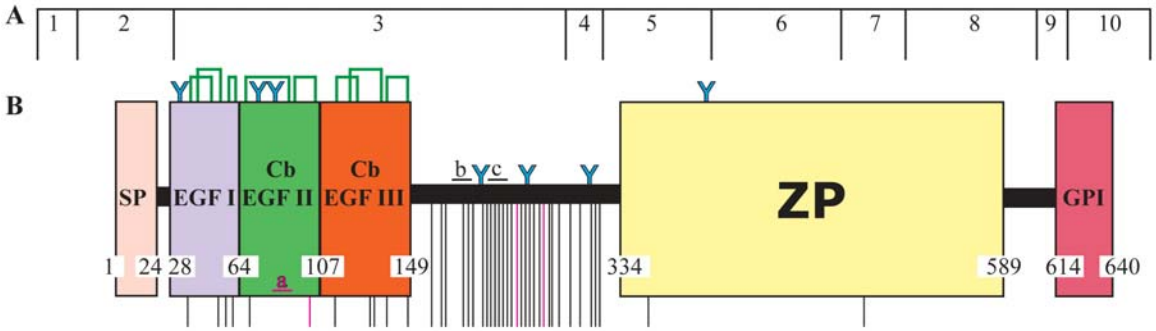

Figure 3: Schematic representation of uromodulin protein.

A Schematic representation includes exons 1 to 10 of *UMOD* gene.

B Schematic picture of uromodulin protein include domains assignation (EGF I, Cb EGF II, Cb EGF III, ZP), signal peptide (SP) and glycosylphosphatidylinositol anchorage (GPI). Amino acid positions of individual domains start and end are shown on the bottom of domain scheme. Missense substitutions associated with FJHN1 are marked as black lines; black b represents mutation delH177_R185; black c represents mutation E188Vdel_L221, both are associated with FJHN1. Missense substitutions associated with MCKD2 are marked as red lines; red a represents mutation V93_G97del, ins AASC associated with MCKD2.

Abbreviations and symbols: Y - potential N-glycosylation site; ⊓ - disulfid bond; SP - signal peptide; EGF - like; Cb EGF - calcium binding epidermal growth factor-like; ZP - *zona pellucida*; GPI - glycosylphosphatidylinositol anchorage; FJHN - familial juvenile hyperuricemic nephropathy; MCKD - medullary cystic kidney disease.

Uromodulin (UMOD) functions

There have been many suggestions regarding to the biological function of UMOD and its role in renal physiology and disease in humans. It has been reported that uromodulin has a role as an inhibitor of renal stone formation, as a modulator of renal immune responses, in protecting against urinary tract infections and helps to maintain the integrity of the loop of Henle and the countercurrent mechanism [van Rooijen et al. 1999; Turner et al. 2003; Vylet'al et al. 2006]. The inhibition of renal stone formation is caused by inhibition of calcium oxalate crystal aggregation and formation of urinary casts. The immunomodulatory functions of UMOD are suggested by its ability to bind to tumor necrosis factor, interleukin 1 alpha, and other cytokines [Zhu et al. 2002]. UMOD prevents urinary tract infections against type I fimbriated *Escherichia coli* by binding to this pathogen and inhibiting its attachment to epithelial cells of urinary tract [Hart et al. 2002;

Serafini-Cessi et al. 2003]. UMOD has the ability to polymerize and to form reversible gel-like structure [Devuyst et al. 2005]. Polymerized UMOD molecules could be responsible for water impermeability and maintenance of integrity of Henle´s loop [Mattey et al. 1992; Benetti et al. 2009].

Kidneys and urinary tract of THP gene knock-out mice ($THP^{-/-}$) did not show any changes in the morphology of the renal tubules or the glomeruli. $THP^{-/-}$ mice could not concentrate their urine and excreted higher urine volumes than control mice. The GFR in $THP^{-/-}$ mice as estimated by creatinine clearance was reduced. In $THP^{-/-}$ mice were found that major distal transporters were upregulated, whereas juxtaglomerular COX-2 and renin mRNA expression was significantly decreased [Bachmann et al. 2005].

Despite of the above suggestions and information derived from mice with the functionally inactivated *Umod* gene the exact role of UMOD in humans still remains enigmatic.

Uromodulin (UMOD) mutations

Mutations in *UMOD* are associated with FJHN1/MCKD2 phenotype. To these days 46 different heterozygous *UMOD* mutations were identified. Interestingly, over 95% of identified disease associated *UMOD* mutations are in exon 3 and 4, EGF-like domains and cystein-rich region coding exons. Only two of identified mutations are located in exons coding ZP domain [Fig. 3].

All so far characterized *UMOD* mutations retain full-length peptide bone. Hence all observed *UMOD* mutant variants are likely to resulted in the change of protein folding, maturation and trafficking, caused by disruption of the tertiary and quarternary structure **[see results, paper 4. 2; Vyletal et al. 2006]** [Turner et al. 2003].

There are many studies dedicated to expression of individual mutated UMOD proteins in eukaryotic cells *in vitro*. Based on the results of these studies we can separate UMOD mutations into two groups. One group of mutated UMOD variants shows reduced ability to expose UMOD on plasma membrane. The other group of mutated UMOD variants has the defect of UMOD to exit endoplasmic reticulum (ER). The ability of protein to reach the plasma membrane is determined by its GPI modification. Failure in GPI attachment to the protein could impair intracellular trafficking. Mutated proteins which cannot exit ER lumen could induce endoplasmic reticulum stress pathway.

UMOD accumulation in kidney tissue is observed in UAKD patients with *UMOD* mutation, suggesting possibility of ER stress activation **[see results, paper 4. 2; Vyletal et al. 2006]** [Turner et al. 2003; Bernascone et al. 2006; Lhotta et al. 2009; Williams et al. 2009]. ER stress of tubular mutated UMOD producing cells may be pathogenetic mechanism responsible for kidney tubular damage. Accumulation of mutated UMOD in ER of tubular cells may lead to induction of ER stress resulting in apoptosis, deterioration of kidney tissue and subsequent progressive renal failure. The fact, that the heterozygous *UMOD* mutation causes an autosomal dominant disease is consistent with a dominant negative effect [Tinschert et al. 2004; Bernascone et al. 2006].

Hyperuricemia in UAKD patients usually appears at an early age, suggesting that hyperuricemia is somehow directly linked to UMOD dysfunction [Dahan et al. 2003; Vylet'al et al. 2006]. However, the link between early hyperuricemia, damage of kidney and function and mutation in UMOD remains unclear.

Other diseases associated with defect in uromodulin excretion

Significant quantitative and qualitative changes in urinary UMOD excretion were found in patients at various clinical stages of Fabry disease (OMIM 301500). These

changes seemed in most investigated cases to reflect phenotypic severity. The abnormal patterns normalized in all investigated patients on enzyme replacement therapy and in some patients on substrate reduction therapy. These observations warrant evaluation of tubular functions in Fabry disease and suggest UMOD as a potential biochemical marker of therapeutic response of the kidney to therapy **[see results, paper 4. 3; Vyletal et al. 2008]**.

Genome-wide association studies (GWAS) identified SNP in *UMOD* locus, among others, to be associated with chronic kidney disease and glomerular filtration rate [Kottgen et al. 2009]. The common polymorphism (rs4293393) in the *UMOD* gene is associated with higher risk of chronic kidney disease development [Kottgen et al. 2009].

1. 6 Hepatocyte nuclear factor - 1β (HNF-1β)

Hepatocyte nuclear factor - 1β (HNF-1β) expression

Hepatocyte nuclear factor-1β (HNF-1β) is a homeodomain-containing transcription factor which is highly expressed in tubular epithelia of renal, biliary and pancreatic ducts. In kidney is HNF-1β expressed throughout the entire nephron, from proximal tubules to collecting ducts. HNF-1β, as a transcription factor, directly control genetic cascades that are essential for physiology of kidney, pancreas, liver, genital tract and gut [Coffinier et al. 1999; Gresh et al. 2004].

Hepatocyte nuclear factor - 1β (HNF-1β) functions

Mice with renal-specific inactivation of HNF-1β developed polycystic kidney disease with abnormalities localized especially in medullar region [Gresh et al. 2004]. These mice showed specific transcriptional downregulation of several genes known to play crucial role in cystogenesis, such as *Umod* (uromodulin) in medulla, *Pkhd1* (polyductin) in

cystic epithelia, and *Pkd2* (polycystin 2) in cystic cells. Inactivation of *HNF-1β* in tubular epithelial cells results in increased proliferation of these cells in vivo [Gresh et al. 2004].

HNF-1β binding sites were detected in DNA elements of the *Umod, Pkhd1* and *Pkd2* genes using chromatin immunoprecipitation of mice pooled kidney lysates. These genes are known to be mutated in distinct cystic kidney diseases in men. Mutations in *PKD1* and *PKD2* are associated with autosomal dominant polycystic kidney disease [Mochizuki et al. 1996], autosomal recessive polycystic kidney disease is associated with mutations in *PKHD1* [Ward et al. 2002], and medullary cystic kidney disease type 2 is associated with mutations in *UMOD* [Hart et al. 2002]. Most of the HNF-1β targets colocalize with the primary cilium, organelle that plays an important role in controlling the proliferation of tubular cells.

Taken together, HNF-1β directly controls the transcription of several genes expressed in tubular epithelial cells and is essential for controlling the proliferation and differentiation of renal tubular epithelial cells [Gresh et al. 2004].

Hepatocyte nuclear factor - 1β (HNF-1β) mutations

Human heterozygous mutations in the *HNF-1β* gene are associated with autosomal dominant type of inheritance. The most common phenotype observed in patients with *HNF-1β* mutation is called renal cysts and diabetes (RCAD, OMIM 137920) syndrome. This syndrome combines a form of type II diabetes called maturity onset diabetes of the young type 5 (MODY5) with a nondiabetic renal disease [Horikawa et al. 1997; Bingham et al. 2004]. In some kindreds hyperuricemia, gout and renal cystic disease was reported [Bingham et al. 2003]. Some patients also present genital malformations, liver dysfunctions and pancreatic atrophy [Bellanne-Chantelot et al. 2004; Edghill et al. 2008].

The wide spectrum of clinical manifestations associated with mutations in *HNF-1β* suggests the importance of this transcription factor in pancreatic and renal development.

1. 7 Renin and prorenin

Renin was discovered in 1898 by Robert Tigerstedt and Per Bergman. They injected rabbits with fresh homogenate of rabbit kidney and observed increase in blood pressure in the recipients. They concluded that in kidney is pressor substance and named this substance according its habitat renin [Tigerstedt et al. 1898].

Renin expression

Renin is an aspartyl protease expressed from early stages of human kidney development by epitheloid juxtaglomerular cells [Schutz et al. 1996]. Epitheloid juxtaglomerular cells (JGC) are located in the wall of renal afferent arterioles at the entrance of the glomerular capillary network. Juxtaglomerular apparatus (JGA) is the main source but not the only one of renin. Messenger RNA as well as protein of renin was observed in other segments of kidney as well. The renin was detected in cells of glomeruli and proximal and distal nephron [Moe et al. 1993; Rohrwasser et al. 1999; Zivna et al. 2009]. Other tissues that were found to produce renin are adrenal glands, brain, lung and vasculature [Persson et al. 2003; Kobori et al. 2007].

Renin and prorenin structure and secretion

Renin is synthesized as 406 amino acids enzymaticaly inactive preprorenin which includes 23 amino acids N-terminal "pre-region" signal peptide [Imai et al. 1983]. Signal peptide is required for the targeting and translocation of nascent preprorenin into the lumen

of rough endoplasmic reticulum [Walter et al. 1994]. Signal peptide is followed by 43 amino acids "pro-region" which prevent renin from being catalytically active. The mature protein has 340 amino acids, two predicted N-glycosylation sites and two active sites [Fig. 4]. Electrophoretical mobility of mature renin is 43 kDa.

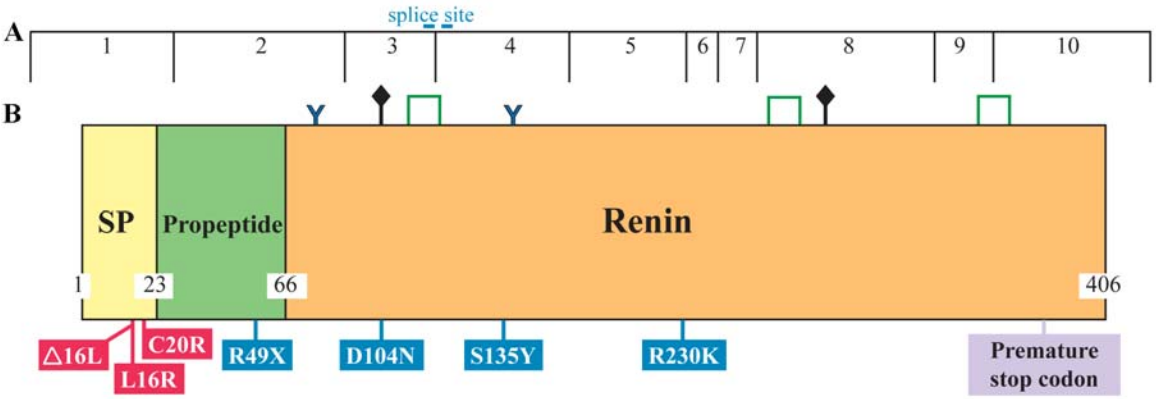

Figure 4: Schematic representation of renin protein.
A Schematic representation includes exons 1 to 10 of *REN* gene.
B Schematic picture of renin protein include signal peptide (SP), propeptide and mature renin. Amino acid positions of individual parts start and end are shown on the bottom of protein scheme. Missense substitutions associated with FJHN2 are marked in red boxes; Mutations associated with renal tubular dysgenesis are marked in blue boxes; Mutation associated with benign hyperproreninemia is marked in purple box.
Abbreviations and symbols: Y - potential N-glycosylation site; ⊓ - disulphid bond; ♦ - acive site; SP - signal peptide; FJHN - familial juvenile hyperuricemic nephropathy.

Preprorenin is processed to prorenin, which has two major fates. Prorenin is either released from the Golgi to the circulation through exocytosis or packaged into secretory granules and converted to renin by processing endopeptidases such as proconvertase and cathepsin B. Prorenin is principally secreted by the constitutive pathway [Pratt et al. 1987; Ichihara et al. 2009]. The plasma prorenin level is 10-fold higher than renin in normal subjects [Danser et al. 1998]. Mature renin is released from the secretory granules after cell

stimulation. Renin secretion, especially from JGA in the kidney, is regulated by arterial blood pressure, sympathetic nervous system activity, sodium balance and negative feedback regulation by angiotensin II (ANG II) [Persson 2003; Brown 2007].

Renin and prorenin functions

Prorenin and renin are active in two distinct pathways - the renin-angiotensin system (RAS) [Paul et al. 2006], and the (pro)renin receptor signal transduction [Campbell 2008]. Both pathways play an important role in kidney physiology and pathology.

Renin-angiotensin system (RAS)

RAS is a cascade of catalytic reactions where renin acts as the first and limiting step. Renin cleaves angiotensinogen (AGT) to the decapeptide angiotensin I (ANG I), which is further converted by angiotensin-converting enzyme (ACE) to the active octapeptide angiotensin II (ANG II). ANG II is the most powerful biologically active product of the RAS and acts through its binding to angiotensin II type 1 (AT1) or type 2 (AT2) receptors. RAS regulates blood pressure, cell growth, apoptosis, erythropoiesis, electrolyte balance, and volume homeostasis [Kurtz et al. 1999; Persson 2003; Schweda et al. 2007]. Besides the circulating RAS components, local RAS was documented in many tissues with possible paracrine and autocrine regulatory role. This universal paracrine and autocrine action may be important in many organ systems and can mediate important physiological stimuli [Paul et al. 2006]. Locally produced ANG II has direct effect at the cellular level and can influence, for example, cell growth, differentiation, and may play a role as a mediator of apoptosis [Paul et al. 2006]. Although every organ system in the body has individual elements of the RAS, the kidney is unique in having all components of the RAS. All of the components necessary to generate intrarenal ANG II are present along the

nephron [Kobori et al. 2007]. ANG II enhances the sensitivity of the vascular and mesangial elements that mediate tubuloglomerular feedback-induced alterations in single nephron function. These effects probably are mediated by direct actions on the vascular smooth muscle cells and mesangial cells as well as by modulating the Na^+/H^+ exchange activity of the macula densa cells [Peti-Peterdi et al. 1998; Kovacs et al. 2002; Navar et al. 2004]. Intrarenal ANG II contribution to increased tubular reabsorption is complex, including constriction of glomerular arterioles, which alter peritubular capillary dynamics and renal medullary blood flow, and direct actions on tubular epithelial cell transport.

From the studies with ACE inhibitors and AGT II receptor blockers the fact that intrarenally formed ANG II may be more important than circulating ANG II in controlling renal function emerged [Kobori et al. 2007].

Renin and prorenin receptors

Other functions of renin and prorenin is likely related to their binding with receptors. Two receptors able to bind both renin and prorenin, mannose-6-phosphate (M6P) receptor and (pro)renin receptor, were found.

The M6P receptor may bind every phosphomannosylated protein including renin and prorenin. Binding is followed by the internalization and proteolytic activation of prorenin, which is a result of unknown prorenin activating enzyme [van den Eijnden et al. 2001]. It seems that cleavage of prorenin to renin after internalization is the first step toward intracellular prorenin and renin degradation way. M6P receptor is likely to clearance receptor for renin and prorenin [van den Eijnden et al. 2001; Nguyen 2007].

The (pro)renin receptor mRNA was detected in human brain, heart, placenta, kidney, liver, pancreas, and eye [Nguyen et al. 2002]. Nguyen et al in 2002 showed that (pro)renin receptor in kidney is localized in distal renal tubule, within the mesangial area of

glomeruli, and in vascular smooth muscle cells [Nguyen et al. 2002] Contrary to that, our group detected the (pro)renin receptor in basolateral pole of distal convoluted tubules and thick ascending loop of Henle without any other positivity **[see results, supplement of paper 4. 4; Zivna et al. 2009]**.

The binding of prorenin to (pro)renin receptor seem to trigger different consequences compared to binding renin [Huang et al. 2007]. The binding of prorenin to the (pro)renin receptor is followed by conformational change which lead to the unmasking of active sites without cleavage of prosegment. The result is cleavage angiotensinogen with kinetics similar to that of fully active renin in solution. Thus, (pro)renin receptor may induce prorenin catalytic activity functionally comparable to renin [Jan Danser et al. 2002; Nguyen 2005; Nguyen et al. 2008]. Renin binding to the (pro)renin receptor induces rapid phosphorylation of mitogen-activated protein (MAP) kinases extracellular-signal regulated kinase 1 and 2 (ERK1 and ERK2) in rat and human mesangial cells. Activation of ERK1/2 signaling pathway increases expression of transforming growth factor - beta1 (TGF-β1) and plasminogen activator inhibitor-1 (PAI-1) [Nguyen 2006; Huang et al. 2007]. TGF- β1 and PAI-1 are both key medaitors of tissue fibrosis [Border et al. 1998]. The renin signaling mediated by (pro)renin receptor may induce profibrotic changes, cell growth and tissue remodeling in the heart and kidney [Huang et al. 2006; Huang et al. 2007; Kaneshiro et al. 2007; Nguyen 2007].

The transgenic rats that overexpress human (pro)renin receptor developed slowly progressive nephropathy with proteinuria and significant glomerulosclerosis. In the kidney of the transgenic rats MAPKs and expression of TGF-β1 was increased. Human (pro)renin receptor was unable to evoke the enzyme activity of rat prorenin suggesting the changes are independent on angiotensin part of RAS. This transgenic rat model provide *in vivo*

evidence for the AngII-independent MAPKs activation by human (pro)renin receptor [Kaneshiro et al. 2007].

Except of the kidney, there are emerging evidences suggesting that the (pro)renin receptor and prorenin influence other tissue functions. The increase of circulating prorenin level was associated with state such as diabetes mellitus [Bader 2007], diabetic retinopathy [Moravski et al. 2003; Wilkinson-Berka 2008] and retinopathy of prematurity [Moravski et al. 2000]. The mutation in (pro)renin receptor was identified in a single family and is associated with X-linked mental retardation and epilepsy. These findings indicate importance of (pro)renin receptor in cognitive functions and brain development [Ramser et al. 2005].

Renin mutations

Mutations in human renin gene (*REN*) are associated with three different phenotypes. Severity of the phenotype depends on affected segment of renin and whether the mutation is homozygous or heterozygous.

Benign hyperproreninemia

The first identified mutation in *REN* is heterozygous point mutation creates premature stop codon resulting in a truncated form of renin with 20 amino acids deleted from the carboxyl terminus [Fig. 4]. This mutation was identified in a single Dutch family with 3 probands. All family members, including probands, were normotensive and had normal plasma renin activities. All probands were asymptomatic with benign hyperproreninemia (OMIM 179820) [Villard et al. 1994].

Renal tubular dysgenesis (RTD)

Renal tubular dysgenesis (RTD, OMIM 267430), disorder with autosomal recessive type of inheritance, is associated with various homozygous or compound heterozygous mutations in *REN* [Fig. 4] [Gribouval et al. 2005; Lacoste et al. 2006; Zingg-Schenk et al. 2008]. RTD is severe disorder of renal tubular development characterized by absence or paucity of differentiated proximal tubules, persistent fetal anuria, renal failure, skull ossification defects, large fontanels and pulmonary hypoplasia from early-onset oligohydramnios (Potter syndrome). Affected individuals often die during perinatal period [Gribouval et al. 2005; Lacoste et al. 2006; Zingg-Schenk et al. 2008]. Only two patients with inherited RTD who survived perinatal period are known [Zingg-Schenk et al. 2008]. RTD phenotype is associated not only with mutations in *REN* but also with mutations in other components of RAS. Clinical manifestations of RTD highlight the crucial role of the renin and RAS in human kidney development [Gribouval et al. 2005; Lacoste et al. 2006].

Familial juvenile hyperuricemic nephropathy type 2 (FJHN2)

Patients from three unrelated families with the autosomal dominant inheritance of chronic progressive kidney failure with phenotype similar to FJHN1/MCKD2 were mapped on chromosome 1q41 **[see results, paper 4. 1; Hodanova et al. 2005 and paper 4. 4; Zivna et al. 2009]** and were recently assigned as FJHN2. The FJHN2 phenotype segregates with heterozygous mutations in the signal sequence of renin, single leucine deletion ($\Delta L16^{REN}$), the amino acid exchange leucine to arginin ($L16R^{REN}$) and the amino acid exchange cystein to arginin ($C20R^{REN}$) [Fig. 4]. Clinical and biochemical findings of FJHN2 are early anemia, hypouricosuric hyperuricemia, small sized kidney with no evidence of cysts formation, progressive kidney failure resulting in end-stage renal failure between ages 43 - 68. Family BE1 [Hodanova et al. 2005] was in next paper assigned as

family A [Zivna et al. 2009] and is further referred as family A ($\Delta L16^{REN}$). Patients from family A have low excretion of urinary UMOD, caused by strongly reduced expression of UMOD in tubular cells **[see results, paper 4. 1; Hodanova et al. 2005]**. Urinary UMOD excretion was not measured in other families with mutation in *REN*. Kidney biopsy revealed focal tubular atrophy and dystrophy, focal and segmental glomerular sclerosis, and interstitial fibrosis. Renin expression was either strongly reduced or absent in JGA and surrounding tubules compared to age matched controls. Interestingly, expression of renin and prorenin was detected inside the wall of small size renal vessels. The ectopic expression of renin and prorenin in kidney vessel wall was more prominent in adult than in patients in an early stage of the disease. Renin was not detected immunologicaly in the biopsy specimen from family C ($L16R^{REN}$), but renin mRNA was strongly expressed in sparse cells regarded as pericytes, along peritubular capillary without positivity in JGA **[see results, paper 4. 4; Zivna et al. 2009]**. In addition to decreased renin expression in JGA and ectopic renin and prorenin expression in kidney patients from family A revealed reduced kidney angiotensinogen, angiotensin II, and (pro)renin receptor. All of these RAS components were localized in the similar kidney segments compared to control kidneys. The reduction level of respective signals correlated with stage of the disease **[see results, paper 4. 4; Zivna et al. 2009 and supplement of paper 4. 4]**.

Over 20 mutations in signal sequences of proteins are associated with various diseases. More than half of the identified mutations are shown to impair the signal peptide function and thus influence protein transportation [Jarjanazi et al. 2008]. Proteins entering the secretory pathway as well as membrane proteins contain on their N-terminal part signal sequence. Signal sequence is essential for nascent polypeptide chain to target and translocate across the membrane of endoplasmic reticulum (ER). In the simplified view of protein translocation the first step is recognition and interaction of signal sequence with the

signal recognition particle (SRP). Nascent polypeptide chain is through SRP directed to the ER membrane. SRP dissociates from the nascent polypeptide chain upon interaction with SRP receptor which is embedded in the membrane of ER. Both SRP and SRP receptor are GTPases which control specific docking to the translocation machinery. Once the C-terminus of the protein has passed through the ER membrane into the ER lumen the signal sequence is cleaved from nascent polypeptide chain by signal peptidase and rapidly degraded to amino acids by other proteases known as signal peptide peptidase. Although signal sequences of proteins have widely variable amino acid sequence they all are recognized by SRP based on hydrophobic interaction. Three typical structural motifs are responsible for proper function of signal sequence. N-terminal hydrophilic region, hydrophobic core which is critical for cotranslational processing, and polar C-terminal amino acids region contains the signal sequence cleavage site.

Mutations in signal sequence of renin which were identified in patients with FJHN2 affected translocation of nascent preprorenin into lumen ER. The mutant variant $\Delta L16^{REN}$ reduced translocation ability, significantly impaired prorenin and renin biosynthesis, secretion and activity. Cells stably producing $\Delta L16^{REN}$ had reduced growth rate, activated ER stress, and unfolded protein response. Mutant variant $L16R^{REN}$ was not translocated at all and renin granule-like structures were detected in cytosol. Mutant variant $C20R^{REN}$ was not translocated, similarly to variant $L16R^{REN}$, but no granule-like structures were detected in cytosol. Instead, diffuse accumulation of unprocessed protein was found in the cytosol **[see results, paper 4. 5; submitted manuscript]**. Untranslocated preprorenin stay in nascent form without glycosylation, further processing and secretion.

The mechanism responsible for damage of renin producing cells in patients with renin signal sequence mutation may depend on the type of mutation. Molecular markers of ER stress can be identified in cells stably transfected with $\Delta L16^{REN}$ renin variant. Chronic

ER stress can lead to site-specific attenuation of renin biosynthesis and RAS dysregulation. Reduced viability of juxtaglomerular cells and limited renin availability then affect renal development, intrarenal RAS homeostasis, and kidney autoregulation resulting in anemia, reduced glomerular filtration rate, and hyperuricemia. Over time, accelerated apoptosis in juxtaglomerular cells results, and, similar to mice with ablated juxtaglomerular cells [Pentz et al. 2004], in nephron loss and progressive kidney failure. Proposed pathogenetic cascade correlates with the clinical picture of slowly advancing kidney failure, progressive tubulointerstitial nephropathy, secondary, focal and segmental glomerular sclerosis. Described pathogenetic partial steps are resulting in early-onset hyperuricemia, anemia, and progressive kidney failure.

For clinical, biochemical, immunohistochemical details as well as for molecular characterization of the $\Delta L16^{REN}$ and $L16R^{REN}$ renin variant **[see results, paper 4. 4; Zivna et al. 2009 and supplement of paper 4. 4]** and $C20R^{REN}$ renin variant **[see results, paper 4. 5; submitted manuscript]**.

1. 8 Summary and future research

In recent years the pathological and clinical approach to the diagnosis of FJHN and MCKD has been shown to be insufficient to distinguished different molecular mechanisms responsible for clinical signs and symptoms. Using positional cloning approach we identified and described mutations in two genes with very different kidney localization and biological function. It implies that future research must be aimed at further dissection of genetic heterogeneity of FJHN by genetic mapping approach. This will be greatly facilitated within next couple of years by availability and application of novel sequencing technologies which will enable massive resequencing of candidate loci identified in previous linkage studies and also by whole-exome and later also whole-genome sequencing

studies in affected individuals. This approach will inevitably lead to definition of all of FJHN causing genes and together with subsequent targeted molecular studies it will suggest key mechanisms and pathways involved in pathogenesis of clinical and biochemical symptoms. This may open an avenue to early presymptomatic diagnosis in affected individuals and families, development of targeted treatments and early intervention reducing and/or preventing development of kidney disease.

2 References

Auranen, M., Ala-Mello, S., Turunen, J. A. and Jarvela, I. (2001). Further evidence for linkage of autosomal-dominant medullary cystic kidney disease on chromosome 1q21. Kidney Int 60(4): 1225-32.

Bader, M. (2007). The second life of the (pro)renin receptor. J Renin Angiotensin Aldosterone Syst 8(4): 205-8.

Bachmann, S., Mutig, K., Bates, J., Welker, P., Geist, B., Gross, V., Luft, F. C., Alenina, N., Bader, M., Thiele, B. J., Prasadan, K., Raffi, H. S. and Kumar, S. (2005). Renal effects of Tamm-Horsfall protein (uromodulin) deficiency in mice. Am J Physiol Renal Physiol 288(3): F559-67.

Bellanne-Chantelot, C., Chauveau, D., Gautier, J. F., Dubois-Laforgue, D., Clauin, S., Beaufils, S., Wilhelm, J. M., Boitard, C., Noel, L. H., Velho, G. and Timsit, J. (2004). Clinical spectrum associated with hepatocyte nuclear factor-1beta mutations. Ann Intern Med 140(7): 510-7.

Benetti, E., Caridi, G., Vella, M. D., Rampoldi, L., Ghiggeri, G. M., Artifoni, L. and Murer, L. (2009). Immature renal structures associated with a novel UMOD sequence variant. Am J Kidney Dis 53(2): 327-31.

Bernascone, I., Vavassori, S., Di Pentima, A., Santambrogio, S., Lamorte, G., Amoroso, A., Scolari, F., Ghiggeri, G. M., Casari, G., Polishchuk, R. and Rampoldi, L. (2006). Defective intracellular trafficking of uromodulin mutant isoforms. Traffic 7(11): 1567-79.

Bingham, C., Ellard, S., van't Hoff, W. G., Simmonds, H. A., Marinaki, A. M., Badman, M. K., Winocour, P. H., Stride, A., Lockwood, C. R., Nicholls, A. J., Owen, K. R., Spyer, G., Pearson, E. R. and Hattersley, A. T. (2003). Atypical familial juvenile hyperuricemic nephropathy associated with a hepatocyte nuclear factor-1beta gene mutation. Kidney Int 63(5): 1645-51.

Bingham, C. and Hattersley, A. T. (2004). Renal cysts and diabetes syndrome resulting from mutations in hepatocyte nuclear factor-1beta. Nephrol Dial Transplant 19(11): 2703-8.

Bleyer, A. J., Hart, T. C., Shihabi, Z., Robins, V. and Hoyer, J. R. (2004). Mutations in the uromodulin gene decrease urinary excretion of Tamm-Horsfall protein. Kidney Int 66(3): 974-7.

Bleyer, A. J., Trachtman, H., Sandhu, J., Gorry, M. C. and Hart, T. C. (2003). Renal manifestations of a mutation in the uromodulin (Tamm Horsfall protein) gene. Am J Kidney Dis 42(2): E20-6.

Border, W. A. and Noble, N. A. (1998). Interactions of transforming growth factor-beta and angiotensin II in renal fibrosis. Hypertension 31(1 Pt 2): 181-8.

Brown, M. J. (2007). Renin: friend or foe? Heart 93(9): 1026-33.

Cameron, J. S., Moro, F. and Simmonds, H. A. (1993). Gout, uric acid and purine metabolism in paediatric nephrology. Pediatr Nephrol 7(1): 105-18.

Cameron, J. S. and Simmonds, H. A. (2005). Hereditary hyperuricemia and renal disease. Semin Nephrol 25(1): 9-18.

Campbell, D. J. (2008). Critical review of prorenin and (pro)renin receptor research. Hypertension 51(5): 1259-64.

Cavallone, D., Malagolini, N. and Serafini-Cessi, F. (2001). Mechanism of release of urinary Tamm-Horsfall glycoprotein from the kidney GPI-anchored counterpart. Biochem Biophys Res Commun 280(1): 110-4.

Coffinier, C., Barra, J., Babinet, C. and Yaniv, M. (1999). Expression of the vHNF1/HNF1beta homeoprotein gene during mouse organogenesis. Mech Dev 89(1-2): 211-3.

Cohn, D. H., Shohat, T., Yahav, M., Ilan, T., Rechavi, G., King, L. and Shohat, M. (2000). A locus for an autosomal dominant form of progressive renal failure and hypertension at chromosome 1q21. Am J Hum Genet 67(3): 647-51.

Dahan, K., Devuyst, O., Smaers, M., Vertommen, D., Loute, G., Poux, J. M., Viron, B., Jacquot, C., Gagnadoux, M. F., Chauveau, D., Buchler, M., Cochat, P., Cosyns, J. P., Mougenot, B., Rider, M. H., Antignac, C., Verellen-Dumoulin, C. and Pirson, Y. (2003). A cluster of mutations in the UMOD gene causes familial juvenile hyperuricemic nephropathy with abnormal expression of uromodulin. J Am Soc Nephrol 14(11): 2883-93.

Dahan, K., Fuchshuber, A., Adamis, S., Smaers, M., Kroiss, S., Loute, G., Cosyns, J. P., Hildebrandt, F., Verellen-Dumoulin, C. and Pirson, Y. (2001). Familial juvenile hyperuricemic nephropathy and autosomal dominant medullary cystic kidney disease type 2: two facets of the same disease? J Am Soc Nephrol 12(11): 2348-57.

Danser, A. H., Derkx, F. H., Schalekamp, M. A., Hense, H. W., Riegger, G. A. and Schunkert, H. (1998). Determinants of interindividual variation of renin and prorenin concentrations: evidence for a sexual dimorphism of (pro)renin levels in humans. J Hypertens 16(6): 853-62.

Devuyst, O., Dahan, K. and Pirson, Y. (2005). Tamm-Horsfall protein or uromodulin: new ideas about an old molecule. Nephrol Dial Transplant 20(7): 1290-4.

Duncan, H. and Dixon, A. S. (1960). Gout, familial hypericaemia, and renal disease. Q J Med 29: 127-35.

Edghill, E. L., Oram, R. A., Owens, M., Stals, K. L., Harries, L. W., Hattersley, A. T., Ellard, S. and Bingham, C. (2008). Hepatocyte nuclear factor-1beta gene deletions--a common cause of renal disease. Nephrol Dial Transplant 23(2): 627-35.

Enomoto, A., Kimura, H., Chairoungdua, A., Shigeta, Y., Jutabha, P., Cha, S. H., Hosoyamada, M., Takeda, M., Sekine, T., Igarashi, T., Matsuo, H., Kikuchi, Y., Oda, T., Ichida, K., Hosoya, T., Shimokata, K., Niwa, T., Kanai, Y. and Endou, H. (2002). Molecular identification of a renal urate anion exchanger that regulates blood urate levels. Nature 417(6887): 447-52.

Fuchshuber, A., Deltas, C. C., Berthold, S., Stavrou, C., Vollmer, M., Burton, C., Feest, T., Krieter, D., Gal, A., Brandis, M., Pierides, A. and Hildebrandt, F. (1998). Autosomal dominant medullary cystic kidney disease: evidence of gene locus heterogeneity. Nephrol Dial Transplant 13(8): 1955-7.

Fuchshuber, A., Kroiss, S., Karle, S., Berthold, S., Huck, K., Burton, C., Rahman, N., Koptides, M., Deltas, C., Otto, E., Ruschendorf, F., Feest, T. and Hildebrandt, F. (2001). Refinement of the gene locus for autosomal dominant medullary cystic kidney disease type 1 (MCKD1) and construction of a physical and partial transcriptional map of the region. Genomics 72(3): 278-84.

Gaffo, A. L. and Saag, K. G. (2008). Management of hyperuricemia and gout in CKD. Am J Kidney Dis 52(5): 994-1009.

Gardner, K. D., Jr. (1971). Evolution of clinical signs in adult-onset cystic disease of the renal medulla. Ann Intern Med 74(1): 47-54.

Gresh, L., Fischer, E., Reimann, A., Tanguy, M., Garbay, S., Shao, X., Hiesberger, T., Fiette, L., Igarashi, P., Yaniv, M. and Pontoglio, M. (2004). A transcriptional network in polycystic kidney disease. Embo J 23(7): 1657-68.

Gribouval, O., Gonzales, M., Neuhaus, T., Aziza, J., Bieth, E., Laurent, N., Bouton, J. M., Feuillet, F., Makni, S., Ben Amar, H., Laube, G., Delezoide, A. L., Bouvier, R., Dijoud, F., Ollagnon-Roman, E., Roume, J., Joubert, M., Antignac, C. and Gubler, M. C. (2005). Mutations in genes in the renin-angiotensin system are associated with autosomal recessive renal tubular dysgenesis. Nat Genet 37(9): 964-8.

Hart, T. C., Gorry, M. C., Hart, P. S., Woodard, A. S., Shihabi, Z., Sandhu, J., Shirts, B., Xu, L., Zhu, H., Barmada, M. M. and Bleyer, A. J. (2002). Mutations of the UMOD gene

are responsible for medullary cystic kidney disease 2 and familial juvenile hyperuricaemic nephropathy. J Med Genet 39(12): 882-92.

Hateboer, N., Gumbs, C., Teare, M. D., Coles, G. A., Griffiths, D., Ravine, D., Futreal, P. A. and Rahman, N. (2001). Confirmation of a gene locus for medullary cystic kidney disease (MCKD2) on chromosome 16p12. Kidney Int 60(4): 1233-9.

Hodanova, Kalbacova, M., Stiburkova, B., Majewski, J., Marinaki, A., Simmonds, A., Matthijs, G., Fryns, J., Ott, J. and Kmoch, S. (2003). Familial juvenile hyperuricaemic nephropathy (FJHN): Linkage analysis in 17 families, transcriptional characterization of the FJHN critical region on chromosome 16p11.2 and the analyzes of uromodulin and other candidate genes. Am J Hum Genet 73: 2324.

Hodanova, K., Majewski, J., Kublova, M., Vyletal, P., Kalbacova, M., Stiburkova, B., Hulkova, H., Chagnon, Y. C., Lanouette, C. M., Marinaki, A., Fryns, J. P., Venkat-Raman, G. and Kmoch, S. (2005). Mapping of a new candidate locus for uromodulin-associated kidney disease (UAKD) to chromosome 1q41. Kidney Int 68(4): 1472-82.

Horikawa, Y., Iwasaki, N., Hara, M., Furuta, H., Hinokio, Y., Cockburn, B. N., Lindner, T., Yamagata, K., Ogata, M., Tomonaga, O., Kuroki, H., Kasahara, T., Iwamoto, Y. and Bell, G. I. (1997). Mutation in hepatocyte nuclear factor-1 beta gene (TCF2) associated with MODY. Nat Genet 17(4): 384-5.

Huang, Y., Noble, N. A., Zhang, J., Xu, C. and Border, W. A. (2007). Renin-stimulated TGF-beta1 expression is regulated by a mitogen-activated protein kinase in mesangial cells. Kidney Int 72(1): 45-52.

Huang, Y., Wongamorntham, S., Kasting, J., McQuillan, D., Owens, R. T., Yu, L., Noble, N. A. and Border, W. (2006). Renin increases mesangial cell transforming growth factor-beta1 and matrix proteins through receptor-mediated, angiotensin II-independent mechanisms. Kidney Int 69(1): 105-13.

Chamberlin, B. C., Hagge, W. W. and Stickler, G. B. (1977). Juvenile nephronophthisis and medullary cystic disease. Mayo Clin Proc 52(8): 485-91.

Choi, S. W., Ryu, O. H., Choi, S. J., Song, I. S., Bleyer, A. J. and Hart, T. C. (2005). Mutant tamm-horsfall glycoprotein accumulation in endoplasmic reticulum induces apoptosis reversed by colchicine and sodium 4-phenylbutyrate. J Am Soc Nephrol 16(10): 3006-14.

Christodoulou, K., Tsingis, M., Stavrou, C., Eleftheriou, A., Papapavlou, P., Patsalis, P. C., Ioannou, P., Pierides, A. and Constantinou Deltas, C. (1998). Chromosome 1 localization of a gene for autosomal dominant medullary cystic kidney disease. Hum Mol Genet 7(5): 905-11.

Ichida, K., Hosoyamada, M., Hisatome, I., Enomoto, A., Hikita, M., Endou, H. and Hosoya, T. (2004). Clinical and molecular analysis of patients with renal hypouricemia in Japan-influence of URAT1 gene on urinary urate excretion. J Am Soc Nephrol 15(1): 164-73.

Ichihara, A., Sakoda, M., Kurauchi-Mito, A., Kaneshiro, Y. and Itoh, H. (2009). Renin, prorenin and the kidney: a new chapter in an old saga. J Nephrol 22(3): 306-11.

Imai, T., Miyazaki, H., Hirose, S., Hori, H., Hayashi, T., Kageyama, R., Ohkubo, H., Nakanishi, S. and Murakami, K. (1983). Cloning and sequence analysis of cDNA for human renin precursor. Proc Natl Acad Sci U S A 80(24): 7405-9.

Jan Danser, A. H. and Saris, J. J. (2002). Prorenin uptake in the heart: a prerequisite for local angiotensin generation? J Mol Cell Cardiol 34(11): 1463-72.

Jarjanazi, H., Savas, S., Pabalan, N., Dennis, J. W. and Ozcelik, H. (2008). Biological implications of SNPs in signal peptide domains of human proteins. Proteins 70(2): 394-403.

Jovine, L., Darie, C. C., Litscher, E. S. and Wassarman, P. M. (2005). Zona pellucida domain proteins. Annu Rev Biochem 74: 83-114.

Kamatani, N., Moritani, M., Yamanaka, H., Takeuchi, F., Hosoya, T. and Itakura, M. (2000). Localization of a gene for familial juvenile hyperuricemic nephropathy causing underexcretion-type gout to 16p12 by genome-wide linkage analysis of a large family. Arthritis Rheum 43(4): 925-9.

Kaneshiro, Y., Ichihara, A., Sakoda, M., Takemitsu, T., Nabi, A. H., Uddin, M. N., Nakagawa, T., Nishiyama, A., Suzuki, F., Inagami, T. and Itoh, H. (2007). Slowly progressive, angiotensin II-independent glomerulosclerosis in human (pro)renin receptor-transgenic rats. J Am Soc Nephrol 18(6): 1789-95.

Kobori, H., Nangaku, M., Navar, L. G. and Nishiyama, A. (2007). The intrarenal renin-angiotensin system: from physiology to the pathobiology of hypertension and kidney disease. Pharmacol Rev 59(3): 251-87.

Kottgen, A., Glazer, N. L., Dehghan, A., Hwang, S. J., Katz, R., Li, M., Yang, Q., Gudnason, V., Launer, L. J., Harris, T. B., Smith, A. V., Arking, D. E., Astor, B. C., Boerwinkle, E., Ehret, G. B., Ruczinski, I., Scharpf, R. B., Ida Chen, Y. D., de Boer, I. H., Haritunians, T., Lumley, T., Sarnak, M., Siscovick, D., Benjamin, E. J., Levy, D., Upadhyay, A., Aulchenko, Y. S., Hofman, A., Rivadeneira, F., Uitterlinden, A. G., van Duijn, C. M., Chasman, D. I., Pare, G., Ridker, P. M., Kao, W. H., Witteman, J. C., Coresh, J., Shlipak, M. G. and Fox, C. S. (2009). Multiple loci associated with indices of renal function and chronic kidney disease. Nat Genet.

Kottgen, A., Hwang, S. J., Larson, M. G., Eyk, J. E., Fu, Q., Benjamin, E. J., Dehghan, A., Glazer, N. L., Kao, W. H., Harris, T. B., Gudnason, V., Shlipak, M. G., Yang, Q., Coresh, J., Levy, D. and Fox, C. S. (2009). Uromodulin Levels Associate with a Common UMOD Variant and Risk for Incident CKD. J Am Soc Nephrol.

Kovacs, G., Peti-Peterdi, J., Rosivall, L. and Bell, P. D. (2002). Angiotensin II directly stimulates macula densa Na-2Cl-K cotransport via apical AT(1) receptors. Am J Physiol Renal Physiol 282(2): F301-6.

Kudo, E., Kamatani, N., Tezuka, O., Taniguchi, A., Yamanaka, H., Yabe, S., Osabe, D., Shinohara, S., Nomura, K., Segawa, M., Miyamoto, T., Moritani, M., Kunika, K. and Itakura, M. (2004). Familial juvenile hyperuricemic nephropathy: detection of mutations in the uromodulin gene in five Japanese families. Kidney Int 65(5): 1589-97.

Kurtz, A. and Wagner, C. (1999). Cellular control of renin secretion. J Exp Biol 202(Pt 3): 219-25.

Lacoste, M., Cai, Y., Guicharnaud, L., Mounier, F., Dumez, Y., Bouvier, R., Dijoud, F., Gonzales, M., Chatten, J., Delezoide, A. L., Daniel, L., Joubert, M., Laurent, N., Aziza, J., Sellami, T., Amar, H. B., Jarnet, C., Frances, A. M., Daikha-Dahmane, F., Coulomb, A., Neuhaus, T. J., Foliguet, B., Chenal, P., Marcorelles, P., Gasc, J. M., Corvol, P. and Gubler, M. C. (2006). Renal tubular dysgenesis, a not uncommon autosomal recessive disorder leading to oligohydramnios: Role of the Renin-Angiotensin system. J Am Soc Nephrol 17(8): 2253-63.

Lhotta, K., Gehringer, A., Jennings, P., Kronenberg, F., Brezinka, C., Andersone, I. and Strazdins, V. (2009). Familial juvenile hyperuricemic nephropathy: report on a new mutation and a pregnancy. Clin Nephrol 71(1): 80-3.

Lhotta, K., Gruber, J., Sgonc, R., Fend, F. and Konig, P. (1998). Apoptosis of tubular epithelial cells in familial juvenile gouty nephropathy. Nephron 79(3): 340-4.

Malagolini, N., Cavallone, D. and Serafini-Cessi, F. (1997). Intracellular transport, cell-surface exposure and release of recombinant Tamm-Horsfall glycoprotein. Kidney Int 52(5): 1340-50.

Masuo, K., Kawaguchi, H., Mikami, H., Ogihara, T. and Tuck, M. L. (2003). Serum uric acid and plasma norepinephrine concentrations predict subsequent weight gain and blood pressure elevation. Hypertension 42(4): 474-80.

Mattey, M. and Naftalin, L. (1992). Mechanoelectrical transduction, ion movement and water stasis in uromodulin. Experientia 48(10): 975-80.

McCarty, D. J. and Koopman, W. J. (1989). Arthritis and allied conditions : a textbook of rheumatology. Philadelphia, Lea & Febiger.

Moe, O. W., Ujiie, K., Star, R. A., Miller, R. T., Widell, J., Alpern, R. J. and Henrich, W. L. (1993). Renin expression in renal proximal tubule. J Clin Invest 91(3): 774-9.

Mochizuki, T., Wu, G., Hayashi, T., Xenophontos, S. L., Veldhuisen, B., Saris, J. J., Reynolds, D. M., Cai, Y., Gabow, P. A., Pierides, A., Kimberling, W. J., Breuning, M. H., Deltas, C. C., Peters, D. J. and Somlo, S. (1996). PKD2, a gene for polycystic kidney disease that encodes an integral membrane protein. Science 272(5266): 1339-42.

Monne, M., Han, L., Schwend, T., Burendahl, S. and Jovine, L. (2008). Crystal structure of the ZP-N domain of ZP3 reveals the core fold of animal egg coats. Nature 456(7222): 653-7.

Moravski, C. J., Kelly, D. J., Cooper, M. E., Gilbert, R. E., Bertram, J. F., Shahinfar, S., Skinner, S. L. and Wilkinson-Berka, J. L. (2000). Retinal neovascularization is prevented by blockade of the renin-angiotensin system. Hypertension 36(6): 1099-104.

Moravski, C. J., Skinner, S. L., Stubbs, A. J., Sarlos, S., Kelly, D. J., Cooper, M. E., Gilbert, R. E. and Wilkinson-Berka, J. L. (2003). The renin-angiotensin system influences ocular endothelial cell proliferation in diabetes: transgenic and interventional studies. Am J Pathol 162(1): 151-60.

Muchmore, A. V. and Decker, J. M. (1985). Uromodulin: a unique 85-kilodalton immunosuppressive glycoprotein isolated from urine of pregnant women. Science 229(4712): 479-81.

Muchmore, A. V. and Decker, J. M. (1986). Uromodulin. An immunosuppressive 85-kilodalton glycoprotein isolated from human pregnancy urine is a high affinity ligand for recombinant interleukin 1 alpha. J Biol Chem 261(29): 13404-7.

Navar, L. G. and Nishiyama, A. (2004). Why are angiotensin concentrations so high in the kidney? Curr Opin Nephrol Hypertens 13(1): 107-15.

Nguyen, G. (2005). The (pro)renin receptor: biochemistry and potential significance. J Renin Angiotensin Aldosterone Syst 6(3): 166-7.

Nguyen, G. (2006). Renin/prorenin receptors. Kidney Int 69(9): 1503-6.

Nguyen, G. (2007). The (pro)renin receptor: pathophysiological roles in cardiovascular and renal pathology. Curr Opin Nephrol Hypertens 16(2): 129-33.

Nguyen, G. and Danser, A. H. (2008). Prorenin and (pro)renin receptor: a review of available data from in vitro studies and experimental models in rodents. Exp Physiol 93(5): 557-63.

Nguyen, G., Delarue, F., Burckle, C., Bouzhir, L., Giller, T. and Sraer, J. D. (2002). Pivotal role of the renin/prorenin receptor in angiotensin II production and cellular responses to renin. J Clin Invest 109(11): 1417-27.

Paul, M., Poyan Mehr, A. and Kreutz, R. (2006). Physiology of local renin-angiotensin systems. Physiol Rev 86(3): 747-803.

Pavelka, K., Jr., Sebesta, I., Blovska, J., Maly, J. and Chadimova, M. (1996). [Familial juvenile gouty nephropathy]. Cas Lek Cesk 135(20): 668-71.

Pennica, D., Kohr, W. J., Kuang, W. J., Glaister, D., Aggarwal, B. B., Chen, E. Y. and Goeddel, D. V. (1987). Identification of human uromodulin as the Tamm-Horsfall urinary glycoprotein. Science 236(4797): 83-8.

Pentz, E. S., Moyano, M. A., Thornhill, B. A., Sequeira Lopez, M. L. and Gomez, R. A. (2004). Ablation of renin-expressing juxtaglomerular cells results in a distinct kidney phenotype. Am J Physiol Regul Integr Comp Physiol 286(3): R474-83.

Persson, P. B. (2003). Renin: origin, secretion and synthesis. J Physiol 552(Pt 3): 667-71.

Persson, P. B., Skalweit, A., Mrowka, R. and Thiele, B. J. (2003). Control of renin synthesis. Am J Physiol Regul Integr Comp Physiol 285(3): R491-7.

Peti-Peterdi, J. and Bell, P. D. (1998). Regulation of macula densa Na:H exchange by angiotensin II. Kidney Int 54(6): 2021-8.

Pratt, R. E., Carleton, J. E., Richie, J. P., Heusser, C. and Dzau, V. J. (1987). Human renin biosynthesis and secretion in normal and ischemic kidneys. Proc Natl Acad Sci U S A 84(22): 7837-40.

Prieto, C. and Berrocal, T. (1994). Ultrasound imaging and colour Doppler studies in familial nephropathy associated with hyperuricemia (FNAH). The Spanish Group for the Study of FNAH. Adv Exp Med Biol 370: 65-8.

Puig, J. G., Miranda, M. E., Mateos, F. A., Picazo, M. L., Jimenez, M. L., Calvin, T. S. and Gil, A. A. (1993). Hereditary nephropathy associated with hyperuricemia and gout. Arch Intern Med 153(3): 357-65.

Rampoldi, L., Caridi, G., Santon, D., Boaretto, F., Bernascone, I., Lamorte, G., Tardanico, R., Dagnino, M., Colussi, G., Scolari, F., Ghiggeri, G. M., Amoroso, A. and Casari, G. (2003). Allelism of MCKD, FJHN and GCKD caused by impairment of uromodulin export dynamics. Hum Mol Genet 12(24): 3369-84.

Ramser, J., Abidi, F. E., Burckle, C. A., Lenski, C., Toriello, H., Wen, G., Lubs, H. A., Engert, S., Stevenson, R. E., Meindl, A., Schwartz, C. E. and Nguyen, G. (2005). A unique exonic splice enhancer mutation in a family with X-linked mental retardation and epilepsy points to a novel role of the renin receptor. Hum Mol Genet 14(8): 1019-27.

Riches, P. L., Wright, A. F. and Ralston, S. H. (2009). Recent insights into the pathogenesis of hyperuricaemia and gout. Hum Mol Genet 18(R2): R177-84.

Richmond, J. M., Kincaid-Smith, P., Whitworth, J. A. and Becker, G. J. (1981). Familial urate nephropathy. Clin Nephrol 16(4): 163-8.

Rohrwasser, A., Morgan, T., Dillon, H. F., Zhao, L., Callaway, C. W., Hillas, E., Zhang, S., Cheng, T., Inagami, T., Ward, K., Terreros, D. A. and Lalouel, J. M. (1999). Elements of a paracrine tubular renin-angiotensin system along the entire nephron. Hypertension 34(6): 1265-74.

Saeki, A., Hosoya, T., Okabe, H., Saji, M., Tabe, A., Ichida, K., Itoh, K., Joh, K. and Sakai, O. (1995). Newly discovered familial juvenile gouty nephropathy in a Japanese family. Nephron 70(3): 359-66.

Scolari, F., Puzzer, D., Amoroso, A., Caridi, G., Ghiggeri, G. M., Maiorca, R., Aridon, P., De Fusco, M., Ballabio, A. and Casari, G. (1999). Identification of a new locus for medullary cystic disease, on chromosome 16p12. Am J Hum Genet 64(6): 1655-60.

Sebesta, I., Krijt, J., Pavelka, K., Maly, J., Simmonds, H. A. and McBride, M. B. (1994). Familial juvenile hyperuricaemic nephropathy in adolescents. Adv Exp Med Biol 370: 73-6.

Serafini-Cessi, F., Malagolini, N. and Cavallone, D. (2003). Tamm-Horsfall glycoprotein: biology and clinical relevance. Am J Kidney Dis 42(4): 658-76.

Schaeffer, C., Santambrogio, S., Perucca, S., Casari, G. and Rampoldi, L. (2009). Analysis of uromodulin polymerization provides new insights into the mechanisms regulating ZP domain-mediated protein assembly. Mol Biol Cell 20(2): 589-99.

Schutz, S., Le Moullec, J. M., Corvol, P. and Gasc, J. M. (1996). Early expression of all the components of the renin-angiotensin-system in human development. Am J Pathol 149(6): 2067-79.

Schweda, F., Friis, U., Wagner, C., Skott, O. and Kurtz, A. (2007). Renin release. Physiology (Bethesda) 22: 310-9.

Simmonds, H. A., Warren, D. J., Cameron, J. S., Potter, C. F. and Farebrother, D. A. (1980). Familial gout and renal failure in young women. Clin Nephrol 14(4): 176-82.

Stacey, J. M., Turner, J. J., Harding, B., Nesbit, M. A., Kotanko, P., Lhotta, K., Puig, J. G., Torres, R. J. and Thakker, R. V. (2003). Genetic mapping studies of familial juvenile hyperuricemic nephropathy on chromosome 16p11-p13. J Clin Endocrinol Metab 88(1): 464-70.

Stenflo, J., Stenberg, Y. and Muranyi, A. (2000). Calcium-binding EGF-like modules in coagulation proteinases: function of the calcium ion in module interactions. Biochim Biophys Acta 1477(1-2): 51-63.

Stiburkova, B., Majewski, J., Hodanova, K., Ondrova, L., Jerabkova, M., Zikanova, M., Vylet'al, P., Sebesta, I., Marinaki, A., Simmonds, A., Matthijs, G., Fryns, J. P., Torres, R., Puig, J. G., Ott, J. and Kmoch, S. (2003). Familial juvenile hyperuricaemic nephropathy (FJHN): linkage analysis in 15 families, physical and transcriptional characterisation of the FJHN critical region on chromosome 16p11.2 and the analysis of seven candidate genes. Eur J Hum Genet 11(2): 145-54.

Stiburkova, B., Majewski, J., Sebesta, I., Zhang, W., Ott, J. and Kmoch, S. (2000). Familial juvenile hyperuricemic nephropathy: localization of the gene on chromosome 16p11.2-and evidence for genetic heterogeneity. Am J Hum Genet 66(6): 1989-94.

Swenson, R. S., Kempson, R. L. and Friedland, G. W. (1974). Cystic disease of the renal medulla in the elderly. Jama 228(11): 1401-4.

Tamm, I. and Horsfall, F. L., Jr. (1950). Characterization and separation of an inhibitor of viral hemagglutination present in urine. Proc Soc Exp Biol Med 74(1): 106-8.

Thornley, C., Dawnay, A. and Cattell, W. R. (1985). Human Tamm-Horsfall glycoprotein: urinary and plasma levels in normal subjects and patients with renal disease determined by a fully validated radioimmunoassay. Clin Sci (Lond) 68(5): 529-35.

Tigerstedt, R. and Bergman, P. (1898). Niere und kreislauf. Scand Arch Physiol. 8.

Tinschert, S., Ruf, N., Bernascone, I., Sacherer, K., Lamorte, G., Neumayer, H. H., Nurnberg, P., Luft, F. C. and Rampoldi, L. (2004). Functional consequences of a novel uromodulin mutation in a family with familial juvenile hyperuricaemic nephropathy. Nephrol Dial Transplant 19(12): 3150-4.

Turner, J. J., Stacey, J. M., Harding, B., Kotanko, P., Lhotta, K., Puig, J. G., Roberts, I., Torres, R. J. and Thakker, R. V. (2003). UROMODULIN mutations cause familial juvenile hyperuricemic nephropathy. J Clin Endocrinol Metab 88(3): 1398-401.

van den Eijnden, M. M., Saris, J. J., de Bruin, R. J., de Wit, E., Sluiter, W., Reudelhuber, T. L., Schalekamp, M. A., Derkx, F. H. and Danser, A. H. (2001). Prorenin accumulation and activation in human endothelial cells: importance of mannose 6-phosphate receptors. Arterioscler Thromb Vasc Biol 21(6): 911-6.

van Rooijen, J. J., Voskamp, A. F., Kamerling, J. P. and Vliegenthart, J. F. (1999). Glycosylation sites and site-specific glycosylation in human Tamm-Horsfall glycoprotein. Glycobiology 9(1): 21-30.

Villard, E., Lalau, J. D., van Hooft, I. S., Derkx, F. H., Houot, A. M., Pinet, F., Corvol, P. and Soubrier, F. (1994). A mutant renin gene in familial elevation of prorenin. J Biol Chem 269(48): 30307-12.

Vylet'al, P., Kublova, M., Kalbacova, M., Hodanova, K., Baresova, V., Stiburkova, B., Sikora, J., Hulkova, H., Zivny, J., Majewski, J., Simmonds, A., Fryns, J. P., Venkat-Raman, G., Elleder, M. and Kmoch, S. (2006). Alterations of uromodulin biology: a common denominator of the genetically heterogeneous FJHN/MCKD syndrome. Kidney Int 70(6): 1155-69.

Wallace, K. L., Riedel, A. A., Joseph-Ridge, N. and Wortmann, R. (2004). Increasing prevalence of gout and hyperuricemia over 10 years among older adults in a managed care population. J Rheumatol 31(8): 1582-7.

Walter, P. and Johnson, A. E. (1994). Signal sequence recognition and protein targeting to the endoplasmic reticulum membrane. Annu Rev Cell Biol 10: 87-119.

Ward, C. J., Hogan, M. C., Rossetti, S., Walker, D., Sneddon, T., Wang, X., Kubly, V., Cunningham, J. M., Bacallao, R., Ishibashi, M., Milliner, D. S., Torres, V. E. and Harris, P. C. (2002). The gene mutated in autosomal recessive polycystic kidney disease encodes a large, receptor-like protein. Nat Genet 30(3): 259-69.

Wilkinson-Berka, J. L. (2008). Prorenin and the (pro)renin receptor in ocular pathology. Am J Pathol 173(6): 1591-4.

Williams, S. E., Reed, A. A., Galvanovskis, J., Antignac, C., Goodship, T., Karet, F. E., Kotanko, P., Lhotta, K., Moriniere, V., Williams, P., Wong, W., Rorsman, P. and Thakker, R. V. (2009). Uromodulin mutations causing familial juvenile hyperuricaemic nephropathy lead to protein maturation defects and retention in the endoplasmic reticulum. Hum Mol Genet 18(16): 2963-74.

Wolf, M. T., Beck, B. B., Zaucke, F., Kunze, A., Misselwitz, J., Ruley, J., Ronda, T., Fischer, A., Eifinger, F., Licht, C., Otto, E., Hoppe, B. and Hildebrandt, F. (2007). The Uromodulin C744G mutation causes MCKD2 and FJHN in children and adults and may be due to a possible founder effect. Kidney Int 71(6): 574-81.

Wolf, M. T., Karle, S. M., Schwarz, S., Anlauf, M., Glaeser, L., Kroiss, S., Burton, C., Feest, T., Otto, E., Fuchshuber, A. and Hildebrandt, F. (2003). Refinement of the critical region for MCKD1 by detection of transcontinental haplotype sharing. Kidney Int 64(3): 788-92.

Wolf, M. T., Mucha, B. E., Hennies, H. C., Attanasio, M., Panther, F., Zalewski, I., Karle, S. M., Otto, E. A., Deltas, C. C., Fuchshuber, A. and Hildebrandt, F. (2006). Medullary cystic kidney disease type 1: mutational analysis in 37 genes based on haplotype sharing. Hum Genet 119(6): 649-58.

Yu, A. S. L. and Brenner, B. M. (2004). Tubulointerstitial Diseases of the Kidney. Harrison´s Principles of Internal Medicine. D. L. Kasper. New York, The McGraw Hill Company: 1702 - 1705.

Yuan, X., Werner, J. M., Lack, J., Knott, V., Handford, P. A., Campbell, I. D. and Downing, A. K. (2002). Effects of the N2144S mutation on backbone dynamics of a TB-cbEGF domain pair from human fibrillin-1. J Mol Biol 316(1): 113-25.

Zhu, X., Cheng, J., Gao, J., Lepor, H., Zhang, Z. T., Pak, J. and Wu, X. R. (2002). Isolation of mouse THP gene promoter and demonstration of its kidney-specific activity in transgenic mice. Am J Physiol Renal Physiol 282(4): F608-17.

Zingg-Schenk, A., Bacchetta, J., Corvol, P., Michaud, A., Stallmach, T., Cochat, P., Gribouval, O., Gubler, M. C. and Neuhaus, T. J. (2008). Inherited renal tubular dysgenesis: the first patients surviving the neonatal period. Eur J Pediatr 167(3): 311-316.

Zivna, M., Hulkova, H., Matignon, M., Hodanova, K., Vylet'al, P., Kalbacova, M., Baresova, V., Sikora, J., Blazkova, H., Zivny, J., Ivanek, R., Stranecky, V., Sovova, J., Claes, K., Lerut, E., Fryns, J. P., Hart, P. S., Hart, T. C., Adams, J. N., Pawtowski, A., Clemessy, M., Gasc, J. M., Gubler, M. C., Antignac, C., Elleder, M., Kapp, K., Grimbert, P., Bleyer, A. J. and Kmoch, S. (2009). Dominant renin gene mutations associated with early-onset hyperuricemia, anemia, and chronic kidney failure. Am J Hum Genet 85(2): 204-13.

3 Summary and Conclusions

To elucidate the genetic basis of hyperuricemic nephropathies and to solve pathogenetic mechanisms leading to the clinical and biochemical signs and subsequent kidney failure we systematically collect samples (urine, blood, tissue biopsies) from patients and families and analyze clinical, biochemical, molecular and physiological results.

We use linkage analysis, candidate gene prioritizing, candidate gene sequencing and functional analysis of identified mutated genes. Finally, we correlate clinical, biochemical and histological findings with our experimental data to identify pathophysiology of the disease.

Within the frame of this research my work resulted in and contributed to the following points:

- **We confirmed extensive genetic heterogeneity of familial hyperuricemic nephropathies**
  - We identified new locus on chromosome 1q41 segregates with the disease.
  - Only 40% of cases link to known loci associated with the disease (16p11.2, 1q21, 17q21.3 and 1q41).
- **We identified and functionally characterized several mutations in *UMOD* gene (locus 16p.11.2) in FJHN1/MCKD2 patients**
  - Mutated UMOD showed aberrant glycosylation patterns, impaired cellular trafficking, and decreased ability to be exposed on the plasma membrane of transfected cells compared to wild type UMOD. These changes in UMOD protein processing led to various degree of UMOD accumulation in endoplasmic reticulum which could induce stress of endoplasmic reticulum.

- The observed accumulation of mutated UMOD in the endoplasmic reticulum corresponded with the histological finding in patient´s kidney.

- **We suggested UMOD as a key molecule in pathogenesis of development of hyperuricemic nephropathies, FJHN1/MCKD2 and FJHN2**
  - We found that FHJN1/MCKD2 and FJHN2 diseases of different genetic background are commonly associated with reduction of UMOD urinary excretion.
- **We defined and characterized molecular and pathogenetic mechanisms of new disease now named familial juvenile hyperuricemic nephropathy type 2 (FJHN2)**
  - We described patients with early onset hyperuricemia, anemia and chronic kidney failure and identified mutations in renin signal sequence (locus 1q41) segregated with this phenotype in 4 unrelated families.
  - This phenotype was enrolled into database of human genes and genetic disorders Online Mendelian Inheritance in Man (OMIM) administrated by National Center for Biotechnology Information (NCBI) as new disease under evidence number 613092 and named familial juvenile hyperuricemic nephropathy type 2 (FJHN2).
  - All identified mutations significantly impaired prorenin and renin biosynthesis, secretion and enzymatic activity.
  - We proposed that the identified mutations in renin signal sequence likely expose juxtaglomerular cells to chronic ER stress and lead to site-specific attenuation of renin biosynthesis and RAS dysregulation. Reduced viability of juxtaglomerular cells and limited renin availability then affect renal development, intrarenal

RAS homeostasis, and kidney blood flow autoregulation resulting in anemia, reduced glomerular filtration rate, and hyperuricemia.

- Important therapeutic implications are based on our finding and are currently tested on selected patients

- **We established ongoing co-operation with nephrology clinicians and researchers from Czech Republic, Europe and USA.**

4 Results

4. 1 Mapping of a new candidate locus for uromodulin-associated kidney disease (UAKD) to chromosome 1q41.

Hodanová K, Majewski J, **Kublová M**, Vyletal P, Kalbácová M, Stibůrková B, Hůlková H, Chagnon YC, Lanouette CM, Marinaki A, Fryns JP, Venkat-Raman G, Kmoch S.

Kidney Int. 2005 Oct;68(4):1472-82., **IF 4, 927**

Kidney International, Vol. 68 (2005), pp. 1472–1482

GENETIC DISORDERS – DEVELOPMENT

Mapping of a new candidate locus for uromodulin-associated kidney disease (UAKD) to chromosome 1q41

Kateřina Hodaňová, Jacek Majewski, Martina Kublová, Petr Vyleťal, Marie Kalbáčová, Blanka Stibůrková, Helena Hůlková, Yvon C. Chagnon, Christian-Marc Lanouette, Anthony Marinaki, Jean-Pierre Fryns, Gopalakrishnan Venkat-Raman, and Stanislav Kmoch

Center for Applied Genomics, Institute for Inherited Metabolic Disorders, Charles University 1st School of Medicine, Prague, Czech Republic; Laboratory of Statistical Genetics, Rockefeller University, New York, New York; Laval University Research Center Robert-Giffard, Beauport, Québec, Canada; Purine Research Unit, GKT, Guy's Hospital, London, United Kingdom; Center for Human Genetics, University of Leuven, Belgium; and Renal Unit, Queen Alexandra Hospital, Portsmouth, United Kingdom

Mapping of a new candidate locus for uromodulin-associated kidney disease (UAKD) to chromosome 1q41.

Background. Autosomal-dominant juvenile hyperuricemia, gouty arthritis, medullary cysts, and progressive renal insufficiency are features associated with familial juvenile hyperuricemic nephropathy (FJHN), medullary cystic kidney disease type 1 (MCKD1) and type 2 (MCKD2). *MCKD1* has been mapped to chromosome 1q21. *FJHN* and *MCKD2* have been mapped to chromosome 16p11.2. FJHN and MCKD2 are allelic, result from uromodulin *(UMOD)* mutations and the term uromodulin-associated kidney disease (UAKD) has been proposed for them. Linkage studies also reveal families that do not show linkage to any of the identified loci. To identify additional *UAKD* loci, we analyzed one of these families, with features suggestive of FJHN.

Methods. Clinical, biochemical, and immunohistochemical investigations were used for phenotype characterization. Genotyping, linkage and haplotype analyses were employed to identify the candidate disease region. Bioinformatics and sequencing were used for candidate gene selection and analyses.

Results. We identified a new candidate *UAKD* locus on chromosome 1q41, bounded by markers D1S3470 and D1S1644. We analyzed and found no linkage to this region in eight additional families, who did not map to the previously established loci. We noted that affected individuals showed, in addition to the characteristic urate hypoexcretion, significant reductions in urinary excretion of calcium and UMOD. Immunohistochemical analysis showed that low UMOD excretion resulted from its reduced expression, which is a different mechanism to intracellular UMOD accumulation observed in cases with *UMOD* mutations.

Conclusion. We have mapped a new candidate *UAKD* locus and shown that UAKD may be a consequence of various defects affecting uromodulin biology.

Key words: familial juvenile hyperuricemic nephropathy, hyperuricemia, linkage mapping, uromodulin, renal failure.

Received for publication October 18, 2004
and in revised form January 18, 2005, and March 7, 2005
Accepted for publication April 15, 2005

Familial juvenile hyperuricemic nephropathy (FJHN) (OMIM 162000) [1, 2] and medullary cystic kidney diseases type 1 (MCKD1) (OMIM 174000) [3] and type 2 (MCKD2) (OMIM 603860) [4] represent a constellation of autosomal-dominant tubulointerstitial nephropathies, which are accompanied to a variable extent by hyperuricemia, gouty arthritis, medullary cysts, and progressive renal insufficiency. The phenotypic expression of the diseases is inconsistent, overlaps, and indicates broader genetic and allelic heterogeneity. Several independent studies showed linkage of FJHN [5, 6] and MCKD2 [4, 7] to the same genomic region on chromosome 16 p11.2. Recent studies confirmed that FJHN and MCKD2 are allelic disorders resulting from mutations of uromodulin (UMOD) [8–15] and therefore the term uromodulin-associated kidney disease (UAKD) has been proposed [8]. MCKD1 was mapped to chromosome 1q21 [16–19], to which region also an autosomal-dominant form of progressive renal failure (OMIM 161900) was localized [20, 21]. The above studies further confirmed that both FJHN [22–25] and MCKD [18, 26] are genetically heterogeneous, and that in approximately 40% to 75% of analyzed families the diseases are likely to be caused by a gene(s) located outside of the16p11.2. and 1q21 intervals [11, 12, 25]. To search for other UAKD loci we performed a genome-wide mapping in a single Belgian family BE1, which displayed some features of FJHN but in which previous analyses excluded linkage to FJHN/MCKD2 loci on chromosome 16p11.2 [25] and to *MCKD1* locus on chromosome 1q21 [logarithm of odds (LOD) < -3.8 within the *MCKD1* critical region, analyzing markers D1S534,

D1S1595, D1S394, and D1S1653]. We identified a new candidate UAKD gene locus on chromosome 1q41. Haplotype analysis and recombination events detected in affected individuals delimited the candidate disease region to be bounded by markers D1S3470 and D1S1644. We also tested and found no linkage to the newly identified region in eight families from our previous studies that did not show evidence of linkage to the already established FJHN/MCKD2 locus on 16p11.2 and MCKD1 locus on 1q21 [18, 23, 25].

Assessing the phenotype, we found that affected individuals showed, in addition to characteristic urate hypoexcretion, significant reduction in urinary excretion of calcium and UMOD. The immunohistochemical analysis of kidney biopsies showed that low UMOD excretion in family BE1 originated from significantly reduced UMOD expression. This observation is clearly different from the characteristic intracellular UMOD accumulation observed in the previously studied cases of FJHN with UMOD mutations and suggests that various defects affecting UMOD biology may play a central role in development of UAKD.

METHODS

Patients

The investigated families were described and referred in our previous studies, family C [23], families BE1, GB1, GB4, GB5, GB6, GB9, GB10, and E2 [25, 27], and MCKD family 6 [18]. Family BE1 described in this study was ascertained at the Department of Nephrology at the University Hospital in Leuven. The family GB6 (for pedigree [25] and for clinical details [27], kindred 7) was ascertained at the Renal Clinics at Guy's Hospital and Portsmouth Hospital. Medical histories were obtained as a part of all the patients' clinical workup by consultants of the above referred institutions. Clinical and biochemical investigations essential for the investigation were explained to the patients prior to performance. Patient privacy was protected by restricting access to family names, addresses, and written health records.

Biochemical investigations

Random spot urine samples were collected from available individuals and were stored until the analyses at −80°C. Urine total protein, creatinine, uric acid, magnesium, calcium, and phosphate were determined by the protein (urine) (BioSystems, Costa Brava, Barcelona, Spain), CREA (Roche, Prague, Czech Republic), UA Plus (Roche), Mg (Roche), Ca (Roche), and PHOS (Roche) kits, respectively, on a Hitachi Modular Analyzer (Roche). Sodium, potassium, and chloride were determined by ion-selective electrodes. Osmolality was determined by freezing point technology using FISKE 2400 osmometer.

For quantitative UMOD analysis, thawed urine samples were diluted (1:250) in tetraethylammonium (TEA) buffer according to Kobayashi and Fukuoka [28]. UMOD was quantified by sandwich enzyme-linked immunosorbent assay (ELISA) method with antihuman Tamm-Horsfall protein mouse IgG2b monoclonal antibodies (Cedarlane, Hornby, Ontario, Canada) as capture antibodies and rabbit antihuman Tamm-Horsfall protein polyclonal antibodies (Biogenesis, Pool, England) and goat antirabbit IgG-horseradish peroxidase conjugate as detection antibodies. As a quantitative standard, UMOD purified from healthy male urine (according to the method of Kobayashi and Fukuoka [28]) was used.

For qualitative analysis of urinary UMOD, 250 μL of urine was concentrated on Microcon YM-30 filters (Millipore, Bedford, MA, USA) and total protein was recovered. For analysis of UMOD in sediment, 35 μL of total urine was centrifuged at 5 000*g* for 10 minutes. About 10 μg of total urinary protein and entire sediment pellet were dissolved in sodium dodecyl sulfate (SDS) sample buffer. Proteins were separated by SDS-polyacrylamide gel electrophoresis (PAGE) and either stained by SYPRO Ruby (Molecular Probes, Eugene, OR, USA), or blotted in a semidry system (Biotec-Fischer, Reiskirchen, Germany) on polyvinylidine difluoride (PVDF) membranes (Immobilon-P) (Millipore). Western blot analysis was performed with UMOD monoclonal mouse antibodies (Cedarlane) (primary antibodies) and antimouse Ig antibody conjugated to horseradish peroxidase (Pierce, Rockford, IL, USA) (secondary antibodies). Chemiluminescent signal was obtained using SuperSignal West Pico Chemiluminescent Substrate Kit (Pierce).

Statistical analyses were performed using nonparametric methods. The Mann-Whitney test was used for the comparison of continuous variables. The significantly different parameters (disease status characteristics) were used for discriminant analysis which calculated the posterior probability of an individual being a carrier or not (Fig. 3). All the statistical analyses were performed using the software Statistica, version 4.5 (StatSoft, Tulsa, OK, USA).

Immunohistochemical analysis

Formaldehyde- or ethanol-fixed kidney samples from a control, a patient with a mutation in *UMOD* gene, three individuals from family BE1 (DIII6, DIV3, and DIV7) and a single proband from family GB6 were analyzed. Immunodetection of UMOD was done on paraffin sections using rabbit anti-Tamm-Horsfall protein antibody (Biogenesis). The paraffin sections were stained after deparaffination, hydration, and standard blocking procedures [blocking of endogenous peroxidase with 1% sodium azide and 0.3% H_2O_2 for 10 minutes and blocking with 5% fetal bovine serum (FBS) in phosphate-buffered

saline (PBS) for 30 minutes, both at room temperature]. The primary antibody was applied diluted 1:800 in 5% FBS in PBS overnight at 40°C. Detection of bound primary antibody was achieved using Dako EnVision+™ Peroxidase Rabbit Kit (Dako, Glostrup, Denmark) with 3,3′-diaminobenzidine (DAB) as substrate.

Genotype analysis

Genomic DNA was isolated by standard methodology. Genotyping was performed with Li-Cor IR2 and ALFExpress sequencer systems as previously described [23, 29]. A medium density genome scan of 93 markers with an average spacing of 30 cM was carried out in 17 individuals from family BE1. The markers were all part of the Marshfield version 9 screening set. For further fine mapping on chromosome 1q41 additional markers were selected and their order and distances between the markers were obtained from Genethon [30] and Marshfield databases [31].Genotyping data were screened for errors using the PEDCHECK program [32]. Mendelian inconsistencies were corrected using the original gels or, in cases where bands could not be unambiguously resolved, assigned an "unknown" genotype.

Linkage analysis

Two-point and multipoint linkage analyses, along with determination of the most likely haplotypes, were performed using the Allegro software (deCode Genetics, Reykjavik, Iceland) [33]. The analyses were carried out under the assumption of a dominant mode of inheritance with a 0.99 constant, age independent penetrance, 0.01 phenocopy rate, and 0.001 frequency of the disease allele.

Critical region and candidate genes analyses

Genetic markers were positioned on human genome contigs by searching actual builds of major human genome databases–MapViewer (*http://www.ncbi.nlm.nih.gov/*), Ensembl (*http://www.ensembl.org/*), and Human Genome Working Draft at UCSC, (*http://genome.ucsc.edu/*). Individual genes present in delimited critical region were evaluated according to their expression profiles, knowledge or assumption of their function, and analysis of hypothetical functional domains.

To identify kidney-specific genes and expressed sequence tag (EST) clusters, we (*1*) downloaded from Gene Expression Omnibus Database (GEO) (*http://www.ncbi.nlm.nih.gov/geo/*) data sets of normal human tissue mRNA expression profiling experiments (GDS422-GDS426), queried kidney expression data sets against all other available tissues, extracted all genes showing four times higher kidney expression and intersected resulting expression set with candidate region gene content; (*2*) used the Digital Differential Display approach (*http://www.ncbi.nlm.nih.gov/UniGene/*) to compare EST sequences derived from kidney cDNA libraries against EST sequences derived from the pool of normal human tissues cDNA libraries and intersected resulting set with candidate region gene content; (*3*) evaluated the gene content in a view of recently published kidney specific gene expression data [34]; (*4*) focused on genes that may be connected to UMOD biogenesis [e.g., inability of glycosyl-phosphatidylinositol (GPI) anchor synthesis, proper membrane targeting or proteolytic release of GPI-anchored membrane proteins; (*5*) searched for genes which are known to be involved in hypertension and/or renal failure; and (*6*) searched for transcription factors and proteins which might regulate UMOD expression.

Genomic fragments covering promoter region (about 500 bp upstream from the most cDNA 5′end) and all of the exons and intron-exon boundaries of selected candidate genes were polymerase chain reaction (PCR) amplified from genomic DNA and sequenced as previously described [35]. All candidate genes were analyzed in one proband and one unaffected family member. Genetic variations were screened against single nucleotide polymorphism (SNP) and UNIGENE databases.

RESULTS

Clinical and biochemical findings

The pedigree of the family BE1 is shown in Figure 1. In this family, the first signs of the disease were mild anemia, hyperuricemia, and slowly progressive renal insufficiency. All the patients had small, echogenic kidneys on renal echography, but renal cysts were not reported. Gout was not a feature in any of the subjects.

Terminal renal failure developed at 68, 50, and 66 years of age in DI1, DI3, and DII1, respectively. In the last case this was treated successfully with renal transplantation. Individual DII3 (71 years old) showed the main clinical and biochemical features of the disease. The patient's current clinical status is unknown.

Individual DIII4 (44 years old) is reported as having anemia, hyperuricemia, small kidneys, and evidence of renal insufficiency.

Individual DIII6 (43 years old) has been followed clinically and biochemically for 5 years. Following the correction of hyperuricemia by allopurinol, the patient has shown permanently elevated concentration of plasma creatinine (range 210 to 305 μmol/L) and urea (range 19 to 22 mmol/L), mild persistent anemia (hemoglobin range 10.5 to 14 g/dL), and mild intermittent hyperkalemia (range 5.11 to 5.79 mmol/L).The 24-hour urine collection samples were analyzed six times and showed reduced creatinine clearance (34 to 37 mL/min/1.73 m^2) with normal concentrations of sodium, potassium, and chloride. Uric acid excretion was not measured.

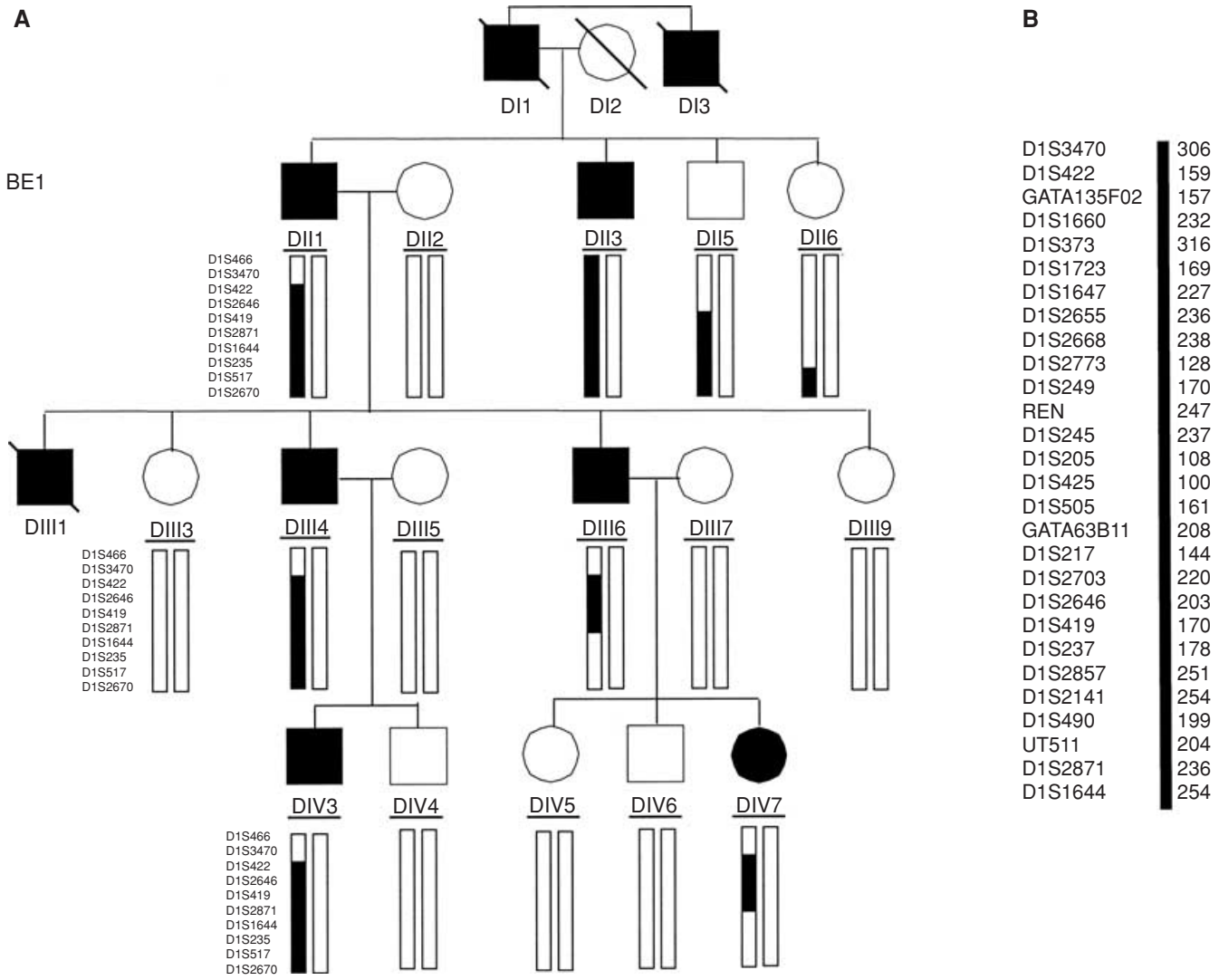

Fig. 1. Pedigree diagram of the investigated uromodulin-associated kidney disease (UAKD) family linked to 1q41. (*A*) Black symbols denote affected individuals and white symbols denote unaffected individuals. Genotyped individuals are underlined. Recombinant markers forming the haplotype segregating with the disease locus are indicated. (*B*) Actual allele sizes forming the disease haplotype.

Individual DIV3 (16 years old) was investigated for the first time at 8 years of age. He showed anemia (hemoglobin 10 g/dL), hyperuricemia (435 μmol/L), elevated concentration of plasma creatinine (80 μmol/L) and urea (9 mmol/L), and reduced creatinine (51 mL/min/1.73 m^2) and inulin (68 mL/min/1.73 m^2) clearance. Hyperuricemia was corrected by allopurinol and the patient has been followed up for 6 years. He has shown persistent anemia (hemoglobin range 9.5 to 11 g/dL), gradually rising creatinine plasma concentration (80 to 130 μmol/L) and urea concentration (9 to 12 mmol/L). Plasma potassium concentrations were within the normal range. The 24-hour urine collection samples showed reduced creatinine clearance (49 to 64 mL/min/1.73 m^2) and reduced uric acid excretion (0.7 to 1 mmol/24 hours, controls 1.25 to 5 mmol/24 hours). Kidney sizes were –2.1 SD bilaterally for the corresponding body height.

Individual DIV7 (12 years old) was investigated for the first time at 4 years of age. The patient showed anemia (10.1 g of hemoglobin/dL), hyperuricemia (400 μmol/L), elevated concentration of plasma creatinine (80 μmol/L) and urea (9.6 mmol/L), and reduced creatinine (60 mL/min/1.73 m^2) and inulin (68 mL/min/1.73 m^2) clearance. Hyperuricemia was corrected by allopurinol and patient has been followed up for 8 years. The patient has shown persistent anemia (hemoglobin range 8.8 to 11.9 g/dL), gradually rising creatinine plasma concentration (80 to 135 μmol/L) and urea concentration (9.6 to 18.5 mmol/L). Mild persistent hyperkalemia (range 5.00 to 5.86 mmol/L) was observed. The 24-hour urine collection samples showed reduced creatinine clearance (46 to 68 mL/min/1.73 m^2) and reduced uric acid excretion (1.2 mmol/24 hours). Kidney sizes were –3.5 SD (right) and –3.3 SD (left) for the corresponding body height.

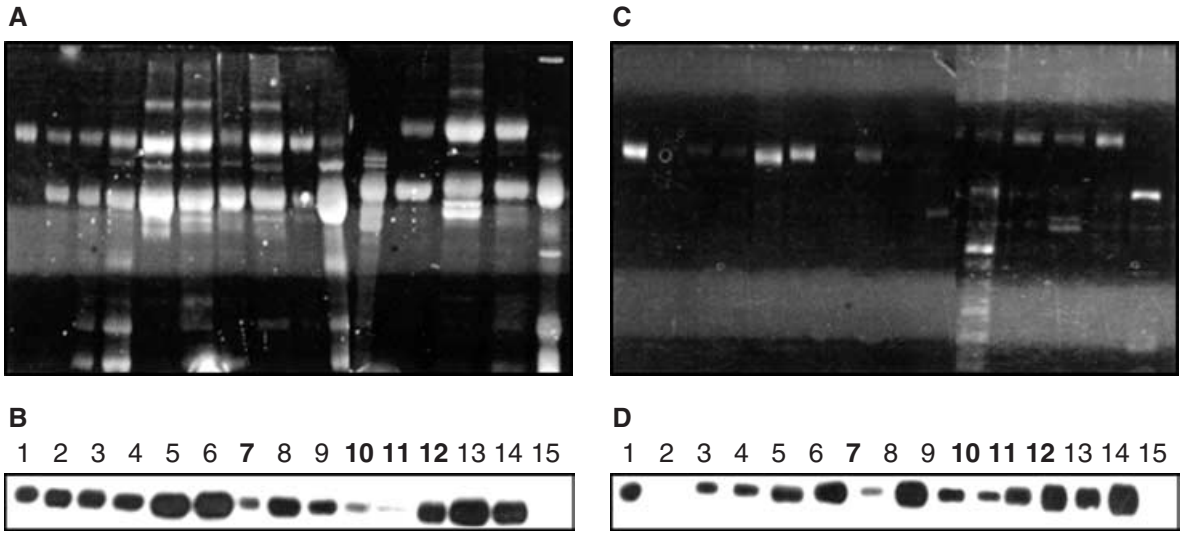

Fig. 2. Sodium dodecyl sulfate-polyacrylamide gel electrophoresis (SDS-PAGE) and Western blot analysis of urinary uromodulin (UMOD). (*A* and *C*) SYPRO Ruby–labeled proteins in urine and urinary sediment, respectively. (*B* and *D*) UMOD detected in the same samples by Western blot. Lane 1, purified UMOD, 1.5μg; lane 2, female control; lane 3, male control; lane 4, DII5; lane 5, DIV4; lane 6, DIV5; lane 7, DIV7; lane 8, DIV6; lane 9, DII6; lane 10, DIII6; lane 11, DIII4; lane 12, DIV3; lane 13, DIII3; lane 14, control; and lane 15, patient from familial juvenile hyperuricemic nephropathy (FJHN) family with mutation in *UMOD* gene. Samples from affected individuals are bold.

Table 1. Urine biochemical parameters measured in individuals from family BEI and controls

	Group			Mann-Whitney test *P* values		
Parameter	Healthy ((*N* = 6)	Disease (*N* = 4)	Control (*N* = 77)	Disease/ Healthy	Disease/ Control	Healthy/ Control
Age	37 (14–67)	29 (12–44)	36 (22–81)	*NS*	*NS*	*NS*
Creatinine *mmol/L*	14.0 (5.7–22)	13.4 (7.0–25.0)	9.0 (0.9–24.6)	*NS*	*NS*	*NS*
PO4/creatinine *mmol/mmol*	1.75 (0.63–2.23)	1.20 (0.70–2.03)	1.96 (0.27–7.3)	*NS*	*NS*	*NS*
UCB/creatinine *mg/mmol*	10.5 (6.7–16.7)	17.1 (6.3–33.7)	8.5 (0.0–49.5)	*NS*	$P \leq 0.05$	*NS*
Potassium/creatinine *mmol/mmol*	5.65 (1.84–9.67)	3.48 (2.00–4.79)	6.54 (1.61–34.29)	*NS*	$P \leq 0.05$	*NS*
Sodium/creatinine *mmol/mmol*	10.6 (5.1–14.4)	6.2 (2.7–11.7)	13.9 (1.6–49.2)	*NS*	$P \leq 0.05$	*NS*
Mg^{2+}/creatinine *mmol/mmol*	0.26 (0.18–0.42)	0.20 (0.15–0.30)	0.37 (0.14–1.82)	*NS*	$P \leq 0.05$	*NS*
Osmolality/creatinine *mOsm/mmol*	63 (42–88)	39 (20–70)	71 (35–160)	*NS*	$P \leq 0.05$	*NS*
Chloride/creatinine *mmol/mmol*	12.4 (5.3–17.7)	5.6 (1.4–11.5)	17.3 (3.5–49.2)	*NS*	$P \leq 0.01$	*NS*
Ca^{2+}/creatinine *mmol/mmol*	0.38 (0.13–0.58)	0.04 (0.01–0.05)	0.35 (0.04–1.56)	$P \leq 0.01$	$P \leq 0.001$	*NS*
Uromodulin /creatinine *mg/g*	30.3 (19.7–53.8)	9.2 (0.0–15.5)	35.7 (7.7–111.0)	$P \leq 0.01$	$P \leq 0.001$	*NS*
Uric acid/creatinine *mmol/mmol*	222 (116–362)	49 (17–102)	247 (90–990)	$P \leq 0.01$	$P \leq 0.001$	*NS*

Values are reported as median (range). *P* values correspond to the comparison between groups. *NS* is not significant.

Individuals DIV4, DIV5, and DIV6 are 14, 19, and 17 years old, respectively. They were thoroughly investigated at the age of 8, 11, and 16 years of age, and 9 and 14 years of age, respectively. They showed no biochemical abnormality in any of above-mentioned parameters. Their clinical status remains stable up to now, with normal renal function.

To assess the most current biochemical status of the individuals enrolled in the study, we collected spot urine, analyzed qualitatively and quantitatively UMOD protein, measured creatinine, uric acid, sodium, potassium, calcium, magnesium, phosphates, chlorides, and total protein concentrations and determined urine osmolality.

Qualitative protein analysis showed that UMOD was reduced or absent in the patients' urine. The same was observed in urinary sediment. No abnormality in electrophoretic mobility of residual UMOD protein was observed in patients (Fig. 2).

To correlate individual analyte concentrations, we normalized them to creatinine content and correlated resulting values between affected individuals, nonaffected individuals, and external controls. We found no statistically significant ($P > 0.05$) changes in any of the parameters between healthy individuals and controls. In contrast, except for phosphate, all the parameters were significantly different in affected individuals compared to controls ($P < 0.05$). Comparing the affected and unaffected individuals within the family, significant reduction in excretion of urate, calcium, and UMOD were found (Table 1). We next considered all the significantly different parameters found between affected individuals and controls, (Table 1) as disease status characteristics

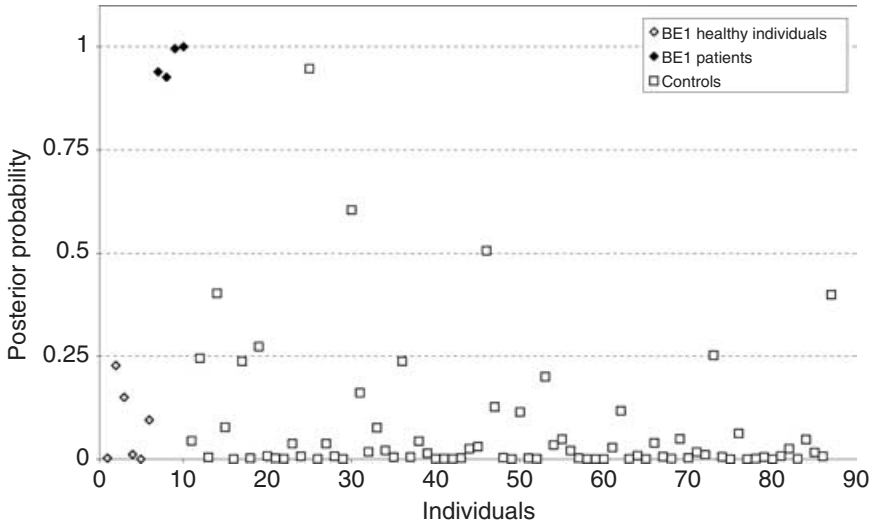

Fig. 3. Posterior probabilities of having the disease observed in 87 individuals. Gray symbols represent, from left to right, DIV4, DIV6, DIV5, DIII3, DII6, and DII5, respectively. Black symbols represent, in the same order, affected individuals DIV7, DIV3, DIII6, and DIII4, respectively. Controls are represented in white.

Table 2. Clinical and biochemical data used for individual's status classification (individuals classified as affected are in bold)

Individuals	Age *year*	Anemia	Hyperuricemia	Renal insufficiency	Uric acid *mmol/mmol creatinine*	Ca^{2+} *mmol/mmol creatinine*	Uromodulin *mmol/mmol creatinine*	Disease probablity
DI1	**Died at 68**	**Yes**	**Yes**	**Yes**	**ND**	**ND**	**ND**	**ND**
DI3	**Died at 50**		**NA**	**yes**	**ND**	**ND**	**ND**	**ND**
DII1	**72**	**Yes**	**Yes**	**Transplantation at 60**	**ND**	**ND**	**ND**	**ND**
DII3	**71**	**Yes**	**Yes**	**Yes**	**ND**	**ND**	**ND**	**ND**
DII5	67	No	No	No	243	0.42	25.67	0.09
DII6	59	No	No	No	362	0.33	53.78	0.00
DIII1	**Died at 37**	**Yes**	**Yes**	**Yes**	**ND**	**ND**	**ND**	**ND**
DIII3	47	No	No	No	202	0.58	34.27	0.01
DIII4	**44**	**Yes**	**Yes**	**Yes**	**17**	**0.05**	**0.00**	**1.00**
DIII6	**43**	**Yes**	**Yes**	**Yes**	**35**	**0.03**	**7.34**	**1.00**
DIII9	41	No	No	No	ND	ND	ND	ND
DIV3	**16**	**Yes**	**Yes**	**Yes**	**43**	**0.01**	**13.79**	**0.93**
DIV4	14	No	No	No	283	0.49	28.05	0.00
DIV5	19	No	No	No	116	0.30	20.14	0.15
DIV6	17	No	No	No	128	0.13	19.66	0.22
DIV7	**12**	**Yes**	**Yes**	**Yes**	**102**	**0.05**	**15.52**	**0.94**
Controls($N = 77$)								
Average ± SD	36 ± 13	NA	NA	NA	246 ± 108	0.35 ± 0.25	35.23 ± 17.63	0,07 ± 0.15
Median	36				240	0.29	33.69	0.01
Range	22–18				90–990	0.04–7.50	7.71–110.97	0.00–0.95

Abbreviations are: ND, not determined; NA, not available.

and performed multivariate discriminant analysis. The analysis revealed a highly significant discrimination between patients and controls (Wilks' Lambda 0.68 approximately F (8.72) = 4.15) ($P < 0.0004$). The variables contributing the most to the discrimination were urine uric acid/creatinine ratio (partial Wilks' Lambda 0.91) ($P < 0.01$) and urine UMOD/creatinine ratio (partial Wilks' Lambda 0.87) ($P < 0.001$). In order to classify each individual from family BE1, we used the resulting discriminant function and based on equal priors we calculated posterior probabilities that the individuals belong to the disease or control group (Fig. 3). This analysis showed that affected and unaffected individuals form separate clusters and corroborated previous clinical observations and biochemical investigations, which are summarized in Table 2.

Immunohistochemical analysis

In control kidney tissue (Fig. 4A), UMOD was expressed strongly in the ascending limb of the loop of Henle. The distribution was cytoplasmic; however, maximal staining intensity was seen on the apical membranes of epithelial cells.

In kidney tissue from the FJHN patient with the UMOD mutation (Fig. 4B), epithelium of the loop of Henle displayed strong coarsely granular cytoplasmic staining suggesting accumulation of UMOD in vesicular compartment (i.e., endoplasmic reticulum).

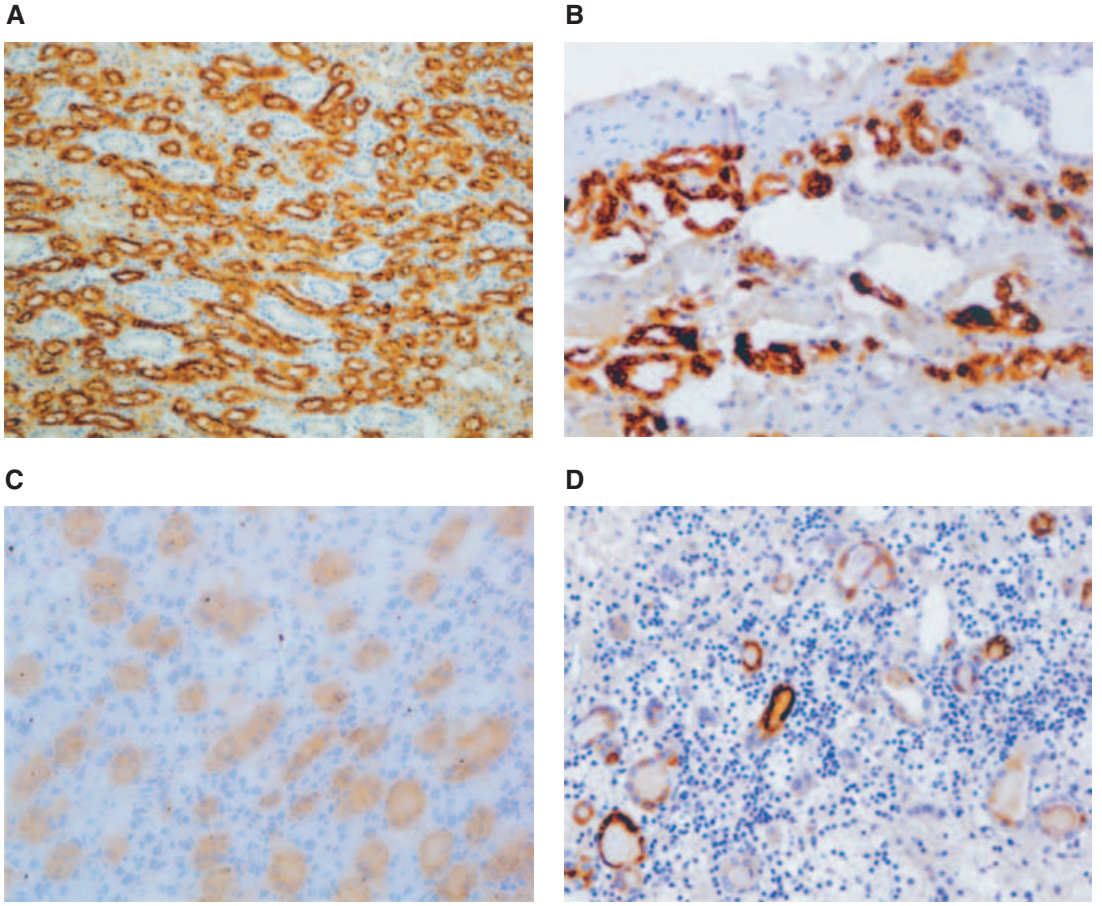

Fig. 4. Immunohistochemical analysis of uromodulin (UMOD) in kidney from control (*A*), familial juvenile hyperuricemic (FJHN) patient with mutation in UMOD gene (*B*) and in affected individuals from families BE1 (*C*) and GB6 (*D*). Three different mechanism of UMOD dysfunction associated with the uromodulin-associated kidney disease (UAKD) can be predicted. Massive UMOD storage along the secretory pathway (B), strongly reduced expression of UMOD (C) and decreased and irregular UMOD staining on the background of interstitial fibrosis and tubular atrophy (D).

In kidney tissue from patients from family BE1 (Fig. 4C), UMOD staining was significantly and uniformly reduced in the epithelium of the loop of Henle in all three studied cases (DIII6, DIV3, and DIV7). Minimal signs of tubulointerstitial injury were observed.

In kidney from the patient from family GB6 (Fig. 4D), decreased and irregular UMOD staining was observed in tubules on the background of interstitial fibrosis and tubular atrophy.

Positively stained tubular casts were seen occasionally in control and patients samples except for the case with the UMOD mutation.

Linkage analysis

Preliminary results from a two-point genome-wide linkage analysis of 93 microsatellite markers in family BE1 produced no conclusive proof of linkage; however, one candidate region on chromosome 1, including markers D1S398 and D1S202 (LOD = 1.69) was identified for further analysis. There were no other markers or regions with LOD scores exceeding 1. For our candidate region, we carried out fine mapping using 38 additional markers and obtained a maximum multipoint LOD score of 3.27 (Fig. 5). Haplotype analysis uncovered a single haplotype segregating with the disease and recombination events detected in affected individuals delimited the candidate region bound by markers D1S3470 and D1S1644 (Fig. 1). We then tested for linkage to the newly identified 1q41 locus in eight FJHN families from our previous studies, family C [23], families GB1, GB4, GB5, GB6, GB9, GB10, and E2 [25], and MCKD family 6 [18], that did not show evidence of linkage to the already established FJHN/MCKD loci on chromosomes 16p11.2 and 1q21. All but one of the families produced negative LOD scores within the entire candidate interval. Families C, GB2, GB4, and GB5 had LOD scores < -2 within the entire 1q41 interval, as well as the 16p11.2 interval, excluding linkage to those loci and thus providing evidence of further genetic heterogeneity in UAKD.

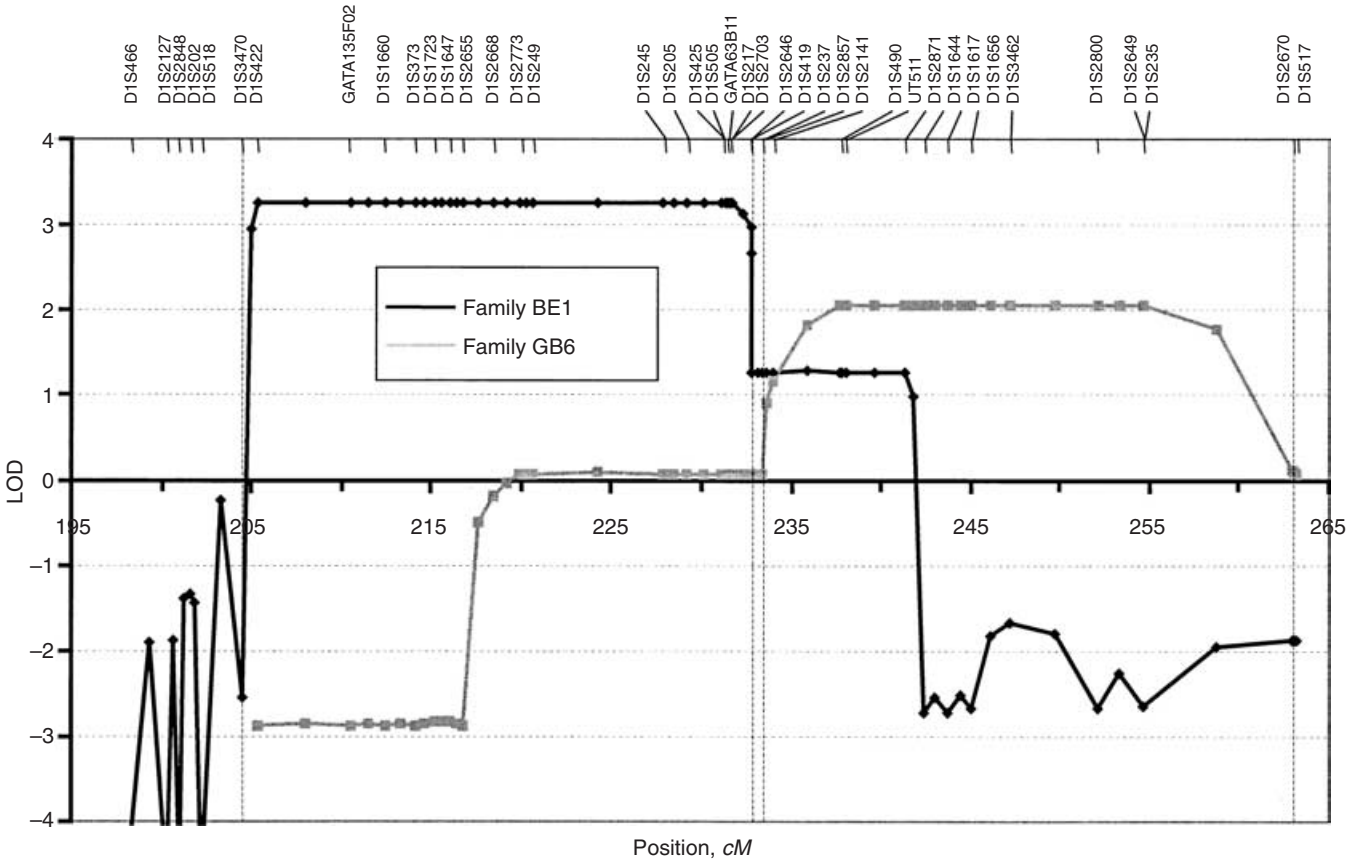

Fig. 5. Multipoint overlapping logarithm of the odds (LOD) score analysis of the markers in the linked region on chromosome 1q41. The candidate region in family BE1 is delimited by markers D1S3470 and D1S1644 based on recombination events in affected individuals. Note that using a less stringent criterion of one LOD unit drop from the maximum (which includes also information from unaffected individuals), the candidate region may be further restricted to D1S3470-D1S2857.

The single family with a positive LOD score within the 1q41 interval, family GB6, initially showed LOD = 0.6 at markers D1S425, D1S2703, and D1S419. After genotyping additional markers, we found for this family a maximum LOD score of 2.07. Haplotype analysis demonstrated in affected individuals a single haplotype, delimited by markers D1S237 and D1S2670, that segregated with the disease phenotype. Both identified disease regions were, however, distinct and nonoverlapping (Fig. 5). Because parallel immunohistochemical analysis supported the possibility of genetically distinct origin of the diseases (Fig. 4C and D), and since the LOD score 2.07 did not reach the generally accepted limit for determining linkage, we conclude that the segregation of the candidate region haplotype on 1q41 with disease phenotype in family GB6 is likely to be a chance finding.

Candidate gene analysis

The critical region we have delimited in family BE1 spans 37.2 million bases, is fully sequenced, and contains about 300 genes. Evaluating gene content, we have selected and sequenced, in probands and healthy individuals from the family, nine candidate genes—ATPase, H+ transporting, lysosomal 13 kD, V1 subunit G isoform (3ATP6VIG3), feline leukemia virus subgroup C cellular receptor (FLVCR), hypothetical protein FLJ20605 (Unigene clusterHS.4932A), transforming growth factor beta 2 precursor (TGFβ2), 5′-bisphosphate nucleotidase 1(BPNT1), transmembrane 7 superfamily member 1 protein (TM7SF1), guanine nucleotide binding protein (GNG4), and Jun dimerization protein p21 (SNFT). Although several genetic variants were found in some of the genes (data not shown), no "classic" deleterious mutation was detected within the analyzed promoter regions, exon/intron junctions, and coding sequences.

DISCUSSION

We describe here localization of a new *UAKD* locus on chromosome1q41. We identified this locus by genome scan and linkage analysis in a single family, which showed the clinical and biochemical symptoms of UAKD and did not show linkage to any of previously identified *UAKD*-associated loci.

Since the family size was not sufficient for the "affected only" analysis, we focused first on detailed clinical and biochemical characterization which would minimize the possibility of disease status misclassification. Within the family all the main signs of the disease, small kidney size, anemia, hyperuricemia, elevated plasma creatinine and hypouricuria, appeared at an early age, in probands DIV3 and DIV7 at the ages of 8 and 4 years old, respectively. Renal insufficiency appeared in all affected individuals in the third and fourth decades of life. The end stage renal disease developed in the sixth to seventh decade of life, which is relatively late compared to the typical cases of FJHN. The early onset of biochemical signs and relatively uniform clinical picture of the disease suggests that it is not necessary to use age-based penetrance models in subsequent linkage analysis. To assess the most current biochemical status, we collected urines from available individuals (all individuals from the youngest generation) and analyzed several biochemical parameters potentially helpful in assessment of kidney function. Compared to controls, in the patients we found significant changes in excretion patterns of almost all of the tested biochemical parameters. We used all these disease characteristics in discriminant analysis, which calculated posterior probabilities that the individuals belong to the disease or healthy group. This analysis allowed us to classify and confirm the affection status in the healthy individuals with a very high degree of certainty.

The most significant biochemical changes observed in patients were reduced excretion of urate, UMOD, and calcium. Reduced excretion of urate, which is a key diagnostic marker of FJHN/MCKD, was not surprising. Excretion patterns of UMOD observed in our study correlate well with recent observation in patients with mutations in the *UMOD* gene [36]. Our observation of reduced UMOD excretion even in patients with no mutation in UMOD gene is interesting. It suggests, that UMOD dysfunction plays a central role in UAKD development, and implies that UAKD symptoms may result from various defects affecting UMOD transcription, translation, posttranslational processing, cellular trafficking, GPI anchoring, cell surface stability, and release. Three distinct pathogenetic mechanisms leading to UMOD deficiency can already be seen in immunohistochemical analysis of kidney sections from patients with mutation in the *UMOD* gene, probands from the family reported here, and a proband from family GB6 (Fig. 4). Reasons for low calcium excretions observed in the patients are not clear. We can only hypothesize that through its calcium-binding domains UMOD contributes to the regulation of calcium metabolism. There are no data on urinary calcium excretion in other FJHN/MCKD patients, and such investigations are therefore warranted.

Having a high degree of certainty in the determination of affection status, following the preliminary results of genome scan, and analyzing 38 markers in 1q41 candidate locus, we observed in this family a statistically significant evidence of linkage with a maximum multipoint LOD score of 3.27. Analysis of the recombination events in affected individuals uncovered a single haplotype segregating with the disease and delimited candidate region by markers D1S3470 and D1S1644. Unfortunately, we were not able to confirm linkage to this candidate region in eight additional FJHN families which did not map to any of currently known FJHN/MCKD loci on 16p11.2 and 1q21. This result however does not lessen the probability or rule out the existence of the 1q41 candidate region we have identified. The phenotype observed in family BE1 is unusual among all the previously reported FJHN/MCKD families in having precocious anemia**,** absence of gout, abnormalities in ion**s** metabolism, different pattern of UMOD expression in kidney biopsy, and relatively late onset of renal insufficiency and therefore does not match the typical criteria set for FJHN earlier [37]. This presentation is suggestive of a genetically distinct origin of the disease in family BE1 and it is therefore probable that the locus we have identified really represents a new *UAKD* locus which is distinct from that one involved in previously investigated FJHN families.

The identified locus overlaps with three other kidney related diseases, autosomal-dominant fibronectin glomerulopathy [38], autosomal-recessive form of steroid-resistant nephrotic syndrome [39], and pseudohypoaldosteronism type II, [40], the phenotypes of which are however distinct from the phenotype defined in family BE1.

The critical region we have delimited is fully sequenced and contains about 300 genes. In our gene content evaluation and candidate gene selection we first focused on genes with prominent kidney expression. Applying several bioinformatic approaches, we did not identify any gene, the expression pattern of which would be kidney and nephron segment-specific as is UMOD or genes causing other kidney specific diseases [34]. Second, we focused on genes the defect of which may explain the observation of significantly reduced UMOD expression in kidney biopsies. Since we had no tissue for in situ hybridization analysis available, we considered two possibilities. First, reduced UMOD expression may be caused by a mutation in a transcription factor or hormone involved in UMOD gene transcription activation. Atypical FJHN associated with diabetes was found in a family with HNF1B mutation [41], and a pathogenic mechanism linking HNF1B mutation and FJHN symptoms was experimentally established in mice in which the kidney-specific inactivation of HNF1B led to greatly reduced UMOD expression [42]. A severe reduction in UMOD expression was also observed in patients with hyperprostaglandin E syndrome [43] and in two animal models, Brn1-deficient mouse [44] and in hypothyroid rats [45].

Second, reduced UMOD expression may be caused by a mutation affecting a protein involved in posttranslational modification or cellular traffic of UMOD. The improper modification and/or mistargeting of UMOD may then lead to a loss or masking of immunoreactive epitopes and protein does not crossreact with available antibodies.

Considering both possibilities we selected and sequenced in a first round nine candidate genes. In all of the selected genes no "classic" deleterious mutation was detected within the promoter regions, exon/intron junctions, and coding sequences. This finding, however, can not completely rule out the involvement of those genes in the disease development. The transcription of any of those genes can be greatly affected by mutations in distant promoter regions or by intronic mutations affecting mRNA processing. The cDNA studies, which would be very useful in this respect, could not be performed, as we did not have sufficient amounts of affected kidney tissues.

In addition to these analyzed genes, several transcription factors, G protein regulators, protein kinases, ion channels, and as yet uncharacterized proteins that may be hypothetically involved in regulation of UMOD expression are located within the critical interval. Further positional cloning efforts and efficient candidate gene selection are, however, currently greatly hampered by the size of delimited critical interval. Further progress depends on identification of other families linked to the region proposed here. Our work provides a new "genomic address" for such studies which may be performed in FJHN/MCKD families in which genetic linkage has not yet been demonstrated [11, 12, 22]. Positive results may not only confirm and further narrow the identified 1q41 region but may also have direct diagnostic/clinical relevance in affected families, enabling early treatment and preventing the progression of the renal lesion [37].

ACKNOWLEDGMENTS

This work was supported by grant 5NE/7046 from the Grant Agency of Ministry of Health of the Czech Republic. Institutional support was provided by grant VZ-111100003 from the Ministry of Education of the Czech Republic. We thank Stewart Cameron for critical reading the manuscript, Anne Simmonds for vital and long-standing contribution, Gert Matthijs, Elly Pijkels, and Sirpa Ala-Mello for their effort in collection of biological materials and patient data, Jana Sovová for performing the immunohistochemical analysis, Zdislava Vaníčková for help in ELISA analysis, and Květa Pelinková for performing the clinical biochemistry analyses.

Reprint requests to Stan Kmoch, Center for Applied Genomics, Institute for Inherited Metabolic Disorders, Ke Karlovu 2, 128 00 Prague 2, Czech Republic.
E-mail: skmoch@lf1.cuni.cz

REFERENCES

1. Duncan H, Dixon A: Gout, familial hyperuricaemia and renal disease. *Q J Med* 29:127–136, 1960
2. Cameron JS, Moro F, Simmonds HA: Gout, uric acid and purine metabolism in paediatric nephrology. *Pediatr Nephrol* 7:105–118, 1993
3. Goldman SH, Walker SR, Merigan TC, Jr., *et al*: Hereditary occurrence of cystic disease of the renal medulla. *N Engl J Med* 274:984–992, 1966
4. Scolari F, Puzzer D, Amoroso A, *et al*: Identification of a new locus for medullary cystic disease, on chromosome 16p12. *Am J Hum Genet* 64:1655–1660, 1999
5. Dahan K, Fuchshuber A, Adamis S, *et al*: Familial juvenile hyperuricemic nephropathy and autosomal dominant medullary cystic kidney disease type 2: Two facets of the same disease? *J Am Soc Nephrol* 12:2348–2357, 2001
6. Kamatani N, Moritani M, Yamanaka H, *et al*: Localization of a gene for familial juvenile hyperuricemic nephropathy causing underexcretion-type gout to 16p12 by genome-wide linkage analysis of a large family. *Arthritis Rheum* 43:925–929, 2000
7. Hateboer N, Gumbs C, Teare MD, *et al*: Confirmation of a gene locus for medullary cystic kidney disease (MCKD2) on chromosome 16p12. *Kidney Int* 60:1233–1239, 2001
8. Hart TC, Gorry MC, Hart PS, *et al*: Mutations of the UMOD gene are responsible for medullary cystic kidney disease 2 and familial juvenile hyperuricaemic nephropathy. *J Med Genet* 39:882–892, 2002
9. Turner JJ, Stacey JM, Harding B, *et al*: UROMODULIN mutations cause familial juvenile hyperuricemic nephropathy. *J Clin Endocrinol Metab* 88:1398–1401, 2003
10. Bleyer AJ, Woodard AS, Shihabi Z, *et al*: Clinical characterization of a family with a mutation in the uromodulin (Tamm-Horsfall glycoprotein) gene. *Kidney Int* 64:36–42, 2003
11. Wolf MT, Mucha BE, Attanasio M, *et al*: Mutations of the uromodulin gene in MCKD type 2 patients cluster in exon 4, which encodes three EGF-like domains. *Kidney Int* 64:1580–1587, 2003
12. Dahan K, Devuyst O, Smaers M, *et al*: A cluster of mutations in the UMOD gene causes familial juvenile hyperuricemic nephropathy with abnormal expression of uromodulin. *J Am Soc Nephrol* 14:2883–2893, 2003
13. Rampoldi L, Caridi G, Santon D, *et al*: Allelism of MCKD, FJHN and GCKD caused by impairment of uromodulin export dynamics. *Hum Mol Genet* 12:3369–3384, 2003
14. Kudo E, Kamatani N, Tezuka O, *et al*: Familial juvenile hyperuricemic nephropathy: Detection of mutations in the uromodulin gene in five Japanese families. *Kidney Int* 65:1589–1597, 2004
15. Rezende-Lima W, Parreira KS, Garcia-Gonzalez M, *et al*: Homozygosity for uromodulin disorders: FJHN and MCKD-type 2. *Kidney Int* 66:558–563, 2004
16. Christodoulou K, Tsingis M, Stavrou C, *et al*: Chromosome 1 localization of a gene for autosomal dominant medullary cystic kidney disease. *Hum Mol Genet* 7:905–911, 1998
17. Fuchshuber A, Kroiss S, Karle S, *et al*: Refinement of the gene locus for autosomal dominant medullary cystic kidney disease type 1 (MCKD1) and construction of a physical and partial transcriptional map of the region. *Genomics* 72:278–284, 2001
18. Auranen M, Ala-Mello S, Turunen JA, *et al*: Further evidence for linkage of autosomal-dominant medullary cystic kidney disease on chromosome 1q21. *Kidney Int* 60:1225–1232, 2001
19. Wolf MT, Karle SM, Schwarz S, *et al*: Refinement of the critical region for MCKD1 by detection of transcontinental haplotype sharing. *Kidney Int* 64:788–792, 2003
20. Cohn DH, Shohat T, Yahav M, *et al*: A locus for an autosomal dominant form of progressive renal failure and hypertension at chromosome 1q21. *Am J Hum Genet* 67:647–651, 2000
21. Parvari R, Shnaider A, Basok A, *et al*: Clinical and genetic characterization of an autosomal dominant nephropathy. *Am J Med Genet* 99:204–209, 2001
22. Ohno I, Ichida K, Okabe H, *et al*: Familial juvenile gouty nephropathy: Exclusion of 16p12 from the candidate locus. *Nephron* 92:573–575, 2002
23. Stiburkova B, Majewski J, Sebesta I, *et al*: Familial juvenile hyperuricemic nephropathy: Localization of the gene on chromosome 16p11.2-and evidence for genetic heterogeneity. *Am J Hum Genet* 66:1989- -1994, 2000
24. Stacey JM, Turner JJ, Harding B, *et al*: Genetic mapping studies of familial juvenile hyperuricemic nephropathy on chromosome 16p11-p13. *J Clin Endocrinol Metab* 88:464–470, 2003

25. Stiburkova B, Majewski J, Hodanova K, *et al*: Familial juvenile hyperuricaemic nephropathy (FJHN): Linkage analysis in 15 families, physical and transcriptional characterisation of the FJHN critical region on chromosome 16p11.2 and the analysis of seven candidate genes. *Eur J Hum Genet* 11:145–154, 2003
26. Kroiss S, Huck K, Berthold S, *et al*: Evidence of further genetic heterogeneity in autosomal dominant medullary cystic kidney disease. *Nephrol Dial Transplant* 15:818–821, 2000
27. McBride MB, Rigden S, Haycock GB, *et al*: Presymptomatic detection of familial juvenile hyperuricaemic nephropathy in children. *Pediatr Nephrol* 12:357–364, 1998
28. Kobayashi K, Fukuoka S: Conditions for solubilization of Tamm-Horsfall protein/uromodulin in human urine and establishment of a sensitive and accurate enzyme-linked immunosorbent assay (ELISA) method. *Arch Biochem Biophys* 388:113–120, 2001
29. Chagnon YC, Borecki IB, Perusse L, *et al*: Genome-wide search for genes related to the fat-free body mass in the Quebec family study. *Metabolism* 49:203–207, 2000
30. Dib C, Faure S, Fizames C, *et al*: A comprehensive genetic map of the human genome based on 5,264 microsatellites. *Nature* 380:152–154, 1996
31. Broman KW, Murray JC, Sheffield VC, *et al*: Comprehensive human genetic maps: Individual and sex-specific variation in recombination. *Am J Hum Genet* 63:861–869, 1998
32. O'Connell JR, Weeks DE: PedCheck: a program for identification of genotype incompatibilities in linkage analysis. *Am J Hum Genet* 63:259–266, 1998
33. Gudbjartsson DF, Jonasson K, Frigge ML, *et al*: Allegro, a new computer program for multipoint linkage analysis. *Nat Genet* 25:12–13, 2000
34. Chabardes-Garonne D, Mejean A, Aude JC, *et al*: A panoramic view of gene expression in the human kidney. *Proc Natl Acad Sci USA* 100:13710–13715, 2003
35. Kmoch S, Hartmannova H, Stiburkova B, *et al*: Human adenylosuccinate lyase (ADSL), cloning and characterization of full-length cDNA and its isoform, gene structure and molecular basis for ADSL deficiency in six patients. *Hum Mol Genet* 9:1501–1513, 2000
36. Bleyer AJ, Hart TC, Shihabi Z, *et al*: Mutations in the uromodulin gene decrease urinary excretion of Tamm-Horsfall protein. *Kidney Int* 66:974–977, 2004
37. Fairbanks L, Cameron J, Venkat-Raman G, *et al*: Early treatment with allopurinol in familial juvenile hyperuricaemic nephropathy (FJHN) ameliorates progression of renal disease in long-term studies. *Q J Med* 95:597–607, 2002
38. Vollmer M, Kremer M, Ruf R, *et al*: Molecular cloning of the critical region for glomerulopathy with fibronectin deposits (GFND) and evaluation of candidate genes. *Genomics* 68:127–135, 2000
39. Fuchshuber A, Jean G, Gribouval O, *et al*: Mapping a gene (SRN1) to chromosome 1q25-q31 in idiopathic nephrotic syndrome confirms a distinct entity of autosomal recessive nephrosis. *Hum Mol Genet* 4:2155–2158, 1995
40. Mansfield TA, Simon DB, Farfel Z, *et al*: Multilocus linkage of familial hyperkalaemia and hypertension, pseudohypoaldosteronism type II, to chromosomes 1q31-42 and 17p11-q21. *Nat Genet* 16:202–205, 1997
41. Bingham C, Ellard S, van't Hoff WG, *et al*: Atypical familial juvenile hyperuricemic nephropathy associated with a hepatocyte nuclear factor-1beta gene mutation. *Kidney Int* 63:1645–1651, 2003
42. Gresh L, Fischer E, Reimann A, *et al*: A transcriptional network in polycystic kidney disease. *EMBO J* 23:1657–1668, 2004
43. Schroter J, Timmermans G, Seyberth HW, *et al*: Marked reduction of Tamm-Horsfall protein synthesis in hyperprostaglandin E-syndrome. *Kidney Int* 44:401–410, 1993
44. Nakai S, Sugitani Y, Sato H, *et al*: Crucial roles of Brn1 in distal tubule formation and function in mouse kidney. *Development* 130:4751–4759, 2003
45. Schmitt R, Kahl T, Mutig K, *et al*: Selectively reduced expression of thick ascending limb Tamm-Horsfall protein in hypothyroid kidneys. *Histochem Cell Biol* 121:319–327, 2004

4 Results

4. 2 Alterations of uromodulin biology: a common denominator of the genetically heterogeneous FJHN/MCKD syndrome.

Vylet'al P*, **Kublová M***, Kalbácová M, Hodanová K, Baresová V, Stibůrková B, Sikora J, Hůlková H, Zivný J, Majewski J, Simmonds A, Fryns JP, Venkat-Raman G, Elleder M, Kmoch S.

Kidney Int. 2006 Sep;70(6):1155-69. Epub 2006 Aug 2., **IF 4, 773**

*** these authors contibuted equally**

Figure 5 (title of figure: Cellular localization of wild-type UMOD and individual UMOD mutants in permeabilized AtT-20 cells studied 18 h after Transfection) from this article was chosen by the editor of Kidney International as cover page of the second September issue (6^{th} issue of 70^{th} volume) in 2006

Alterations of uromodulin biology: a common denominator of the genetically heterogeneous FJHN/MCKD syndrome

P Vylet'al[1,2,8], M Kublová[1,2,8], M Kalbáčová[1,2], K Hodaňová[1,2], V Barešová[1,2], B Stibůrková[2], J Sikora[2], H Hůlková[2], J Živný[3], J Majewski[4], A Simmonds[5], J-P Fryns[6], G Venkat-Raman[7], M Elleder[2] and S Kmoch[1,2]

[1]Center for Applied Genomics, Charles University 1st School of Medicine, Prague, Czech Republic; [2]Institute for Inherited Metabolic Disorders, Charles University 1st School of Medicine, Prague, Czech Republic; [3]Department of Pathophysiology, Charles University 1st School of Medicine, Prague, Czech Republic; [4]Department of Human Genetics, McGill University and Genome Quebec Innovation Center, Montreal, Quebec, Canada; [5]Purine Research Unit, GKT, Guy's Hospital, London, UK; [6]Center for Human Genetics, University of Leuven, Leuven, Belgium and [7]Renal Unit, Queen Alexandra Hospital, Portsmouth, UK

Autosomal dominant hyperuricemia, gout, renal cysts, and progressive renal insufficiency are hallmarks of a disease complex comprising familial juvenile hyperuricemic nephropathy and medullary cystic kidney diseases type 1 and type 2. In some families the disease is associated with mutations of the gene coding for uromodulin, but the link between the genetic heterogeneity and mechanism(s) leading to the common phenotype symptoms is not clear. In 19 families, we investigated relevant biochemical parameters, performed linkage analysis to known disease loci, sequenced *uromodulin* gene, expressed and characterized mutant uromodulin proteins, and performed immunohistochemical and electronoptical investigation in kidney tissues. We proved genetic heterogeneity of the disease. *Uromodulin* mutations were identified in six families. Expressed, mutant proteins showed distinct glycosylation patterns, impaired intracellular trafficking, and decreased ability to be exposed on the plasma membrane, which corresponded with the observations in the patient's kidney tissue. We found a reduction in urinary uromodulin excretion as a common feature shared by almost all of the families. This was associated with case-specific differences in the uromodulin immunohistochemical staining patterns in kidney. Our results suggest that various genetic defects interfere with uromodulin biology, which could lead to the development of the common disease phenotype. 'Uromodulin-associated kidney diseases' may be thus a more appropriate term for this syndrome.

Kidney International advance online publication, 2 August 2006; doi:10.1038/sj.ki.5001728

KEYWORDS: familial nephropathy; genetic renal disease; uromodulin; Tamm–Horsfall protein; hyperuricemia

Correspondence: *S Kmoch, Center for Applied Genomics, Institute for Inherited Metabolic Disorders, Ke Karlovu 2, 128 00 Prague 2, Czech Republic. E-mail: skmoch@lf1.cuni.cz*

[8]These authors contributed equally to this work

Received 18 January 2006; revised 7 June 2006; accepted 13 June 2006

Familial juvenile hyperuricemic nephropathy (FJHN) (OMIM 162000),[1,2] and medullary cystic kidney diseases type 1 (MCKD1; OMIM 174000),[3] and type 2 (MCKD2; OMIM 603860)[4] are autosomal dominant tubulointerstitial nephropathies characterized by combinations of hyperuricemia, gouty arthritis, progressive renal insufficiency, and in some but not all families, medullary cysts. Recently it was found that in some families FJHN and MCKD2 are allelic disorders associated with mutations of the uromodulin gene (*UMOD*) coding for uromodulin (UMOD), Tamm–Horsfall protein.[5–12] However, *UMOD* mutations are not the only cause of the FJHN/MCKD phenotype,[8,9] which confirmed the broader genetic heterogeneity suggested by linkage studies.[13–18] The other candidate loci for FJHN/MCKD were identified on chromosome 1q21,[18–21] chromosome 1q41,[22] and a disease causing mutation in *HNF-1β* gene was found in a single family with features of FJHN and diabetes.[23] The mechanism linking the genetic heterogeneity to common disease symptom development in families with no *UMOD* mutations is not clear but it was suggested that UMOD dysfunction might be a common pathogenic mechanism.[22]

In this study, we have investigated 19 families showing characteristics of the FJHN/MCKD phenotype. In all families we performed linkage analysis to all known FJHN/MCKD loci, and analyzed the *UMOD* genomic sequence. Disease causing *UMOD* mutations were identified in only six families. We transiently expressed mutant proteins in eucaryotic cells and correlated its properties with biochemical, immunohistochemical, electron microscopy observations and specific disease symptoms. We also found that decreased urinary UMOD excretion is common to almost all patients independent of their corresponding linkage groups. The changes in urinary UMOD excretion were accompanied by case-specific differences of UMOD immunohistochemical staining patterns in kidney tissues.

Our work suggests that various genetic defects and mechanisms hamper UMOD biology, which lead to the

development of the FJHN/MCKD phenotype, and this lends support to the term of 'uromodulin-associated kidney diseases' (UAKD)[5,22] as a more appropriate for the FJHN/MCKD syndrome.

RESULTS

Clinical and biochemical findings

The pedigrees of families not yet reported are shown in Figure 1.

The family CZ4 came to attention through the probands N IV.3 (39 years old), and N IV.4 (31 years old), who suffered from gout. Biochemical investigation showed hyperuricemia, reduced fractional excretion of uric acid, and elevated concentration of plasma creatinine. Urinary UMOD excretion was absent. Their father N III.3 (62 years old) suffered from gout, which appeared for the first time at 23 years of age. He gradually developed renal insufficiency, which was treated at 55 years of age by dialysis and two years later by renal transplantation.

The family CZ5 came to attention through the proband F II.1 who suffered from gout, which appeared for the first time at 26 years of age. Biochemical investigation showed hyperuricemia (over 700 μmol/l), reduced fractional excretion of uric acid (5.9%), and elevated concentration of plasma creatinine (204 μmol/l). Following treatment with allopurinol, uricemia normalized, but the gouty attacks have persisted and patient (now 36 years old) has developed hypertension and chronic renal insufficiency. Sonography showed bilateral small kidneys with reduced parenchyma and single cyst (5 mm). Urinary UMOD excretion was absent. Molecular investigation revealed a pathogenic mutation resulting in C32Y substitution in UMOD protein. All the relatives have been reported healthy, their biochemical investigations showed no abnormalities, molecular investigation has not revealed in any of them the presence of pathogenic *UMOD* mutation. The possibility of nonpaternity was excluded by STR analysis.

The family US1 came to attention through the proband US I.1., who developed gout during pregnancy at the age of 27 years. Biochemical investigation showed hyperuricemia which did not responded to any treatment, reduced fractional excretion of uric acid and elevated concentration of plasma creatinine (185 μmol/l). Sonography showed small kidneys and renal biopsy revealed glomerular sclerosis and glomerular cysts. Individuals US II.1 (23 years old) and US II.2 (21 years old) showed hyperuricemia (>700 μmol/l), elevated concentration of plasma creatinine (>200 μmol/l), and urea (>7.5 mmol/l). Both patients responded to allopurinol and had no further gout. No urine was available for investigation of UMOD excretion.

The other families have been described previously.[13,15,18,24,25] The diagnosis of FJHN/MCKD was based on the familial occurrence of chronic renal disease associated with or preceded by early onset of hyperuricemia associated with reduced fractional excretion of uric acid $<5\%$. Biochemical investigations showed no notable abnormalities in other serum ion concentration. Urine biochemical parameters measured in available individuals are shown in Table 1. Clinical information on individuals with *UMOD* mutations is provided in Table 2.

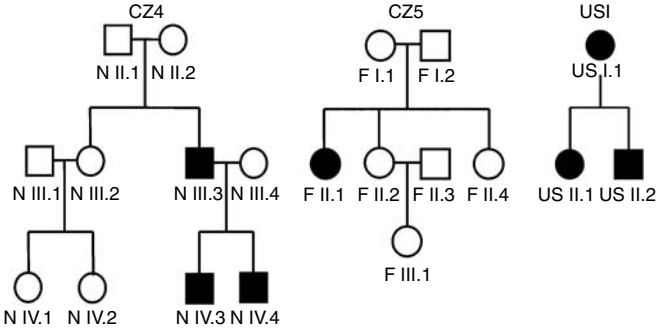

Figure 1 | Pedigree diagram of the investigated and not yet reported UAKD families. Black symbols denote affected individuals, open symbols denote unaffected individuals.

Genotyping and linkage analysis

Linkage analyses to the *UMOD* candidate locus in 16 families have been reported previously.[13,15] Families US1, CZ4, and CZ5 are reported here for the first time. As summarized in Table 3, the genetic linkage to the *UMOD* candidate locus on chromosome 16p11.2 was found in nine of the analyzed families and excluded, based on the logarithm of odds (LOD) $=-2$ criterion, in three families. A single family BE1 has been linked to UAKD locus on 1q41 previously[22] and in family GB4, a disease-causing mutation in *HNF-1β* gene was found.[23] In the rest of the families, no consistent haplotypes segregating with any of the currently known FJHN/MCKD loci were found.

UMOD gene analysis

Sequence analysis revealed missense mutations in six families (Table 3, Figure 2) and several novel single-nucleotide polymorphisms (Table 4). In families, which showed genetic linkage to the *UMOD* candidate locus on chromosome 16p11.2, and in which no *UMOD* mutation was identified, the 5.7-kb promoter sequence of the *UMOD* gene was also analyzed. Identified nucleotide changes are shown in Table 4.

Transient expression of UMOD

We cloned wild type and identified mutated *UMOD* cDNA sequences into mammalian expression vector and transiently expressed wt-UMOD protein in HEK-293, MDCK, CHO, and AtT-20 cells. The UMOD processing and localization patterns were essentially identical in all the cell lines (data not shown).[26] AtT-20 cells were chosen for further experiments as they were the most easy to culture, showed higher transfection efficiency, and performed best with available compartment markers antibodies.

Flow cytometry

The amount of the UMOD expressed on the plasma membrane was measured 6, 12, 18, and 24 h after transfection

Table 1 | Urine biochemical parameters measured in patients with mutation in *UMOD* gene (*UMOD*+), in patients with no mutation in *UMOD* gene (*UMOD*−), and in controls

Parameter	*UMOD*+ (*n*)	*P*	*UMOD*− (*n*)	*P*	Control (*n*=77)
Age	40±18 (21)	NS	40±16 (11)	NS	36±13
Creatinine (mmol/l)	6.5±3.2 (16)	NS	7.8±4.7 (31)	NS	9.0±5.4
Na/Cr (mmol/mmol)	13.9±7.9 (16)	NS	12.4±8.0 (31)	NS	13.9±8.8
K/Cr (mmol/mmol)	4.93±1.74 (16)	NS	4.45±2.18 (31)	⩽0.05	6.54±4.30
Mg^{2+}/Cr (mmol/mmol)	0.30±0.11 (14)	NS	0.29±0.18 (24)	NS	0.37±0.27
PO_4/Cr (mmol/mmol)	1.80±0.67 (14)	NS	2.01±1.27 (24)	NS	1.96±1.22
Cl/Cr (mmol/mmol)	12.3±7.5 (16)	NS	10.6±6.7 (31)	⩽0.01	17.2±11.6
Ca^{2+}/Cr (mmol/mmol)	0.19±0.19 (14)	⩽0.05	0.10±0.10 (24)	⩽0.0001	0.35±0.25
Osmolality (mOsm/kg)	329±65 (14)	⩽0.01	414±88 (13)	⩽0.05	572±278
UCB/Cr (mg/mmol)	69±167 (16)	⩽0.001	30±47 (31)	⩽0.001	8.5±8.7
UA/Cr (mmol/mol)	103±81 (14)	⩽0.0001	120±90 (24)	⩽0.0001	247±109
Umod/Cr (mg/g)	1.8±5.5 (14)	⩽0.0001	9.1±14.7 (32)	⩽0.0001	35.7±17.8

Values are reported as means±s.d.; *P*-values (*t*-test) correspond to the comparisons between the corresponding group and controls.
Cr, creatinine; NS, not significant; UA, uric acid; UCB, total protein.

Table 2 | Clinical information on individuals and families in which UMOD mutations were identified

Family (ID)	Sex/age	Age of onset	First symptoms	Blood pressure	Gout	Cr	UA	Renal ultrasound	Present status
Family CZ1, kindred A in Stiburkova et al[13]									
AI2	F/†	30y	Gout	+/?	+/30y	+/?	+/?	SK/single C	TR 58y; †63y
AII3	F/52y	18y	Gout	+/25y	+/18y	+/18y	+18y	SK, no C	RKF, arthritis
AII5	M/55y	20y	Gout	+/40y	+/20y	+/20y	+20y	SK, no C	TR 54y, no problems
AIII2	F/22y	6y[a]	HU	+/17y	No	+/6y	+/6y	SK, no C	No problems
AIII3	M/25y	12y[a]	HT	+/12y	No	+/12y	+/6y	Normal	RKF
Family CZ2, kindred B in Stiburkova et al[13]									
BI2	F/†	NA	NA	NA	NA	NA	NA	NA	RF/†49y
BI3	M/†	NA	NA	NA	+/?	NA	NA	NA	RF/†56y
BII1	M/39y	26y	Gout	NA	+/26y	+/31	+/26y	NA	RKF
BII2	M/53y	20y	Gout, HU	+/40y	+/20y	+/25y	+/20y	SK/multiple C	RKF
BII6	M/55y	17y	Gout	+/25y	+/?	+/20y	+/20y	NA	RF, TR 28y, 42y
BII9	F/53y	20y	HT	+/?	+/30y	+/23y	+/25y	SK/multiple C	RF, TR 43y
BIII1	F/31y	17y	Gout	+/23y	+/17y	+/17y	+/17y	SK/single C	RKF
BIII2	M/28y	15y[a]	FH	No	No	+/22y	+/15y	Normal	No problems
BIII3	F/27y	10y[a]	FH	+/25y	+/10y	+/10y	+/10y	Normal	No problems
BIII7	F/29y	24y[a]	FH	+/29y	No	+/26y	+/24y	Normal	HT
Family CZ5 (this report)									
II1	F/36y	26y	Gout	+/28y	+/26y	+/26y	+/26y	Normal	HT, obesity
Family BE[2], (15)									
EII3	M/68y	20y	Albuminuria	NA	+/30y	+/30y	+/30y	NA	TR 65y, no problems
EII4	M/62y	20y	Gout	NA	+/20y	+/20y	+/20y	NA	60y, hemodialysis
EII5	M/NA	40y	Gout	NA	+/40y	+/40y	+/40y	NA	NA
Family GB2[25]									
C4	F/†	31y	Gout	+/31y	+/31y	+/31y	+/31y	NA	TR; †36y
C1	F/43y	19y[a]	HU	No	No	No	No	No	No problems
C2	M/40y	16y[a]	HU	No	No	No	No	No	No problems
Family GB7, kindred 6 in McBride et al[24]									
L7	F	NA	HU	NA	+/?	NA	NA	NA	RF
L4	F	NA	HU	NA	+/?	NA	NA	NA	NA
L12	F	NA	HU	NA	NA	NA	NA	NA	NA
L10	F/†	15y	Gout	+/25y	+/15y	NA	NA	NA	Dialysis; †63y
L15	M	NA	HU	NA	NA	NA	NA	NA	NA

[a]Or when the first signs of the disease were recognized; +/y, + the symptom is present/age of onset.
C, renal cysts; Cr, serum (plasma) creatinine; FH, family history; HU, hyperuricemia; HT, hypertension; NA, not available; RF, renal failure; RKF, reduced kidney function; SK, small kidney size; TR, kidney transplantation; UA, serum (plasma) uric acid; UMOD, uromodulin; y, years.
†Died.

Table 3 | Summary of linkage analysis to all of currently known FJHN/MCKD loci with results of *UMOD* sequence analysis

Family	UMOD 16p11.2	UMOD mutation	MCKD1 1q21	UAKD 1q41
CZ1	+	C317Y	ND	ND
CZ2	+	M229R	ND	ND
CZ3	Ex	No	Ex	Ex
BE1	Ex	No	Ex	+
BE2	+	V273F	ND	ND
GB1	–	No	Ex	–
GB2	+	C126R	ND	Ex
GB3	+	No	–	–
GB4[a]	Ex	ND	ND	Ex
GB5	–	No	–	Ex
GB6	–	No	–	–
GB7	–/+[b]	P236L	ND	ND
GB8	+	No	ND	–
GB9	–	No	–	–
GB10	–	No	–	–
MCKD6	–	No	–	–
CZ4	+	No	–	–
CZ5	ND	C32Y	ND	ND
US1	+	No	–	–

Ex, families excluded for linkage on LOD $\leqslant -2$ criterion; +, Families segregating haplotypes consistent with linkage; –, Families with haplotypes inconsistent with linkage. ND, not done.
[a]Family GB4 with a disease-causing mutation in *HNF-1β* gene.
[b]Changing the original status in person L11 (GB7) to healthy, the LOD for that family goes up from –0.49 (before) to 1.47 (now) and the haplotypes are consistent with linkage.
FJHN, familial juvenile hyperuricemic nephropathy; LOD, Logarithm of odds; MCKD, medullary cystic kidney diseases; ND, not done; UMOD, uromodulin.

(Figure 3a). The time-course experiments showed a gradual increase of the wild-type UMOD protein expressed on plasma membrane with a plateau being reached in 18–24 h. Mutant proteins – 32Y, 229R, and 317Y (group I mutants) – showed patterns similar to the wild-type protein but the amount of protein localized on the plasma membrane was always lower as compared to the wild-type protein. The other mutant proteins – 126R, 236L, and 273F (group II mutants) showed a poor ability to reach the plasma membrane as compared to both, wild-type protein and group I mutants. The differences were statistically significant when measured 18 h post-transfection (Figure 3b).

SDS-PAGE and Western blot analysis

UMOD protein was analyzed in cell lyzates and medium (Figure 4). Wild-type protein was present in two 85 and 71 kDa zones (Figure 4a) as observed previously.[26] Both zones were smeared as they were probably composed of several poorly resolved bands corresponding to heterogeneous oligosaccharide processing of UMOD.[27] Complex deglycosylation treatment with peptide *N*-glycosidase F (PNGase F, Figure 4c), sialidase A (Figure 4e), and endo-*O*-glycosidase (Figure 4b) showed that both zones represent different UMOD glycoforms. The 85 kDa zone represents properly glycosylated, glycosyl-phosphatidylinositol (GPI)-modified and membrane-anchored UMOD protein as it corresponds to that of the molecular weight of UMOD excreted in urine. The 71 kDa zone represents a UMOD precursor probably lacking branched sialic acids and terminal sialic acid residues as its molecular weight corresponds to that of the 71 kDa zone appearing after the treatment of the urinary and recombinant wt-UMOD with sialidase A (Figure 4e). This 71 kDa UMOD precursor probably accumulates owing to protein overexpression, as it is not markedly observed in a stable UMOD-expressing cell line (Figure 4f), and probably represents a protein intermediate along the secretory pathway. No detectable effect on the wild-type mobility was observed after endo-*O*-glycosidase treatment (Figure 4b), which suggests that either no significant *O*-glycosylation of UMOD occurs in AtT-20 cells, or that the action of the enzyme is blocked by extended modification of the core structure by other saccharides.[28] In agreement with Rindler *et al.*,[26] neither wild-type and later nor any of the mutant UMOD proteins were detected in medium of cultured cells (data not shown).

As seen in Figure 4a, group I mutants – 32Y, 229R, and 317Y – showed similar amounts of the fully processed 85 kDa form as the wild-type protein. The 229R mutant differed from the other two by the absence of 71 kDa form and the appearance of a 69 kDa band, which probably corresponds to the endoplasmic reticulum (ER)-retained intermediate lacking GPI anchor (see below) and missing Golgi-mediated glycosylation trimming. Group II mutants showed low amounts of the fully processed 85 kDa form and retention of the 69 kDa intermediate protein.

Following the treatment of expressed proteins with PNGase F (Figure 4c), the group I mutants as well as the wild-type protein appeared in two 57 and 52 kDa forms which represent, respectively, the protein precursor and the protein with cleaved C-terminal ecto-domain and covalently linked GPI anchor. Observed incomplete processing may be attributed to protein overexpression as reported previously.[29,30] GPI anchor attachment was less pronounced in the 229R mutant and no precursor processing and GPI linkage was observed in group II mutants.

Treatment with sialidase A (Figure 4e) showed that two proteins from group I mutants – 32Y and 317Y – as well as the wild-type protein sialidase A were sensitive and corresponded to a single zone of ~71 kDa. Partial resistance to sialidase treatment was observed in the 229 R and 236L mutants, which produced two zones of 71 and 65 kDa. Other group II mutants showed the original 71 kDa zone and the processed form of 62 kDa.

Complex deglycosylation with a mixture of all three enzymes (Figure 4d) showed comparable results as for the PNGase F treatment (Figure 4c).

Immunofluorescence

Images of the individual UMOD proteins are shown in Figure 5. The wild-type protein localized on the plasma membrane, with almost no detectable intracellular retention. All the mutant proteins showed granular retention of UMOD in the ER. The ER retention was less pronounced in group I

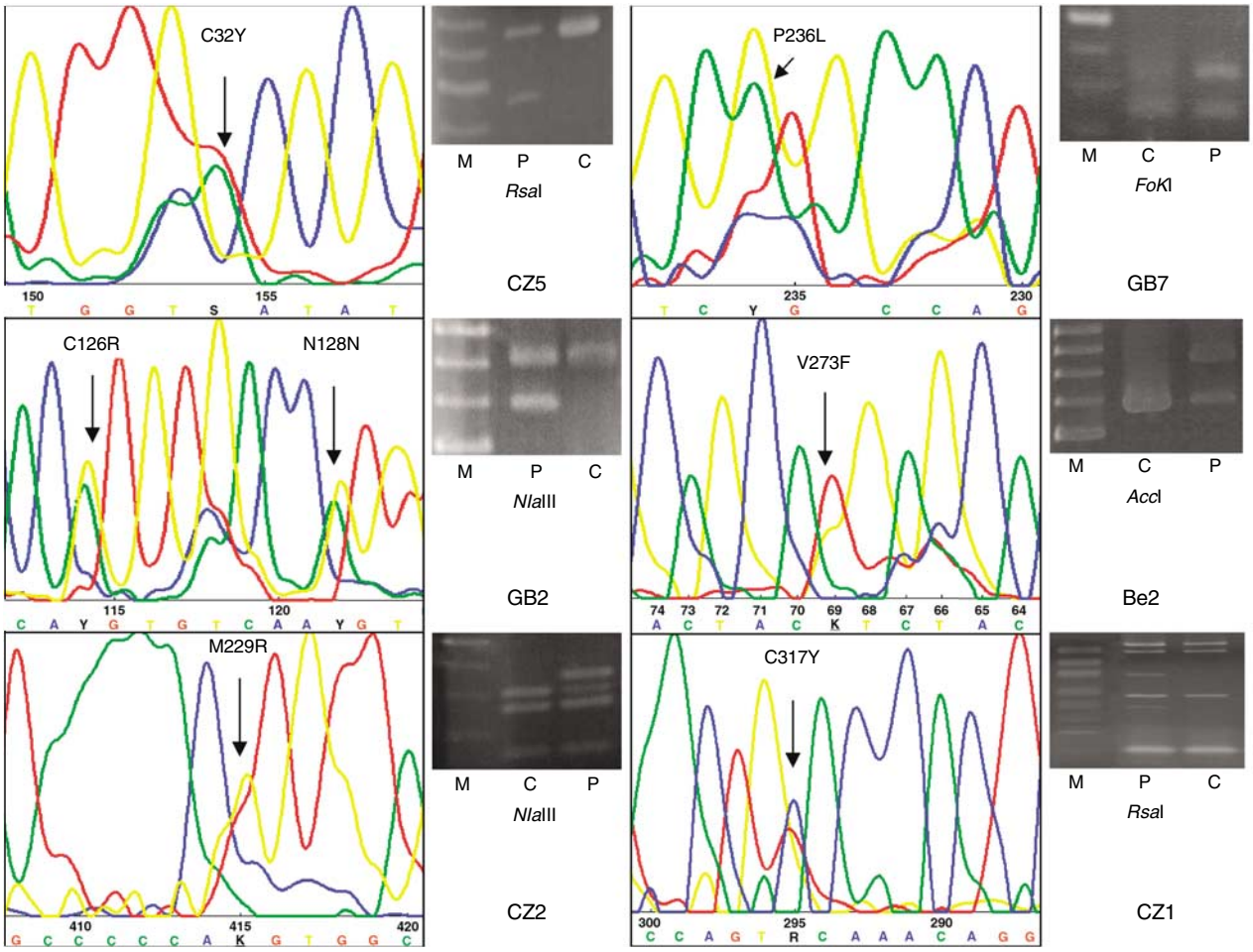

Figure 2 | *UMOD* mutations detected in indicated families and polymerase chain reaction-restriction fragment length polymorphism assays employed in genotyping and mutation analysis. M: size marker standard, P: patient, C: control individual.

mutant proteins, which also showed strong presence on the plasma membrane. The group II mutants showed almost no plasma membrane localization. No significant presence of the proteins in Golgi apparatus was observed (data not shown).

Urinary UMOD analysis

UMOD excretion was investigated in spot urine collected from 71 controls and 96 subjects originating from the 15 affected families. From the 96 subjects, 49 have been classified as affected, based on the clinical and biochemical data obtained. Of those 49 patients, 14 patients have the *UMOD* mutation, 14 patients are from families linked to the *UMOD* region on chromosome 16p11.2 but in whom no *UMOD* mutations have been found, 16 patients are from families in which a linkage has not yet been found, and four patients are from a single family which mapped to the region on chromosome 1q41.[22] One other patient with *UMOD* mutation was investigated after kidney transplantation (T). Qualitative analysis showed the absence or decrease of urinary UMOD excretion in almost all affected individuals. Abnormal UMOD processing has been observed in several individuals, classified as healthy and originated from different families (Figure 6). No co-segregation of the abnormal UMOD processing and disease phenotype has been found.

Quantitative analysis showed that the UMOD excretion was significantly reduced in almost all affected individuals, independent of the linkage groups they belonged to (Figure 7a). Analysis performed separately for each family (Figure 7b) showed that UMOD excretion was reduced in all families except family CZ3. Decreased UMOD excretion was present also in young patients with relatively preserved renal function (Figure 7c). UMOD excretion normalized in a single patient with the *UMOD* mutation after kidney transplantation.

Immunohistochemistry and electron microscopy

Prominent differences in the patterns of UMOD immunohistochemical staining were observed in available kidney tissues. They encompass massive intracellular UMOD accumulation in the patients with *UMOD* mutation, and presence of UMOD in hyaline casts with low intracellular positivity, irregular pattern of UMOD staining or strongly reduced UMOD expression in patients with not yet established molecular defects. Patterns of UMOD staining were correlated and mostly parallel with that of the epithelial membrane antigen (MUC1) (Figure 8).

Table 4 | Nucleotide changes found in *UMOD* genomic sequence

gDNA position	Nucleotide change	Exon/intron	Protein change	dbSNP	Family
UMOD promotor					
−5634	C→C/A				
−5589	G→G/A				
−5494	G→G/A				
−5316	T→T/C				US1
−5074	T→T/C				
−4893	A→A/G				
−4754	G→G/A				
−2531	T→T/C				
−1379	T→T/C				GB3
UMOD-coding sequence					
110	G→G/A	Int 3			
1821	C→C/T	Ex 4	128Asn→Asn		GB2
1959	T→T/C	Ex 4	174Cys→Cys	rs7193058	
2061	G→G/A	Ex 4	208Gln→Gln		
2229	G→G/A	Ex 4	264Val→Val	rs13335818	
2352	G→G/T	Int 4			
2380	T→A	Int 4			
2427	C→C/A	Int 5			CZ3
2793	C→C/A	Int 5			
4662	C→C/T	Int 6		rs4506906	
4779	G→G/A	Int 6			
4805	G→G/A	Int 6			
9192	C→G	Int 7		rs9928757	GB5
9299	T→T/C	Int 7		rs9646256	
9370	C→C/T	Int 7			
9377	C→C/A	Int 7			
13 540	C→C/A	Int 9			

[a]Numbering: initiation codon ATG=1.
Underline values indicate nucleotide changes observed exclusively in indicated families.
Ex, exon; Int, intron; UMOD, uromodulin.

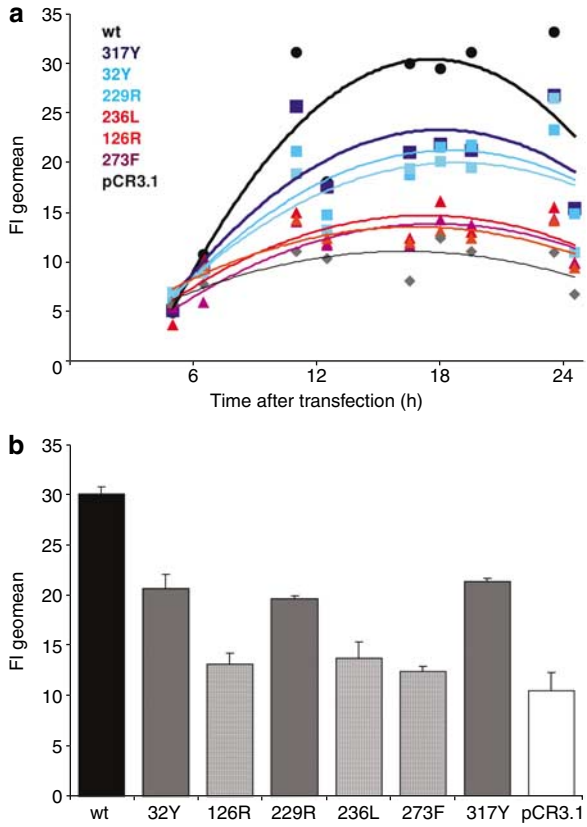

Figure 3 | Fluorescence-activated cell sorter analysis of UMOD-positive AtT-20 cells transfected with pCR3.1 eucaryotic expression vector containing wild-type and identified mutant *UMOD* cDNAs. (**a**) Time course showing saturation of the UMOD plasma membrane exposition in between 18 and 24 h after the transfection. Two groups of mutants, either showing similar dynamics of the plasma membrane exposition as the wild-type protein but with the final amount of the protein significantly reduced (group I mutants, blue lines), and mutants not exposed on the plasma membrane (group II mutants, red lines), are clearly separated. (**b**) The differences in UMOD plasma membrane exposition between wild-type UMOD (black column), group I mutants (gray columns), and group II mutants (dashed columns) measured 18 h after transfection. The values represent means of fluorescence ±s.d. of three transfection experiments carried out in triplicates. The differences between wild-type UMOD, group I mutants, and group II mutants were statistically significant when tested by one-way analysis of variance using Tukey's multiple comparison procedure ($P<0.001$).

Material for ultrastructural studies was available from a single case with M229R UMOD mutation. The tubular epithelium displayed a number of nonspecific changes such as atrophy, hyper regeneration, and increase in dense lysosomal residual bodies. Significant changes related to molecular pathology of the disorder are shown and described in Figure 9. The ER storage material has been identified as an accumulated UMOD protein by immunofluorescence analysis of renal biopsy tissue (Figure 10).

DISCUSSION

FJHN/MCKD is a genetically heterogeneous disease with only a proportion of families having a demonstrable mutation in the *UMOD* gene.

In this work, we characterized in more detail 19 families fulfilling the basic clinical and biochemical criteria of FJHN/MCKD. We completed linkage analysis to three currently known FJHN/MCKD loci – *UMOD* loci on chromosome 16p11.2, MCKD1 loci on chromosome 1q21, and the UAKD loci on chromosome 1q41. The greatest proportion, nine families, showed linkage to the *UMOD* candidate region, the rate of which is comparable with results in several other studies.[8,9,14] Linkage to the UAKD loci on chromosome 1q41 was detected in just a single family and linkage to MCKD1 was not found. Finally, no linkage to any of the above loci was detected in eight families and in a single family, family CZ3, all three loci were even excluded on the LOD = −2 criterion. This result suggests that a second major or several other FJHN/MCKD loci exist and remain to be discovered. Another explanation for such a low detection rate might be false negative results of linkage analysis. In the FJHN/MCKD phenotype, this might be caused by late onset and/or reduced penetrance of the disease,[13,31] phenocopy or by co-occurrence of the disease trait with relatively common phenotypes such as hyperuricemia,[9] gout, or the metabolic syndrome.[32] However, analysis of the *UMOD* genomic sequence showed the false negativity of linkage analysis only in a single family GB7. Interestingly, *UMOD* mutations were found in five but

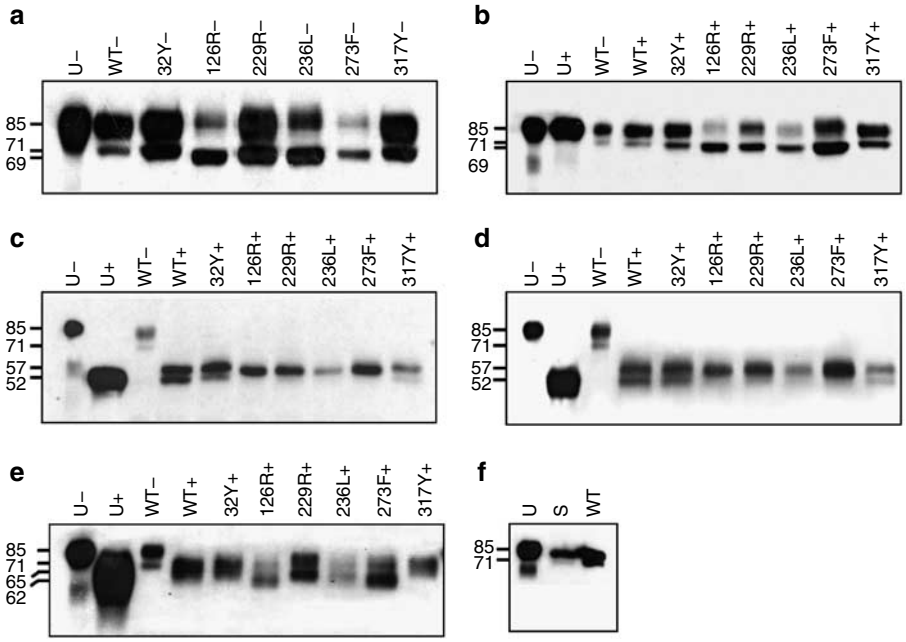

Figure 4 | Western blot analyses of wild-type (WT) and individual mutated UMOD-expressing AtT-20 cell lyzates treated by various glycosidases. Lyzates of transfected cells, (**a**) harvested 24 h after transfection, were treated by (**b**) *O*-glycanase, (**c**) PNGase F, (**e**) sialidase A, and (**d**) mixture of PNGase F, *O*-glycanase, and sialidase. Panel (**f**) shows Western blot analysis of lyzates of stable (S) and transiently (WT) UMOD-expressing cell lines. Uromodulin isolated from urine (U) was used as a control; + indicates treatment and − indicates no treatment with corresponding glycosidase. Molecular weights are given in kilodaltons on the left-hand side of the individual panels. The molecular weight calibration curve was constructed by plotting decadic logarithm of molecular weights versus distance of corresponding bands of the protein molecular weight marker (Precision Plus Protein Kaleidoscope Standards, Biorad) from the upper edge of the SDS-PAGE gel after blotting. Molecular weights of different UMOD glycoforms were calculated from their distances using logarithmic regression equation.

not in the other four families originally linked to *UMOD* candidate region on chromosome 16p11.2. This finding may be explained by false positivity of the linkage analysis that has arisen from the small number of investigated individuals or indicates the existence of other disease gene located in the *UMOD* candidate region. The other explanation may be undetected mutations in *UMOD* promoter sequence or the existence of synonymous exonic mutations and/or intronic mutations affecting proper *UMOD* mRNA processing. We found several such 'private mutations' in the promoter sequence in families US1 and GB3 but their potential pathogenic effect has not yet been further investigated. Overall, only six disease-causing mutations in the *UMOD* gene were identified in 19 FJHN/MCKD families. Such a low detection rate is in agreement with at least two similar extensive studies[8,9] and further confirms the considerable degree of genetic heterogeneity of the FJHN/MCKD phenotype.

Functional consequences of *UMOD* mutations

From the identified mutations, three mutations have been already reported in other families. Mutation C126R was found in family GB2, in Italian family F5,[9] and an Austrian family 13/00,[6] which is a branch of family GB2. Mutation C317Y was found in Czech family CZ1 and in an Italian family MCKD no. 1.[7] Mutation P236L was found in GB7 and in the Japanese family no. 1.[10] Three identified mutations, C32Y, M229R, and V273F are novel. To prove their pathogenity, we cloned all the mutations and characterized transiently expressed mutant proteins. All the mutant proteins differed from the wild-type protein in their ability to reach the exoplasmic face of the plasma membrane and according to it they clustered into two groups. Group I mutants showed reduced ability and group II mutants were not able to reach the plasma membrane. The ability of the protein to reach the plasma membrane was determined by GPI modification. GPI-modified proteins (group I mutants) may exit endoplasmic reticulum, enter secretory pathway and reach the plasma membrane. In these mutants, the associated pathogenic mechanism may thus be related to impaired intracellular trafficking, decreased ability of the protein to be properly internalized and exposed on the exoplasmic face of the plasma membrane, or defective assembly of UMOD filaments. In contrary, mutants lacking GPI (group II mutants) cannot exit and remain retained within ER lumen, which leads to marked expansion of the organelle, attenuation of the translation of other polypeptides, activation of the stress signaling pathway, and progressive tissue damage.[30] Both mechanisms are compatible with a concept of autosomal dominant negative effect of the disease. In the group I mutants, both the wild-type and misfolded mutant protein may be trapped together in transport cargo vesicles where their co-occurrence may delay or hamper intracellular

Figure 5 | Cellular localization of wild-type UMOD and individual UMOD mutants in permeabilized AtT-20 cells studied 18 h after transfection. Columns (**a, i, q, y, gg, oo, ww, l, m, u, cc, kk, ss, aaa**) UMOD; columns (**b, j, r, z, hh, pp, xx**) PDI as a marker of ER; column (**f, n, v, dd, ll, tt, bbb**) pan-Cadherin as a marker of plasma membrane. Column (**c, k, s, aa, ii, qq, yy**) show merged signals of individual UMOD proteins (red fluorescence) with the markers of ER (green fluorescence). In column (**d, l, t, bb, jj, rr, zz**), the resulting colocalization map of UMOD and PDI is shown. Column (**g, o, w, ee, mm, uu, ccc**) show merged signals of individual UMOD proteins (red fluorescence) with the marker of plasma membrane (green fluorescence). In column (**h, p, x, ff, nn, vv, ddd**), the resulting colocalization map of UMOD and pan-Cadherin is shown. Wild-type UMOD localized exclusively on the (**g, h**) plasma membrane, with only minor presence in the (**c, d**) ER. (**k, s, aa, ii, qq, yy** and **l, t, bb, jj, rr, zz**) All the mutant proteins show retention of UMOD in the ER. The ER retention is less pronounced in the properly GPI-modified group I mutants 32Y (**k, l**), and 317 Y(**yy, zz**), which show also strong presence on the plasma membrane (**o, p** and **ccc, ddd**), respectively. Only partly GPI-processed 229R mutant (row **y–ff**), and GPI-unprocessed 126R mutant (row **q–x**) show irregular plasma membrane localization (**ee, ff** and **w, x** respectively). The transport compromised group II mutants 236L (row **gg–nn**) and 273F (row **oo–vv**) show almost no plasma membrane localization (**mm, nn** and **uu, vv** respectively).

trafficking process or lateral transmembrane transport as in several other kidney diseases.[33] Another alternatives might be that the presence of the mutant protein on the cell surface hampers proper copolymerization and assembly of UMOD filaments,[34] which then affects the proper biological function(s) of UMOD on the plasma membrane. In the group II mutants, the disease mechanism might be different. The mutant protein is probably retained and accumulates gradually in the ER. The accumulation of unfolded proteins in the ER leads to marked expansion of the organelle, attenuation of the translation of other polypeptides, activation of the stress signaling pathway, and progressive tissue damage.[35] Two questions however remain to be answered. First, to what extent the results of *in vitro* studies correlate with the real situation in kidney tissues of affected individuals and second, whether any particular phenotypic patterns might be assigned to individual UMOD mutant groups. Such a correlation might have been done only for the mutation 229R. According to the expression studies, this mutation seems to have both the suggested pathogenic effects. The protein should reach to a certain extent the plasma membrane but it should also be less efficiently GPI modified and retained in the ER. This possibility corresponds well with the immunohistochemistry and electron microscopy investigations of the kidney tissue available from the patient. Eventual genotype-specific phenotypic differences cannot be judged easily since only a small number of families and inadequate clinical data are currently available. More

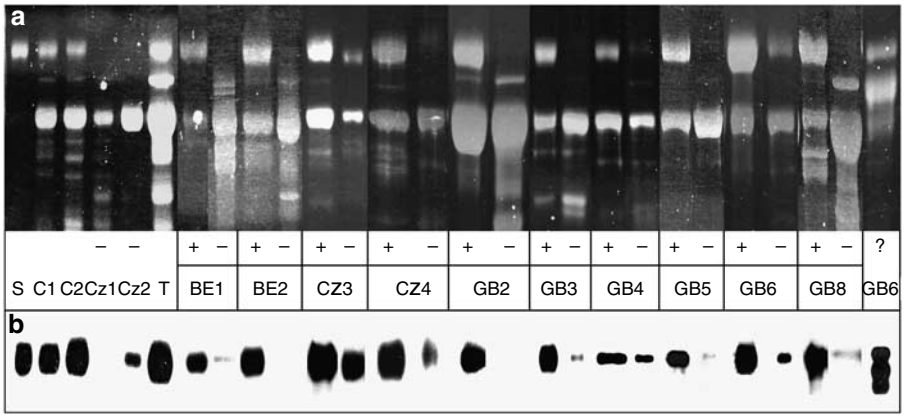

Figure 6 | Qualitative analysis (SDS-PAGE and Western blot) of urinary UMOD in a single affected proband (–) and healthy individual (+) from UAKD families showing the absence or significant reduction in urinary UMOD excretion. S: uromodulin standard isolated from control urine, C: control urines, T: urine from patient with UMOD mutation after successful kidney transplantation ?: abnormal UMOD processing that has been observed in several healthy individuals from various families.

work in this direction is warranted since different pathogenic mechanisms might be targeted more effectively by different therapeutic approaches.[36]

Defects in UMOD biology seems to be common to the pathogenesis of FJHN/MCKD

The link between UMOD mutations, intracellular protein aggregation, and absence of the protein in urine has been shown in several studies.[7,9,37] However, not much information is available on UMOD excretion in FJHN/MCKD patients having no *UMOD* mutation. Analysis in a single such family showed normal UMOD excretion[9] and it has been suggested that a drop in the UMOD urinary excretion is specific only for cases with *UMOD* mutations.[38] Our investigations however showed that UMOD excretion was significantly decreased in all but one family. Decreased UMOD excretion could be considered as being secondary to renal disease.[39] While this might be true we favor the explanation that our findings reflect and highlight the central role of UMOD dysfunction in the development of common FJHN/MCKD symptoms. This central role might be attributed to the absence of proper UMOD function on the plasma membrane and/or in the urine, as this factor seems to be common to all the cases we have had the opportunity to investigate. The absence of UMOD properly expressed on the plasma membrane might result from different molecular mechanisms such as reduced gene expression resulting from a mutation of transcription factor as demonstrated in the case of the *HNF1-β* mutation[23,40] or in hypothyroidism,[41] from protein mistargeting, inability of the protein to be properly GPI-anchored, from gradual gene expression silencing resulting from aberrant developmental processes or from aberrant cellular differentiation or proliferation.[42]

UAKD

Possible pathogenic mechanisms linking *UMOD* mutations with characteristic disease symptoms have been discussed recently.[43] Hyperuricemia in UAKD results from the underexcretion of uric acid. This feature usually appears at an early age, well before the renal disease becomes apparent, so it seems that hyperuricemia is somehow directly linked to UMOD dysfunction. Our data from 36 UAKD patients show positive correlation between urinary urate and urinary UMOD concentrations ($r = 0.62$; $P < 0.0001$), and this trend has been observed also in 113 healthy individuals ($r = 0.18$; $P \leqslant 0.05$). As minor *UMOD* expression has been found also in proximal tubule cells,[44] abnormal urate handling and UMOD dysfunction linked through enhanced urate reabsorption in the proximal tubule is a distinct possibility. Another mechanism linked to hyperuricemia might be a dysfunction of the UMOD containing water barrier on the apical membrane of the loop of Henle cells, which may result in nonspecific transcellular transport of urate in this segment. Defects in the secretion, or enhanced postsecretory reabsorption of urate linked to UMOD absence in the distal convoluted tubule or collecting duct is yet another possibility.

A common feature present in UAKD patients is also a loss of urine concentrating efficiency.[31,43] It has been suggested that low urine osmolality may be attributed to dysregulation of ion transport and electrolyte homeostasis. We hypothesize that decreased urine concentrating efficiency might result from the absence of released UMOD in both, the distal convoluted tubule and the collecting duct. UMOD is fundamental in cast formation, which takes place in the late section of the distal tubules and the early section of the collecting duct. Absence of UMOD may thus prevent cast formation, enhance urine flow, impair water reabsorption, and result in low urine osmolality. Abnormality in urine flow and dysregulation of major distal tubule transporters in UMOD−/− mice[45] supports this hypothesis.

To conclude, in our work we have shown that various genetic defects and mechanisms hamper various steps in UMOD biology, which probably leads to the development of

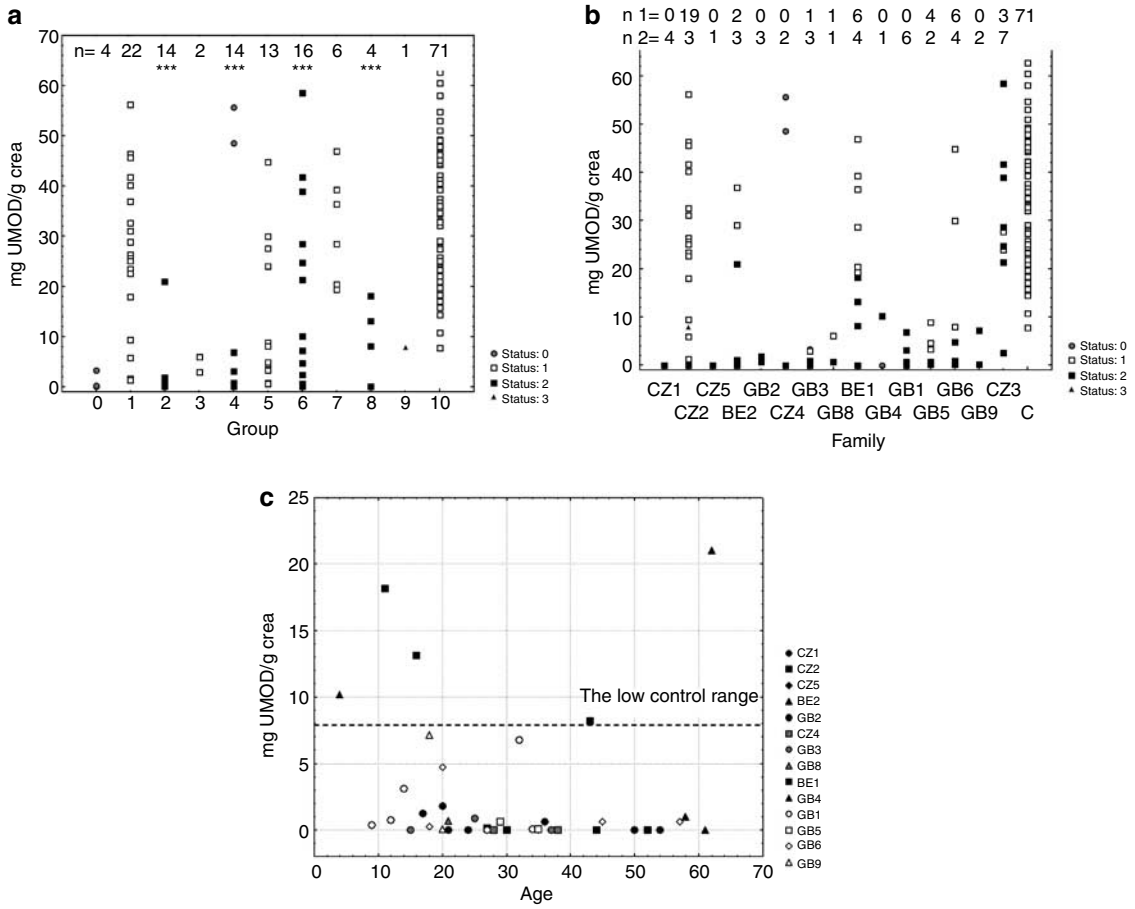

Figure 7 | Quantitative analysis (enzyme-linked immunosorbent assay) of urinary UMOD excretion. (**a**) Data plotted for the individual linkage groups. 0: individuals of unknown status; 1: healthy individuals and 2: affected individuals from families with the *UMOD* mutation; 3: healthy individuals and 4: affected individuals from families linked to the *UMOD* candidate region on chromosome 16p11.2 but in which no mutation in the *UMOD* gene has been detected; 5: healthy individuals and 6: affected individuals from families in which no linkage to any of UAKD loci has been detected; 7: healthy individuals and 8: affected individuals from a family linked to UAKD loci on chromosome 1q41; 9: a patient with UMOD mutation after successful kidney transplantation; 10: controls. The number of individuals investigated in each of the groups is indicated above corresponding columns. *P*-values (*t*-test) correspond to the comparisons between indicated group and controls; ***$P < 0.001$. (**b**) The same results of quantitative urinary UMOD excretion plotted for individual families and showing reduction of UMOD excretion in all families with an exception of CZ3. The number of individuals investigated in each group is indicated above the corresponding columns; n 1 and n 2 denotes the number of healthy and affected individuals, respectively. Status 0 represents an unknown phenotype, status 1 and 2 represent healthy and affected individual, respectively. Status 3 represents a patient with UMOD mutation after successful kidney transplantation. (**c**) Decreased UMOD excretion is present also in young patients with relatively preserved renal function. It is suggestive that in the reported families the UMOD dysfunction precedes the onset of renal insufficiency. Black symbols denote patients from families with *UMOD* mutations. Gray symbols denote patients from families with no *UMOD* mutations but showing linkage to UAKD-associated loci. Black/white symbols denote patients from families in which no linkage to any of UAKD loci has been detected. Patients from family CZ3 showing normal UMOD excretion are not included in this figure. Control values of UMOD excretion are reported in Table 1 and its distribution is shown in panels **a** and **b**.

common FJHN/MCKD phenotype. This finding supports the term of UAKD[5,22] as the most appropriate for the FJHN/MCKD designation. Given the frequency of urate abnormalities, an alternative designation might be 'familial urate–uromodulin nephropathy'.

UMOD urinary excretion analysis with subsequent *UMOD* sequencing is currently the primary diagnostic test in UAKD patients. As suggested previously[9] and clearly documented here in family CZ5, this investigation should be undertaken even in sporadic cases, in the absence of family history as *de novo* mutations do appear. However, as the protein has tendency to aggregate, a caution should be exercised in interpretation of UMOD quantitative data.[37,46] Qualitative Western blot analysis represents at least in our hands the preferred method for extensive urinary UMOD testing which has the potential to identify more UAKD families without *UMOD* mutations. In these families, linkage analysis to already defined loci or alternatively, whole genome scans may be performed to confirm and narrow the existing loci, or to reveal not yet identified UAKD loci. Identification and characterization of other UAKD loci may help to clarify the exact biological roles of UMOD, provide better diagnostic techniques, and finally suggest potential therapeutic targets and therapeutic approaches.[36]

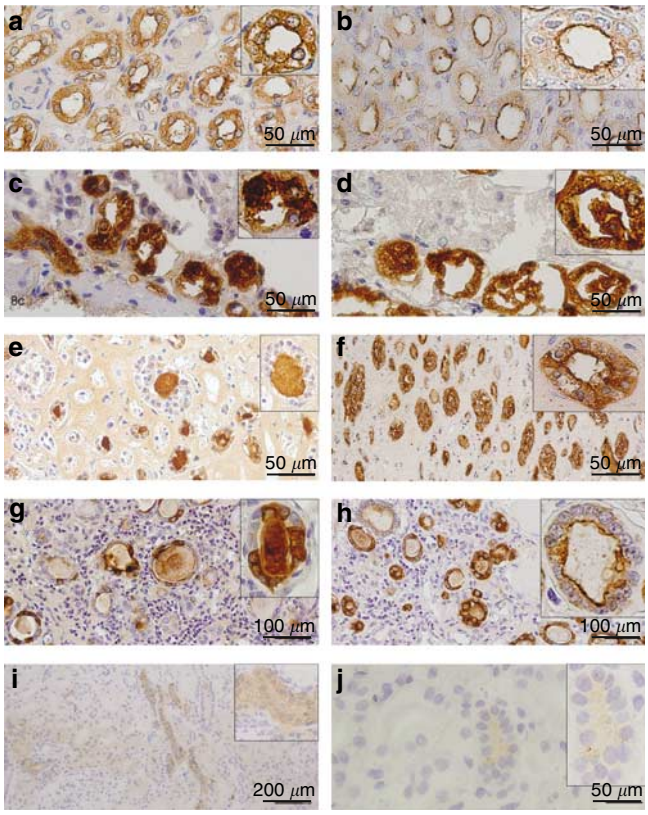

Figure 8 | Immunohistochemical analysis of UMOD and MUC1 in kidney biopsies. In control tissue, (**a**) UMOD shows diffuse cytoplasmic staining with maximal intensity on the apical membranes and (**b**) MUC1 is expressed almost exclusively on the apical membrane of the cells of the ascending limb of the loop of Henle. The tissue of patient with the *UMOD* mutation shows (**c**) massive intracellular accumulation of UMOD and (**d**) abundant MUC1 presence with strong uniform intracellular positivity. In a case from family GB3 linked to the *UMOD* region on chromosome 16p11.2 but in which no *UMOD* mutation has been found, shows (**e**) UMOD to be present in hyaline casts with low intracellular positivity and (**f**) normal or variable intracellular increase of MUC1 exceeding this of UMOD. A case from family GB6, in which no linkage to any of the UAKD loci has been found shows (**g**) an irregular pattern of UMOD staining and (**h**) normal or close to normal expression of MUC1. In three patients from a family linked to 1q41, (**i**) UMOD and (**j**) MUC1 expression is strongly reduced and both proteins are present in the form of tiny intracellular granules.

MATERIALS AND METHODS

Patients

In total, 19 families were enrolled in this study. Five families are from the Czech Republic. Pedigrees of families CZ1, CZ2, and CZ3 have been reported (A, B, and C, respectively) previously;[13] CZ4, CZ5, and a single family from the USA (US1) are reported here for the first time. Ten families are from Great Britain (GB1–GB10) and two families are from Belgium (BE1, BE2).[15] The single family is from Finland (MCKD family 6).[18]

Biochemical investigations

Collected random spot urine samples were stored at −80°C. Urine total protein, creatinine, uric acid, magnesium, calcium, phosphate, sodium, potassium, chloride, osmolality, and qualitative and quantitative UMOD excretion were determined as previously described.[22]

Genotyping and linkage analysis

For MCKD/FJHN locus on chromosome 16p11.2, a set of 13 microsatellite markers D16S499–D16S501–D16S3056–D16S3041–D16S3036–D16S3046–D16S403–D16S412–D16S3130–D16S417–D16-S420–D16S3113–D16S401; for MCKD1 locus on chromosome 1q21, a set of three microsatellite markers D1S1153–D1S2624–D1S2125; and for UAKD locus on chromosome 1q41, a set of 11 markers GATA31D05–D1S373–D1S2773–D1S245–D1S2703–D1S490–D1S1644–D1S1656–D1S2649–D1S2850–D1S2670 were used. Genotyping and linkage analysis were performed as previously described.[15,22]

UMOD gene analysis

Genomic organization, upstream promoter region sequence, and genomic sequence of the *UMOD* gene were obtained using pairwise BLASTN comparison of the *UMOD* cDNA sequence with the corresponding genomic sequences. Primers for polymerase chain reaction amplification and sequencing were designed using software Oligo (National Biosciences, Plymouth, MN, USA). Genomic fragments covering the promoter and all of the exons and intron–exon boundaries were polymerase chain reaction amplified and sequenced as previously described[47] in a single proband and unaffected individual in each family.

UMOD cDNA expression constructs

UMOD cDNA was prepared from kidney cDNA using primers UcDNA1U and UcDNA2L, cloned into pCR4-TOPO sequencing vector (Invitrogen, Paisley, UK) and introduced into the *Escherichia coli* TOP 10'F strain (Invitrogen, Paisley, UK). Mammalian expression construct UcDNAwt/pCR3.1 was prepared by subcloning of the UcDNAwt/pCR4-TOPO insert into pCR3.1 vector (Invitrogen, Paisley, UK) using *Eco*RI restriction sites. Mutated constructs UcDNA229R/pCR3.1, UcDNA126R/pCR3.1, and UcDNA236L/pCR3.1 were prepared by cloning of mutation bearing polymerase chain reaction fragments, first into UcDNAwt/pCR4-TOPO construct (UMODE4,5: 51980U and Cy5ex4,5-A primers, *Sac*I a BstAPI restriction sites), and then into pCR3.1 vector (Invitrogen, Paisley, UK), using *Eco*RI restriction sites as described above.

Mutated constructs UcDNA32Y/pCR3.1, UcDNA273F/pCR3.1, and UcDNA317Y/pCR3.1 were prepared by site-directed mutagenesis of UcDNAwt/pCR3.1 construct (GeneTailor kit, Invitrogen, Paisley, UK). All the primer sequences are available upon request.

Cell culture and transfection experiments

AtT-20 pituitary cells were maintained in DMEM high glucose medium supplemented with 10% (vol/vol) fetal calf serum, 100 U/ml penicillin G, and 100 μg/ml streptomycin sulfate (PAA Laboratories GmbH, Pashing, Austria). Cells were used at 80% confluence. Transfection was carried out with 4 μg of DNA using Lipofectamine 2000™ (Invitrogen, Paisley, UK).

Flow cytometry

AtT-20 cells were seeded in six-well tissue culture plates (BD Falcon, Palo Alto, CA, USA). Following 24-h incubation, the cells were transfected and harvested at the indicated time after the transfection. 2×10^5 cells were washed, stained for 30 min with 1.5 μg of fluorescein isothiocyanate-labeled (Fluorescent Labelling Kit, Roche, Prague, Czech Republic) anti-UMOD – rabbit polyclonal IgG (Biogenesis, Pool, UK), washed and fixed in 2% paraformaldehyde. Fluorescence was measured using FACSCalibur flow cytometer and analyzed using the Cell Quest software version 3.3 (Becton Dickinson, San Jose, CA, USA). Cell-surface expression of UMOD was quantified as the geomean of the fluorescence of gated fluorescein isothiocyanate-positive cells.

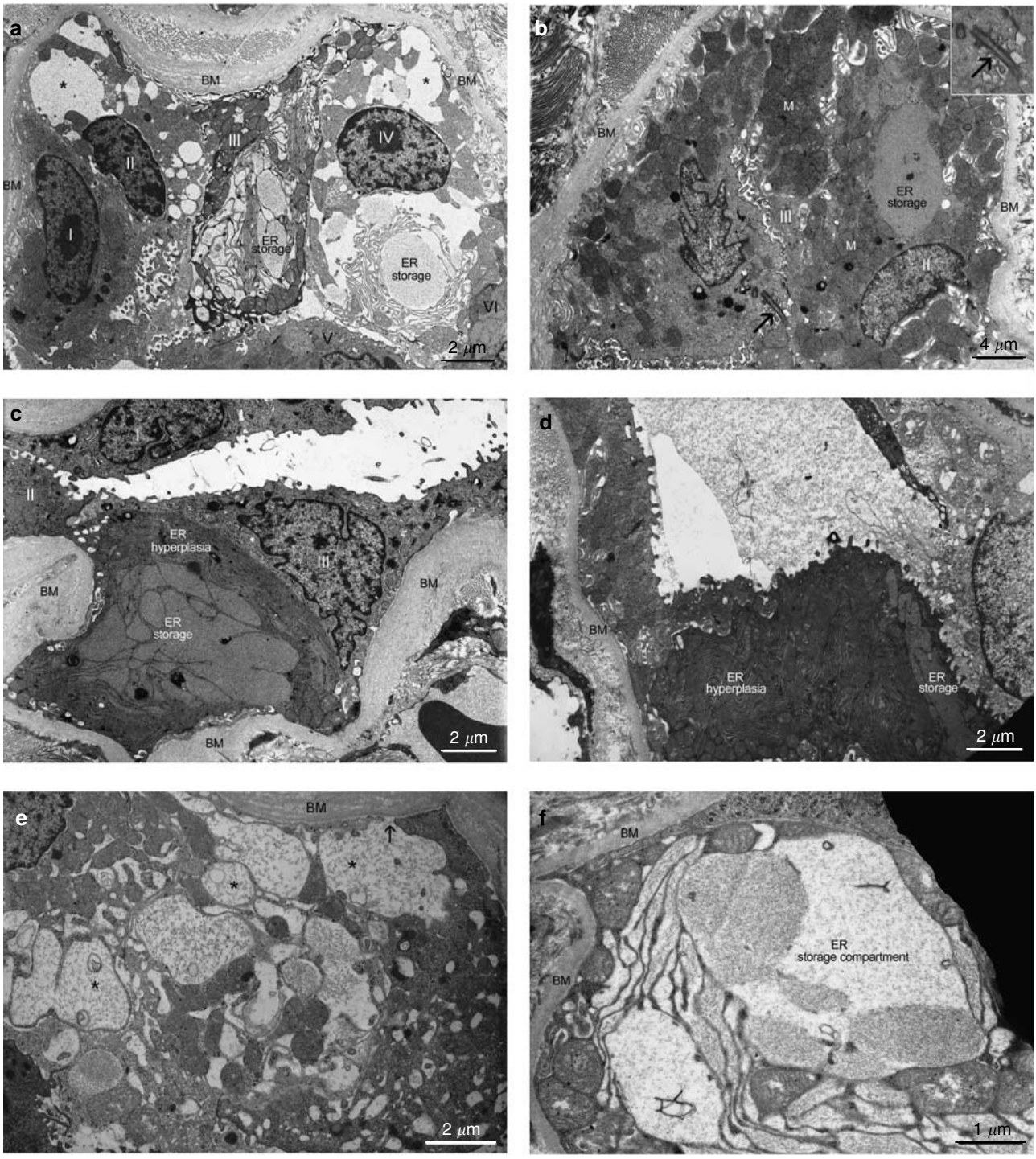

Figure 9 | Ultrastructural changes in renal tubules compatible with the ascending loop of Henle prepared from the kidney biopsy from a patient with the M229R UMOD mutation. Individual cells are labeled with Roman numerals, ER: endoplasmic reticulum, BM: basal membranes, M: mitochondria, *: distended basal invaginations. (**a**) Considerably distended basal invagination of many tubules projected into the cell interior. (**b**) Thickened and partly multilayered basement membrane with increase in the number of mitochondria, which were generally rich in the inner membrane system. Cilia is shown by arrow and enlarged in the insert. (**c**, **d**) Abundant slender rough ER cisternae arranged in slightly curved or whirled stacks present in flat tubular epithelia and in those exhibiting expansion of ER with amorphous moderately dense content ranging from slight to massive distension. (**e**) Detail of distension of the basal cisternae with an arrow pointing to their communication with the extracellular space. (**f**) Detail of the ER storage areas either bulging into the apical pole luminally or facing the basolateral pole.

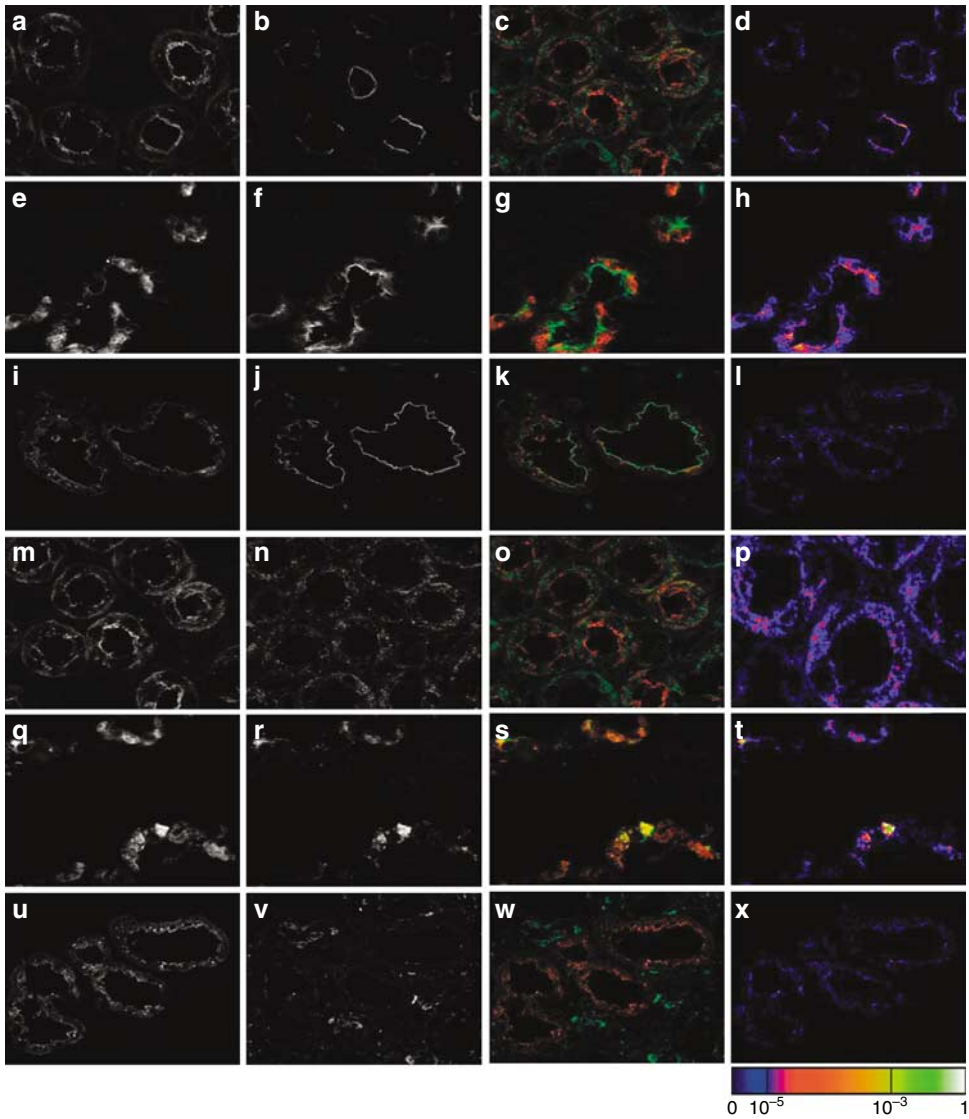

Figure 10 | Cellular localization of the UMOD in the renal biopsy tissue from control (rows a–d, m–p), from patient with the M229R UMOD mutation (rows e–h, q–t), and from patient with no *UMOD* mutation (rows i–l, u–x). In control, (**a**) UMOD is clearly present on apical membrane of the ascending limb of the loop of Henle cells as is the plasma membrane marker (**b**) MUC1. In patient with the M229R UMOD mutation, both (**e**) UMOD and (**f**) MUC1 show diffuse intracellular staining pattern suggesting decreased efficiency in targeting of membrane cargo proteins into plasma membrane. In patient with no *UMOD* mutation, (**i**) UMOD shows diffuse intracellular staining pattern as in the case with UMOD mutation, but (**j**) MUC1 expression is clearly normal. (**c, g, k**) Merged fluorescence signals of UMOD (red) and MUC1 (green), and (**d, h, l**) colocalization maps employing overlap coefficient values are shown for control, patient with the M229R UMOD mutation and patient with no *UMOD* mutation, respectively. In patient with the M229R UMOD mutation, the intracellular localization of (**q**) UMOD was assigned almost exclusively into (**r**) ER as seen by fluorescence signal merge of UMOD (red) with (**s**) ER marker PDI (green) and the corresponding (**t**) colocalization map. The degree of UMOD signal retention in ER is demonstrated by the overlap coefficient value (note the scale of the lookup tables, compare to (**p**), and see the massive ER storage in Figure 9). In patient with no *UMOD* mutation, the intracellular localization of (**u**) UMOD could not be attributed to (**v**) ER, as seen by fluorescence signal merge of UMOD (red) with (**w**) ER marker PDI (green) and the (**x**) corresponding colocalization map. In this case, the defect seems to affect either proper UMOD internalization into plasma membrane or inefficient targeting and/or processing of UMOD in ER (compare colocalization maps for (**p**) control and (**x**) patient).

SDS-PAGE and Western blotting analysis

Harvested cells were resuspended in phosphate-buffered saline containing Protease inhibitor coctail (Sigma, Prague, Czech Republic) and sonicated. UMOD was detected as described previously.[22]

Deglycosylation experiments

Deglycosylation experiments were performed on cell lyzates using the GlycoPro™ enzymatic deglycosylation kit (ProZyme Inc., San Leandro, CA, USA). Deglycosylated products were analyzed by sodium dodecyl sulfate-polyacrylamide gel electrophoresis (SDS-PAGE) and Western blot as described above.

Immunofluorescence

For immunofluorescence, 6.5×10^4 of AtT-20 cells were grown on 70 mm^2 glass chamber slides (BD Falcon – 4Chamber Polystyrene Vessel Tissue Culture Treated Glass Slide) for 24 h and transfected as described above. At 18 h after the transfection, the cells were fixed with 100% methanol at −20°C, washed, blocked with 5% FCS

and incubated for 1 h at 37°C with primary antibodies: rabbit Anti-Human THP polyclonal antibodies (Biogenesis, Poole, UK) or Anti-Human THP mouse IgG2b monoclonal antibodies (Cedarlane, Hornby, Ontario, Canada) for UMOD detection; anti-PDI – mouse monoclonal IgG1 (Stressgen, San Diego, CA, USA) for ER localization; anti-GS28 mouse monoclonal IgG (Stressgen, San Diego, CA, USA) for Golgi localization, and anti-pan Cadherin rabbit polyclonal IgG (Abcam, Cambridge, UK) for plasma membrane localization. For fluorescence detection, secondary antibodies – Alexa 568 goat anti-rabbit IgG and Alexa 488 goat anti-mouse IgG (Molecular Probes, Invitrogen, Paisley, UK) were used. Prepared slides were mounted in fluorescence mounting medium Immu-Mount (Shandon Lipshaw, Pittsburgh, PA, USA) and analyzed by confocal microscopy.

Image acquisition and analysis

XYZ images sampled according to Nyquist criterion were acquired using Nikon Eclipse E800 microscope equipped with C1 confocal head, Nikon PlanApo objective (60X, N.A.1.40), 488 and 543 nm laser lines, and 515 ± 15 and 590 ± 15 nm band pass filters. Images were deconvolved using classic maximum likelihood restoration algorithm in the Huygens Professional Software (SVI, Hilversum, The Netherlands).[48] The colocalization maps employing single pixel overlap coefficient values ranging from 0 to 1[49] were created in the Huygens Professional Software. The resulting overlap coefficient values are presented as the pseudocolor whose scale is shown in corresponding lookup tables.

Immunohistochemistry studies

Formaldehyde- or ethanol-fixed kidney samples were analyzed. Immunodetection of UMOD was performed as previously described.[22] Immunodetection of mucine 1 (MUC1, epithelial membrane antigen) was carried out using anti-MUC1 monoclonal antibody (DAKO, Carpinteria, CA, USA).

Electron microscopy

Renal biopsy specimen was fixed with 4% paraformaldehyde (PFA) in 0.1 M phosphate buffer for 30 min and by buffered 1% OsO_4 for 2 h, dehydrated and embedded into Epon. Thin sections were double contrasted with uranyl acetate and lead nitrate. Photographs were obtained on a TESLA 500 electron microscope.

ACKNOWLEDGMENTS

We thank Gert Matthijs, Elly Pijkels, Bernard Kaplan, Sirpa Ala-Mello, Miroslav Ryba for their efforts in collection of biological materials and patient's data; Jana Sovová for performing the immunohistochemical analysis; Květa Pelinková and Slávka Vaníčková for performing the clinical biochemistry analyses; and Stewart Cameron for critical reading of the manuscript. This work was supported by grant 5NE/7046 from the Grant Agency of the Ministry of Health of the Czech Republic and grant 203 200 from the Grant Agency of Charles University of Prague. Institutional support was provided by grant MSM0021620806 from the Ministry of Education of the Czech Republic.

REFERENCES

1. Duncan H, Dixon A. Gout, familial hyperuricaemia and renal disease. *Q J Med* 1960; **29**: 127–136.
2. Cameron JS, Moro F, Simmonds HA. Gout, uric acid and purine metabolism in paediatric nephrology. *Pediatr Nephrol* 1993; **7**: 105–118.
3. Goldman SH, Walker SR, Merigan Jr TC *et al.* Hereditary occurrence of cystic disease of the renal medulla. *N Engl J Med* 1966; **274**: 984–992.
4. Scolari F, Puzzer D, Amoroso A *et al.* Identification of a new locus for medullary cystic disease on chromosome 16p12. *Am J Hum Genet* 1999; **64**: 1655–1660.
5. Hart TC, Gorry MC, Hart PS *et al.* Mutations of the UMOD gene are responsible for medullary cystic kidney disease 2 and familial juvenile hyperuricaemic nephropathy. *J Med Genet* 2002; **39**: 882–892.
6. Turner JJ, Stacey JM, Harding B *et al.* UROMODULIN mutations cause familial juvenile hyperuricemic nephropathy. *J Clin Endocrinol Metab* 2003; **88**: 1398–1401.
7. Rampoldi L, Caridi G, Santon D *et al.* Allelism of MCKD, FJHN and GCKD caused by impairment of uromodulin export dynamics. *Hum Mol Genet* 2003; **12**: 3369–3384.
8. Wolf MT, Mucha BE, Attanasio M *et al.* Mutations of the uromodulin gene in MCKD type 2 patients cluster in exon 4, which encodes three EGF-like domains. *Kidney Int* 2003; **64**: 1580–1587.
9. Dahan K, Devuyst O, Smaers M *et al.* A cluster of mutations in the UMOD gene causes familial juvenile hyperuricemic nephropathy with abnormal expression of uromodulin. *J Am Soc Nephrol* 2003; **14**: 2883–2893.
10. Kudo E, Kamatani N, Tezuka O *et al.* Familial juvenile hyperuricemic nephropathy: detection of mutations in the uromodulin gene in five Japanese families. *Kidney Int* 2004; **65**: 1589–1597.
11. Rezende-Lima W, Parreira KS, Garcia-Gonzalez M *et al.* Homozygosity for uromodulin disorders: FJHN and MCKD-type 2. *Kidney Int* 2004; **66**: 558–563.
12. Tinschert S, Ruf N, Bernascone I *et al.* Functional consequences of a novel uromodulin mutation in a family with familial juvenile hyperuricaemic nephropathy. *Nephrol Dial Transplant* 2004; **19**: 3150–3154.
13. Stiburkova B, Majewski J, Sebesta I *et al.* Familial juvenile hyperuricemic nephropathy: localization of the gene on chromosome 16p11.2- and evidence for genetic heterogeneity. *Am J Hum Genet* 2000; **66**: 1989–1994.
14. Stacey JM, Turner JJ, Harding B *et al.* Genetic mapping studies of familial juvenile hyperuricemic nephropathy on chromosome 16p11–p13. *J Clin Endocrinol Metab* 2003; **88**: 464–470.
15. Stiburkova B, Majewski J, Hodanova K *et al.* Familial juvenile hyperuricaemic nephropathy (FJHN): linkage analysis in 15 families, physical and transcriptional characterisation of the FJHN critical region on chromosome 16p11.2 and the analysis of seven candidate genes. *Eur J Hum Genet* 2003; **11**: 145–154.
16. Ohno I, Ichida K, Okabe H *et al.* Familial juvenile gouty nephropathy: exclusion of 16p12 from the candidate locus. *Nephron* 2002; **92**: 573–575.
17. Kroiss S, Huck K, Berthold S *et al.* Evidence of further genetic heterogeneity in autosomal dominant medullary cystic kidney disease. *Nephrol Dial Transplant* 2000; **15**: 818–821.
18. Auranen M, Ala-Mello S, Turunen JA *et al.* Further evidence for linkage of autosomal-dominant medullary cystic kidney disease on chromosome 1q21. *Kidney Int* 2001; **60**: 1225–1232.
19. Christodoulou K, Tsingis M, Stavrou C *et al.* Chromosome 1 localization of a gene for autosomal dominant medullary cystic kidney disease. *Hum Mol Genet* 1998; **7**: 905–911.
20. Fuchshuber A, Kroiss S, Karle S *et al.* Refinement of the gene locus for autosomal dominant medullary cystic kidney disease type 1 (MCKD1) and construction of a physical and partial transcriptional map of the region. *Genomics* 2001; **72**: 278–284.
21. Wolf MT, Karle SM, Schwarz S *et al.* Refinement of the critical region for MCKD1 by detection of transcontinental haplotype sharing. *Kidney Int* 2003; **64**: 788–792.
22. Hodanova K, Majewski J, Kublova M *et al.* Mapping of a new candidate locus for uromodulin-associated kidney disease (UAKD) to chromosome 1q41. *Kidney Int* 2005; **68**: 1472–1482.
23. Bingham C, Ellard S, van't Hoff WG *et al.* Atypical familial juvenile hyperuricemic nephropathy associated with a hepatocyte nuclear factor-1beta gene mutation. *Kidney Int* 2003; **63**: 1645–1651.
24. McBride MB, Rigden S, Haycock GB *et al.* Presymptomatic detection of familial juvenile hyperuricaemic nephropathy in children. *Pediatr Nephrol* 1998; **12**: 357–364.
25. Fairbanks L, Cameron J, Venkat-Raman G *et al.* Early treatment with allopurinol in familial juvenile hyperuricaemic nephropathy (FJHN) ameliorates progression of renal disease in long-term studies. *QJM* 2002; **95**: 597–607.
26. Rindler MJ, Naik SS, Li N *et al.* Uromodulin (Tamm–Horsfall glycoprotein/uromucoid) is a phosphatidylinositol-linked membrane protein. *J Biol Chem* 1990; **265**: 20784–20789.
27. van Rooijen JJ, Voskamp AF, Kamerling JP *et al.* Glycosylation sites and site-specific glycosylation in human Tamm–Horsfall glycoprotein. *Glycobiology* 1999; **9**: 21–30.

28. Easton RL, Patankar MS, Clark GF *et al.* Pregnancy-associated changes in the glycosylation of Tamm–Horsfall glycoprotein. Expression of sialyl Lewis(x) sequences on core 2 type O-glycans derived from uromodulin. *J Biol Chem* 2000; **275**: 21928–21938.
29. Moran P, Raab H, Kohr WJ *et al.* Glycophospholipid membrane anchor attachment. Molecular analysis of the cleavage/attachment site. *J Biol Chem* 1991; **266**: 1250–1257.
30. Field MC, Moran P, Li W *et al.* Retention and degradation of proteins containing an uncleaved glycosylphosphatidylinositol signal. *J Biol Chem* 1994; **269**: 10830–10837.
31. Bleyer AJ, Woodard AS, Shihabi Z *et al.* Clinical characterization of a family with a mutation in the uromodulin (Tamm–Horsfall glycoprotein) gene. *Kidney Int* 2003; **64**: 36–42.
32. Short RA, Tuttle KR. Clinical evidence for the influence of uric acid on hypertension, cardiovascular disease, and kidney disease: a statistical modeling perspective. *Semin Nephrol* 2005; **25**: 25–31.
33. Devonald MA, Karet FE. Renal epithelial traffic jams and one-way streets. *J Am Soc Nephrol* 2004; **15**: 1370–1381.
34. Jovine L, Qi H, Williams Z *et al.* The ZP domain is a conserved module for polymerization of extracellular proteins. *Nat Cell Biol* 2002; **4**: 457–461.
35. Rutishauser J, Spiess M. Endoplasmic reticulum storage diseases. *Swiss Med Wkly* 2002; **132**: 211–222.
36. Choi SW, Ryu OH, Choi SJ *et al.* Mutant Tamm–Horsfall glycoprotein accumulation in endoplasmic reticulum induces apoptosis reversed by colchicine and sodium 4-phenylbutyrate. *J Am Soc Nephrol* 2005; **10**: 3006–3014.
37. Bleyer AJ, Hart TC, Shihabi Z *et al.* Mutations in the uromodulin gene decrease urinary excretion of Tamm–Horsfall protein. *Kidney Int* 2004; **66**: 974–977.
38. Devuyst O, Dahan K, Pirson Y. Tamm–Horsfall protein or uromodulin: new ideas about an old molecule. *Nephrol Dial Transplant* 2005; **20**: 1290–1294.
39. Serafini-Cessi F, Malagolini N, Cavallone D. Tamm–Horsfall glycoprotein: biology and clinical relevance. *Am J Kidney Dis* 2003; **42**: 658–676.
40. Gresh L, Fischer E, Reimann A *et al.* A transcriptional network in polycystic kidney disease. *EMBO J* 2004; **23**: 1657–1668.
41. Schmitt R, Kahl T, Mutig K *et al.* Selectively reduced expression of thick ascending limb Tamm–Horsfall protein in hypothyroid kidneys. *Histochem Cell Biol* 2004; **121**: 319–327.
42. Chakraborty J, Below AA, Solaiman D. Tamm–Horsfall protein in patients with kidney damage and diabetes. *Urol Res* 2004; **32**: 79–83.
43. Scolari F, Caridi G, Rampoldi L *et al.* Uromodulin storage diseases: clinical aspects and mechanisms. *Am J Kidney Dis* 2004; **44**: 987–999.
44. Chabardes-Garonne D, Mejean A, Aude JC *et al.* A panoramic view of gene expression in the human kidney. *Proc Natl Acad Sci USA* 2003; **100**: 13710–13715.
45. Bachmann S, Mutig K, Bates J *et al.* Renal effects of Tamm–Horsfall protein (uromodulin) deficiency in mice. *Am J Physiol Renal Physiol* 2005; **288**: F559–F567.
46. Kobayashi K, Fukuoka S. Conditions for solubilization of Tamm–Horsfall protein/uromodulin in human urine and establishment of a sensitive and accurate enzyme-linked immunosorbent assay (ELISA) method. *Arch Biochem Biophys* 2001; **388**: 113–120.
47. Kmoch S, Hartmannova H, Stiburkova B *et al.* Human adenylosuccinate lyase (ADSL), cloning and characterization of full-length cDNA and its isoform, gene structure and molecular basis for ADSL deficiency in six patients. *Hum Mol Genet* 2000; **9**: 1501–1513.
48. Landmann L. Deconvolution improves colocalization analysis of multiple fluorochromes in 3D confocal data sets more than filtering techniques. *J Microsc* 2002; **208**: 134–147.
49. Manders EMM, Verbeek FJ, Aten JA. Measurement of colocalization of objects in dual-color confocal images. *J Microsc* 1993; **169**: 375–382.

OFFICIAL JOURNAL OF THE INTERNATIONAL SOCIETY OF NEPHROLOGY

kidney INTERNATIONAL

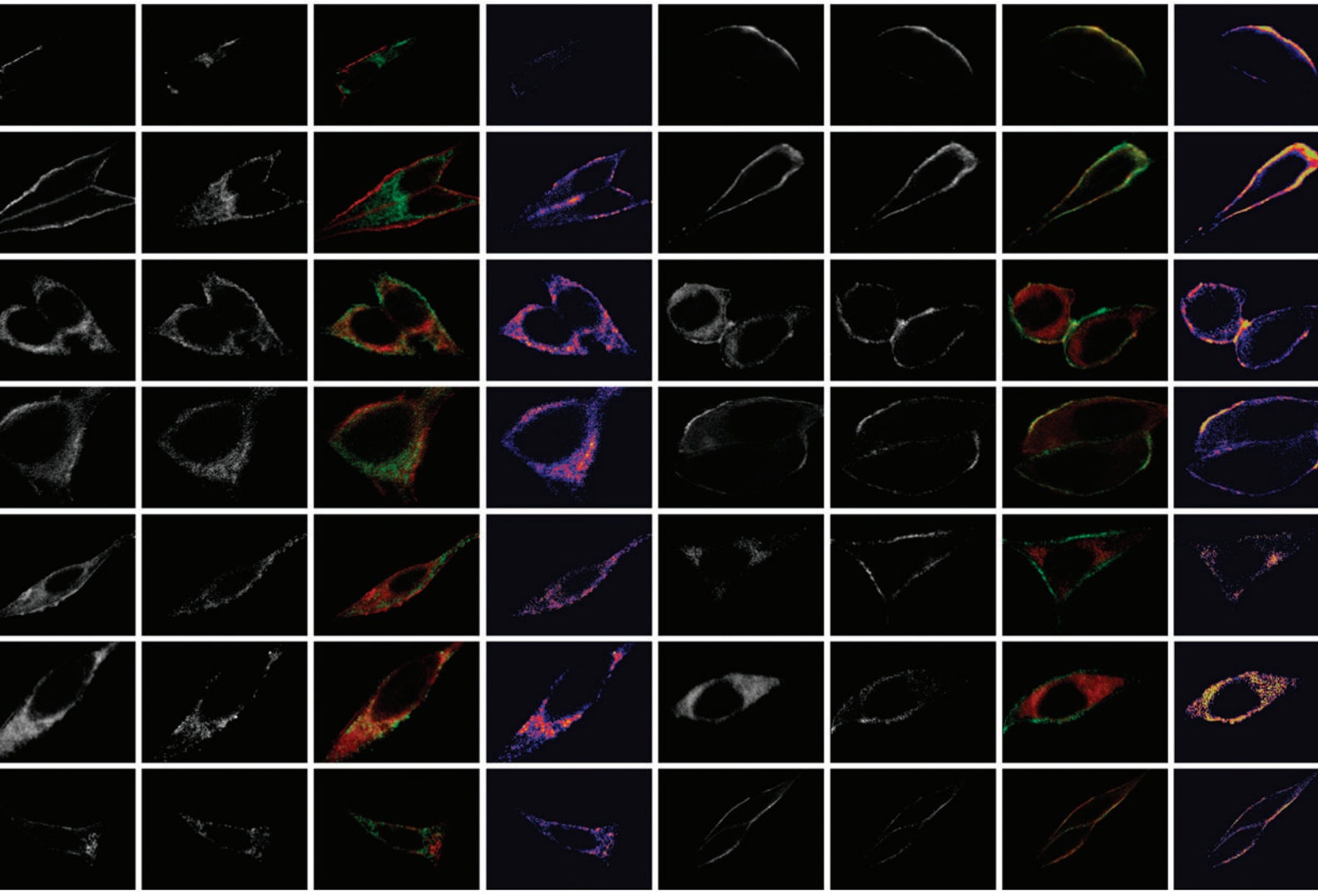

VOLUME 70 | ISSUE 6 | SEPTEMBER (2) 2006

http://www.kidney-international.org

Complexity of congenital nephritic syndrome

Organ transplantation in hyperoxaluria type I

Prostaglandin agonists in renal therapy

4 Results

4. 3 Abnormal expression and processing of uromodulin in Fabry disease reflects tubular cell storage alteration and is reversible by enzyme replacement therapy.

Vylet'al P, Hůlková H, **Zivná M**, Berná, Novák P, Elleder M, Kmoch S.

J Inherit Metab Dis. 2008 Aug;31(4):508-17. Epub 2008 Jul 27., **IF 2,691**

J Inherit Metab Dis
DOI 10.1007/s10545-008-0900-3

ORIGINAL ARTICLE

Abnormal expression and processing of uromodulin in Fabry disease reflects tubular cell storage alteration and is reversible by enzyme replacement therapy

P. Vylet'al · H. Hůlková · M. Živná · L. Berná · P. Novák · M. Elleder · S. Kmoch

Received: 20 February 2008 / Submitted in revised form: 21 April 2008 / Accepted: 23 April 2008 / Published online: 27 July 2008

Summary Uromodulin (UMOD) malfunction has been found in a range of autosomal dominant tubulointerstitial nephropathies associated with hyperuricaemia, gouty arthritis, medullary cysts and renal failure—labelled as familial juvenile hyperuricaemic nephropathy, medullary cystic disease type 2 and glomerulocystic kidney disease. To gain knowledge of the spectrum of UMOD changes in various genetic diseases with renal involvement we examined urinary UMOD excretion and found significant quantitative and qualitative changes in 15 male patients at various clinical stages of Fabry disease. In untreated patients, the changes ranged from normal to a marked decrease, or even absence of urinary UMOD. This was accompanied frequently by the presence of aberrantly processed UMOD lacking the C-terminal part following the K432 residue. The abnormal patterns normalized in all patients on enzyme replacement therapy and in some patients on substrate reduction therapy. Immunohistochemical analysis of the affected kidney revealed abnormal UMOD localization in the thick ascending limb of Henle's loop and the distal convoluted tubule, with UMOD expression inversely proportional to the degree of storage. Our observations warrant evaluation of tubular functions in Fabry disease and suggest UMOD as a potential biochemical marker of therapeutic response of the kidney to therapy. Extended comparative studies of UMOD expression in kidney specimens obtained during individual types of therapies are therefore of great interest.

Communicating editor: Ed Wraith

Competing interests: None declared

References to electronic databases: Fabry disease: OMIM 301500. α-Galactosidase A: EC 3.2.1.22. Uromodulin, OMIM 191845.

P. Vylet'al · M. Živná · M. Elleder · S. Kmoch
Center for Applied Genomics and Institute for Inherited Metabolic Disorders, Charles University 1st Faculty of Medicine, Prague, Czech Republic

H. Hůlková · L. Berná
Institute for Inherited Metabolic Disorders, Charles University 1st Faculty of Medicine, Prague, Czech Republic

P. Novák
Laboratory of Molecular Structure Characterization, Institute of Microbiology, Academy of Sciences of the Czech Republic, Prague, Czech Republic

S. Kmoch (✉)
Center for Applied Genomics and Institute for Inherited Metabolic Disorders, Ke Karlovu 2, 128 00 Prague 2, Czech Republic
e-mail: skmoch@lf1.cuni.cz

Abbreviations

DCT	distal convoluted tubule
ERT	enzyme replacement therapy
Gb_3	globotriaosylceramide
GLA	α-galactosidase A
MALDI-TOF	matrix assisted lased desorption/ ionization-time of flight
SRT	substrate reduction therapy
TALH	thick ascending limb of Henle's loop
UAKD	uromodulin-associated kidney disease
UMOD	uromodulin

Introduction

Uromodulin (UMOD; OMIM 191845) or Tamm–Horsfall protein (THP) is a protein selectively expressed in the

thick ascending limb of Henle's loop (TALH), the macula densa segment and the distal convoluted tubule (DCT) (Hoyer and Seiler 1979; Peach et al 1988; Schenk et al 1971; Sikri et al 1981). Normally the synthesized protein is glycosylated, glypiated, secreted and glycosylphosphatidylinositol-anchored in the apical membrane of the polarized renal tubular epithelial cells (Kreft et al 2002; Rindler et al 1990; Serafini-Cessi et al 1993), from where it is continuously released by a specific but not yet identified protease (Cavallone et al 2001; Fukuoka and Kobayashi 2001). UMOD is excreted in the urine at the rate of 50–100 mg/day, which makes it one of the most abundant urinary proteins (Kumar and Muchmore 1990). UMOD precipitates in the urine and is the main constituent of urinary casts (Cohen 1981; Fairley et al 1983; Wenk et al 1981).

Mutations in the uromodulin gene (HGNC *UMOD*) were found in a subset of patients suffering from a range of autosomal dominant tubulointerstitial nephropathies associated with hyperuricaemia, gouty arthritis, medullary cysts and renal failure—labelled as familial juvenile hyperuricaemic nephropathy (FJHN, OMIM 162000), medullary cystic disease type 2 (MCKD2, OMIM 603860) (Hart et al 2002) and glomerulocystic kidney disease (GCKD, OMIM 609886) (Rampoldi et al 2003). In these patients *UMOD* mutations led to intracellular UMOD accumulation, absence of the protein on the plasma membrane and decreased urinary excretion (Bernascone et al 2006; Bleyer et al 2004; Dahan et al 2003; Hodanova et al 2005; Rampoldi et al 2003; Vylet'al et al 2006). Changes in UMOD expression, cellular localization and urinary excretion were found also in FJHN/MCKD patients with no *UMOD* mutation and this led to introduction of the term '*uromodulin-associated kidney diseases*' (UAKD) (Hart et al 2002; Hodanova et al 2005; Vylet'al et al 2006).

As it is unclear as to what extent the changes in UMOD expression, cellular localization and urinary excretion are specific to FJHN/MCKD/UAKD, we are examining these parameters in other genetic diseases with severely compromised renal functions.

Fabry disease (OMIM 301500) is an X-linked, gonosomal recessive disorder caused by deficiency of α-galactosidase A (GLA; EC 3.2.1.22.). The enzyme defect leads to massive accumulation and storage of non-degraded substrate globotriaosylceramide (Gb_3) in lysosomes of various cell types. Hemizygous male patients manifest a wide range of symptoms, including characteristic skin lesions, chronic progressive painful small-fibre neuropathy, corneal opacities, renal failure, heart disease and stroke due to systemic vasculopathy. If untreated, the disease is lethal, renal failure being the usual cause of death (Desnick et al 1989; Masson et al 2004).

The Fabry storage nephropathy has attracted biomedical interest mainly owing to deterioration of glomerular function, starting with increased protein permeability, followed by progressive hyalinization and loss of the filtration capacity. This process as such has been studied intensively at clinical and pathological levels (Burkholder et al 1980; Glass et al 2004; McNary and Lowenstein 1965; Morel-Maroger et al 1966; Pabico et al 1973) among others with the intention of defining 'the point of no return' for enzyme replacement therapy (ERT) (Breunig and Wanner 2003; De Schoenmakere et al 2003; del Toro et al 2004). Renal tubular dysfunction in Fabry disease was described earlier by Pabico and colleagues (Pabico et al 1973) but attracted little attention. However, tubular dysfunction has been described as being prominent during the early clinical course (Parchoux et al 1978; Wornell et al 2006).

In this study of 15 male Fabry disease patients in various clinical stages of the disease, we examined UMOD urinary excretion and protein proteolytic processing and found significant quantitative and qualitative abnormalities. Interestingly, these changes normalized in every single patient treated by ERT (Fabrazyme or Replagal) but not as successfully in the patients on substrate reduction therapy (SRT) using the ceramide glucosyltransferase inhibitor Zavesca.

To explain the observed abnormalities we studied UMOD cellular localization in different parts of the nephron and collecting duct in kidney tissue from three untreated patients. These studies revealed abnormal UMOD localization in TALH and collecting tubules, with UMOD expression in TALH epithelia being inversely proportional to the degree of storage. In contrast to previous studies, which have largely looked at functional changes, our study shows for the first time a biochemically defined alteration of tubular cell biology reflecting the process of storage in defined parts of the nephron. Although the mechanisms by which the enzyme defect and/or storage process lead to abnormal UMOD expression, processing and urinary excretion remain unknown. Our observations warrant further evaluation of tubular functions in Fabry disease patients and suggest UMOD as a potential biochemical marker of response of the kidney to therapy.

Materials and methods

Patients

For the analyses, urine samples were collected from 15 male patients with Fabry disease with a range of ages, severity of symptoms and types of treatment. The diagnosis of Fabry disease in the selected patients was made following the finding of reduced GLA activity in leukocytes and the presence of a pathogenic mutation in the *GLA* gene (HGNC *GLA*). Basic clinical, biochemical and molecular data as well as the treatment regimens for all 15 patients are summarized in Table 1. All the patients were from the Czech Republic and were diagnosed and studied in our Institute (Dobrovolny et al 2005).

SDS-PAGE and western blot

Urine samples stored at −80°C were thawed and 15 µl of sample was denatured using standard SDS-PAGE loading buffer. Proteins were separated on 10% SDS–polyacrylamide gel and UMOD was detected using western blot analysis as described previously (Hodanova et al 2005).

Deglycosylation experiments

Deglycosylation experiments were performed on 15 µl of total urine using the GlycoPro enzymatic deglycosylation kit (ProZyme Inc., San Leandro, CA, USA) according to the manufacturer's instructions. Deglycosylated protein products were directly analysed on 10% SDS–polyacrylamide gel and UMOD was detected by western blot as described above.

Mass spectrometry

To characterize UMOD variants, total protein from 500 µl of each patient's urine was recovered on Microcon YM-50 columns (Milipore, Bedford, MA, USA) and separated on 10% SDS–polyacrylamide gel. Coomassie blue R 250 stained protein bands were extracted from the gel and digested with trypsin (Promega, Madison, WI, USA, 5 ng/µl). The resulting peptides were extracted and subjected to mass-spectrometric analysis.

Mass spectra were measured using the following. (a) A matrix-assisted laser desorption/ionization reflectron time-of-flight MALDI-TOF mass spectrometer BIFLEX II (Bruker-Franzen, Bremen, Germany) equipped with a nitrogen laser (337 nm) and gridless delayed extraction ion source. Spectra were calibrated externally using the monoisotopic $[M+H]^+$ ion of peptide standard somatostatin (Sigma-Aldrich, Prague, Czech Republic). A saturated solution of α-cyano-4-hydroxycinnamic acid in 50% CAN–0.2% TFA was used as a MALDI matrix. (b) A LCQ^{DECA} ion trap mass spectrometer (ThermoQuest, San Jose, CA, USA) equipped with a nanoelectrospray ion source (ESI LC-MS/MS). Magic-C18 column, 0.2×150 mm, 200 Å, 5 µm (Michrom Bioresources, Auburn, CA,

Table 1 Clinical, biochemical and molecular information on patients

Patient	DOB	GLA mutation	GLA activity[a]	Mainz score	Renal index	Treatment[b]
P1	1945	c.801ins36	2.4	34	0	Z(12), F(12)
P2	1949	delEx2	2.6	56	18	Z(12), F(45)
P3	1952	R301X	2.9	54	18	Z(12), F
P4	1957	L294X	1.0	54	18	Z, T, F(5)
P5	1960	c.801ins36	1.7	41	4	Z, F(14)
P6	1968	c.674del59	0.7	41	18	R(2)
P7	1972	N215S	7.2	–	0	N
P8	1978	D155H	1.7	41	18	Z, F
P9	1979	N215S	5.2	5	0	N
P10	1985	G360S	1.9	–	0	N
P11	1956	Q280K	1.2	35	4	Z(12), F(45)
P12	1978	R342Q	3.4	32	8	R(3)
P13	1972	R342Q	0.3	41	4	R(3)
P14	1966	R342Q	1.8	28	0	Z(12)
P15	1948	R301X	1.9	44	4	Z(12), F(13)

[a] GLA activity in leukocytes measured at 37°C; average of 100 controls 53.8±11,5 and range 32–89 nmol/mg per hour.
[b] Z, Zavesca; F, Fabrazyme; R, Replagal; N, none; T, transplantation; duration of the treatment is given in months in parentheses.

USA) and MeCN–acetic acid gradient was used for peptide separation. Positive-ion full scan and CID mass spectra over *m/z* range 350–1600 were acquired and interpreted by SEQUEST software against the human NCBI database.

Immunohistochemistry studies

Archived formalin-fixed paraffin-embedded kidney samples originated from two autopsied adult males and one female with Fabry disease, who died at 47, 44 and 63 years respectively. The storage was detected in fixed frozen section, using the periodic acid–Schiff (PAS) method (checked by lipid extraction) and by birefringence. In paraffin sections, it was indicated by the typical foamy appearance of the storage cells.

Immunodetection of UMOD and of the apical cell membrane marker MUC1 was done in paraffin sections as previously described (Vylet'al et al 2006). For designation of individual parts of the kidney tubular system the nomenclatures of Clapp and Croker was used (Clapp and Croker 1997), i.e. nephron (consisting of proximal tubule, Henle loop and distal convoluted tubule) and the collecting tubule.

Results

Analysis of urinary UMOD

For an overview on the nature and range of eventual changes in urinary UMOD excretion we analysed urine samples from 15 Fabry patients with a range of age, severity of symptoms and treatment regimens (Table 1).

Initially, we analysed UMOD excretion patterns in urine samples collected before any treatment was started (Fig. 1). The analysis showed that in some of the patients UMOD excretion was strongly decreased (P3, P8) or reduced (P5), along with abnormal forms of anti-UMOD immunoreactive protein (P1, P2, P3, P5, P6, P8, P11, P15). In other patients, UMOD excretion seemed to be normal (P4, P7, P9, P10, P12, P13, P14). As indicated in Table 1, P4 was tested after kidney transplantation and patients P7, P9 and P10 showed a mild clinical phenotype.

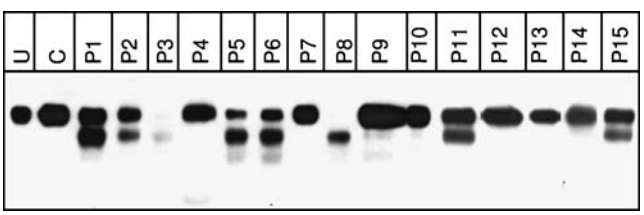

Fig. 1 Qualitative analysis (western blot) of urinary UMOD in patients with Fabry disease before the therapy. U: UMOD standard isolated from control urine. C: control urine. P1–P15: patient designation as provided in Table 1

To identify the nature of the anti-UMOD immunoreactive protein found in urines of some Fabry disease patients, we first deglycosylated urine from patient P1 with *N*-glycanase (PGNase F) and subjected the resulting UMOD profile to western blot analysis (Fig. 2a). The analysis suggested that the abnormal anti-UMOD immunoreactive protein did not represent a different UMOD glycoform but rather a UMOD protein differing in its peptide moiety. We therefore recovered total protein from the urine sample of P1, separated the proteins on SDS-polyacrylamide gel, detected corresponding protein bands by Coomassie blue staining (Fig. 2b), excised them and analysed them by mass spectrometry (Fig. 2c). The analysis showed that the abnormal protein with the lower molecular mass was UMOD lacking a C-terminal part. With K432 being the last amino acid positively identified, the cleavage site leading to this abnormal proteolytic processing is most likely to be located between amino acid residues K432 and R449 (Fig. 2d).

The patients chosen for this study were enrolled in three different treatment protocols using either the synthetic ceramide glucosyltransferase inhibitor Zavesca (miglustat; Actelion Pharmaceuticals Ltd, Allschwil, Switzerland) or two available recombinant GLA preparations, Fabrazyme (Genzyme, Cambridge, MA, USA) and Replagal (Shire Human Genetic Therapies AB, Danderyd, Sweden). To investigate eventual effects of the treatment protocols on abnormal UMOD excretion and processing, we analysed urine samples collected before and during the individual trials (Fig. 3). Abnormal processing of UMOD clearly normalized in all patients receiving ERT with Fabrazyme (Fig. 3b) and Replagal (Fig. 3c). The effect of Zavesca treatment was not as striking (Fig. 3a).

UMOD expression *in situ* and its relation to the storage process

To explain the observed abnormalities in urinary UMOD excretion and processing, we studied UMOD cellular expression and its relation to the storage in different parts of nephron and collecting duct in archived kidney tissues from two untreated hemizygotes and one heterozygous patient whose urine samples were unfortunately not available for correlation.

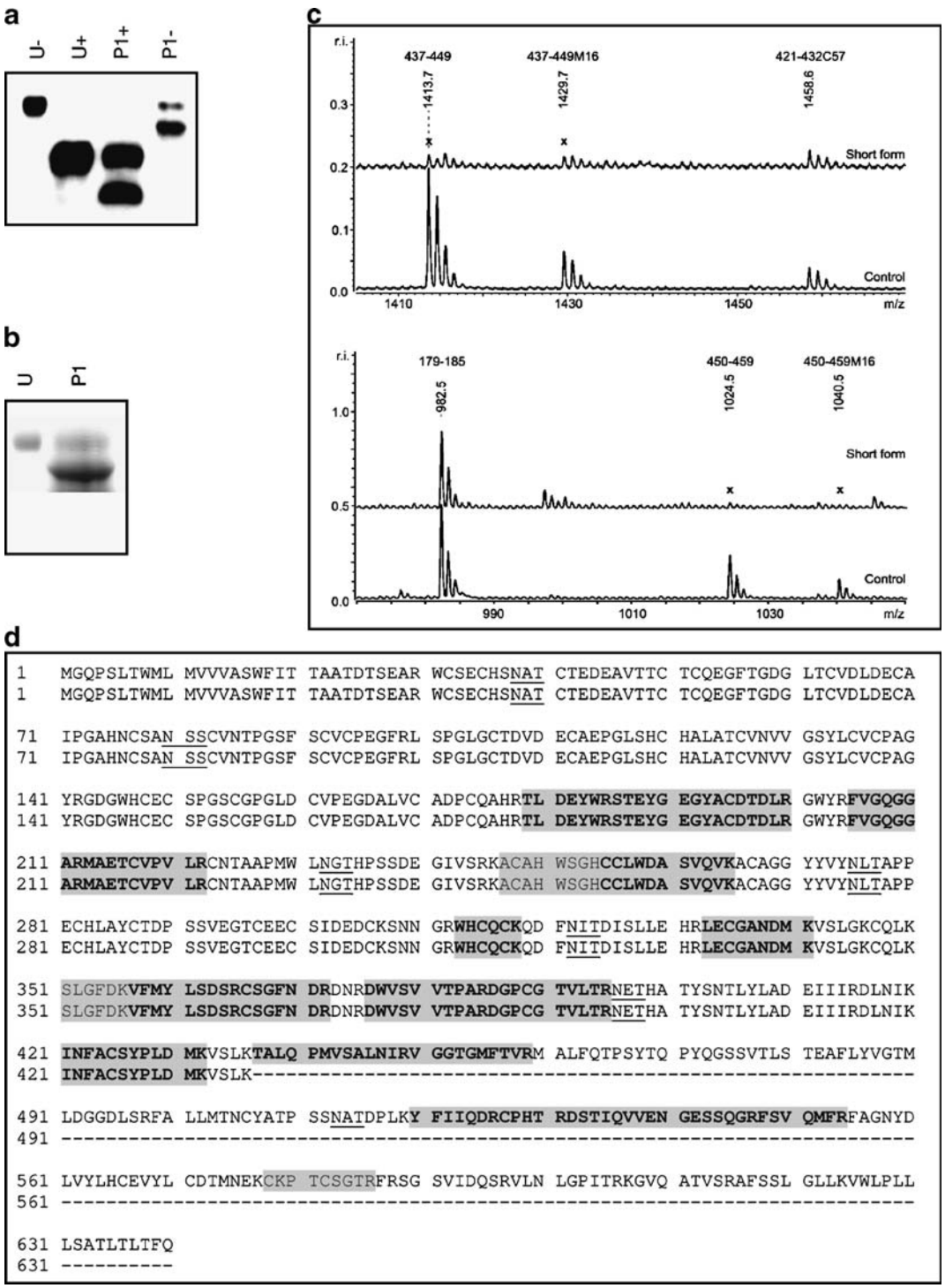

Fig. 2 Characterization of abnormal UMOD processing. (**a**) Qualitative analysis (western blot) of UMOD isolated from healthy male urine before (U−) and (U+) after deglycosylation treatment with *N*-glycanase. P1− indicates urine from patient P1 before and P1+ after deglycosylation treatment with *N*-glycanase. (**b**) Qualitative analysis (Coomassie blue-stained SDS-PAGE gel) of total protein extract obtained from 500 µl of urine from patient P1 on Amicon YM-50. U: UMOD standard isolated from control urine. (**c**) Peptide mass fingerprinting of UMOD standard (control) and isolated protein of interest confirms that 'short form' is UMOD protein lacking the N-terminal part following 432K residue. M16 indicates oxidized methionine. C57 indicates cysteine iodoacetamide. (**d**) Sequence alignment of the control urinary UMOD (upper sequence) and the patient 'short form' (lower sequence) shows with grey highlight peptides detected by peptide mass fingerprinting and in bold type peptides that were confirmed by peptide microsequencing. Theoretical N-glycosylation sites of UMOD are underlined

UMOD in situ *expression in control kidney samples* was restricted to the epithelial cells of the TALH and the DCT. In the latter, the expression was lower and variable. UMOD was maximally expressed in the apical pole with less intracellular positivity. Exceptionally there was also staining at the basolateral pole. Rarely there was slight positivity in some cells in collecting tubules.

Distribution of the storage in Fabry disease kidneys. In the cortex, storage was absent in both the proximal and the distal tubules. It was present only in glomeruli and in vessels (endothelia and smooth-muscle cells). The tubular storage dominated in the medullary parts of the nephron (both descending and ascending limbs of the loop of Henle) and in the system of collecting tubules, decreasing from the outer medulla to the papilla. Corresponding tubular segments (parts) differed considerably in the degree of storage. In the collecting tubules, the storage was more pronounced in the intercalated cells. There were also signs of tubular regeneration (binucleate cells, cells with flat cytoplasm) and degeneration (cell shrinkage and nuclear pycnosis) and focal fibrosis in the medulla, mainly in its outer part. The storage pattern in the heterozygous Fabry kidney was the same as described in both hemizygotes.

UMOD in situ expression in Fabry disease kidneys. UMOD signal was present with similar intensity as in controls in the non-storing TALH and in the DCT. The number of tubules strongly positive for UMOD in the cortex was comparable to that in control kidneys (Fig. 4a, b) but was decreased in the outer medulla (Fig. 4c, d). In many cross-sections of TALH, there were strongly UMOD-positive epithelia free of recognizable storage mixed with cells in advanced stage of storage and decreased or absent UMOD staining (Fig. 4e). In general, the degree of UMOD expression was inversely proportional to the degree of lysosomal storage (Fig. 4f). In cells with lesser degrees of storage, UMOD apical presentation was preserved but often combined with staining at the basolateral pole (Fig. 4g). In some collecting tubules there was UMOD signal at the cell membrane as well as intracellularly, suggesting ectopic expression (Fig. 4h). This finding was more frequent than in controls but was not entirely bound to advanced lysosomal storage. Several UMOD-positive luminal casts were also observed. UMOD staining in the heterozygous Fabry kidney did not differ from that in the samples from the hemizygous patients.

In parallel the marker of the apical membrane, MUC1, was present throughout the whole nephron

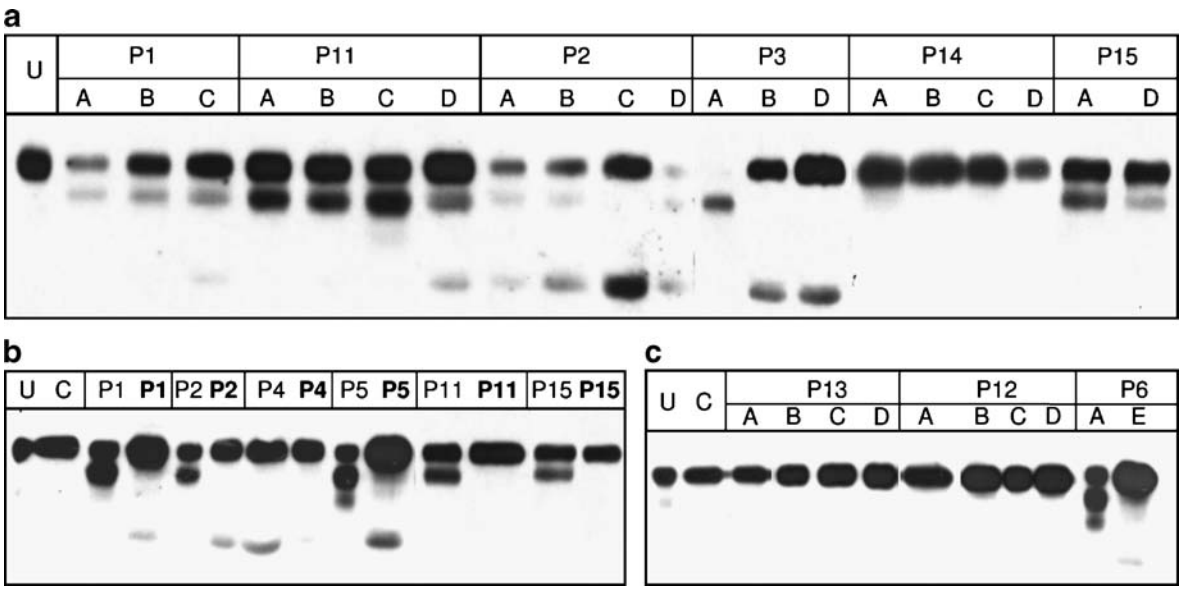

Fig. 3 Qualitative analysis (western blot) of urinary UMOD in patients with Fabry disease on various therapy protocols. (**a**) Zavesca protocol. Urine samples were collected (A) before treatment, (B) at 6 months, (C) at the end of treatment (12 months) and (D) 1 month after termination of the treatment. (**b**) Fabrazyme protocol. Samples taken before and during the treatment are in plain and bold characters, respectively. (**c**) Replagal protocol. Urine samples were collected (A) before treatment, (B) at 1 month, (E) at 2 months, (C) at 3 months and (D) 1 month after termination of the treatment. U: uromodulin standard isolated from control urine, C: control urine, P1–P15: patient designation as provided in Table 1. The low molecular weight bands seen at the bottom of images most probably represent albumin, reflecting disease-related proteinuria

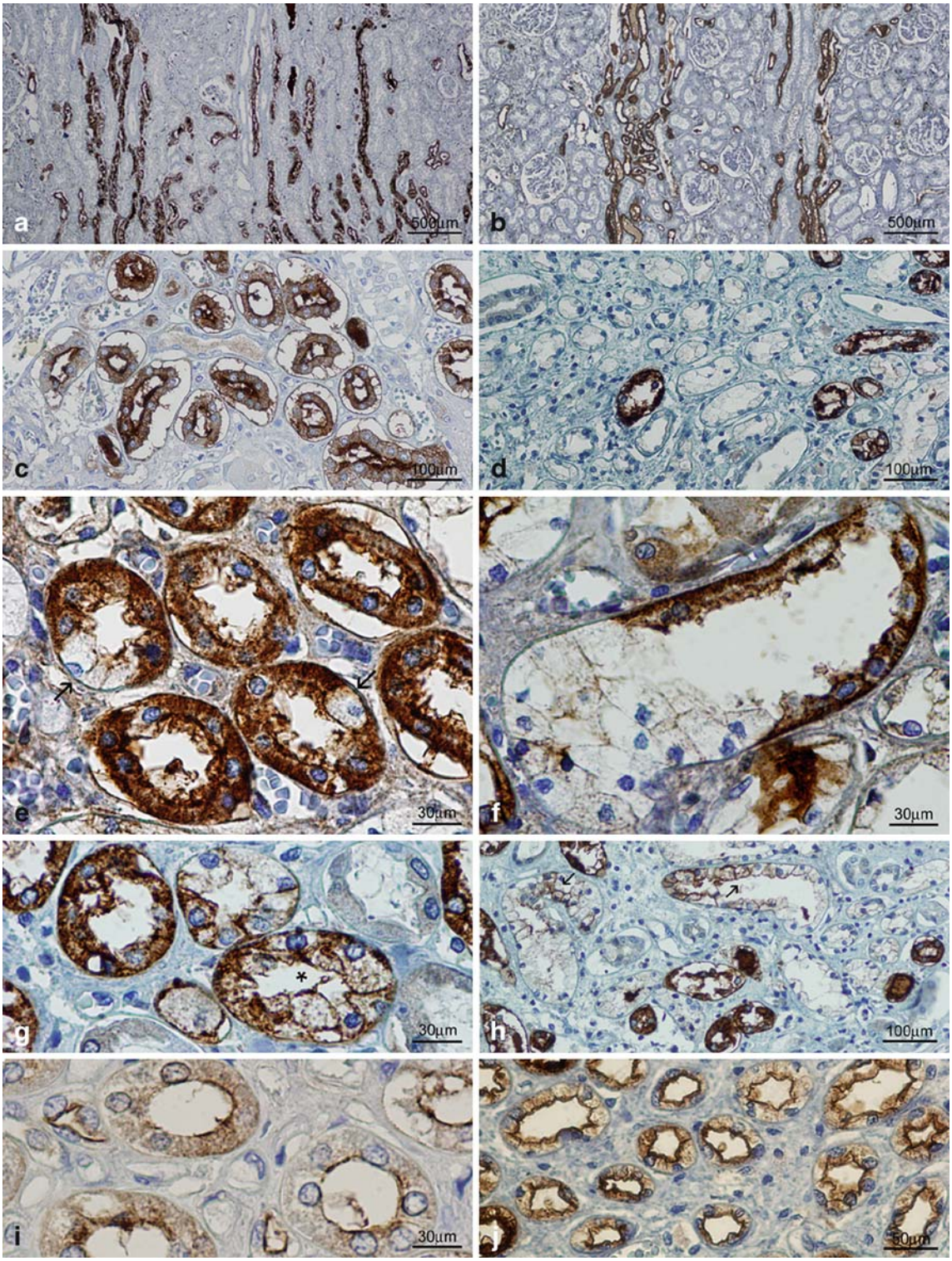

Fig. 4 Immunohistochemical analysis of UMOD and MUC1 in kidney biopsies. Survey of the cortical medullary rays shows strong and comparable UMOD expression (**a**) in control and (**b**) in Fabry disease kidney where cortical TALH is without prominent lysosomal storage. Differences in UMOD expression were present in the outer medulla. (**c**) In the control the staining in TALH is uniform whereas (**d**) in Fabry disease kidney the absence of UMOD staining is seen in many cross-sectioned TALH displaying storage. Details of the outer medulla in Fabry disease kidney show (**e**) absence of UMOD expression in individual storage TALH cells (arrows) and (**f**) UMOD expression in TALH inversely proportional to the degree of storage. (**g**) Storage TALH epithelium with persistent decreased apical UMOD expression (asterisk). (**h**) Collecting tubules (arrows) with distinct apical and basolateral UMOD positivity. MUC1 expression is identical in both (**i**) control and (**j**) despite the storage also in Fabry disease kidney

with the exception of proximal convoluted tubules, and in the collecting tubules as in controls. There was no significant reduction of MUC1 expression due to storage (Fig. 4i, j).

Discussion

We present here the results of a pilot study investigating UMOD urinary excretion, processing and expression in patients with Fabry disease at different clinical stages of the disease and during treatment with ERT or SRT. This work has been undertaken with the aim of extending knowledge of the range of UMOD changes in various genetic diseases with severe renal involvement, starting with the model of Fabry disease. In about half of the untreated hemizygous male patients as well as in 7 out of 9 heterozygous carriers (data not shown), we found significant quantitative and qualitative changes in urinary UMOD excretion, which indicate a gradual decrease in urinary UMOD excretion accompanied in some cases by aberrant proteolytic UMOD processing. Variability in UMOD excretion seemed in most patients to reflect phenotypic severity (with the exception of P12 and P13) as it correlates with the reported Mainz severity score index. This speculation is further supported by the finding that UMOD urinary excretion patterns normalized in all patients enrolled in ERT and, to a lesser extent, in patients on SRT. Reversibility of abnormal UMOD excretion profile after ERT and SRT represents a key observation as it links the changes of UMOD biology to the storage process in TALH and the DCT.

Existing studies addressing the nephron storage distribution in Fabry disease differ surprisingly with regard to definition of the individual affected segments. Storage in the proximal part has been reported only rarely (Alroy et al 2002; Farge et al 1985; McNary and Lowenstein 1965; Wornell et al 2006). Storage in collecting tubules was found to be present in only two reports (Alroy et al 2002; Burkholder et al 1980), while others described storage in the distal tubules (Burkholder et al 1980; Dempsey et al 1965; Faraggiana et al 1981; Farge et al 1985; Gubler et al 1978; McNary and Lowenstein 1965; Pabico et al 1973; Tondeur and Resibois 1969; Wornell et al 2006). The distal tubule and the Henle loop are thus considered to be affected most prominently in Fabry disease (Okuda 2000). The storage pattern in heterozygotes did not differ substantially from that in hemizygous male patients (Farge et al 1985; Gubler et al 1978).

We observed storage in the loop of Henle and in the collecting ducts with notable degrees of variability between individual tubules. In particular, storage in the TALH had a mosaic character. Similar variability in storage has been described before (Gubler et al 1978). As in previous studies on UMOD expression in control kidney, we observed prominent expression of UMOD in the TALH and less so in the DCT in normal kidneys (Hoyer and Seiler 1979; Peach et al 1988; Schenk et al 1971; Sikri et al 1981). Thus, both processes, lysosomal storage and UMOD expression, meet in the TALH.

Normal, fully processed UMOD detected in the patient urine samples is most probably produced by cells not affected by storage process and showing UMOD staining like that in controls. Decrease in UMOD excretion might be attributed to its attenuated expression as shown by the UMOD staining pattern, which is inversely proportional to the degree of storage in patient kidney. Attenuated UMOD expression, however, cannot be attributed to generally compromised proteosynthesis because another marker of apical membrane, MUC1, showed normal expression pattern in unaffected as well as storing cells. Attenuated UMOD expression is thus probably linked directly to the lysosomal storage process. Similar decrease in UMOD transcription and expression was found recently in mice with renal-specific inactivation of *HNF1β* (Gresh et al 2004), *Brn1*$^{-/-}$ mice (Nakai et al 2003), an ischaemia-reperfusion model of ARF in rat (Yoshida et al 2002), in some patients with UAKD (Hodanova et al 2005; Vylet'al et al 2006), and in kidney damage (Chakraborty et al 2004).

The other interesting observation of our study represents aberrant proteolytic processing of UMOD. Our results do not define the site and mechanism of this process. It may be intracellular as a result of storage-related proteosome and/or specific protease activation. It may also occur on the cell membrane by a process of abnormal ectodomain shedding. This process may be activated by glomerulopathy-related changes in tubular fluid composition (proteinuria, osmolarity, pH), which may alter the tertiary structure of UMOD and make it susceptible to aberrant cleavage either by UMOD-specific or other proteases present in urine. This latter explanation seems more likely as distinct UMOD staining may be seen on the apical membrane of storing as well as non-storing epithelial

cells (Fig. 4). The alternative processing can also reflect alternative proteolytic cleavage in desquamated tubular storage epithelia responsible for the massive urinary lipid excretion.

In conclusion, storage processes in Fabry disease trigger mechanisms that lead to reduced expression, alternative proteolytic processing and decreased urinary excretion of UMOD. Lack of UMOD function(s) has been shown to be associated with impairment of tubular function, particularly of the urine-concentrating process, accounting for water depletion in UAKD (Bleyer et al 2003; Scolari et al 2004; Vylet'al et al 2006). It is therefore reasonable to speculate that the observed changes in UMOD expression may contribute to altered tubular functions in Fabry disease as well. Association of UMOD changes with the degree of the storage process and its reversibility by ERT and partly also by SRT suggests that UMOD excretion monitoring may be a useful marker, particularly of response to treatment. We suggest that UMOD might be an additional marker of therapeutic *in situ* effect on Gb_3, the excretion of which may be affected by cleavage of lipid released from the desquamated storage epithelia by the applied recombinant enzyme (Christensen et al 2007). Extended study and especially detailed comparative studies of UMOD expression in kidney specimens obtained before and during individual types of available therapies are therefore of great interest.

Acknowledgements We thank Dr Venkat Raman for comments and critical reading of the manuscript. This work was supported by grant MSM0021620806 from the Ministry of Education of the Czech Republic and partly by grant number 257750 from the Grant Agency of Charles University in Prague (GAUK).

References

Alroy J, Sabnis S, Kopp JB (2002) Renal pathology in Fabry disease. *J Am Soc Nephrol* **13**(Supplement 2): S134–138.

Bernascone I, Vavassori S, Di Pentima A, et al (2006) Defective intracellular trafficking of uromodulin mutant isoforms. *Traffic* **7**: 1567–1579.

Bleyer AJ, Trachtman H, Sandhu J, Gorry MC, Hart TC (2003) Renal manifestations of a mutation in the uromodulin (Tamm Horsfall protein) gene. *Am J Kidney Dis* **42**: E20–26.

Bleyer AJ, Hart TC, Shihabi Z, Robins V, Hoyer JR (2004) Mutations in the uromodulin gene decrease urinary excretion of Tamm-Horsfall protein. *Kidney Int* **66**: 974–977.

Breunig F, Wanner C (2003) Enzyme replacement therapy for Fabry disease: proving the clinical benefit. *Nephrol Dial Transplant* **18**: 7–9.

Burkholder PM, Updike SJ, Ware RA, Reese OG (1980) Clinicopathologic, enzymatic, and genetic features in a case of Fabry's disease. *Arch Pathol Lab Med* **104**: 17–25.

Cavallone D, Malagolini N, Serafini-Cessi F (2001) Mechanism of release of urinary Tamm-Horsfall glycoprotein from the kidney GPI-anchored counterpart. *Biochem Biophys Res Commun* **280**: 110–114.

Chakraborty J, Below AA, Solaiman D (2004) Tamm-Horsfall protein in patients with kidney damage and diabetes. *Urol Res* **32**: 79–83.

Christensen EI, Zhou Q, Sorensen SS, et al (2007) Distribution of alpha-galactosidase A in normal human kidney and renal accumulation and distribution of recombinant alpha-galactosidase A in Fabry mice. *J Am Soc Nephrol* **18**: 698–706.

Clapp WL, Croker BP (1997) Adult kidney. In: Sternberg SS, ed. *Histology for Pathologists*, 2nd edn. Philadelphia: Lippincott-Raven, 799–834.

Cohen AH (1981) Morphology of renal tubular hyaline casts. *Lab Invest* **44**: 280–287.

Dahan K, Devuyst O, Smaers M, et al (2003) A cluster of mutations in the UMOD gene causes familial juvenile hyperuricemic nephropathy with abnormal expression of uromodulin. *J Am Soc Nephrol* **14**: 2883–2893.

De Schoenmakere G, Chauveau D, Grunfeld JP (2003) Enzyme replacement therapy in Anderson-Fabry's disease: beneficial clinical effect on vital organ function. *Nephrol Dial Transplant* **18**: 33–35.

del Toro N, Milan JA, Palma A (2004) Enzyme replacement in the treatment of Fabry's disease. Is there a point-of-no-return? *Nephrol Dial Transplant* **19**: 1018.

Dempsey H, Hartley MW, Carroll J, Balint J, Miller RE, Frommeyer WB Jr. (1965) Fabry's disease (angiokeratoma corporis diffusum): case report on a rare disease. *Ann Intern Med* **63**: 1059–1068.

Desnick RJ, Astrin KH, Bishop DF (1989) Fabry disease: molecular genetics of the inherited nephropathy. *Adv Nephrol Necker Hosp* **18**: 113–127.

Dobrovolny R, Dvorakova L, Ledvinova J, et al (2005) Relationship between X-inactivation and clinical involvement in Fabry heterozygotes. Eleven novel mutations in the alpha-galactosidase A gene in the Czech and Slovak population. *J Mol Med* **83**: 647–654.

Fairley JK, Owen JE, Birch DF (1983) Protein composition of urinary casts from healthy subjects and patients with glomerulonephritis. *Br Med J (Clin Res Ed)* **287**: 1838–1840.

Faraggiana T, Churg J, Grishman E, et al (1981) Light- and electron-microscopic histochemistry of Fabry's disease. *Am J Pathol* **103**: 247–262.

Farge D, Nadler S, Wolfe LS, Barre P, Jothy S (1985) Diagnostic value of kidney biopsy in heterozygous Fabry's disease. *Arch Pathol Lab Med* **109**: 85–88.

Fukuoka S, Kobayashi K (2001) Analysis of the C-terminal structure of urinary Tamm-Horsfall protein reveals that the release of the glycosyl phosphatidylinositol-anchored counterpart from the kidney occurs by phenylalanine-specific proteolysis. *Biochem Biophys Res Commun* **289**: 1044–1048.

Glass RB, Astrin KH, Norton KI, et al (2004) Fabry disease: renal sonographic and magnetic resonance imaging findings in affected males and carrier females with the classic and cardiac variant phenotypes. *J Comput Assist Tomogr* **28**: 158–168.

Gresh L, Fischer E, Reimann A, et al (2004) A transcriptional network in polycystic kidney disease. *Embo J* **23**: 1657–1668.

Gubler MC, Lenoir G, Grunfeld JP, Ulmann A, Droz D, Habib R (1978) Early renal changes in hemizygous and heterozygous patients with Fabry's disease. *Kidney Int* **13**: 223–235.

Hart TC, Gorry MC, Hart PS, et al (2002) Mutations of the UMOD gene are responsible for medullary cystic kidney disease 2 and familial juvenile hyperuricaemic nephropathy. *J Med Genet* **39**: 882–892.

Hodanova K, Majewski J, Kublova M, et al (2005) Mapping of a new candidate locus for uromodulin-associated kidney disease (UAKD) to chromosome 1q41. *Kidney Int* **68**: 1472–1482.

Hoyer JR, Seiler MW (1979) Pathophysiology of Tamm-Horsfall protein. *Kidney Int* **16**: 279–289.

Kreft B, Jabs WJ, Laskay T, et al (2002) Polarized expression of Tamm-Horsfall protein by renal tubular epithelial cells activates human granulocytes. *Infect Immun* **70**: 2650–2656.

Kumar S, Muchmore A (1990) Tamm-Horsfall protein—uromodulin (1950–1990). *Kidney Int* **37**: 1395–1401.

Masson C, Cisse I, Simon V, Insalaco P, Audran M (2004) Fabry disease: a review. *Joint Bone Spine* **71**: 381–383.

McNary WF, Lowenstein LM (1965) A morphological study of the renal lesion in angiokeratoma corporis diffusum universale (Fabry's disease). *J Urol* **93**: 641–648.

Morel-Maroger L, Ganter P, Ardaillou R, Cathelineau G, Richet G (1966) [Histochemical study of a lipid thesaurismosis with renal, cutaneous and neurologic involvement. Its relation to Fabry's angiokeratosis and familial renal cytodystrophy]. *Bull Mem Soc Med Hop Paris* **117**: 49–57.

Nakai S, Sugitani Y, Sato H, et al (2003) Crucial roles of Brn1 in distal tubule formation and function in mouse kidney. *Development* **130**: 4751–4759.

Okuda S (2000) Renal involvement in Fabry's disease. *Intern Med* **39**: 601–602.

Pabico RC, Atancio BC, McKenna BA, Pamukcoglu T, Yodaiken R (1973) Renal pathologic lesions and functional alterations in a man with Fabry's disease. *Am J Med* **55**: 415–425.

Parchoux B, Guibaud P, Maire I, et al (1978) [Fabry's disease. Initial nephrogenic diabetes insipidus in children]. *Pediatrie* **33**: 757–765.

Peach RJ, Day WA, Ellingsen PJ, McGiven AR (1988) Ultrastructural localization of Tamm-Horsfall protein in human kidney using immunogold electron microscopy. *Histochem J* **20**: 156–164.

Rampoldi L, Caridi G, Santon D, et al (2003) Allelism of MCKD, FJHN and GCKD caused by impairment of uromodulin export dynamics. *Hum Mol Genet* **12**: 3369–3384.

Rindler MJ, Naik SS, Li N, Hoops TC, Peraldi MN (1990) Uromodulin (Tamm-Horsfall glycoprotein/uromucoid) is a phosphatidylinositol-linked membrane protein. *J Biol Chem* **265**: 20784–20789.

Scolari F, Caridi G, Rampoldi L, et al (2004) Uromodulin storage diseases: clinical aspects and mechanisms. *Am J Kidney Dis* **44**: 987–999.

Serafini-Cessi F, Malagolini N, Hoops TC, Rindler MJ (1993) Biosynthesis and oligosaccharide processing of human Tamm-Horsfall glycoprotein permanently expressed in HeLa cells. *Biochem Biophys Res Commun* **194**: 784–790.

Schenk EA, Schwartz RH, Lewis RA (1971) Tamm-Horsfall mucoprotein. I. Localization in the kidney. *Lab Invest* **25**: 92–95.

Sikri KL, Foster CL, MacHugh N, Marshall RD (1981) Localization of Tamm-Horsfall glycoprotein in the human kidney using immuno-fluorescence and immuno-electron microscopical techniques. *J Anat* **132**: 597–605.

Tondeur M, Resibois A (1969) Fabry's disease in children. An electron microscopic study. *Virchows Arch B Cell Pathol* **2**: 239–254.

Vylet'al P, Kublova M, Kalbacova M, et al (2006) Alterations of uromodulin biology: a common denominator of the genetically heterogeneous FJHN/MCKD syndrome. *Kidney Int* **70**: 1155–1169.

Wenk RE, Bhagavan BS, Rudert J (1981) Tamm-Horsfall uromucoprotein and the pathogenesis of casts, reflux nephropathy, and nephritides. *Pathobiol Annu* **11**: 229–257.

Wornell P, Dyack S, Crocker J, Yu W, Acott P (2006) Fabry disease and nephrogenic diabetes insipidus. *Pediatr Nephrol* **21**: 1185–1188.

Yoshida T, Kurella M, Beato F, et al (2002) Monitoring changes in gene expression in renal ischemia-reperfusion in the rat. *Kidney Int* **61**: 1646–1654.

4 Results

4. 4 Dominant renin gene mutations associated with early-onset hyperuricemia, anemia, and chronic kidney failure.

Zivná M, Hůlková H, Matignon M, Hodanová K, Vylet'al P, Kalbácová M, Baresová V, Sikora J, Blazková H, Zivný J, Iványek R, Stránecký V, Sovová J, Claes K, Lerut E, Fryns JP, Hart PS, Hart TC, Adams JN, Pawtowski A, Clemessy M, Gasc JM, Gübler MC, Antignac C, Elleder M, Kapp K, Grimbert P, Bleyer AJ, Kmoch S.

Am J Hum Genet. 2009 Aug;85(2):204-13. Epub 2009 Aug 6., **IF 10,153**

And supplemental data of this article

Please cite this article in press as: Živná et al., Dominant Renin Gene Mutations Associated with Early-Onset Hyperuricemia, Anemia, and Chronic Kidney Failure, The American Journal of Human Genetics (2009), doi:10.1016/j.ajhg.2009.07.010

ARTICLE

Dominant Renin Gene Mutations Associated with Early-Onset Hyperuricemia, Anemia, and Chronic Kidney Failure

Martina Živná,[1,2] Helena Hůlková,[2] Marie Matignon,[4,5] Kateřina Hodaňová,[1,2] Petr Vylet'al,[1,2] Marie Kalbáčová,[1,2] Veronika Barešová,[1,2] Jakub Sikora,[2] Hana Blažková,[2] Jan Živný,[3] Robert Iványek,[1,2] Viktor Stránecký,[1,2] Jana Sovová,[2] Kathleen Claes,[6] Evelyne Lerut,[6] Jean-Pierre Fryns,[7] P. Suzanne Hart,[8] Thomas C. Hart,[9] Jeremy N. Adams,[8] Audrey Pawtowski,[10] Maud Clemessy,[12] Jean-Marie Gasc,[12] Marie-Claire Gübler,[11,13] Corinne Antignac,[10,11,13] Milan Elleder,[1,2] Katja Kapp,[14] Philippe Grimbert,[4,5] Anthony J. Bleyer,[15] and Stanislav Kmoch[1,2,*]

Through linkage analysis and candidate gene sequencing, we identified three unrelated families with the autosomal-dominant inheritance of early onset anemia, hypouricosuric hyperuricemia, progressive kidney failure, and mutations resulting either in the deletion (p.Leu16del) or the amino acid exchange (p.Leu16Arg) of a single leucine residue in the signal sequence of renin. Both mutations decrease signal sequence hydrophobicity and are predicted by bioinformatic analyses to damage targeting and cotranslational translocation of preprorenin into the endoplasmic reticulum (ER). Transfection and in vitro studies confirmed that both mutations affect ER translocation and processing of nascent preprorenin, resulting either in reduced (p.Leu16del) or abolished (p.Leu16Arg) prorenin and renin biosynthesis and secretion. Expression of renin and other components of the renin-angiotensin system was decreased accordingly in kidney biopsy specimens from affected individuals. Cells stably expressing the p.Leu16del protein showed activated ER stress, unfolded protein response, and reduced growth rate. It is likely that expression of the mutant proteins has a dominant toxic effect gradually reducing the viability of renin-expressing cells. This alters the intrarenal renin-angiotensin system and the juxtaglomerular apparatus functionality and leads to nephron dropout and progressive kidney failure. Our findings provide insight into the functionality of renin-angiotensin system and stress the importance of renin analysis in families and individuals with early onset hyperuricemia, anemia, and progressive kidney failure.

Introduction

The physiologic importance of the renin-angiotensin system (RAS) has been well described in more than 25,000 medical publications, with substantial interest in the effect of angiotensin converting enzyme gene polymorphisms on renal function.[1] Recessive mutations causing complete loss of renin synthesis resulting in renal tubular dysgenesis (RTD [MIM 267430]) have been described.[2] With the exception of premature stop codon mutation leading to benign hyperproreninemia[3] (REN [MIM 179820]), no other nonlethal mutations of the renin gene have been reported to date. Identification and characterization of such mutations may provide unique insight into the physiology of the RAS and its organ-specific functionality and regulation. The gene responsible for renin production is located on chromosome 1, and it is primarily expressed by granular cells in the juxtaglomerular apparatus of the kidney. The gene product preprorenin contains a signal sequence that directs ER targeting, glycosylation, and proteolytic processing of the nascent preproprotein, resulting in prorenin and renin production.[4] A primary function of renin is the hydrolytic cleavage of angiotensinogen to angiotensin, with the subsequent stimulation of aldosterone production. The RAS has also been found to have widespread and diverse roles, including modulating vascular tone, renal sodium handling, erythropoiesis, thirst, cardiac hypertrophy, and functioning through local RAS systems in many organs.[5]

In this work, by using positional cloning, we identify two unrelated families with mutations resulting in the deletion (p.Leu16del) of a single leucine residue in the signal sequence of renin. On the other hand, renin mutation (p.Leu16Arg) in the third family was detected through a candidate gene approach based on the association of anemia and hyperkalemia with low-normal and orthostatism-unresponsive plasma renin concentration (PRC) and aldosterone levels in the proband.

Detailed clinical, biochemical, and immunohistochemical studies and molecular characterization of the identified

[1]Center for Applied Genomics, [2]Institute for Inherited Metabolic Disorders, [3]Institute of Pathophysiology, Charles University in Prague, First Faculty of Medicine, Prague 12000, Czech Republic; [4]Assistance Publique-Hôpitaux de Paris (AP-HP), Nephrology and Transplantation Unit, Henri Mondor Hospital, Créteil 94010, France; [5]Paris XII University, Créteil 94010, France; [6]Department of Nephrology, University Hospital Gasthuisberg, Leuven 3000, Belgium; [7]Center for Human Genetics, University of Leuven, Leuven 3000, Belgium; [8]Office of the Clinical Director, National Human Genome Research Institute, [9]Human Craniofacial Genetics Section, National Institute of Dental and Craniofacial Research, National Institutes of Health, Bethesda, MD 20892-4320, USA; [10]Assistance Publique-Hôpitaux de Paris (AP-HP), Département de Génétique, [11]INSERM U574, Hôpital Necker-Enfants Malades, Paris 75015, France; [12]INSERM U833, Collège de France, Paris 75005, France; [13]Université Paris Descartes, Faculté de Médecine, Paris 75006, France; [14]ZMBH (Center for Molecular Biology Heidelberg), University of Heidelberg, Heidelberg D-69120, Germany; [15]Section on Nephrology, Wake Forest University School of Medicine, Winston-Salem, NC 27157, USA

*Correspondence: skmoch@lf1.cuni.cz

DOI 10.1016/j.ajhg.2009.07.010.

mutations suggested that juxtaglomerular cells, sustaining the highest expression rate of the mutant protein expression, are likely exposed to chronic ER stress and unfolded protein response. This led to site-specific attenuation of renin biosynthesis, RAS dysregulation, and altered juxtaglomerular apparatus functionality that result in a newly described clinical syndrome characterized by early-onset anemia, hyperuricemia, and progressive kidney failure.

Material and Methods

Patients

Family A was ascertained at the Department of Nephrology at the University Hospital in Leuven and was described, labeled as BE1, in our previous studies.[6,7] Families B and C were ascertained at the Section on Nephrology, Wake Forest University School of Medicine (Winston-Salem, NC) and Nephrology and Transplantation Unit, Henri Mondor Hospital (Creteil, France), respectively. Medical histories were obtained as a part of all the patients' clinical work-up by consultants of the above referred institutions. Investigations were approved by the participating center's Institutional Review Boards and were conducted according to the Declaration of Helsinki principles.

Genotyping, Linkage Analysis, and DNA Sequencing

Members of family A were genotyped with Affymetrix GeneChip Mapping 10K 2.0 Xba Arrays. Multipoint parametric linkage analysis, along with determination of the most likely haplotypes, was carried out under the assumption of a dominant mode of inheritance with a 0.99 constant, age-independent penetrance, 0.01 phenocopy rate, and 0.001 frequency of disease allele. Genomic fragments covering promoter region (about 500 bp upstream from most cDNA 5′ end) and all of the exons and exon-intron boundaries of selected candidate genes were PCR amplified from genomic DNA and sequenced in single proband and healthy individual from family A. The renin gene (*REN*) was analyzed in all three families as previously described.[2,8] Segregation of *REN* mutations in the families and absence of the mutations in a control white population were assessed by combination of genotyping and direct sequencing of the corresponding genomic DNA fragment. Disease haplotypes in families A and B were assessed with a set of microsatellite markers flanking the *REN* region.

In Silico Analysis

Preprorenin signal sequences from the presented species were obtained from the UniProtKB/Swiss-Prot database. Multiple alignment and evaluation of the amino acids conservation were performed by ClustalW2 software (EMBL-EBI database). Properties of the signal sequences were assessed with the SignalP 3.0 server[9] and the Kyte and Doolittle method.[10]

REN cDNA Expression Constructs

Wild-type *REN* mRNA was reverse transcribed from human total kidney RNA, PCR amplified, and cloned into pCR3.1 vector (Invitrogen, Paisley, UK). Constructs were introduced into the *Escherichia coli* TOP 10′F strain (Invitrogen, Paisley, UK) and the wild-type (WT^{REN}) clones were selected by sequencing. Mutant construct c.45_47 delGCT ($\Delta L16^{REN}$) was prepared by subcloning of the corresponding DNA fragments into the WT^{REN}/pCR3.1 construct. Mutant construct c.47T>G ($L16R^{REN}$) was prepared by site-directed mutagenesis.

Transient Expression of REN

HEK293 cells were maintained in DMEM high-glucose medium supplemented with 10% (vol/vol) fetal calf serum (PAA), 100 U/ml penicillin G (Sigma, Prague, Czech Republic), and 100 μg/ml streptomycin sulfate (PAA Laboratories GmbH, Pashing, Austria). Transfections were carried out with Lipofectamine 2000 (Invitrogen, Paisley, UK) with either 1.5 μg or 4 μg DNA for 1.5×10^5 or 8×10^5 cells, respectively.

REN-Expressing Stable Cell Lines

HEK293 cells were maintained as described above and transfected at 85% confluence with Amaxa nucleofector system (Amaxa, Köln, Germany). Three days after nucleofection, cells were trypsinized, diluted, and cultured in selective medium containing 0.8 mg/ml G418 (Invitrogen-GIBCO, Paisley, UK). REN-expressing clones were selected with PCR, sequencing, and western blot analyses.

In Vitro Translation and Translocation

Wild-type (WT^{REN}), c.45_47delGCT ($\Delta L16^{REN}$), and c.47T>G ($L16R^{REN}$) encoding plasmid DNA were linearized, purified, and used for in vitro transcription with T7 polymerase as described before.[11] In vitro translation was performed with rabbit reticulocyte lysate (Promega, Mannheim, Germany) and [^{35}S] EasyTag EXPRESS Protein Labeling Mix (Perkin Elmer, Rodgau Jügesheim, Germany). Reactions were incubated at 30°C for 30 min in the absence or presence of 1 eq *Micrococcus* nuclease-treated rough microsomes (RMs) produced according to the protocol of Walter and Blobel.[12] In vitro reactions were either directly precipitated or the membranes were separated by centrifugation through a sucrose cushion as described elsewhere.[13] Translation products were separated in 10% SDS gels (T: 10%, C: 0.8% according to Lämmli) or in Tris/Bicine gels.[14]

Prorenin and Renin Analysis

Western Blot Analysis and Deglycosylation Studies

Cells were grown in standard, serum-supplemented medium. 24 hr before the analyses, the supplemented medium was replaced by serum-free medium. For secreted renin analysis, the medium was collected and centrifuged first at 800 × g/5 min and then at 15,000 × g/5 min for residual cells and cellular debris removal. Resulting supernatant was mixed with protease inhibitor cocktail (Sigma, Prague, Czech Republic) in ratio 100:1 (vol/vol). 500 μl of the medium was then concentrated on Microcon YM-10 filters (Millipore, Billerica, MA), and total protein was recovered and dissolved in SDS sample buffer. Harvested cells were resuspended in PBS containing protease inhibitor cocktail, sonicated 2 times for 30 s on ice, and centrifuged for 15,000 × g/5 min. Pellet was dissolved in SDS sample buffer. Denatured protein samples were separated on 13% SDS-PAGE, blotted onto PVDF membrane, probed with rabbit anti-preprorenin (recognizing amino acid residues 21–64) antibody (Yanaihara, Shizuoka, Japan), and detected with anti-rabbit IgG antibody conjugated to horseradish peroxidase (Pierce, Rockford, IL). Deglycosylation experiments were performed on protein extracts and cell lysates with the GlycoPro enzymatic deglycosylation kit (ProZyme Inc., San Leandro, CA). Deglycosylated products were analyzed by SDS-PAGE and western blot as described above.

Quantitative Renin Measurement

Cell lysate was prepared as described above. The medium was centrifuged at 15,000 × g for 5 min and resulting supernatant was mixed with protease inhibitor cocktail in ratio 100:1 (vol/vol).

For renin amount, 50 μl of the medium and 5 μl of the lysate were diluted to final volume of 200 μl with PBS. For trypsin-activated total renin and prorenin amount, 5 μl of medium and 2.5 μl of lysate were incubated at 37°C for 30 min in a 50 μl PBS reactions containing 20 μg and 5 μg of trypsin, respectively. The reactions were stopped by 1 μl of 10 mg/mL trypsin inhibitor (PMSF, Roche, Prague, Czech Republic) and diluted to a final volume of 200 μl with PBS. 10 μl of the resulting mixtures were mixed with 190 μl of PBS and 100 μl of the anti-hRenin (I-125) reagent (Active Renin IRMA kit, DSL, Webster, TX), and the renin amount was measured according to manufacturer instructions.

Renin Secretion Measurement

Stably transfected HEK293 cells were cultured in 96-well plates in standard, serum-supplemented medium without phenol red. After 20 hr, the medium was replaced with medium containing renin substrate conjugated with 5-FAM and QXL520 (part of SensoLyte 520 Renin Assay Kit, AnaSpec, San Jose, CA). Fluorescent signal was monitored at 520 nm every 5 min for 8 hr at 37°C on Synergy 2 microplate reader (BioTek, Winooski, VT).

Immunofluorescence Analysis

Transfected HEK293 cells were grown on glass chamber slides (BD Falcon - 4Chamber Polystyrene Vessel Tissue Culture Treated Glass Slide). After 48 hr, the cells were washed with PBS, fixed with 100% ice-cold methanol, blocked with 5% FBS, and incubated with rabbit anti-preprorenin (288-317) antibodies. Organelle-specific primary antibodies and fluorescently labeled secondary antibodies were described previously.[7] Nuclei were stained with 4′,6-diamidino-2-phenylindole (DAPI). Prepared slides were mounted in fluorescence mounting medium Immu-Mount (Shandon Lipshaw, Pittsburgh, PA) and analyzed by confocal microscopy.[7]

Growth Rate Analysis

Stably transfected HEK293 cells were seeded in a 6-well plate at 4×10^5 cells per well and cultured in the selective, G418-containing medium. Cells were counted every 24 hr for 7 days via a standard Bürker cell counting chamber. The medium was changed at the third, fifth, and sixth days.

XBP1 Analysis

Total RNA was isolated from cells via TRIZOL (Invitrogen, Carlsbad, CA) and reverse transcribed with oligo-dT primer and SuperScript II (Invitrogen). *XBP1* was PCR amplified from the corresponding cDNA with gene-specific primers.

Electron Microscopy

Pellets of stably transfected HEK293 cells were fixed with 3% glutaraldehyde in 0.1 M phosphate buffer for 30 min, postfixed with buffered 1% OsO_4 for 2 hr, dehydrated, and embedded into Epon. Thin sections were double contrasted with uranyl acetate and lead nitrate. Grids were observed and photographs were obtained on JEOL 1200 electron microscope.

Immunohistochemistry Studies

Formaldehyde- or ethanol-fixed kidney samples from 5 controls and patients DII1, DIV3, and DIV7 were analyzed essentially as previously described.[7] Selected antigens were investigated with the following primary antibodies: prorenin, rabbit anti-preprorenin (amino acid residues 21–64); prorenin + renin, rabbit anti-preprorenin (amino acid residues 288–317), both (Yanaihara, Shizuoka, Japan); active renin, mouse anti-renin (clone R3-36-16, gift from Novartis AG, Basel Switzerland); Pro/renin receptor, rabbit anti-/P/RR (gift from Genevieve Nguyen, Paris); angiotensinogen, mouse anti-angiotensinogen (US Biological, Swampscott, MA); angiotensin II, mouse anti-angiotensin II (Acris, Herford, Germany). Immunohistochemical detection of renin and in situ detection of renin mRNA in kidney biopsy from Family C patient CIII1 was performed as previously described.[2]

Results

Clinical and Biochemical Findings

In this work, we analyzed three families with the autosomal-dominant inheritance of chronic progressive kidney failure (Figure 1A). All three families were of European ancestry, by family report. In Family A, the youngest family member (DIV7) was studied at age of 4 years, at which time the patient was asymptomatic. The blood pressure was 92/50 mm Hg. Physical examination was unremarkable. Laboratory studies revealed a hemoglobin level of 9.5 g/dl (normal 11.5–13.5 g/dl), serum uric acid level of 6.0 mg/dl (normal 1.8–5.4 mg/dl), and an inulin clearance of 68 ml/min/1.73 m^2. Renal ultrasound performed at 7 years revealed kidney sizes of 7.4 and 6.9 cm (normal 8.5–11.5 cm) with no evidence of cyst formation. Kidney biopsy revealed focal tubular atrophy and dystrophy, focal and segmental glomerular sclerosis, and interstitial fibrosis (Figures 2K and 2L). The patient was started on allopurinol and followed with annual laboratory studies. The serum potassium values ranged between 4.8 and 5.9 mEq/l with serum bicarbonate levels between 19.6 and 25 mEq/l. Plasma renin and aldosterone levels were low but not entirely suppressed. Very similar clinical presentation and biochemical data were observed in all affected individuals in the three families (Table 1). Hemoglobin values were consistently low in children with the disease, with hemoglobin measurement at age 1 year in BIV2 already low at 10.2 g/dl. However, affected adults in the 4^{th} and 5^{th} decades of life had normal hemoglobin values if renal failure was not severe. Individuals with anemia had low reticulocyte counts and normal mean corpuscular volume. B12 and folate levels were normal in those who were studied. Individuals had normal iron stores or remained anemic after iron was repleted. Bone marrow aspirate was normal in an anemic individual from Family A. Anemia responded well to erythropoietin. There was a tendency to hyperkalemia in some individuals, though this was a variable finding. Hyperuricemia was present in many but not all patients, and the fractional excretion of uric acid was low in all individuals studied. Uric acid excretion and proteinuria stayed quite constant over time. Renal disease was characterized by a bland urinalysis and absence of proteinuria. Reduced glomerular filtration was present from an early age and developed in all affected individuals. Kidney failure was slowly progressive with end-stage kidney disease developing at ages 50, 66, and 68 years in Family A, and at ages 43, 50, and 63 years in Family B.

Please cite this article in press as: Živná et al., Dominant Renin Gene Mutations Associated with Early-Onset Hyperuricemia, Anemia, and Chronic Kidney Failure, The American Journal of Human Genetics (2009), doi:10.1016/j.ajhg.2009.07.010

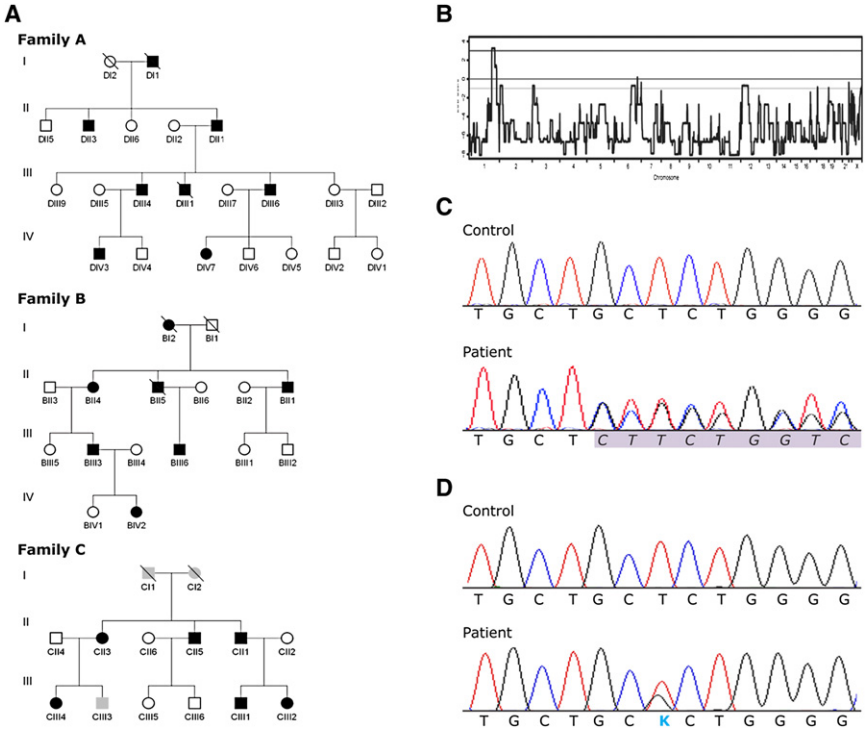

Figure 1. Pedigrees, Linkage and DNA Analysis

(A) Pedigrees of the investigated families. Black symbols denote affected individuals; open symbols denote unaffected individuals; and gray symbols denote individuals in whom clinical, biochemical, and genetic investigations were not yet performed.

(B) A whole-genome parametric linkage analysis showing a single statistically significant region on chromosome 1q41 detected in family A.

(C) Chromatograms showing genomic DNA sequence of the *REN* exon 1 in control and a heterozygous deletion c.45_47 delGCT in patient from family A.

(D) Chromatograms showing genomic DNA sequence of the *REN* exon 1 in control and a heterozygous mutation c.47T>G in patient from family C.

Genotyping, Linkage Analysis, and DNA Sequencing Revealed Mutations in the Signal Sequence of Preprorenin

To identify the genetic defect, we corroborated the results of the previous medium-dense scan in family A,[6] performed a genome-wide linkage analysis, and identified a single genomic region with statistically significant LOD score of 3.24 on chromosome 1 (Figure 1B). By using haplotype analysis, we delimited the candidate region between the SNP_A-1517951 and SNP_A-1509750 markers. The critical region we have delimited (genomic position chr1:188,333,009-213,216,882) spans 25 million bases and contains about 300 genes. After the analysis of nine candidate genes reported in our previous study,[6] we sequenced promoter and coding regions of six additional genes (*ELF3* (ELF3 [MIM 602191]), *ATF3* (ATF3 [MIM 603148]), *KCNK2* (KCNK2 [MIM 603219]), *KCTD3* (MIM n.a.); *PTGS2* (PTGS2 [MIM 600262]), and *REN* (REN [MIM 179820]) and identified a heterozygous deletion c.45_47delGCT in exon 1 of the *REN* gene in the proband (Figure 1C). Genotyping showed that the identified deletion was present in all affected individuals, whereas healthy individuals from the family as well as 385 unrelated white controls had a normal genotype. Targeted *REN* sequencing among probands from other families investigated in the Czech laboratory[7] and families followed by investigator A.J.B. revealed an additional family (Family B) having an identical mutation present on a distinct haplotype, indicating that the families are not related (Supplemental Data available online). Family C of Portuguese origin, with a missense mutation c.47T>G (Figure 1D), was revealed by M.M. and P.G. This mutation also segregated with the disease and was absent in 185 white controls and 50 controls from Portugal.

In Silico Analysis Suggested Altered Targeting Properties of Mutant Renin Signal Sequences

Human prorenin and renin are synthesized in juxtaglomerular (JG) cells from a 406-amino-acid-residues-long preproprotein composed of a 23-residues-long N-terminal signal sequence, 43-residues-long "pro" domain, and the mature renin comprising 340 residues.[4] Mutation c.45_47delGCT causes a deletion, p.Leu16del ($\Delta L16^{REN}$), whereas mutation c.47T>G results in the amino acid exchange p.Leu16Arg ($L16R^{REN}$) of a single leucine residue, L16, forming a hydrophobic penta-leucine motif of the preprorenin signal sequence mediating protein insertion in the ER membrane (Figure 3A). The hydrophobic region of the human preprorenin signal sequence is not entirely conserved among mammals. However, the penta-leucine motive is conserved within primates (Figure 3B). With the SignalP 3.0 server,[9] we noticed that both mutations decrease the signal sequence prediction probability (*D* score value)[15] and have no effect on the predicted signal peptide cleavage site (data not shown). Another calculation, the Kyte-Doolittle algorithm,[10] showed a decrease in the hydrophobicity of the $\Delta L16^{REN}$ and $L16R^{REN}$ signal sequences compared to that of the WT^{REN} (Figure 3C).

Functional Studies Showed that Signal Sequence Mutations Affect Renin Biosynthesis

WT^{REN}, $\Delta L16^{REN}$, and $L16R^{REN}$ proteins were transiently expressed in HEK293 cells and detected by western blot analysis (Figure 4A). $WT^{REN}$and $\Delta L16^{REN}$ were expressed as 47 kDa proteins whereas $L16R^{REN}$ was expressed as 45 kDa protein. Deglycosylation reduced molecular weight of the $WT^{REN}$and $\Delta L16^{REN}$ proteins to 43 kDa, which corresponds to complete loss of N-glycosylation on both of the predicted N-glycosylation sites in the preprorenin sequence (N71 and N141). Molecular weight of $L16R^{REN}$ remained unchanged. Analysis of molecular weights

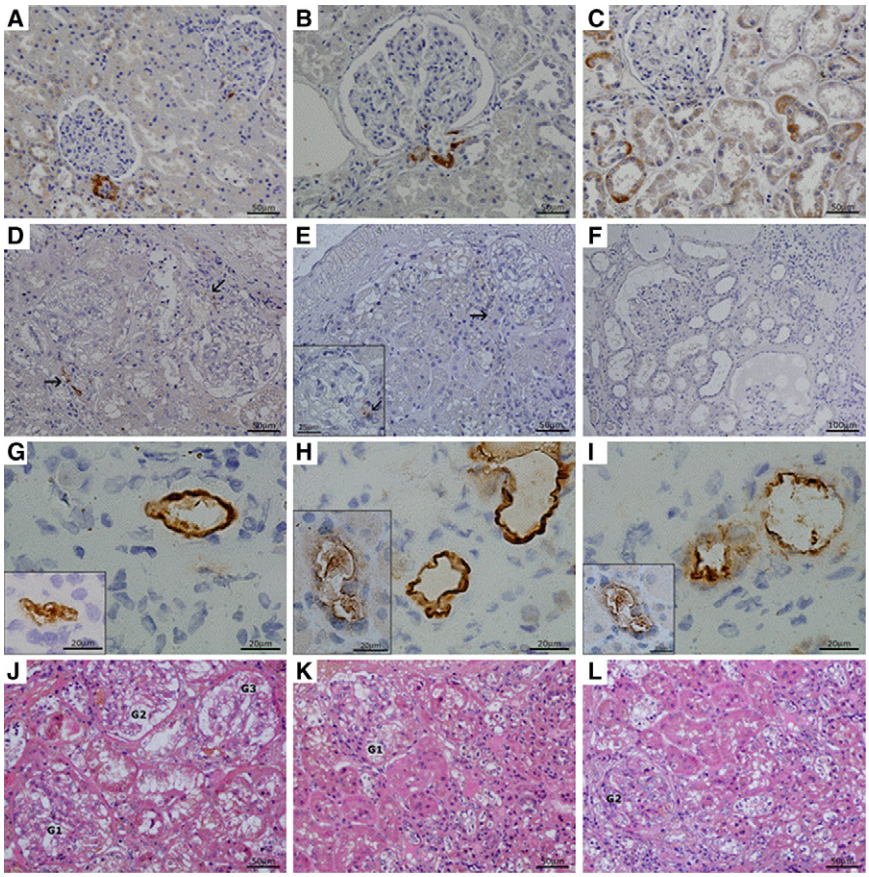

Figure 2. Renin Immunohistochemistry and Nephropathology

Family A, patients DIV3, DIV7, and DII1.

(A–C) Renin expression in control kidney.

(A) Control aged 7 years; renin expression in JG cells and individual cells of collecting ducts.

(B and C) Adult control; renin staining (B) in JG cells and (C) in renal cortical tubules where the signal is restricted to individual cells of the collecting ducts.

(D and E) Kidney biopsies in an early disease stage. Patient DIV3 (D) and patient DIV7 (E) shown. The common denominator is a strong reduction of renin signal in the JG apparatus (marked by arrows) and its absence in the surrounding tubules. Insert in (E) shows glomerulus in detail.

(F) Patient in advanced stage of kidney disease (DII1). Renin staining is absent in both JG apparatus and tubular epithelium even in relatively well-preserved regions.

(G–I) Renin and prorenin expression inside the wall of small size renal vessels, probably in a sub/endothelial localization, more prominent in adult patient DII1 (the main pictures) than in patients in an early stage of the disease (inserts). Preprorenin antibody detecting prorenin and renin (G), monoclonal antibody detecting active renin (H), and polyclonal antibody detecting prorenin (I). Insert in (G) demonstrates this phenomenon in patient DIV7, inserts in (H) and (I) in patient DIV3.

(J–L) Nephropathology in early stage of the disease (HE staining).

(J) Morphology in patient DIV3 was dominated by irregular dystrophic changes in tubular epithelium mainly in proximal tubules (coarsely vacuolated or granular cytoplasm) and focal segmental sclerosis of glomerular tufts with adhesions to Bowman's capsule. Tubular atrophy and interstitial fibrosis was less expressed (sampling?).

(K and L) Kidney biopsy from patient DIV7 demonstrated more pronounced glomerular sclerosis and hyalinosis (1 out of 8 glomeruli was totally sclerosed, not shown) and focal tubular atrophy accompanied with moderate interstitial fibrosis. Glomeruli, marked as Gs, in various degrees of sclerosis and areas of tubulointerstitial fibrosis are shown. In advanced stage of the disease (patient DII1, not shown), morphology of progressive nephropathy was modified by haemodialysis lasting for 1 year.

suggested that $WT^{REN}$and $\Delta L16^{REN}$ produce the signal sequence-cleaved, ER-translocated, and fully glycosylated prorenin whereas $L16R^{REN}$ produce nonglycosylated and therefore secretion-incompetent and enzymatically inactive preprorenin[16] (Figure 4A).

Immunofluorescence and confocal microscopy of transfected cells demonstrated the expected localization of rennin-containing granules in the cytosol of the investigated cells. No visible differences in the amount, shape, and cellular localization of WT^{REN}, $\Delta L16^{REN}$, and $L16R^{REN}$ granules were observed and/or detected by colocalization with ER marker (Supplemental Data).

In vitro translation/translocation assays confirmed that $L16R^{REN}$ is not translocated across the ER membrane and suggested a reduced translocation ability of $\Delta L16^{REN}$ (Figures 4B and 4C). The latter was supported by densitometry analysis of the products obtained in three independent experiments which demonstrated that only 39% of the $\Delta L16^{REN}$ precursor was processed to the 47 kDa form, compared to 75% of the WT^{REN}. In addition, an analysis of the signal peptide processing (Figure 4C) showed that compared to $\Delta L16^{REN}$, the WT^{REN} signal peptide is evidently more stable and only slightly affected by signal peptide peptidase-mediated processing.

To assess prorenin and renin amounts produced by $\Delta L16^{REN}$ exactly, we prepared cell lines stably expressing WT^{REN} and $\Delta L16^{REN}$ and measured prorenin and renin production by quantitative radioimmunoassay. The analysis showed that $\Delta L16^{REN}$ mutation significantly impaired prorenin and renin biosynthesis (Figure 4D), secretion (Figure 4E), and activity (Figure 4F). Cells expressing $\Delta L16^{REN}$ also had a reduced growth rate (Figure 4G), activated endoplasmic reticulum stress, and unfolded protein response, demonstrated by the presence of spliced X-Box Protein 1 (XBP1) mRNA form[17] (Figure 4H).

Ultrastructural analysis showed in the WT^{REN}-expressing cells numerous electron-dense cytoplasmic vesicles compatible with those of previously reported secretory renin granules[18] (Figure 4I), whereas there was a decreased number of cytoplasmic vesicles, considerable distension of rough endoplasmic reticulum cisteranae, and pronounced macroautophagy in $\Delta L16^{REN}$-expressing cells (Figure 4J).

Table 1. Representative Clinical and Biochemical Findings in Affected Family Members

Patient[a]	Gender	Age at Clinical Measurement (y) unless Otherwise Noted	Blood Pressure (mm Hg)	Serum Creatinine (mg/dl)	GFR[b]	Serum Potassium (mEq/L)[c]	Serum Bicarbonate (mEq/L)[d]	Serum Uric Acid (mg/dl)[e]	Fractional Excretion Urate[f]	Hemoglobin (g/L)[g]	Random Plasma Renin Activity (ng/ml/h)[h]	Random serum Aldosterone (ng/dl)[i]	Renal Size Left, Right Kidney (Age of Measurement)
DIV7	F	4	92/50	0.8	68[j]	4.6	21	6.0	0.01	9.5			7.4, 6.9 (7)
DIV7	F	16	115/56	1.5	66[k]	5.2	22	4.4[l]	0.05	12.9	0.5	25	8.2, 8.3 (16)
DIV3	M	8	102/50	0.9	68[j]	4.5	21	7.3	0.04	10.2			8.7, 8.0 (10)
DIV3	M	20	120/70	1.8	72[m]	4.2	24	5.7[l]	0.04	10.9	2.2	15	9.9, 10.9 (19)
DIII4	M	43		3.0	24[m]	4.6	22	4.1[l]		11.5	1.6	18	
DIII6	M	47	120/85	2.5	38[m]	4.9	23	3.8[l]	0.05	13.1	0.6	23	10.7, 10.5 (47)
BIV2	F	8	100/62	0.6	95[k]	4.6	24	5.1	0.03	10.1	1.7	2.8	
BIII6	M	30		1.3	69[m]	4.6	27	9.9	0.04	15.7			
BIII3	M	32	106/63	1.6	54[m]	4.3	29	6.5	0.03	13.1	2.6	6.0	
BII4	F	59		1.8	31[m]	4.7	20			10.8	0.4	6.4	10.3, 9.0 (58)
CIII2	F	12	100/50	1.3	63[k]	6	23	8.0		9.9			
CIII4	F	16	110/60	1.2	83[k]	5.1	24	8.1[l]	0.03	10.9			
CIII1	M	18	95/50	1.9	49[m]	5.7	28	10.5	0.03	8.3[n]	10.3 mU/L[o]	21	9.5, 10.0 (18)
CII5	M	42	135/70	1.6	51[m]	5.4	28	8.1[l]		13.0			
CII3	F	45	125/80	1.1	57[m]	4.1	25	6.3[l]		13.0			
CII1	M	48	120/70	1.5	53[m]	4.0	29	8.3[l]		15.3			

[a] See Figure 1 for pedigree.
[b] GFR, glomerular filtration rate (ml/min/1.73 m^2).
[c] Serum potassium normal range 3.5–5.0 mEq/L.
[d] Serum bicarbonate normal range 22–30 mEq/L.
[e] Serum uric acid normal values:[34] adults, 2.5–8.0 mg/dl; children <5 years, 1.8–5.3 mg/dl; children 5 to 10 years, 2.1–6.1 mg/dl; female 12–16 years, 2.7–6.3 mg/dl.
[f] Fractional urate excretion normal values > 0.10 for children, > 0.05 for men, and > 0.06 for women.
[g] Hemoglobin normal range 11.5–13.5 g/dl for female children, 11.5–15.5 g/dl for male children, 12–16 g/dl for female adult, and 14–18 g/dl for male adult.
[h] Plasma renin activity normal range 0.5–5.9 ng/ml/hr.
[i] Random serum aldosterone level normal range 3–28 ng/dL.
[j] Determined by inulin clearance.
[k] GFR determined by Schwartz Formula.[36]
[l] Determined while on allopurinol.
[m] Estimated by the Modification of Diet in Renal Disease Study equation.[35]
[n] Measured at age 16 prior to erythropoietin therapy.
[o] Active renin normal range 3.3–41 mU/L.

Please cite this article in press as: Živná et al., Dominant Renin Gene Mutations Associated with Early-Onset Hyperuricemia, Anemia, and Chronic Kidney Failure, The American Journal of Human Genetics (2009), doi:10.1016/j.ajhg.2009.07.010

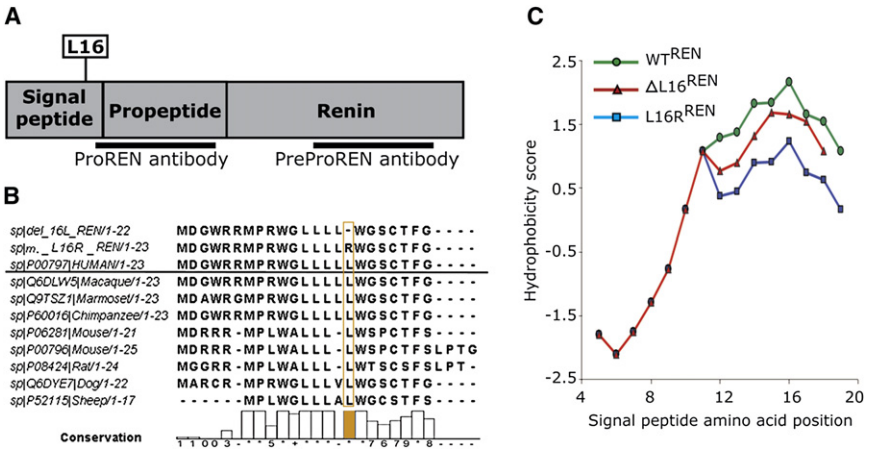

Figure 3. Bioinformatic Analysis of the Preprorenin

(A) Diagram of the preprorenin sequence showing the locations of the identified mutations and epitopes recognized by prorenin (amino acid residues 21–64) and preprorenin (amino acid residues 288–317) antibodies used in this study.

(B) Homology of the mutant and wild-type human preprorenin signal sequences with those of higher mammals.

(C) Hydrophobicity plot of the WT^{REN}, $\Delta L16^{REN}$, and $L16R^{REN}$ signal sequences calculated via the Kyte and Doolittle method and scale.

Mutations Lead to Reduced Expression and Abnormal Localization of Prorenin and Renin and Altered Expression of RAS Components in Patient Kidney

Immunohistochemical staining with antibodies detecting prorenin (amino acids residues 21–64); preprorenin, prorenin, and renin (amino acids residues 288–317); and active renin (clone R3-36-16) was performed in kidney biopsies from three patients with p.Leu16del mutation. Compared to control tissues (Figures 2A–2C), staining for renin and prorenin was strongly decreased in juxtaglomerular granular cells and undetectable in tubular cells in the early disease stage (Figures 2D and 2E). In an advanced stage of the disease, the signal was absent in both the juxtaglomerular apparatus and the tubular epithelium (Figure 2F). However, in all three patients we observed an abnormal localization of both renin and prorenin inside the vessel wall of several arterioles and small arteries (Figures 2G–2I). Staining intensities of the other analyzed renal RAS components—angiotensinogen, angiotensin II, and pro/renin receptor—were decreased compared to controls. The decrease was proportional to the stage of the disease (Supplemental Data). No renin labeling was detected in the biopsy specimen from patient CIII1 with p.Leu16Arg mutation by immunohistochemical staining. According to in situ hybridization, renin mRNA was not detected in juxtaglomerular cells but it was strongly expressed in sparse cells regarded as pericytes, along peritubular capillary (not shown).

Discussion

We identified two mutations, a deletion and an amino acid exchange of a single leucine residue in the signal sequence of renin segregating with a phenotype of anemia, hypouricosuric hyperuricemia, and slowly progressive chronic kidney disease in three unrelated families.

Bioinformatic analysis showed that both mutations affect the signal sequence properties and function. Functional studies proved that $L16R^{REN}$ mutation prevents ER cotranslational translocation and processing, which are necessary for prorenin/renin secretion and activity.[19] Instead, the nascent preproprotein is synthesized and accumulates in cytoplasm. In contrast, $\Delta L16^{REN}$ mutation reduces translocation efficiency of the nascent protein into ER and decreases prorenin and renin biosynthesis and secretion. Interestingly, the $\Delta L16^{REN}$ mutation evidently reduces signal peptide accumulation, which is suggestive that preprorenin-derived signal peptide may fulfill a post-targeting function within the ER membrane or in a different compartment as known for other signal peptides.[20] Expression of the $\Delta L16^{REN}$ protein also significantly affected cells growth, activated ER stress, and unfolded protein response.

Clinical studies correlated these findings: immunohistologic examination revealed a decrease in immunostaining for renin in affected children, with an even more marked decline with aging in juxtaglomerular cells and abnormal localization/induction of both renin and prorenin inside the vessel wall of arterioles, small arteries, and pericytes. Patients were able to sustain plasma renin concentrations, though low normal blood pressures in the setting of chronic kidney disease and mild hyperkalemia suggested, in agreement with immunohistochemistry analysis, a relative decrease in RAS activity.

Reduced fractional excretion of uric acid and resulting hyperuricemia are consistent with a model of increased proximal tubular reabsorption of uric acid resulting from mild volume depletion because of relative aldosterone deficiency. In contrast, if hyperuricemia was due to renal insufficiency, the fractional excretion of uric acid would have been elevated.[21] Hyperuricemia resulting from increased proximal tubular reabsorption of uric acid has been seen in other genetic syndromes associated with salt wasting and mild volume depletion such as uromodulin-associated kidney disease.[22]

Anemia is also consistent with decreased RAS activity. Anemia has been noted in individuals receiving angiotensin converting enzyme inhibitors[23] and diabetics with hyporeninemic hypoaldosteronism.[24] The degree of anemia was out of proportion to the level of kidney failure; one individual with normal renal function at age 8 years

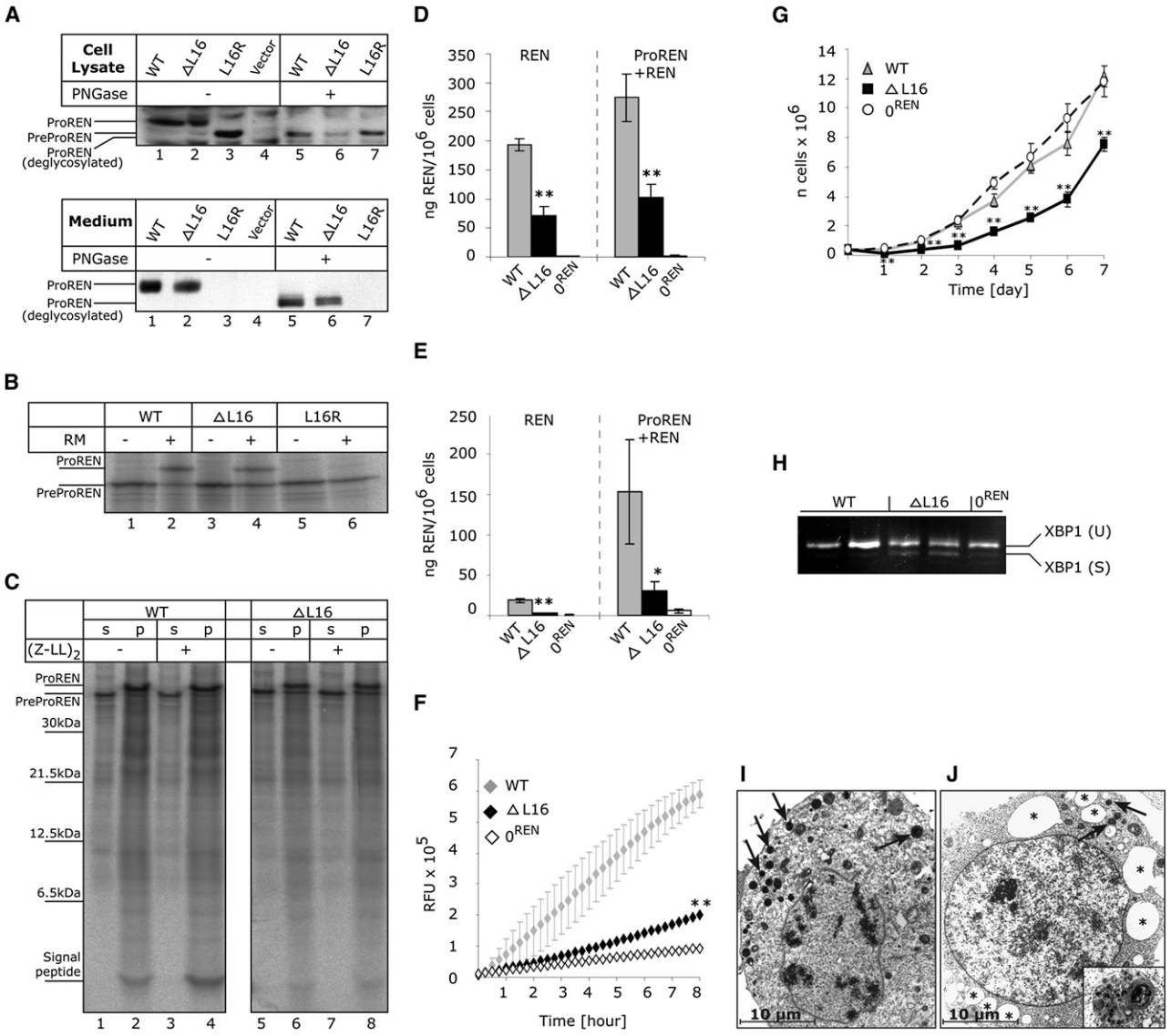

Figure 4. Functional Studies

(A) Western blot analysis of WT^{REN}, $\Delta L16^{REN}$, and $L16R^{REN}$ proteins transiently expressed in HEK293 cells. Products of biosynthesis—preprorenin (PreProREN) and prorenin (ProREN)—were analyzed in cell lysates and cell culturing medium. To distinguish proteolytic processing and glycosylation status, the proteins were always analyzed before (−) and after (+) deglycosylation with PNGase.

(B and C) In vitro translation and translocation.

(B) Nascent WT^{REN}, $\Delta L16^{REN}$, and $L16R^{REN}$ proteins translated from corresponding mRNAs in nuclease-treated rabbit reticulocyte lysate in the absence (−) or presence (+) of rough endoplasmic reticulum microsomes (RM). Without RM, only nascent preprorenin (PreProREN) is formed. With RM, the translocated preprorenin is converted into prorenin (ProREN). In comparing lane 2 to lane 4 (as well as lanes 2 and 4 to lanes 6 and 8 in C), one can see that significantly more WT^{REN} is translocated into the RM and converted to prorenin than with the $\Delta L16^{REN}$ mutant. The difference in translocation efficiency between WT^{REN} and $\Delta L16^{REN}$ was assessed by densitometry. The L16R mutation completely prevents translocation and $L16R^{REN}$ protein is present as preprorenin.

(C) Translation/translocation assay performed in the presence of RM and in the absence (−) or presence (+) of the signal peptide peptidase inhibitor $(ZZ\text{-}L)_2$ketone. Upon centrifugation, prorenin as well as out cleaved signal peptide were present in RM pellet fractions (p), whereas preprorenin that does not translocate is found in supernatant (s). The inhibitor only slightly affected preprorenin signal peptide processing (lanes 4 and 8). Compared to $\Delta L16^{REN}$, the WT^{REN} signal peptide is evidently more stable and only slightly affected by signal peptide peptidase-mediated processing.

(D and E) Prorenin and renin produced by stably transfected HEK293 cells. Active renin (REN) and trypsin activated total renin + prorenin (ProREN+REN) amounts measured in (D) lysates and (E) medium of the corresponding cell lines. The values represent means ± SD of the measurements performed in two independent clones for each of the constructs. The individual measurements were carried out in triplicate. The statistical significance of the differences between WT^{REN} and $\Delta L16^{REN}$ protein amounts was tested by t test. *$p < 0.05$; **$p < 0.01$; ***$p < 0.001$. 0^{REN} is an antibiotic-selected cell line originally transfected with WT^{REN} construct, but showing later no renin expression by RT-PCR and western blot analysis.

(F) Renin secretion from living stably transfected HEK293 cell lines. The fluorescent signal is released from 5-FAM and QXL520 conjugated renin substrate and corresponds to the activity of renin secreted in the medium.

(G and H) Reduced growth rate (G) and activated *XBP1* splicing (H) indicating ER stress in $\Delta L16^{REN}$-expressing cells.

suffered from persistent anemia since measurements performed at age 1 year. The patients in this study were able to reach target hemoglobin levels with use of erythropoietin. It is unclear why the hemoglobin values tended to be higher or normal in older individuals with the renin mutation, though the increase in testosterone secretion after adolescence may have been responsible in men.[25]

The ability of signal sequence mutations to activate ER stress, unfolded protein response, and pronounced autophagy has been noted with other signal sequence mutations.[26–30] These events usually reduce the client protein expression rate, trigger apoptosis and inflammation, and lead to a reduced viability of secretory cells[31] and disease development.[32]

In agreement with this model, we propose that the identified mutations in renin signal sequence likely expose juxtaglomerular cells, sustaining the highest expression rate of the mutant protein, to chronic ER stress and lead to site-specific attenuation of renin biosynthesis and RAS dysregulation. Reduced viability of juxtaglomerular cells and limited renin availability then affect renal development, intrarenal RAS homeostasis, and kidney autoregulation resulting in anemia, reduced glomerular filtration rate, and hyperuricemia. Over time, accelerated apoptosis in juxtaglomerular cells results, and, similar to mice with ablated juxtaglomerular cells,[33] nephron loss and progressive kidney failure occurs. Proposed pathogenetic cascade correlates with the clinical picture of slowly advancing kidney failure, progressive tubulointerstitial nephropathy, secondary focal and segmental glomerular sclerosis, and nephron dropout demonstrated by nephropathologic examination.

From a clinical perspective, our findings stress the importance of renin analysis in families with early-onset hyperuricemia, anemia, and progressive kidney failure. We would be most interested in the referral of similar families for genotyping.

Supplemental Data

Supplemental Data include three figures showing haplotype analysis in families A and B, expression of renal RAS components in kidney biopsies, and cellular localization of the transiently expressed wild-type and mutant preprorenin, prorenin, and renin in HEK293 cells and can be found with this article online at http://www.ajhg.org/.

Acknowledgments

We thank Gert Matthijs, Elly Pijkels, Vicki Robins, Sharon Moe, Conceiçao Mota, and Fatima Torres for collection of biological materials and patient data, Olivier Gribouval for contribution to the genetic analysis, Maria Leidenberger and Klaus Meese for in vitro translation experiments, Zdena Vernerová for nephropathologic expertise, Novartis Pharma for R3-36-16 renin antibody, and Pierre Corvol and Genevieve Nguyen for pro/renin antibody. The authors report no conflict of interest. This work was supported by the Grant Agency of Charles University of Prague (projects 257672 and 257750). Institutional support was provided by the Ministry of Education of the Czech Republic (projects MSM0021620806 and 1M6837805002).

Received: June 18, 2009
Revised: July 13, 2009
Accepted: July 14, 2009
Published online: August 6, 2009

Web Resources

The URLs for data presented herein are as follows:

ClustalW2 software (EMBL-EBI database), http://www.ebi.ac.uk/Tools/clustalw2/
Online Mendelian Inheritance in Man (OMIM), http://www.ncbi.nlm.nih.gov/Omim/
SignalP 3.0 server, http://www.cbs.dtu.dk/services/SignalP/
UniProtKB/Swiss-Prot database, http://www.expasy.ch/sprot/

References

1. Wong, C., Kanetsky, P., and Raj, D. (2008). Genetic polymorphisms of the RAS-cytokine pathway and chronic kidney disease. Pediatr. Nephrol. *23*, 1037–1051.
2. Gribouval, O., Gonzales, M., Neuhaus, T., Aziza, J., Bieth, E., Laurent, N., Bouton, J.M., Feuillet, F., Makni, S., Ben Amar, H., et al. (2005). Mutations in genes in the renin-angiotensin system are associated with autosomal recessive renal tubular dysgenesis. Nat. Genet. *37*, 964–968.
3. Villard, E., Lalau, J.D., van Hooft, I.S., Derkx, F.H., Houot, A.M., Pinet, F., Corvol, P., and Soubrier, F. (1994). A mutant renin gene in familial elevation of prorenin. J. Biol. Chem. *269*, 30307–30312.
4. Imai, T., Miyazaki, H., Hirose, S., Hori, H., Hayashi, T., Kageyama, R., Ohkubo, H., Nakanishi, S., and Murakami, K. (1983). Cloning and sequence analysis of cDNA for human renin precursor. Proc. Natl. Acad. Sci. USA *80*, 7405–7409.
5. Paul, M., Poyan Mehr, A., and Kreutz, R. (2006). Physiology of local renin-angiotensin systems. Physiol. Rev. *86*, 747–803.
6. Hodanova, K., Majewski, J., Kublova, M., Vyletal, P., Kalbacova, M., Stiburkova, B., Hulkova, H., Chagnon, Y.C., Lanouette, C.M., Marinaki, A., et al. (2005). Mapping of a new candidate locus for uromodulin-associated kidney disease (UAKD) to chromosome 1q41. Kidney Int. *68*, 1472–1482.
7. Vylet'al, P., Kublova, M., Kalbacova, M., Hodanova, K., Baresova, V., Stiburkova, B., Sikora, J., Hulkova, H., Zivny, J., Majewski, J., et al. (2006). Alterations of uromodulin biology: A common denominator of the genetically heterogeneous FJHN/MCKD syndrome. Kidney Int. *70*, 1155–1169.
8. Kmoch, S., Hartmannova, H., Stiburkova, B., Krijt, J., Zikanova, M., and Sebesta, I. (2000). Human adenylosuccinate

(I and J) Electron microscopy of stably transfected HEK293 cell lines showing (I) overview of the WT^{REN} -expressing cell with numerous electron-dense granules (arrows) and (J) considerable distensions of ER cisternae (asterisk) observed frequently in $\Delta L16^{REN}$ cells. Detail of one of the autophagosomal structures is shown in the insert. These structures were not present in 0^{REN} cells (data not shown).

lyase (ADSL), cloning and characterization of full-length cDNA and its isoform, gene structure and molecular basis for ADSL deficiency in six patients. Hum. Mol. Genet. *9*, 1501–1513.

9. Bendtsen, J.D., Nielsen, H., von Heijne, G., and Brunak, S. (2004). Improved prediction of signal peptides: SignalP 3.0. J. Mol. Biol. *340*, 783–795.
10. Kyte, J., and Doolittle, R.F. (1982). A simple method for displaying the hydropathic character of a protein. J. Mol. Biol. *157*, 105–132.
11. Lyko, F., Martoglio, B., Jungnickel, B., Rapoport, T.A., and Dobberstein, B. (1995). Signal sequence processing in rough microsomes. J. Biol. Chem. *270*, 19873–19878.
12. Walter, P., and Blobel, G. (1983). Preparation of microsomal membranes for cotranslational protein translocation. Methods Enzymol. *96*, 84–93.
13. Dultz, E., Hildenbeutel, M., Martoglio, B., Hochman, J., Dobberstein, B., and Kapp, K. (2008). The signal peptide of the mouse mammary tumor virus Rem protein is released from the endoplasmic reticulum membrane and accumulates in nucleoli. J. Biol. Chem. *283*, 9966–9976.
14. Wiltfang, J., Arold, N., and Neuhoff, V. (1991). A new multiphasic buffer system for sodium dodecyl sulfate-polyacrylamide gel electrophoresis of proteins and peptides with molecular masses 100,000–1000, and their detection with picomolar sensitivity. Electrophoresis *12*, 352–366.
15. Jarjanazi, H., Savas, S., Pabalan, N., Dennis, J.W., and Ozcelik, H. (2008). Biological implications of SNPs in signal peptide domains of human proteins. Proteins *70*, 394–403.
16. Rothwell, V., Kosowski, S., Hadjilambris, O., Baska, R., and Norman, J. (1993). Glycosylation of active human renin is necessary for secretion: effect of targeted modifications of Asn-5 and Asn-75. DNA Cell Biol. *12*, 291–298.
17. Yoshida, H., Matsui, T., Yamamoto, A., Okada, T., and Mori, K. (2001). XBP1 mRNA is induced by ATF6 and spliced by IRE1 in response to ER stress to produce a highly active transcription factor. Cell *107*, 881–891.
18. Sagnella, G.A., and Peart, W.S. (1979). Studies on the isolation and properties of renin granules from the rat kidney cortex. Biochem. J. *182*, 301–309.
19. Paul, M., Nakamura, N., Pratt, R.E., and Dzau, V.J. (1988). Glycosylation influences intracellular transit time and secretion rate of human prorenin in transfected cells. J. Hypertens. Suppl. *6*, S487–S489.
20. Hegde, R.S., and Bernstein, H.D. (2006). The surprising complexity of signal sequences. Trends Biochem. Sci. *31*, 563–571.
21. Danovitch, G.M. (1972). Uric acid transport in renal failure. A review. Nephron *9*, 291–299.
22. Hart, T.C., Gorry, M.C., Hart, P.S., Woodard, A.S., Shihabi, Z., Sandhu, J., Shirts, B., Xu, L., Zhu, H., Barmada, M.M., et al. (2002). Mutations of the UMOD gene are responsible for medullary cystic kidney disease 2 and familial juvenile hyperuricaemic nephropathy. J. Med. Genet. *39*, 882–892.
23. Hubert, C., Savary, K., Gasc, J.M., and Corvol, P. (2006). The hematopoietic system: A new niche for the renin-angiotensin system. Nat. Clin. Pract. Cardiovasc. Med. *3*, 80–85.
24. Donnelly, S., and Shah, B.R. (1999). Erythropoietin deficiency in hyporeninemia. Am. J. Kidney Dis. *33*, 947–953.
25. Yeap, B.B., Beilin, J., Shi, Z., Knuiman, M.W., Olynyk, J.K., Bruce, D.G., and Milward, E.A. (2008). Serum testosterone levels correlate with haemoglobin in middle-aged and older men. Intern. Med. J., in press.Published online August 16, 2008. 10.1111/j.1445-5994.2008.01789.x.
26. Ito, M., Jameson, J.L., and Ito, M. (1997). Molecular basis of autosomal dominant neurohypophyseal diabetes insipidus. Cellular toxicity caused by the accumulation of mutant vasopressin precursors within the endoplasmic reticulum. J. Clin. Invest. *99*, 1897–1905.
27. Bonapace, G., Waheed, A., Shah, G.N., and Sly, W.S. (2004). Chemical chaperones protect from effects of apoptosis-inducing mutation in carbonic anhydrase IV identified in retinitis pigmentosa 17. Proc. Natl. Acad. Sci. USA *101*, 12300–12305.
28. Rebello, G., Ramesar, R., Vorster, A., Roberts, L., Ehrenreich, L., Oppon, E., Gama, D., Bardien, S., Greenberg, J., Bonapace, G., et al. (2004). Apoptosis-inducing signal sequence mutation in carbonic anhydrase IV identified in patients with the RP17 form of retinitis pigmentosa. Proc. Natl. Acad. Sci. USA *101*, 6617–6622.
29. Datta, R., Waheed, A., Shah, G.N., and Sly, W.S. (2007). Signal sequence mutation in autosomal dominant form of hypoparathyroidism induces apoptosis that is corrected by a chemical chaperone. Proc. Natl. Acad. Sci. USA *104*, 19989–19994.
30. Datta, R., Waheed, A., Bonapace, G., Shah, G.N., and Sly, W.S. (2009). Pathogenesis of retinitis pigmentosa associated with apoptosis-inducing mutations in carbonic anhydrase IV. Proc. Natl. Acad. Sci. USA *106*, 3437–3442.
31. Marciniak, S.J., and Ron, D. (2006). Endoplasmic reticulum stress signaling in disease. Physiol. Rev. *86*, 1133–1149.
32. Kaufman, R.J. (2002). Orchestrating the unfolded protein response in health and disease. J. Clin. Invest. *110*, 1389–1398.
33. Pentz, E.S., Moyano, M.A., Thornhill, B.A., Sequeira Lopez, M.L., and Gomez, R.A. (2004). Ablation of renin-expressing juxtaglomerular cells results in a distinct kidney phenotype. Am. J. Physiol. Regul. Integr. Comp. Physiol. *286*, R474–R483.
34. Wilcox, W.D. (1996). Abnormal serum uric acid levels in children. J. Pediatr. *128*, 731–741.
35. Levey, A.S., Bosch, J.P., Lewis, J.B., Greene, T., Rogers, N., and Roth, D. (1999). A more accurate method to estimate glomerular filtration rate from serum creatinine: a new prediction equation. Modification of Diet in Renal Disease Study Group. Ann. Intern. Med. *130*, 461–470.
36. Schwartz, G.J., Haycock, G.B., Edelmann, C.M., Jr., and Spitzer, A. (1976). A simple estimate of glomerular filtration rate in children derived from body length and plasma creatinine. Pediatrics *58*, 259–263.

American Journal of Genetics, Volume *85*

Supplemental Data

Dominant Renin Gene Mutations Associated with Early-Onset Hyperuricemia, Anemia, and Chronic Kidney Failure

Martina Živná, Helena Hůlková, Marie Matignon, Kateřina Hodaňová, Petr Vyleťal, Marie Kalbáčová, Veronika Barešová, Jakub Sikora, Hana Blažková, Jan Živný, Robert Iványek, Viktor Stránecký, Jana Sovová, Kathleen Claes, Evelyne Lerut, Jean-Pierre Fryns, P. Suzanne Hart, Thomas C. Hart, Jeremy N. Adams, Audrey Pawtowski, Maud Clemessy, Jean-Marie Gasc, Marie-Claire Gübler, Corinne Antignac, Milan Elleder, Katja Kapp, Philippe Grimbert, Anthony J. Bleyer, and Stanislav Kmoch

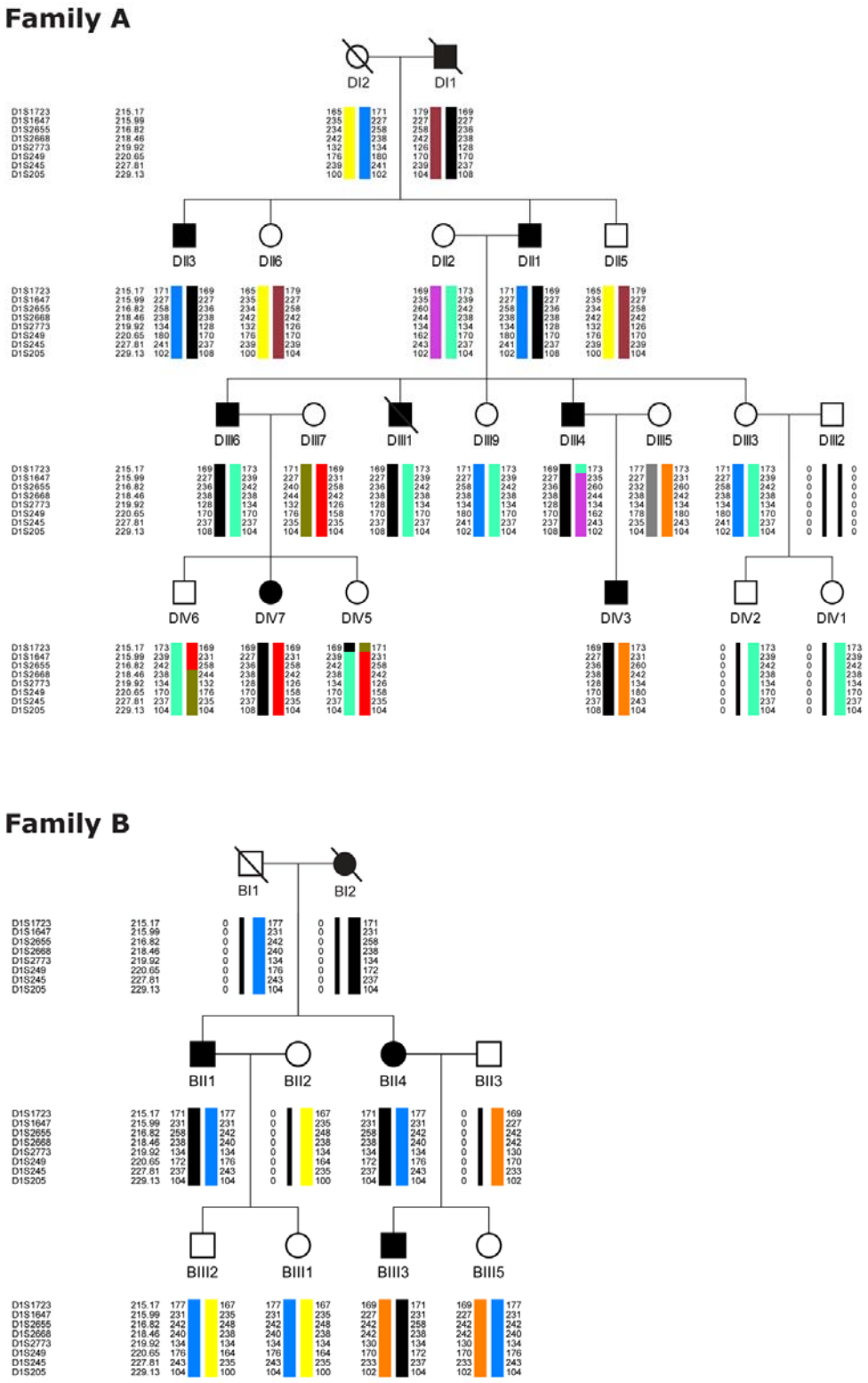

Figure S1. Haplotype analysis in families A and B. Disease haplotypes are shown in black.

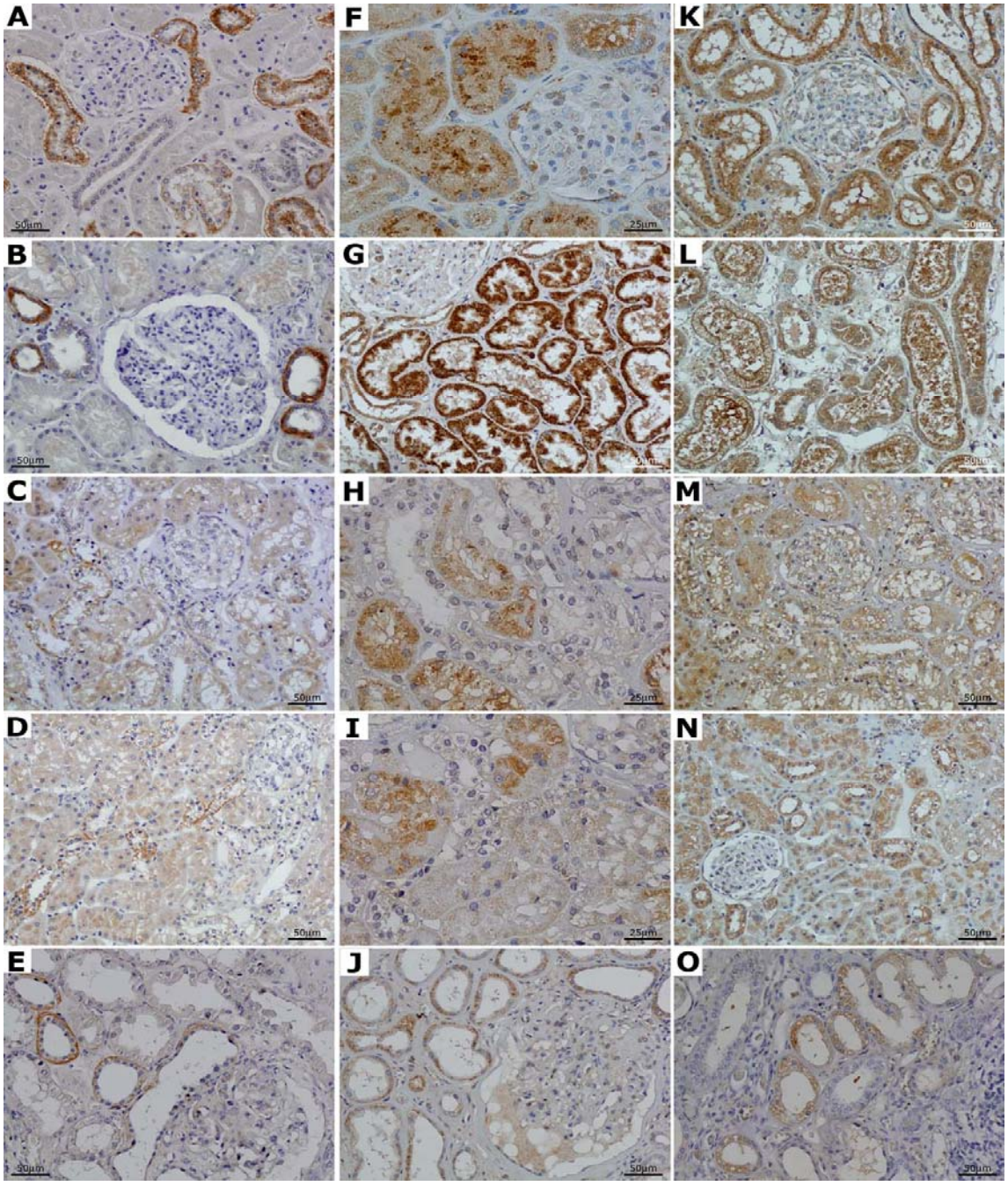

Figure S2. Detection of renal RAS components. (A-E) Immunodetection of pro/renin receptor. (A,B) Strong signal at the basolateral pole of distal convoluted tubules and thick ascending loop of Henle in (A) 7 years aged control, and (B) adult control. Expression of pro/renin receptor is in patients reduced proportionally to the disease stage. (C) patient DIV3, (D) patient DIV7, (E) patient DII1.

(F-J) Immunodetection of angiotensinogen (AGT). (F) Mild and heterogenous intracellular granular positivity in proximal tubules in 7 years aged control and (H,I) comparable or slightly weakened signal in patients in early stage of the disease. (H) patient DIV3, (I) patient DIV7. (G) Pronounced AGT expression in proximal tubules in adult control and (J) significantly decreased intensity in the kidney of patient DII1.

(K-O) Immunodetection of angiotensin II. (K) Presence of angiotensin II at the apical pole of proximal tubules, in the tubular fluid and in distal nephron epithelium in 7 years aged control and reduced signal in both (M) patient DIV3, and (N) patient DIV7. (L) Positivity in adult control kidney is seen in the same locations as in the infantile control but with an increased intensity. This contrasts with (O) markedly decreased signal in adult patient DII1. In the advanced stage of the disease (patient DII1) immunostaining signals of all the followed RAS components were always restricted to the foci of relatively preserved renal parenchyma.

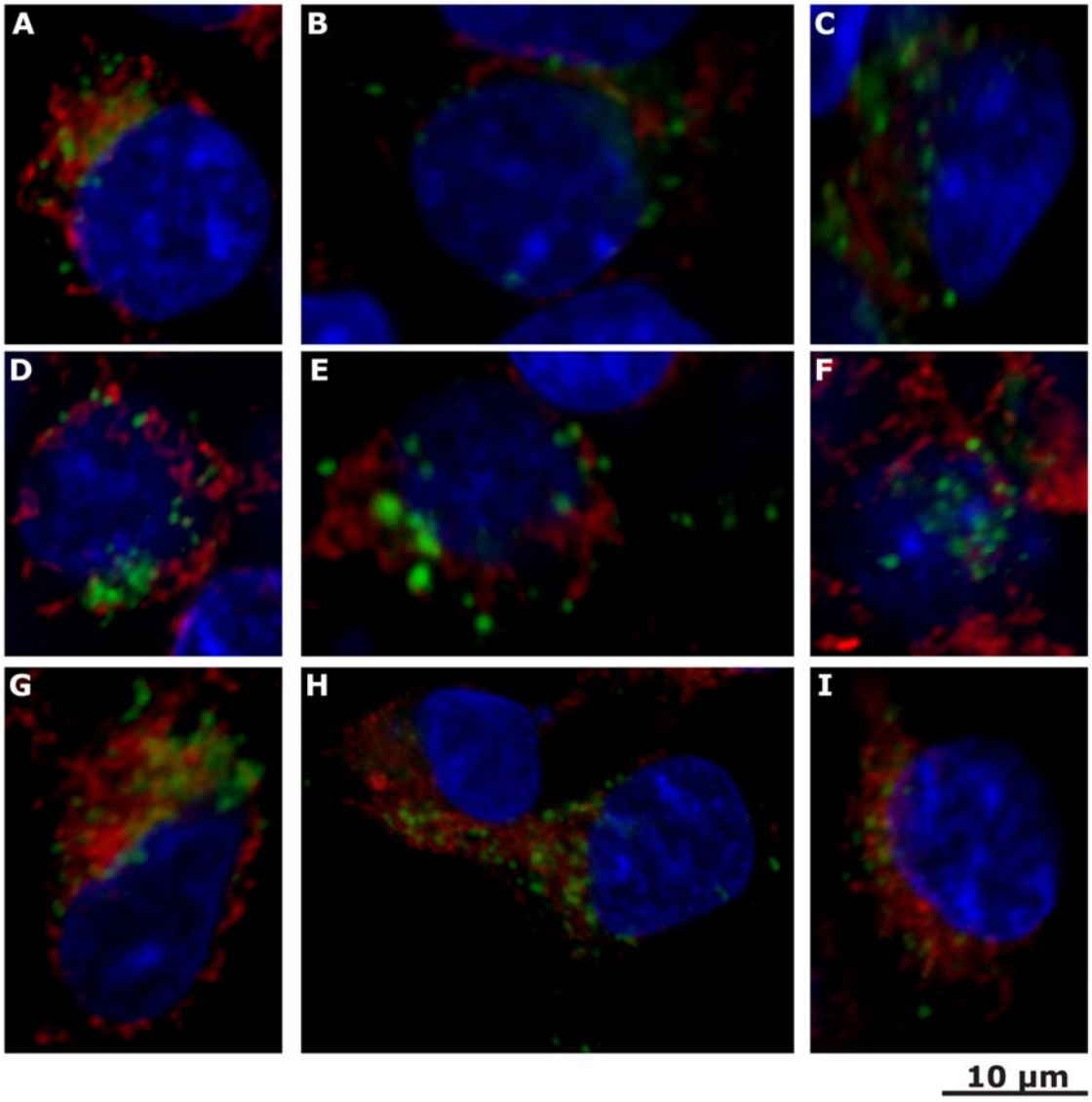

Figure S3. Cellular localization of prorenin and renin in HEK293 cells transiently expressing **(A-C)** WT^{REN}, **(D-F)** $\Delta L16^{REN}$ and **(G-I)** $L16R^{REN}$ proteins. Prorenin and renin were detected using (288-317) antibodies (green). No evidence of prorenin and renin retention in the ER was found by colocalization with ER marker PDI (red).

4 Results

4. 5 Clinical and Molecular Characterization of a New Disorder Resulting From Dominant Renin Gene Mutations and Response to Treatment with Fludrocortisone

Anthony J. Bleyer, **Martina Živná**, Helena Hůlková, Kateřina Hodaňová, Petr Vyleťal, Jakub Sikora, Jan Živný, Jana Sovová, Thomas C. Hart, Jeremy N. Adams, Milan Elleder, Katja Kapp, Robert Haws, Sharon M. Moe, Lynn D. Cornell, Stanislav Kmoch, and P. Suzanne Hart

submitted manuscript

Clinical and Molecular Characterization of a New Disorder Resulting From Dominant Renin Gene Mutations and Response to Treatment with Fludrocortisone

Anthony J. Bleyer[1], Martina Živná[2,3], Helena Hůlková[3], Kateřina Hodaňová[2,3], Petr Vyleťal[2,3], Jakub Sikora[3], Jan Živný[4], Jana Sovová[3], Thomas C. Hart[5], Jeremy N. Adams[6], Milan Elleder[2,3], Katja Kapp[7], Robert Haws[8], Sharon M. Moe[9], Lynn D. Cornell[10], Stanislav Kmoch[2,3], and P. Suzanne Hart[6]

[1]Section on Nephrology, Wake Forest University School of Medicine, Winston-Salem, NC; [2]Center for Applied Genomics, [3]Institute for Inherited Metabolic Disorders, and [4]Institute of Pathophysiology, Charles University in Prague, First Faculty of Medicine, Prague, Czechoslovakia; [5]Human Craniofacial Genetics Section, NIDCR, NIH, Bethesda MD; [6]Office of the Clinical Director, National Human Genome Research Institute, National Institutes of Health, Bethesda, MD; [7]ZMBH (Center for Molecular Biology Heidelberg), University of Heidelberg; [8]Specialty Pediatrics, Marshfield, WI; [9]Department of Medicine, Indiana University School of Medicine, Indianapolis, IN; [10]Division of Anatomic Pathology, Department of Laboratory Medicine and Pathology, Mayo Clinic, Rochester, MN 55905.

Word Count: 3,774

Abstract:

Introduction: A family (Family A) was identified with the autosomal dominant inheritance of early onset anemia, polyuria, and progressive chronic kidney disease.

Methods: Sequence analysis of the *REN* gene was performed. *In vitro* translation/translocation and transient expression of the mutant gene was performed. Laboratory evaluation and clinical characterization was performed on affected family members. Fludrocortisone acetate was administered and changes in clinical condition assessed. Another family (Family B) with a different mutation in the *REN* gene was also characterized.

Results: A novel heterozygous mutation c.58T>C resulting in the amino acid substitution of cysteine for arginine in the preprorenin signal sequence (p.Cys20Arg) occurred in all affected members of Family A. These individuals suffered from anemia, polyuria, and renal insufficiency in childhood, with progressive chronic kidney disease. The polyuria was associated with decreased urinary concentrating ability. Treatment with fludrocortisone in an affected 10 year old child resulted in an increase in blood pressure and estimated glomerular filtration rate, but no improvement in polyuria. The mutation resulted in significantly decreased endoplasmic reticulum cotranslational translocation and post translational processing of the mutant protein, resulting in massive accumulation of non-glycosylated preprorenin in cytoplasm. Family B members had similar clinical characteristics.

Conclusions: Mutations resulting in alterations in the amino acid sequence of the renin signal sequence result in childhood anemia, decreased urinary concentrating ability,

and progressive kidney disease. Treatment with fludrocortisone improved renal function in a child with this condition. Nephrologists should consider *REN* mutational analysis in families with autosomal dominant inheritance of chronic kidney disease, especially if they suffer from anemia and polyuria in childhood.

Introduction: Autosomal dominant inheritance of interstitial kidney disease has previously been attributed to mutations in the *UMOD* gene[1], which produces uromodulin. However, there are other causes of autosomal dominant interstitial kidney disease that have not been elucidated.

In this investigation, we describe a family with a mutation in the *REN* gene encoding renin that alters the preprorenin signal sequence. The mutation results in the autosomal dominant transmission of a clinical syndrome including decreased renin levels, polyuria, anemia, and progressive kidney failure. We describe how the mutation modifies the endoplasmic reticulum (ER) insertion properties of the renin preprotein, the effects of the mutation at the cellular level, and the pathophysiologic changes that result from the mutation. We also further characterize a family previously described with this disorder[2]. For the first time we describe treatment of this condition with fludrocortisone.

Methods:

Patient ascertainment: Family A was referred by RH for evaluation of anemia, polyuria, and chronic kidney disease. According to a protocol approved by the Institutional Review Board of Wake Forest University School of Medicine, blood and urine samples were obtained for chemical and genetic analysis, and a retrospective review of medical records was performed. DNA samples were then collected on affected and unaffected family members, and mutational analysis of the *REN* gene encoding renin was performed.

In affected individuals, 24 hour urine collections were performed on an *ad libitum* diet for urinary electrolytes and aldosterone. Random plasma renin and aldosterone

levels were also determined. When one of the patients (AIII2 - see Figure 1A) was identified as having hypoaldosteronism, the patient's nephrologist started her on fludrocortisone acetate, 0.1 mg orally each day. Laboratory studies were obtained before and after clinical treatment with fludrocortisone acetate. Two other affected individuals were then enrolled in an Institutional Review Board-approved protocol in which baseline blood and urine samples were obtained, and participants were then placed on 3 days of fludrocortisone at a dosage of 0.1 mg orally each day, followed by fludrocortisone at a dosage of 0.2 mg orally for 4 days.

Similar laboratory studies and medical records review were performed on affected individuals from another family (Family B) segregating a recently reported *REN* mutation[2].

Sequence analysis and genotyping: The *REN* gene was PCR amplified from genomic DNA and sequenced in the affected proband, the affected father, and clinically unaffected members of family A using methods previously described [2]. The presence of the novel *REN* mutation identified was evaluated in the complete family and in a control European American population (n=385) by direct sequencing of the corresponding genomic DNA fragment. A set of polymorphic microsatellite markers flanking the *REN* locus were genotyped to identify the disease associated haplotype segregating with the novel *REN* mutation.

Laboratory investigation:

In silico analysis: Preprorenin signal sequences from the presented species were obtained from the UniProtKB/Swiss-Prot database. Multiple alignment and evaluation for amino acid conservation were performed by ClustalW2 software (http://www.ebi.ac.uk/Tools/clustalw2/). Properties of the signal sequences were assessed using the SignalP 3.0 server[3]and the Kyte and Doolittle method[4].

In vitro translation/ translocation and transient expression of the p.Cys20Arg preprorenin: Construction of the wild-type preprorenin (WT^{REN}) eukaryotic expression vector was performed as previously described[2]. The mutant construct c.58T>C, encoding the p.Cys20Arg preprorenin ($C20R^{REN}$), was prepared by site directed mutagenesis of the WT^{REN} vector using a mutation specific oligonucleotide primer and the GeneTailor™ Site – Directed Mutagenesis System Kit (Invitrogen, Paisley, UK).

In vitro translation/ translocation assays, transient transfection of human embryonic kidney (HEK-293) cells, culturing conditions, cell lysate preparation, media collection, and Western blot and immunofluorescence analyses of prorenin and renin were carried out as previously described[2].

Renin granulosity was assessed by the fluorescence-activated cell sorter (FACS) assay, measuring the differences in the fluorescence intensity and the number of granular cells after the transient transfection of HEK293 cells with WT^{REN}, $C20R^{REN}$ and empty pCR3.1 expression vectors and labeling of low-pH secretory granules with fluorescent aminoacridine dye quinacrine. For this assay, 8 x 10^5 HEK293 cells were transfected with 4 μg of the corresponding vectors. Cells were mechanically harvested 24 hours post-transfection using 1.2 mL of supplemented Dulbecco's Modified Eagle's Medium

(DMEM) without phenol red. Five minutes before the analysis, 400 µl of 8 µM quinacrine dihydrochloride (Sigma, Prague, Czech Republic) in DMEM without phenol red was added to 400 µl of the cell suspension containing aproximatively 500,000 cells. Fluorescence was measured using FACS Calibur flow cytometry, and data were analysed using Cell Quest software version 3.3. (Becton Dickinson, San Jose, Ca, USA). Granular cells were counted in gated side scatter high population. The number of low-pH granules was quantified as the mean fluorescence intensity (MFI) of gated quinacrine positive population of 100,000 cells.

Results:

Mutational analysis: Sequencing of the *REN* gene in Family A revealed a novel heterozygous mutation c.58T>C, resulting in the amino acid substitution p.Cys20Arg, ($C20R^{REN}$) in the proband (AIII2) and her affected father (AII6) (Figure 1A). The mutation arose *de novo* in AII6 on the maternal haplotype and was not present in any unaffected family members, even AII3 and AII5 who inherited the same maternal haplotype. The mutation was not present in 385 unrelated Caucasian controls (770 alleles). Affected family members of Family B have a heterozygous deletion p.Leu16del, ($\Delta L16^{REN}$)[2].

Clinical Findings:

FamilyA:

Patient AIII2 (See Figure 1A): The proband was the product of a 38 week gestation and weighed 7 lbs 0 ounces at birth. She presented with acute kidney failure at 3 years. The patient had suffered from a viral syndrome with fevers up to 102 ^{o}F and was placed on non-steroidal anti-inflammatory agents (NSAIDs). Laboratory studies revealed a blood urea nitrogen (BUN) of 71 mg/dl (normal range 5-18 mg/dl), serum creatinine 1.4 mg/dl (normal 0.42-0.57 mg/dl), and hemoglobin 7.6 g/dl (normal 11.5-13.5 g/dl). Acute kidney failure was attributed to NSAIDs, which were stopped with a decline in the serum creatinine to 0.8 mg/dl. The patient was evaluated at age 6 years for a persistently elevated serum creatinine level of 1.2 mg/dl. The patient was asymptomatic except for nocturia.

On physical examination the patient appeared her stated age, with height 46.65 in and weight 50 lbs. The blood pressure was 82/52 mm Hg with pulse 86. The rest of the physical examination was unremarkable. With renal ultrasound, the right kidney was 7 cm and the left kidney 8.5 cm (normal for age 8.5-11.5 cm) without any cysts. A computerized axial tomographic scan revealed no cysts. The serum sodium was 141 mEq/l, potassium 5.5 mEq/l, chloride 106 mEq/l, bicarbonate 23 mEq/l, BUN 55 mg/dl, and serum creatinine 1.2 mg/dl. The serum uric acid was elevated at 6.3 mg/dl (normal range 1.8-5.3 mg/dL), with a fractional excretion of uric acid (FE_{urate}) 5.2% (normal 6-20%). A 24 hour urine collection revealed 6.3 mg/m^2/hour protein (normal < 4 mg/m2/hour), urine sodium 5.2 mEq/kg/day, and volume 57 ml/kg. The creatinine clearance was 58 ml/min/1.73 m^2. The hemoglobin level was low at 10.5 g/dl, with an

iron saturation of 5%, ferritin 135 ng/ml, and erythropoietin level 3.2 mIU/ml (normal 4-21 mIU/ml).

Anemia: The patient was started on iron replacement and darbepoeitin alfa. At age 7 the iron saturation was 33% and ferritin 541 ng/ml, but the patient has subsequently remained dependent on darbepoeitin alfa therapy to maintain hemoglobin levels above 11 g/dl to the present age of 11 years.

Hyperuricemia: The patient's serum uric acid remained elevated, rising to 7.7 mg/dl at age 7. The FE_{urate} remained low with readings less than 5.2%, and the lowest reading of 3.2%.

Renin/aldosterone: A random plasma renin activity was <0.5 ng/ml/h (normal 0.5-5.9 ng/ml/hr) with a random aldosterone measurement <4.0 ng/dl (normal 4-31 ng/dl at age 10 years). A 24 hour urine aldosterone was 2 ug (normal 2-16 ug).

Chronic kidney failure: The eGFR was stable over time (see Figure 2), until the administration of fludrocortisone, which resulted in a sustained improvement (Table 1).

Urinary concentration. While on fludrocortisone, overnight urinary osmolality (from 10 pm to 8 am), was 386 mOsm/kg. Two hours later, with continued fasting, the urine osmolality was 377 mOsm/kg.

Patient AII6: The proband's father presented at age 14 years for unexplained anemia with a hemoglobin 9.3 g/dl, white blood count 5000/ml, and platelet count 101,000/ml. Bone marrow aspirate revealed normoblastic hypoplasia. The patient was diagnosed with hypoplasia of the bone marrow, cause unknown. As part of the evaluation, an intravenous urogram revealed the left kidney to be 12.8 cm and the right

kidney 11.3 cm. The serum creatinine was 1.3 mg/dl. The hemoglobin increased to 11.4 g/dl three months later without treatment.

The patient was diagnosed with gout at age 29 years and placed on allopurinol. The patient was not overweight at the time and did not have excessive alcohol consumption.

At age 33 years the patient was referred to a nephrologist. On physical examination, the height was 6'1", weight 187 lbs., blood pressure 112/78 mmHg, and pulse 52. The urinalysis was bland. The serum sodium was 143 mEq/l, potassium 4.7 mEq/l, BUN 46 mg/dl, serum uric acid level (on allopurinol) 6.4 mg/dl. The hemoglobin was 15.3 g/dl, platelet count 108,000/ml. The 24 hour creatinine clearance was 75 ml/min with 2.25 liters and 245 mg protein. A CT scan revealed no renal lesions, without comment on kidney size. A kidney biopsy (see Figure 3) revealed chronic tubulointerstitial scarring with global glomerulosclerosis. The tubulointerstitial portion of cortex showed atrophy, thickening of the tubular basement membranes, and a tubulointerstitial inflammatory cellular infiltrated consisting primarily of lymphocytes. A larger core of the medulla showed marked tubular atrophy with dilatation and thyroidization. No discrete tubulitis was seen.

Further testing was performed at age 42. The erythropoietin level was 18.5 mIu/ml (normal 4.1 to 19.5 mIu/ml). A 24 hour urine collection was 3450 ml, with 283 mEq sodium, and 111 mEq potassium. The FE_{urate} was 3.6% (normal 5-20%). The 24 hour urinary aldosterone excretion was 9 ug (normal 2-21 on a regular salt diet and 17-44 on a low sodium diet).

Urinary concentration: Urinary osmolality was 426 mOsm/kg after an overnight fast, and two hours later was 427 mOsm/kg with continued fasting.

Chronic kidney failure: eGFR has remained stable over time (see Figure 2).

Family B (Figure 1A):

Patient BIV2 was first evaluated at age 8 as part of this study. There was no history of polyuria. At birth, the patient had a hemoglobin value of 18.2 g/dl. At one year, the hemoglobin had declined to 10.1 g/dl, but there was no workup of anemia. The patient's blood pressure was 100/62 mm Hg. The serum sodium was 136 mEq/l, potassium 4.6 mEq/l, bicarbonate 24 mEq/l, BUN 22 mg/dl, serum creatinine 0.6 mg/dl, and serum uric acid level 5.1 mg/dl. The FE_{urate} was 3.5%. The hemoglobin was 10.1 g/dl, iron saturation 22%, ferritin 23 ng/ml, and serum erythropoietin level 6.2 mIU/ml (9.0 to 28.0 mIU/ml). The plasma renin level was 1.70 ng/ml/hr (0.5-5.9) and aldosterone level 2.8 ngdl (normal 3-28).

Patient BIII3 was first referred to a nephrologist at age 28 years for an elevated serum creatinine level of 1.6 mg/dl. There was no history of enuresis or polyuria. He had been unable to donate blood due to "low blood" in the past. The blood pressure was 110/72 mm Hg, and the rest of the physical examination was unremarkable. The serum creatinine was 1.6 mg/dl with an estimated GFR of 54.5 ml/min/1.73 m^2, serum uric acid 7.1 mg/dl. The hemoglobin was 12.9 g/dl. The patient's serum creatinine remained very stable, with an eGFR of 53.5 ml/min/1.73 m^2 3 years later. At that time, the serum uric

acid level was 6.5 mg/dl, with a The FE_{urate} of 3.5%. There was negligible protein in the urine. A random plasma renin and aldosterone level were 2.6 ng/ml/h and 6.0 ng/dl. A 24 hour urine volume was 1200 cc.

Patient BII4 presented to a nephrologist at age 56 years with a history of longstanding hypertension and chronic kidney disease dating back more than 20 years. The patient had been chronically anemic for greater than 30 years. She was being treated for hypertension with irbesartan, hydrochlorothiazide, carvedilol, and verapamil. Laboratory studies revealed a BUN of 33 mg/dl and serum creatinine of 1.9 mg/dl. With renal ultrasound, the left kidney was 13.7 cm and the right kidney 10.4 cm with marked cortical loss in both kidneys. There were two large renal cysts in each kidney. Figure 4 shows the change in eGFR over time for BII4 and several other family members.

Patient BII1: The patient was evaluated at age 49 years for chronic kidney disease. The patient had a history of several prior gout attacks and was taking 200 mg of allopurinol daily. The patient also had a history of hypertension for which he was on diltiazem, moexipril, and furosemide. The physical examination was unremarkable. Limited available records revealed a serum creatinine of 3.7 mg/dl. The patient's eGFR over time is shown in Figure 4. The patient progressed to end-stage kidney disease and started dialysis at age 50.

Patient BII5 started HD at age 43, and Patient BI2 started dialysis at 58. There were no other records available on these indivdiuals.

Fludrocortisone administration: Patient AIII2 received fludrocortisone as part of clinical care for hypoaldosteronism detected in this investigation. Table 1 shows the changes that occurred with medicine administration. There was a rise in blood pressure

and weight, together with an improvement in BUN and serum creatinine values. Urine output showed a mild increase with the institution of fludrocortisone.

Patients AII6 and BII4 received fludrocortisone as part of the protocol described in the Methods. There was no effect on hemodynamics or eGFR in these patients. The FE_{urate} did not change in any participants. Urine volume did not decrease with fludrocortisone administration.

Laboratory investigations:

In silico analysis: Human prorenin and renin are synthesized in juxtaglomerular cells from a preproprotein composed of a 23 residue N-terminal signal sequence, which mediates insertion of the nascent preprotein into the translocation channel within the ER membrane, a 43 residue "pro" domain, and the mature enzymatically active renin comprising 340 residues[5]. In contrast to the previously reported (p.Leu16del) and (p.Leu16Arg) mutations, which are located within the hydrophobic part of the signal sequence (h-region) and affect protein insertion in the ER membrane, the p.Cys20Arg mutation occurs in the polar C-terminal part (c-region) of the preprorenin signal sequence. This cysteine residue is conserved among mammals except for sheep (Figure 1C). Using the SignalP 3.0 server[3], the p.Cys20Arg mutation decreases the overall hydrophobicity profile of the c-region of the signal sequence and alters its cleavage site score profile and cleavage site probability.

Characterisation of the p.Cys20Arg preprorenin: WT^{REN} and $C20R^{REN}$ proteins were translated and ER-translocated *in vitro* (Figure 5) and transiently expressed in HEK 293 cells (Figure 6). Figure 5 demonstrates that WT^{REN} protein is converted to

glycosylated prorenin in the presence of rough ER microsomes, whereas $C20R^{REN}$ is not. WT^{REN} and $C20R^{REN}$ proteins were transiently expressed in HEK 293 cells, and expressed proteins were detected in cell lysates and medium by Western blot analysis (Figure 6A). In lysates, the WT^{REN} was expressed as a 47 kDa protein whereas the $C20R^{REN}$ was expressed as a 45 kDa protein. Deglycosylation with PNGase reduced the molecular weight of the WT^{REN} to 43 kDa, corresponding to complete loss of N-glycosylation on both of the predicted N-glycosylation sites in the preprorenin sequence (N71 and N141). The molecular weight of $C20R^{REN}$ remained unchanged. Analysis of molecular weights suggests that WT^{REN} produces the fully glycosylated prorenin, and that this protein has successfully completed ER translocation and undergone cleavage of its signal sequence, whereas $C20R^{REN}$ produces only non-glycosylated preprorenin. Analysis of the medium showed however, that the $C20R^{REN}$ protein produces also minute amounts of normally glycosylated, proteolytically processed and therefore secretory competent prorenin. Immunofluorescence analysis (Figure 6C-D) demonstrated that compared to the WT^{REN}, the $C20R^{REN}$ protein does not form cytoplasmic granules and instead has intense diffuse cytoplasmic staining.

Inability of $C20R^{REN}$ to form cytoplasmic granules was confirmed by the FACS based assay. This assay showed that, similar to mock transfection, the expression of $C20R^{REN}$ does not increase either the number of granular cells (Figure 6B), or the quinacrine fluorescence (data not shown) as is the case in cells expressing the WT^{REN} protein.

Discussion:

In this study we identified a family with a novel mutation in the *REN* gene resulting in the autosomal dominant inheritance of early onset anemia, polyuria, and slowly progressive chronic kidney disease. In this family the mutation arose *de novo* in the proband's father. The identified mutation affects the signal sequence properties and function as shown by bioinformatic analysis, *in vitro* translation/translocation studies and transient expression and characterization of the mutant protein. These studies demonstrated that the mutation significantly decreased ER cotranslational translocation and post translational processing of the mutant nascent protein, leading to massive accumulation of non-glycosylated preprorenin in cytoplasm. In contrast to the previously identified p.Leu16del and p.Leu16Arg mutations[2] which affected the hydrophobic region of the signal sequence, the current mutation affects the c-region of the signal sequence and alters its cleavage site score profile and cleavage site probability. The insertion of a positively charged amino acid likely leads to the decreased translocation. This substitution also in some way prevents renin granule formation (which occurred with the other noted mutations), a difference which may be responsible for the phenotypic differences seen in the affected families. Interestingly, affected members of all four families that have been described with this condition have had a mutation in the signal sequence of renin[2].

Mutations in the *REN* gene altering the renin signal peptide have three major effects: First, production of normal renin is markedly reduced in juxtaglomerular cells. Individuals with this disorder have low renin levels, low aldosterone levels, and frequently suffer from mild hyperkalemia. Second, the renin signal peptide is not present in the mutated cells due to aberrant preprotein processing. This may be important

because the wild-type renin signal peptide exhibits uncommon stability and resistance to signal peptide peptidase processing, suggesting that it may have a post-targeting function. Third, non-processed preprorenin is produced and accumulates intracellularly, leading to the unfolded protein response, accelerated apoptosis, subsequent nephron loss, and progressive chronic kidney disease. It is clear that the patients are able to produce some renin, encoded and synthesized from the second unaffected allele. Individuals with genetic mutations resulting in total absence of renin production present with renal tubular dysgenesis and die either *in utero* or early in life[6].

The low renin production manifested itself early on in AIII2 when the patient developed acute kidney failure in the setting of a viral illness together with treatment with non-steroidal anti-inflammatory medications. The decreased renin production likely resulted in the inability to preserve intraglomerular pressure in the setting of volume depletion, and the non-steroidal medication aggravated this problem through inhibition of prostaglandin synthesis. Patients with this disorder should be advised to avoid non-steroidals and volume depletion, similar to individuals receiving angiotensin converting enzyme inhibitors.

Polyuria was a significant finding in family A. Affected family members could not concentrate their urine after an overnight fast. These findings were very similar to the characteristics of mice that undergo Ren1c disruption[7], resulting in the inability to produce renin in the homozygous state. These mice suffer from polyuria and hypotension, with 80% of mice not surviving the first few days of life without salt repletion. These mice also manifest decreased weight, hypotension, and renal failure. Polyuria in these mice is resistant to desmopressin acetate (DDAVP) and unresponsive to

angiotensin infusion. In our patients, fludrocortisone administration did not decrease urinary volume. The link between the renin angiotensin system and urinary concentration requires further investigation and has not been fully appreciated in the past.

Anemia has been observed in all children identified with *REN* mutations. The anemia begins early in life, and hemoglobin values are characteristically between 10 and 12 g/dl. Curiously, the anemia resolves once children enter the teenage years, but then recurs with advancing kidney failure. Production of androgens with puberty may affect hematopoiesis and compensate for the effect of the renin angiotensin system on hematopoiesis early in life.

Chronic kidney failure appears to be very slow in progression, and is likely due to cell death in the setting of progressive intracellular accumulation of abnormal renin. However, the low renin levels likely provide continuous inhibition of aldosterone production and may paradoxically prevent renal failure from worsening.

If the production of abnormal renin leads to cell injury, decreasing production of renin (and hence abnormal renin) might be beneficial in preserving renal function in the long term. Since aldosterone has feedback inhibition on renin secretion, administration of aldosterone should decrease renin production and hence production of abnormal renin. In addition, patients suffer from polyuria, mild hypotension, and hyperkalemia, and renin fludrocortisone administration might reverse these conditions. Therefore, a trial of fludrocortisone was intitiated in three patients. In the 10 year old patient AIII2, fludrocortisone resulted in a decrease in serum potassium, a rise in blood pressure, and a significant improvement in estimated GFR that persisted over 6 weeks of administration. However, its administration had little effect on FE_{urate} or on the polyuria present in this

patient. In the two adult patients, a one week trial of fludrocortisone had little effect. This may be due to the short duration of the study or the presence of irreversible changes in the kidney at this later stage of disease. The potential benefit of fludrocortisone to decrease production of abnormal renin in these patients must be weighed against potential harmful effects of aldosterone in chronic kidney disease.

The two families showed some variation in expression of disease. In Family A, polyuria and mild hypotension were characteristic. In Family B, chronic renal insufficiency went un-noticed throughout childhood, and polyuria was not present. However, chronic kidney disease, childhood anemia, and hypouricosuric hyperuricemia were present in both families.

Weaknesses of this study include the small number of patients in whom fludrocortisone was administered, making it very difficult to provide any firm conclusions. We were of course limited by the very small number of identified families. We plan to pursue investigations with fludrocortisone when more families are diagnosed with this disorder.

In summary, a novel dominant mutation in the *REN* gene is described that results in polyuria, anemia, hypouricosuric hyperuricemia, chronic kidney disease, and manifestations of hypoaldosteronism. Laboratory studies revealed that the mutation affected translocation of preprorenin into the ER with a marked decrease in synthesis of renin, and intracellular accumulation of abnormal renin. These findings are consistent with experimental findings for other *REN* mutations[2]. Treatment with fludrocortisone improved renal function and blood pressure in a child with this condition. Further research will concentrate on the effect of prolonged fludrocortisone treatment in these

patients. Patients with this condition should avoid non-steroidal anti-inflammatory agents and volume depletion.

Acknowledgements: The authors would like to thank Vicki Robins, R.N. for her important contributions to this investigation.

Table 1. Fludrocortisone administration.

Participant	Time	Blood pressure (mm Hg)	Weight	Serum Na (mEq/L)	Serum K (mEq/L)	BUN (mg/dl)	Serum creat-inine (mg/dl)	Serum uric acid (mg/dl)	Fractional excretion urate (%)	Urine vol-ume (ml)	Urine Na (mEq/24h)
AIII2	-11 weeks	87/50		137	5.0	49	1.3	3.2		1825	69
	- 1 week		87.6	137	5.6	62	1.6	5.2		2275	
	1 week	106/69	90	142	4.2	26	1.1	6.1	5.1	2450	72
	6 weeks	112/67		143	4.3	31	1.0	7.0	3.9	2675	70
AII3	0	130/78	201.4	138	4.7	42	1.9	6.1	3.3	3150	91
	Day 3	118/88	201.6	139	4.3	43	2.0	5.9	4.4	3450	98
	Day 7	115/81	201.2	140	4.4	42	1.9	6.3	4.2	2800	81
	Day 8	152/101	203							4650	
BII4	0	126/84	206	144	5.2	28	1.6	7.5	4.8	1825	106
	Day 3	117/85	204.9	143	3.9	29	1.8	8.2	4.8	1750	103
	Day 7	95/70	204.5	144	4.8	30	1.7	9	4.4	1700	77
	Day 8	122/86	206.4							1800	

Figure legends:

Figure 1. *REN* mutation characteristics. 1A. Family pedigree. 1B. Mutation analysis of the *REN* gene. 1C. Amino acid conservation across species. 1D. Hydrophobicity score.

Figure 2. Estimated glomerular filtration rate vs. age in Family A.

Figure 3. Kidney biopsy results of Patient AII6 reveal patchy interstitial fibrosis and tubular atrophy, with focal areas of inflammation within the atrophic areas. The inflammatory infiltrate was composed predominantly of mononuclear cells and plasma cells. Only one glomerulus was present for examination, and it showed periglomerular fibrosis but no other alterations by light microscopy. (Hematoxylin & eosin stain) The atrophic tubules showed markedly thickened and duplicated basement membranes (insert, periodic acid-Schiff).

Figure 4. Estimated glomerular filtration rate vs. age in Family B.

Figure 5. *In vitro* translation and translocation. Nascent WT^{REN} and $C20R^{REN}$ proteins translated from corresponding mRNAs in nuclease-treated rabbit reticulocyte lysate in the absence (-) or presence (+) of rough endoplasmic reticulum microsomes (RM) and tripeptide glycosylation acceptor (AP). Without RM and AP only nascent preprorenin (PreProREN) is formed (lanes 1 and 4). With RM and in the absence of AP most of the ER-translocated WT^{REN} is converted into fully glycosylated prorenin (ProREN); (lane 2) whereas $C20R^{REN}$ produces only minute amounts of ProREN (lane 5). With RM and AP, the glycosylation of the ER-translocated WT^{REN} is inhibited and partially glycosylated

intermediates are present (lane 3); $C20R^{REN}$, which is not ER-translocated, is present as non-glycosylated preprorenin.

Figure 6. Transient expression of WT^{REN} and $C20R^{REN}$ preprorenin in HEK-293 cells. 6A. Western blot analysis of the protein products in cell lysates and medium showing that $C20R^{REN}$ produces only minute amounts of normally glycosylated, proteolytically processed and secretory competent prorenin (ProREN). To distinguish proteolytic processing and glycosylation status, the expressed proteins were analyzed before (-) and after (+) deglycosylation with PNGase. 6B. Fluorescence-activated cell sorter analysis showing inability of the $C20R^{REN}$ to form cytoplasmic granules. The values represent means ± s.d. of the three transfection experiments carried out in triplicates. The differences between the number of granular cells expressing the WT^{REN} and cells expressing either the $C20R^{REN}$ or empty vector were statistically significant ($P< 0,001$). 6C,D Cellular localization of preprorenin, prorenin and renin in HEK293 cells detected using antibodies recognizing amino acid residues 288-317 of the preprorenin (Yanaihara, Shizuoka, Japan). (C) WT^{REN} is present in a form of fine cytoplasmic granules and (D) $C20R^{REN}$ protein is retained intracellularly and shows intense diffuse cytoplasmic staining.

Figure 1.

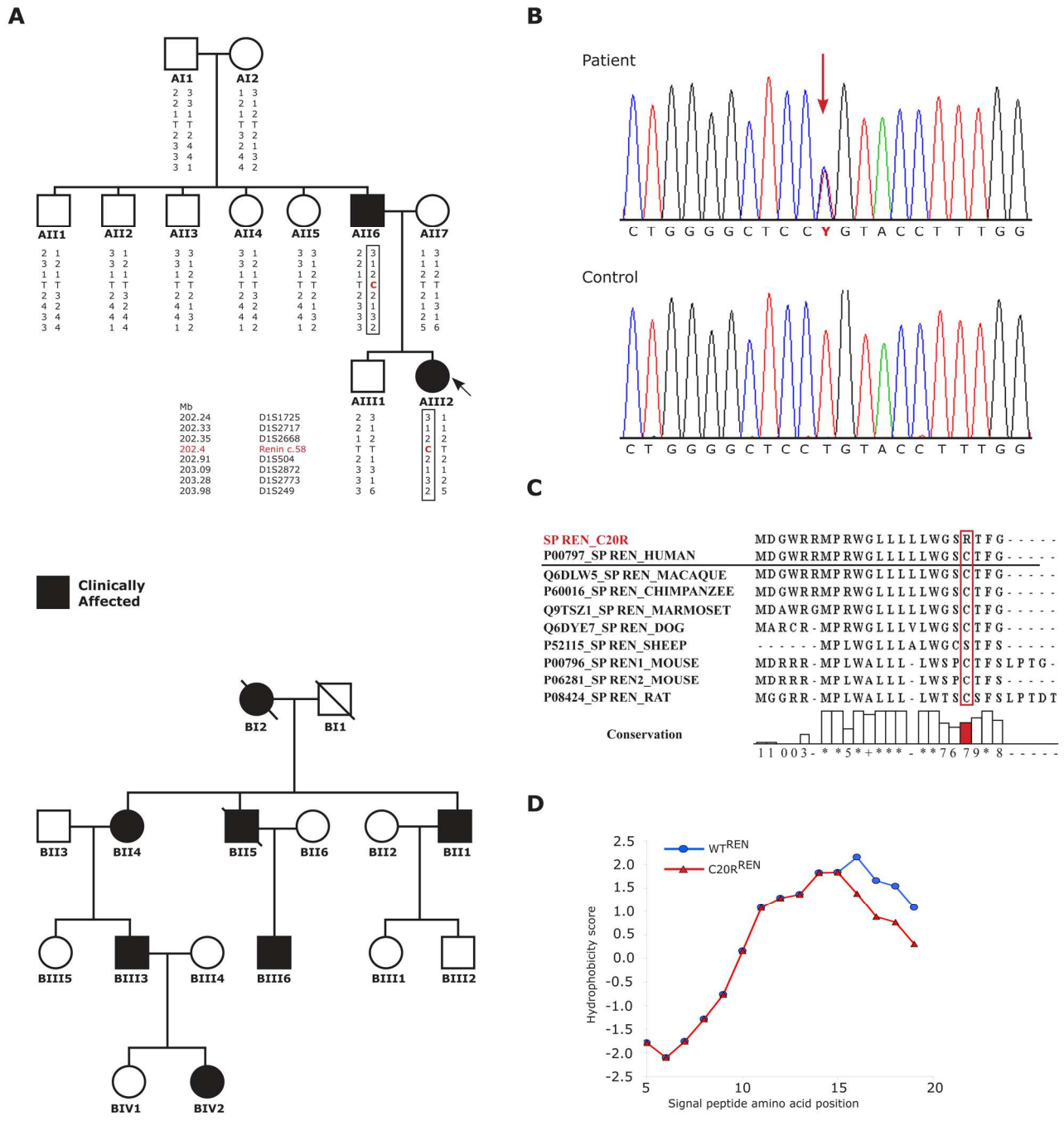
A
AI1
AI2
AII1
AII2
AII3
AII4
AII5
AII6
AII7
AIII1
AIII2
Mb
202.24
202.33
202.35
202.4
202.91
203.09
203.28
203.98
D1S1725
D1S2717
D1S2668
Renin c.58
D1S504
D1S2872
D1S2773
D1S249
Clinically Affected
BI2
BI1
BII3
BII4
BII5
BII6
BII2
BII1
BIII5
BIII3
BIII4
BIII6
BIII1
BIII2
BIV1
BIV2
B
Patient
C T G G G G C T C C Y G T A C C T T T G G
Control
C T G G G G C T C C T G T A C C T T T G G
C
SP REN_C20R MDGWRRMPRWGLLLLLWGSRTFG-----
P00797_SP REN_HUMAN MDGWRRMPRWGLLLLLWGSCTFG-----
Q6DLW5_SP REN_MACAQUE MDGWRRMPRWGLLLLLWGSCTFG-----
P60016_SP REN_CHIMPANZEE MDGWRRMPRWGLLLLLWGSCTFG-----
Q9TSZ1_SP REN_MARMOSET MDAWRGMPRWGLLLLLWGSCTFG-----
Q6DYE7_SP REN_DOG MARCR-MPRWGLLLVLWGSCTFG-----
P52115_SP REN_SHEEP ------MPLWGLLLALWGCSTFS-----
P00796_SP REN1_MOUSE MDRRR-MPLWALLL-LWSPCTFSLPTG-
P06281_SP REN2_MOUSE MDRRR-MPLWALLL-LWSPCTFS-----
P08424_SP REN_RAT MGGRR-MPLWALLL-LWTSCSFSLPTDT
Conservation
11003-***5*+***-**7679*8-----
D
WTREN
C20RREN
Hydrophobicity score
2.5
2.0
1.5
1.0
0.5
0.0
-0.5
-1.0
-1.5
-2.0
-2.5
5
10
15
20
Signal peptide amino acid position

Figure 2.

Figure 2. Estimated Glomerular Filtration Rate vs. Age(Years)

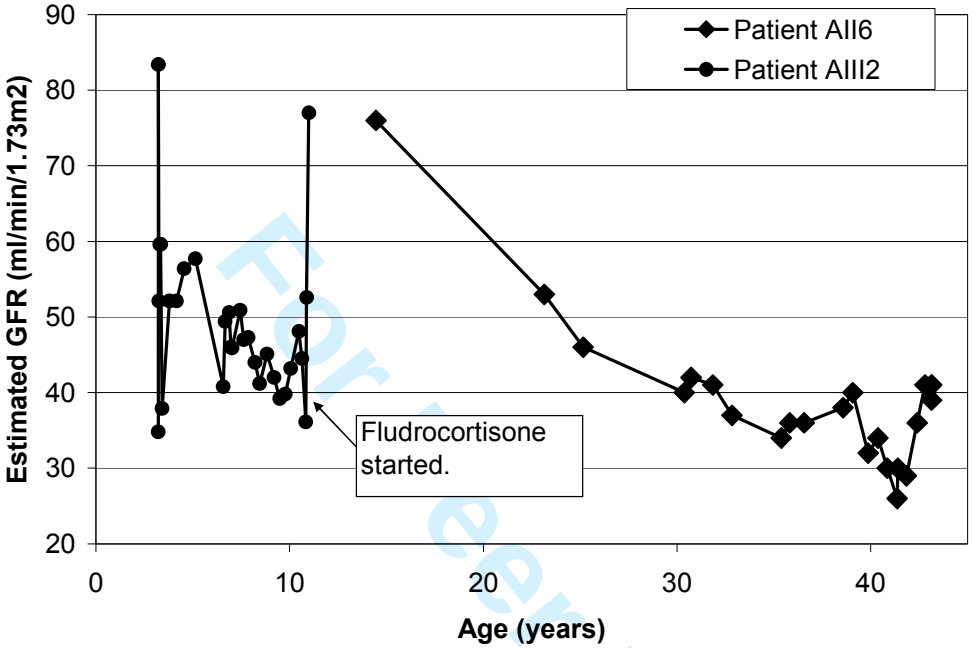

Figure 3. Kidney biopsy of Patient AII6

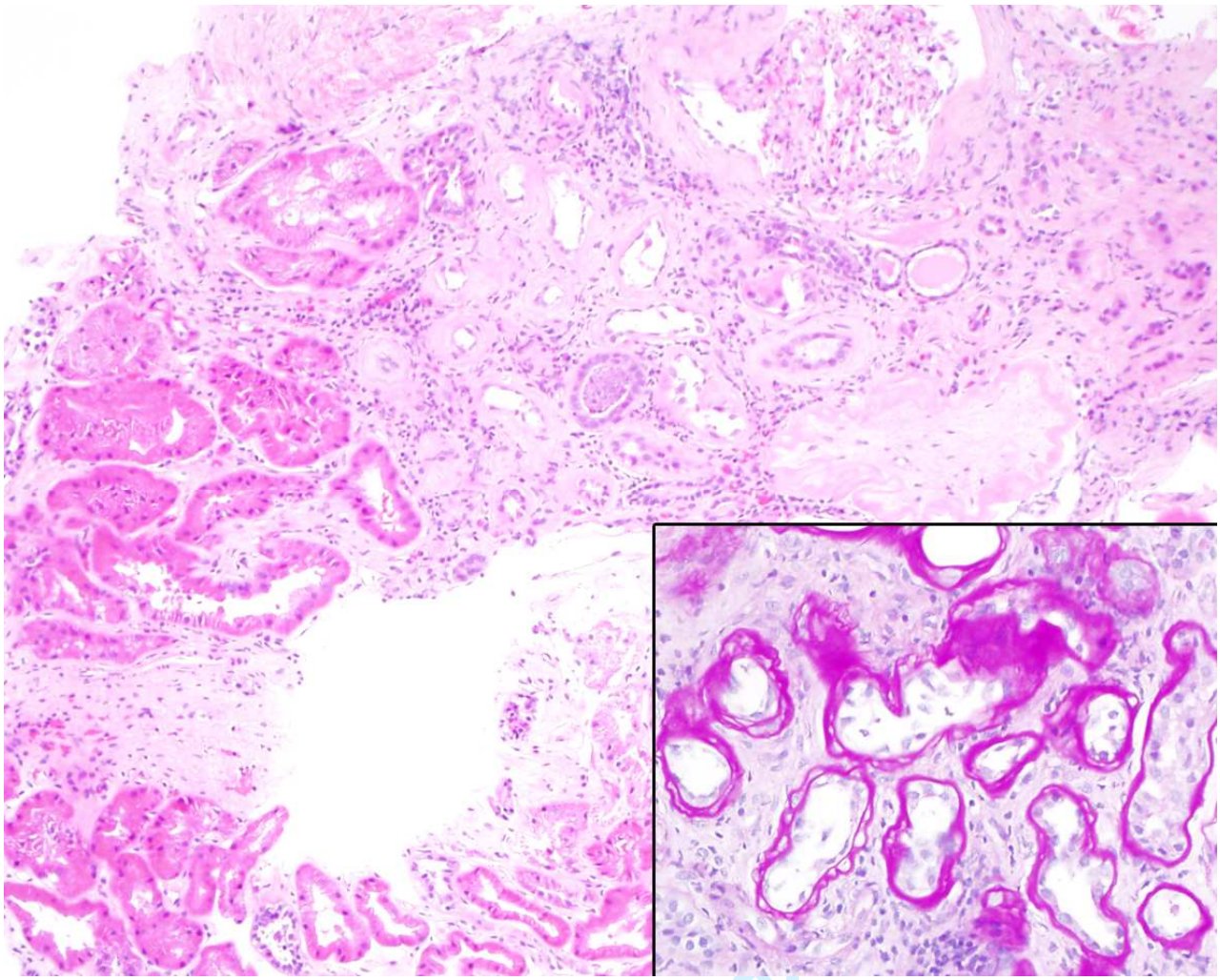

Figure 4.

Figure 5. eGFR vs. Age for Family B

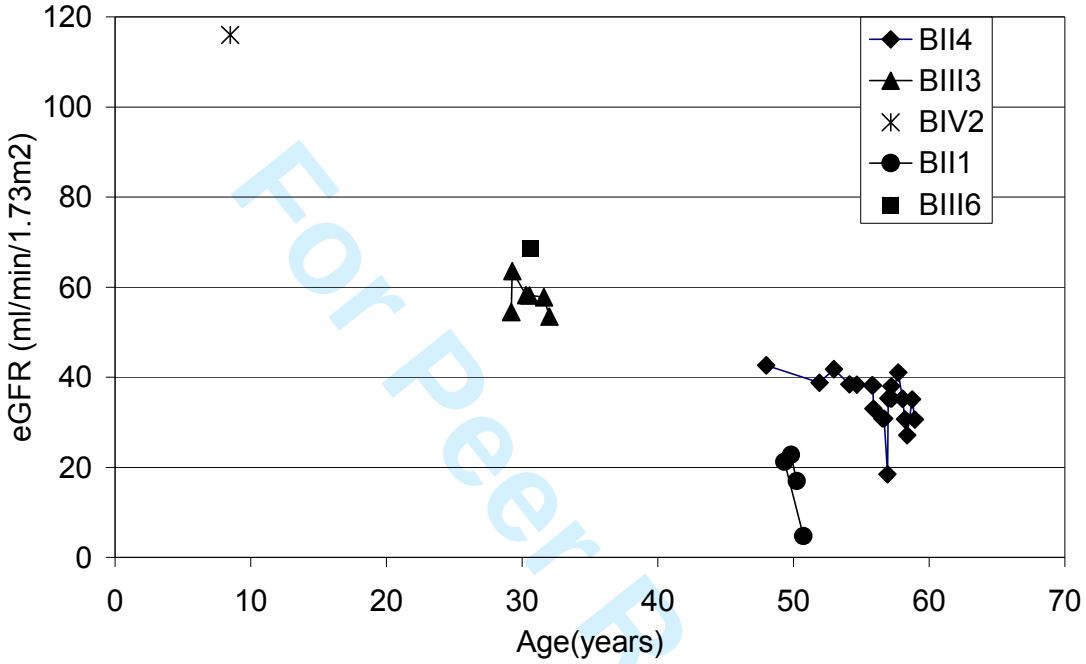

Figure 5. *In vitro* translation and translocation.

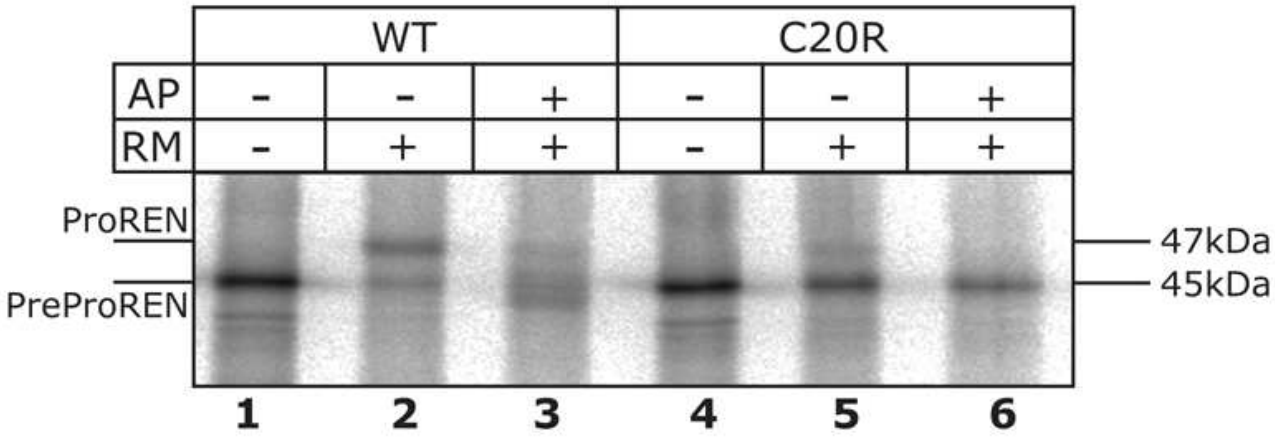

Dominant Renin Gene Mutations 30

Figure 6.

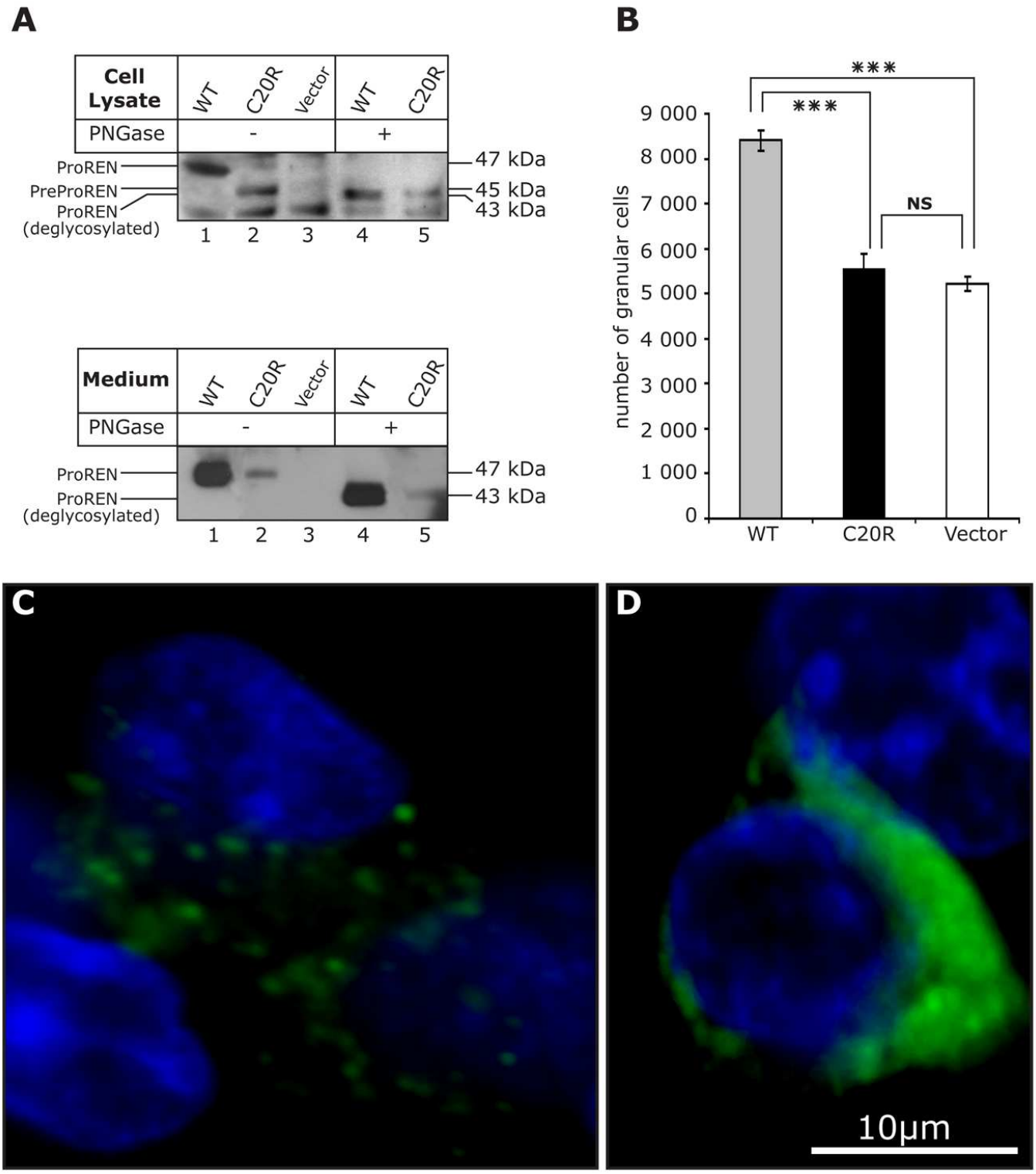

Reference List

(1) Hart TC, Gorry MC, Hart PS et al. Mutations of the UMOD gene are responsible for medullary cystic kidney disease 2 and familial juvenile hyperuricaemic nephropathy. *J Med Genet* 2002 December;39(12):882-92.

(2) Zivna M, Hulkova H, Marignon M et al. Dominant renin gene mutations associated with early-onset hyperuricemia, anemia, and chronic kidney failure. *Am J Human Genet* 2009;In Press.

(3) Bendtsen JD, Nielsen H, von Heijne G, Brunak S. Improved prediction of signal peptides: SignalP 3.0. *J Mol Biol* 2004;340:783-95.

(4) Kyte J, Doolittle RF. A simple method for displaying the hydropathic character of a protein. *J Mol Biol* 1982;157:105-32.

(5) Hegde RS, Bernstein HD. The surprising complexity of signal sequences. *Trends Biochem Sci* 2006;31:563-71.

(6) Gribouval O, Gonzales M, Neuhaus T et al. Mutations in genes in the renin-angiotensin system are associated with autosomal recessive renal tubular dysgenesis. *Nat Genet* 2005;37:964-8.

(7) Takahashi N, Sequeira Lopez ML, Cowhig JE et al. Ren1c homozygous null mice are hypotensive and polyuric, but heterozygotes are indistinguishable from wild-type. *J Am Soc Nephrol* 2004;16:125-32.

5 List of publications, awards, grants and presentations

5. 1 Publications

Hodanová K, Majewski J, **Kublová M**, Vyletal P, Kalbácová M, Stibůrková B, Hůlková H, Chagnon YC, Lanouette CM, Marinaki A, Fryns JP, Venkat-Raman G, Kmoch S.
Mapping of a new candidate locus for uromodulin-associated kidney disease (UAKD) to chromosome 1q41.
Kidney Int. 2005 Oct;68(4):1472-82., **IF 4, 927**

Vylet'al P*, **Kublová M***, Kalbácová M, Hodanová K, Baresová V, Stibůrková B, Sikora J, Hůlková H, Zivný J, Majewski J, Simmonds A, Fryns JP, Venkat-Raman G, Elleder M, Kmoch S.
Alterations of uromodulin biology: a common denominator of the genetically heterogeneous FJHN/MCKD syndrome.
Kidney Int. 2006 Sep;70(6):1155-69. Epub 2006 Aug 2., **IF 4, 773**
*** these authors contibuted equally**

Vylet'al P, Hůlková H, **Zivná M**, Berná L, Novák P, Elleder M, Kmoch S.
Abnormal expression and processing of uromodulin in Fabry disease reflects tubular cell storage alteration and is reversible by enzyme replacement therapy.
J Inherit Metab Dis. 2008 Aug;31(4):508-17. Epub 2008 Jul 27., **IF 2,691**

Zivná M, Hůlková H, Matignon M, Hodanová K, Vylet'al P, Kalbácová M, Baresová V, Sikora J, Blazková H, Zivný J, Ivánek R, Stránecký V, Sovová J, Claes K, Lerut E, Fryns JP, Hart PS, Hart TC, Adams JN, Pawtowski A, Clemessy M, Gasc JM, Gübler MC, Antignac C, Elleder M, Kapp K, Grimbert P, Bleyer AJ, Kmoch S.
Dominant renin gene mutations associated with early-onset hyperuricemia, anemia, and chronic kidney failure.
Am J Hum Genet. 2009 Aug;85(2):204-13. Epub 2009 Aug 6., **IF 10,153**

Anthony J. Bleyer, **Martina Živná**, Helena Hůlková, Kateřina Hodaňová, Petr Vyleťal, Jakub Sikora, Jan Živný, Jana Sovová, Thomas C. Hart, Jeremy N. Adams, Milan Elleder, Katja Kapp, Robert Haws, Sharon M. Moe, Lynn D. Cornell, Stanislav Kmoch, and P. Suzanne Hart
Clinical and Molecular Characterization of a New Disorder Resulting From Dominant Renin Gene Mutations and Response to Treatment with Fludrocortisone (submitted manuscript)

5. 2 Awards

2003 **3rd place in poster session on conference 18th Metabolic Days**, Slušovice, CR
Title of poster: Experimental annotation of a transcription map of familial juvenile hyperuricemic nephropathy (FJHN) critical region on 16p13.12

2005 **Among three best posters on conference 20th Metabolic Days**, Lednice, CR
Title of poster: Familial juvenile hyperuricemic nephropathy (FJHN), molecular analysis of 23 families, identification and functional consequences of 6 uromodulin mutations

2008 **Best poster award on Gordon Research Conference** Proprotein Processing, Trafficking & Secretion, Colby-Sawyer College, New London, NH, USA
Title of poster: Preprorenin signal peptide mutation in a family with uromodulin-associated kidney disease

2009 **Bolzano´s award** – the academic award intended for students who published innovative publication on the medical, natural and humanities field of science
Title of project: Study of molecular basis of familial hyperuricemic nephropathies

5. 3 Grants (PI)

2005 – 2006 Grant awarded by Grant Agency of Charles University, registration number of grant 1/2005 (evidence number 203 200)
Title of project: Pathogenetic mechanisms of mutations in uromodulin and in other genes causing familial juvenile hyperuricemic nephropathy (FJHN)

2007 Grant awarded by Grant Agency of Charles University, registration number of grant 67207
Title of project: Familial juvenile hyperuricaemic nephropathy (FJHN): Identification and characterization of disease causing gene in chromosome 1q41 candidate region

2009 Grant awarded by Grant Agency of Charles University, registration number of grant 44309
Title of project: Analysis of new patients and families with familial juvenile hyperuricemic nephropathy and functional characterization of novel uromodulin (Tamm-Horsfall) mutations

5. 4 Presentations

Kublová M., Kmoch S.: Experimental annotation of a transcription map of FJHN critical region on 16p13.12, Poster presentation. 18th workshop Inherited Metabolic Disorders, Slušovice, Czech Republic, 2003

Kublová M., Vyleťal P., Hodaňová K., Kalbáčová M., Blažková H., Majewski J., Simmonds A., Matthijs G. and Kmoch S.: Uromodulin urinary excretion in patients with familial juvenile hyperuricaemic nephropathy (FJHN). Poster presentation. 19th workshop Inherited Metabolic Disorders, Podbanské, Slovakia, 26. - 28. 5. 2004.

Kublová M., Vyleťal P., Hodaňová K., Kalbáčová M., Hůlková H., Majewski J., Simmonds A., Matthijs G. and Kmoch S.: Uromodulin urinary excretion in patients with familial juvenile hyperuricaemic nephropathy (FJHN). Poster presentation. 45th Annual

Short Course in Medical and Experimental Mammalian Genetics, The Jackson Laboratory, Bar Harbor, Maine, USA, 18. - 30. 7. 2004.

Kublová M.: Familial Juvenile Hyperuricemic Nephropathy (FJHN): Pathogenetic mechanisms of mutations in *UMOD*. Oral presentation. 6th student´s scientific conference 1st Faculty of Medicine, Charles Univerzity, Prague, 23. 5. 2005

Kublová M., Vyleťal P.**,** Hodaňová K., Barešová V., Kalbáčová M., Sikora J., Živný J., Sovová J., Majewski J., Marinaki A., Simmonds A., Fryns J.-P., Venkat-Raman G. and Kmoch S.: Familial Juvenile Hyperuricaemic Nephropathy (FJHN), molecular analysis of 23 families, identification and functional consequences of 6 uromodulin mutations. Poster presentation. 37th European Human Genetics Conference, Prague, Czech Republic, 7. - 10. 5. 2005.

Kublová M., Vyleťal P., Hodaňová K., Barešová V., Kalbáčová M., Sikora J., Živný J., Sovová J., Majewski J., Marinaki A., Simmonds A., Fryns J.-P., Venkat-Raman G. and Kmoch S.: Familial Juvenile Hyperuricaemic nephropathy (FJHN), molecular analysis of 23 families, identification and functional consequences of 6 uromodulin mutations. Poster presentation. 20th workshop Inherited Metabolic Disorders, Lednice, Czech Republic, 18. - 20. 5. 2005.

Kublová M., Hodaňová K., Majewski J., Vyleťal P., Kalbáčová M., Stibůrková B., Hůlková H., Chagnon Y. C., Lanouette Ch. M., Marinaki A., Fryns J.-P., Venkat-Raman G. and Kmoch S.: Mapping of a new candidate locus for uromodulin-associated kidney disease (UAKD) to chromosome 1q41. Poster presentation. Functional Genomics and Disease, 2nd ESF Functional Genomics Conference, Oslo, Norway, 6. - 10. 9. 2005.

Kmoch S., Vyleťal P., **Kublová M.**, Kalbáčová M., Hodaňová K., Stibůrková B., Hůlková H., Majewski J., Simmonds A., Fryns J.-P., Venkat-Raman G. and Elleder M.: Alterations of uromodulin biology: a common denominator of the genetically heterogeneous FJHN/MCKD syndrome. Oral presentation. 31st congress of the Czech Society for Nephrology, Hradec Králové, Czech Republic, 24. 6. 2006.

Živná M., Vyleťal P., Kalbáčová M., Hodaňová K., Barešová V., Stibůrková B., Sikora J., Hůlková H., Živný J., Majewski J., Simmonds A., Fryns J.-P., Venkat-Raman G., Elleder M. and Kmoch S.: Alterations of Uromodulin Biology - a Common Denominator of the Genetically Heterogeneous FJHN/MCKD Syndrome. Poster presentation. The American Society for Cell Biology - 46th Annual Meeting, San Diego, USA, 9. - 13. 12. 2006.

Vyleťal P., Hůlková H., **Živná M.**, Berná L., Novák P., Elleder M. and Kmoch S.: Abnormal processing of uromodulin (UMOD) in Fabry disease patients reflects kidney tubular cell storage alteration and is reversible by enzyme replacement therapy. Poster presentation. The American Society for Cell Biology - 47th Annual Meeting, Washington, DC, USA, 1. - 5. 12. 2007.

Zivna M, Hodanova K, Vyletal P, Sikora J, Baresova V, Hulkova H, Kalbacova M, Zivny J, Ivanek R, Kapp K, Elleder M and Kmoch S: Preprorenin signal peptide mutation in a family with uromodulin-associated kidney disease. Poster presentation. Proprotein Processing, Trafficking and Secretion**,** Gordon Research Conference, New Hampshire, USA, 13. – 18. 7. 2008

K. Hodanova, **M. Zivna**, P. Vyletal, M. Votruba, G. Venkat-Raman, T. Ring, S. Kmoch: Novel uromodulin mutations identified in 8 out of the 21 probands with uromodulin associated kidney disease (UAKD). Poster presentation. The American Society of Human Genetics – 59th Annual Meeting, Honolulu, Hawaii, USA, 20. – 24. 10. 2009

J. N. Adams, A. J. Bleyer, T. C. Hart, **M. Zivna**, S. Kmoch, P. S. Hart: Identification of the second North American family with *REN*-associated medullary cystic kidney disease. Poster presentation. The American Society of Human Genetics – 59th Annual Meeting, Honolulu, Hawaii, USA, 20. – 24. 10. 2009